

**SEDIMENT DYNAMICS, HEAVY MINERAL
DEPLETION AND MORPHOLOGICAL CHANGES OF
A PLACER MINING BEACH OF SW COAST OF INDIA**

Thesis submitted to the



Cochin University of Science and Technology

In partial fulfilment of the requirements for the award of the Degree of

Doctor of Philosophy

in

Physical Oceanography

Under the Faculty of Marine Sciences

by

R. PRASAD



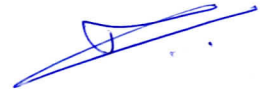
**National Centre for Earth Science Studies
Thiruvananthapuram**

November 2016

DECLARATION

I hereby declare that the thesis entitled "**Sediment Dynamics, Heavy Mineral Depletion and Morphological Changes of a Placer Mining Beach of SW Coast of India**" is an authentic record of research work carried out by me under the supervision and guidance of Dr. N.P. Kurian, former Director, National Centre for Earth Science Studies, Thiruvananthapuram, in partial fulfilment of the requirements for the Ph.D. Degree of the Cochin University of Science and Technology under the Faculty of Marine Sciences and that no part thereof has been presented for the award of any other degree/diploma in any University/Institute.

Thiruvananthapuram
November 1, 2016

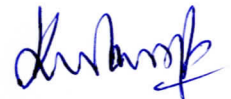


Prasad R.
(Reg. No. 4093)
National Centre for Earth Science Studies
Thiruvananthapuram - 695011

CERTIFICATE

This is to certify that this thesis entitled "**Sediment Dynamics, Heavy Mineral Depletion and Morphological Changes of a Placer Mining Beach of SW Coast of India**" is an authentic record of the research work carried out by Mr. Prasad R. (Reg. No. 4093) under my supervision and guidance at the National Centre for Earth Science Studies, Thiruvananthapuram, in partial fulfilment of the requirements for the Ph.D. Degree of the Cochin University of Science and Technology under the Faculty of Marine Sciences and no part thereof has been presented for the award of any degree/diploma in any University/Institute. All the relevant corrections and modifications suggested by the audience during the pre-synopsis seminar at the National Centre for Earth Science Studies and recommendations by the Doctoral Committee of the candidate have been incorporated in the thesis.

Thiruvananthapuram
November 1, 2016



Dr. N.P. Kurian
Research Guide

Dr. N P Kurian
Director, NCESS (Rtd.)
Eranat, Pullukadu, Karimanal
Trivandrum - 695 583, India

Memories of My Beloved Father
Sri. M.K. Ravindran

Dedicated To
My Beloved Family

ACKNOWLEDGEMENTS

I wish to place on record my deep sense of gratitude to my Research Guide Dr. N.P. Kurian, Former Director, National Centre for Earth Science Studies (NCESS), who has been a source of inspiration and support to me throughout the course of my research work. I owe him a lot for the constant encouragement and guidance and also for sparing his invaluable time, without which this work wouldn't have taken this shape.

I express my immense gratitude to Dr. L. Sheela Nair, Scientist-E, Coastal Processes Group, NCESS for the constant guidance and encouragement received for the research work and for the support in the preparation of this thesis.

I am grateful to Dr. T.N. Prakash, Director-in-charge & Group Head, Coastal Processes and Dr. V.M. Tiwari, Former Director, NCESS for providing all the necessary facilities of the institute for the successful completion of my research work.

Dr. A.N. Balchand, Dean, Faculty of Marine Sciences & Professor, Dept. of Physical Oceanography, School of Marine Sciences, CUSAT has provided me valuable support and guidance in his capacity as Doctoral Committee member. I am thankful to Dr. R. Sajeev, Associate Professor, Dept. of Physical Oceanography, School of Marine Sciences, CUSAT, for the constant encouragement and support during the course of my research work.

It is with great pleasure and gratitude that I acknowledge the valuable guidance received from Dr. K.V. Thomas (former Group Head), Dr. T.S. Shahul Hameed, (Scientist-G, Rtd.), Dr. K.K. Ramachandran (Group Head i/c) and Dr. Reji Srinivas (Scientist-C) of Coastal Processes Group during the course of my work.

I acknowledge with thanks the useful and inspiring discussions I had with Prof. T.S. Murty, Adjunct Professor, University of Ottawa, Canada and Prof. Kerry Black, former Professor, University of Waikato, New Zealand.

I wish to thank Dr. T. Radhakrishna, Dr. G.R. Ravindrakumar, Dr. G. Mohan Kumar, Dr. D. Padmalal, Dr. V. Nandakumar and Dr. D.S. Suresh Babu for their constant encouragement during the course of this research work.

I acknowledge with gratitude the help received from M/s. D. Raju, M. Ramesh Kumar, S. Mohanan, and M. Ajith Kumar, Scientific Officers of NCESS at various stages of this study.

I acknowledge with thanks the support provided by the Chief Manager and other officers and staff of the Administrative and Accounts sections of NCESS. Special thanks are due to Librarian and other staff of the library for extending the Library facilities.

My special thanks to Mrs. Molly Kurian for the moral support extended during the entire period of my work.

It is my pleasure to put on record the support and friendliness I have enjoyed from the company of Dr. C. Sreejith, Dr. V.R. Shamji, Dr. Tiju I. Varghese, Mr. E.K. Sarathraj, Mr. K.C. Vimal, Mr. M.K. Sreeraj, Mr. N. Nishanth, Dr. K.O. Badarees, Dr. C.S. Prasanth, Dr. R. Vishnu, Dr. S.S. Praveen, Mr. S. Arjun, Mr. Anish S. Anand, Mr. V. Noujas., Dr. M.M. Rameshan, Mr. M.K. Rafeeque, Mr. P.B. Vibin, Mr. S.S. Salaj, Mr. T.S. Sreekanth and Mr. K. Eldhose during my tenure at NCESS.

I wish to thank my friends Dr. C.K. Unnikrishnan, Dr. K. Haris and Mr. K.A. Abhinav for their constant encouragement during the course of my research work.

I express my deep gratitude to my mother (N. Radha), my grandmother (M.K. Madhavikutty Amma), my wife (G.S. Soumya), my brother (R. Dileep) and my sister (R. Shailaja) for their prayers and unflinching support for the completion of this work.

Prasad R.

CONTENTS

<i>Acknowledgements</i>	i
<i>Contents</i>	iii
<i>List of tables</i>	ix
<i>List of figures</i>	xi
<i>Symbols/Notations</i>	xvii
<i>Abbreviations/Acronyms</i>	xxi
<i>List of publications from the thesis</i>	xxiii

Chapter 1 INTRODUCTION

1.1	General.....	1
1.2	Coastal Zone.....	1
	1.2.1 Coast.....	1
	1.2.2 Shore.....	2
	1.2.3 Shoreface.....	2
	1.2.4 Continental shelf.....	2
1.3	Coastal Processes.....	2
	1.3.1 Waves.....	3
	1.3.1.1 Wave transformation.....	5
	1.3.1.2 Radiation stress.....	10
	1.3.1.3 Wave spectrum.....	12
	1.3.2 Currents.....	13
	1.3.2.1 Wind-induced current.....	14
	1.3.2.2 Wave-induced current.....	15
	1.3.2.3 Tidal currents.....	17
	1.3.3 Beach Erosion / Accretion.....	18
	1.3.3.1 Coastal structures contributing to erosion/accretion.....	18
	1.3.3.2 Other anthropogenic factors contributing to erosion.....	20
1.4	Sediment Dynamics.....	20
	1.4.1 Modes of sediment transport.....	22
	1.4.1.1 Bed load transport.....	22
	1.4.1.2 Suspended load transport.....	23
	1.4.1.3 Sheet flow.....	24
	1.4.2 Longshore sediment transport.....	24
	1.4.3 Cross-shore sediment transport.....	26
1.5	Sediment Budget.....	27
1.6	Beach States.....	28
	1.6.1 Equilibrium beach profile.....	29
	1.6.2 Beach classification.....	30

1.6.2.1	Reflective beach.....	31
1.6.2.2	Intermediate beach.....	31
1.6.2.3	Dissipative beach.....	32
1.7	Beach Placers.....	32
1.7.1	Formation of placers.....	33
1.7.2	Sorting processes.....	33
1.7.2.1	Settling equivalence.....	33
1.7.2.2	Selective entrainment.....	34
1.7.2.3	Transport sorting.....	34
1.7.2.4	Shear sorting.....	34
1.8	Background of the Study.....	35
1.9	Aim and Objectives.....	37
1.10	Study Area.....	37
1.11	Structure of the Thesis.....	40

Chapter 2 REVIEW OF LITERATURE

2.1	Introduction.....	43
2.2	Coastal Hydrodynamics.....	43
2.2.1	Global scenario.....	43
2.2.2	Indian scenario.....	46
2.3	Nearshore Sediment Transport.....	54
2.3.1	Global scenario.....	54
2.3.2	Indian scenario.....	62
2.4	Beach Placers.....	68
2.4.1	Global scenario.....	68
2.4.2	Indian scenario.....	70
2.5	Beach - Innershelf Morphological Changes.....	74
2.5.1	Global scenario.....	74
2.5.2	Indian scenario.....	83
2.6	Salient Conclusions from the Literature Survey Relevant to the SW Indian Coast.....	90

Chapter 3 DATA AND METHODOLOGY

3.1	Introduction.....	93
3.2	Instruments Used.....	93
3.2.1	Wave rider buoy.....	93
3.2.2	Automatic weather station.....	97
3.2.3	Echo-sounder.....	98
3.2.4	Global positioning system.....	99
3.2.5	Dumpy level.....	100
3.2.6	Sediment traps.....	101

3.2.7	Van Veen grab.....	102
3.2.8	Piston corer.....	102
3.3	Scheme and Methodology Followed for Data Collection.....	103
3.3.1	Waves.....	103
3.3.2	Wind.....	105
3.3.3	Bathymetry.....	105
3.3.4	Beach profile.....	107
3.3.5	Shoreline mapping.....	108
3.3.6	Beach and innershelf sediment sampling.....	111
3.3.7	Suspended sediment sampling.....	111
3.3.8	Littoral Environmental Observations.....	113
3.4	Laboratory Analysis of Sediment Samples.....	115
3.4.1	Textural analysis of sediments.....	115
3.4.1.1	Mechanical analysis.....	115
3.4.1.2	Pipette analysis.....	115
3.4.2	Estimation of heavy mineral content.....	116
3.4.3	Analysis of core sample.....	116
3.4.4	Estimation of quantum of sediment and HM concentration in the sediment trap collections....	117
3.5	Geo-spatial Analysis for Shoreline Change.....	117
3.6	Geo-spatial Analysis for Innershelf Morphological Changes.....	117
3.7	Empirical Orthogonal Function Analysis.....	118
3.8	Numerical Computations.....	119
3.9	Summary.....	120

Chapter 4 NEARSHORE SEDIMENT TRANSPORT REGIME

4.1	Introduction.....	121
4.2	Nearshore Wave Characteristics.....	121
4.2.1	Spectral analysis of waves.....	123
4.3	Coastal Wind Characteristics.....	124
4.4	Beach Profiles.....	127
4.5	Shoreline Orientation.....	129
4.6	Sediment Size.....	129
4.7	Wave Breaking and Breaker Type Estimation.....	130
4.8	Longshore Current (LSC) along the Chavara Coast.....	131
4.9	Estimation of Longshore Transport.....	132
4.9.1	Bulk formulae used.....	132
4.9.1.1	CERC formula.....	133
4.9.1.2	Kamphuis formula.....	133
4.9.2	Processes based model for the estimation of LST.....	134

4.9.2.1	Theoretical background.....	134
4.9.2.2	Input data.....	135
4.9.2.3	Calibration and validation.....	136
4.9.2.4	Surf zone longshore transport along the Chavara coast.....	137
4.9.2.5	Innershelf longshore transport along the Chavara coast.....	140
4.9.3	Estimation of cross-shore transport.....	142
4.9.3.1	Theoretical background.....	142
4.9.3.2	Input data.....	142
4.9.3.3	Calibration and validation.....	142
4.9.3.4	Cross-shore transport along the Chavara coast.....	144
4.10	Discussion.....	148
4.11	Summary.....	151

Chapter 5 HEAVY MINERAL DEPLETION IN THE SEDIMENTS

5.1	Introduction.....	153
5.2	Textural Characteristics of Beach Sediments.....	153
5.2.1	Mean size.....	155
5.2.2	Sorting coefficient.....	155
5.3	Textural Characteristics of Innershelf Sediments.....	157
5.4	Heavy Mineral Distributions of Surficial Sediments.....	161
5.4.1	Beach.....	161
5.4.2	Innershelf.....	162
5.5	Heavy Mineral Concentration in Suspended Sediment...	166
5.6	Sub-Surface Profile of Heavy Mineral Concentration...	167
5.7	Long-Term Change in the Heavy Mineral Concentration.....	170
5.7.1	Surficial distribution.....	170
5.7.2	Sub-surface distribution.....	173
5.8	Discussion.....	175
5.9	Summary.....	178

Chapter 6 BEACH-INNERSHELF MORPHOLOGICAL CHANGES

6.1	Introduction.....	179
6.2	Short-Term Beach Morphological Changes.....	179
6.2.1	Short-term changes derived from beach profiles	179
6.2.1.1	Station NK-1.....	180
6.2.1.2	Station NK-5.....	181
6.2.1.3	Station NK-6.....	182

6.2.1.4	Correlation between beach volume and beach width.....	185
6.2.2	Short-term shoreline changes.....	186
6.3	Long-Term Shoreline Changes.....	189
6.4	Empirical Orthogonal Function Analyses of Beach Profiles.....	194
6.5	Numerical Simulation of Shoreline Evolution.....	195
6.5.1	Theoretical background.....	196
6.5.2	Input data.....	199
6.5.3	Calibration and validation of the model.....	200
6.5.4	Shoreline evolution along the Chavara coast.....	201
6.6	Innershelf Morphological Changes.....	204
6.7	Discussion.....	209
6.8	Summary.....	216

Chapter 7 SUMMARY, CONCLUSIONS AND RECOMMENDATIONS

7.1	Summary.....	217
7.2	Conclusions and Recommendations.....	221
7.3	Recommendations for Future Research.....	223

REFERENCES 225

APPENDIX

Cover and First Page of Publications from the Thesis	251
--	-----

LIST OF TABLES

Table No.	Description	Page No.
1.1	Ledger of sediment budget.....	28
3.1	Specification of wave rider buoy DWR-MKIII.....	96
3.2	Bathymetry, beach profile and shoreline data used for the present study.....	110
3.3	Details of sediment cores collected from the innershelf of Neendakara-Aratupuzha coastal sector.....	113
3.4	Details of sediment traps deployed at Chavara offshore and nearshore sites.....	114
4.1	Monthly LSC values at Srayikkadu obtained from the LEO.....	132
4.2	Sediment characteristics of cross-shore profile used for the LITDRIFT model.....	136
4.3	Climatic description for the LITDRIFT model.....	137
4.4	Monthly LST in the surf zone at Srayikkadu computed using Kamphuis formula, CERC formula and LITDRIFT module of LITPACK.....	139
4.5	Annual longshore sediment transport in the surf zone at Srayikkadu estimated by using Kamphuis formula, CERC formula and LITDRIFT module of LITPACK.....	140
4.6	Monthly LST in the innershelf at Srayikkadu estimated by using LITDRIFT module of LITPACK.....	141
4.7	Annual LST in the innershelf at Srayikkadu estimated by using LITDRIFT module of LITPACK.....	141
4.8	Climatic description for the LITPROF model.....	142
4.9	Calibration terms used for the LITPROF model.....	144
4.10	Classification of BSS.....	144
4.11	Error estimation for the beach profiles using the measured beach profile and simulated cross-shore profile (from LITPROF) during January-December 2014.....	146
4.12	Estimation of BSS from the measured and simulated beach volume (from the LITPROF cross-shore profile) during January-December 2014.....	147
4.13	Monthly cross-shore sediment transport at Srayikkadu estimated by using LITPROF module of LITPACK during January-December 2014	148
4.14	Annual cross-shore sediment transport at Srayikkadu estimated by using LITPROF module of LITPACK during January-December 2014	149
5.1	Textural characteristics of beach sediment samples from different locations of the Neendakara-Arattupuzha coast during the pre-monsoon period.....	156

5.2	Textural characteristics of beach sediment samples from different locations of the Neendakara-Arattupuzha coast during the monsoon period.....	156
5.3	Textural characteristics of beach sediment samples from different locations of the Neendakara-Arattupuzha coast during the post-monsoon period.....	157
5.4	Textural characteristics of the innershelf sediments during the pre-monsoon.....	160
5.5	Textural characteristics of the innershelf sediments during the monsoon.....	162
5.6	Textural characteristics of the innershelf sediments during the post-monsoon.....	163
5.7	Sediment trap collections and heavy mineral content at different levels of nearshore and offshore sites off Chavara during 23-29 th July 2010...	168
5.8	Sediment trap collections and heavy mineral content at different levels of nearshore and offshore sites off Chavara during 20-30 th November 2010.....	168
5.9	Sediment trap collections and heavy mineral content at different levels of nearshore and offshore sites off Chavara during 30 th April to 5 th May 2011.....	168
5.10	Long-term variation in average heavy mineral concentration in the beach samples from Chavara coast.....	170
5.11	Long-term variation in average heavy mineral concentration in the surficial sediment samples of the innershelf.....	172
5.12	Total average heavy mineral concentrations of 0-0.5 m column of seabed for different sectors along the Chavara coast.....	174
5.13	Total heavy mineral concentration of 0-1.0 m column of seabed for different sectors along the Chavara coast.....	174
5.14	Long-term variation in down-core average heavy mineral concentration in the innershelf at different sectors of the Chavara coast.....	174
6.1	Monthly shoreline change (m) along the northern sector of Chavara coast estimated from shorelines mapped using GPS during the year 2014.....	188
6.2	Monthly shoreline change (m) along the northern sector of Chavara coast estimated from shorelines mapped using GPS during the year 2015.....	191
6.3	Long-term shoreline change (m) along the Chavara coast during different periods.....	194
6.4	Results of EOF analysis showing the percentage of variance contained by each eigen function.....	195
6.5	Statistical error estimates for the simulated and measured shoreline along the Chavara coast for the years 2006, 2010 and 2015.....	201
6.6	Shift in isobaths at different locations of the Chavara coast: area calculated from bathymetric contours per unit width over different time periods for 10 m, 14 m and 20 m depth.....	210

LIST OF FIGURES

Fig. No.	Description	Page No.
1.1	Different zones and features of the coastal zone.....	3
1.2	Particle orbits in the deep and shallow waters.....	4
1.3	(a) Refraction along a straight beach with parallel bottom contours, (b) Refraction along an irregular shoreline.....	7
1.4	(a) Definition sketch for wave diffraction, (b) diffraction around an island.....	8
1.5	Classification of wave breaking on the beach.....	10
1.6	(a) Variance density spectrum, (b) Two-dimensional frequency-direction spectrum.....	13
1.7	Typical Pierson-Moskowitz and JONSWAP spectrum.....	13
1.8	Ekman spiral and Ekman transport direction.....	15
1.9	Wave-induced longshore current.....	16
1.10	(a) Rip current and associated current vectors, (b) Nearshore circulation system including rip currents.....	17
1.11	(a) Shore response to perpendicular structure, (b) series of shore perpendicular structures.....	20
1.12	Longshore (q_x) and cross-shore (q_y) sediment transport components.....	21
1.13	Modes of sediment transport showing sliding, rolling and saltation.....	22
1.14	Definition sketch of suspended sediment transport.....	24
1.15	Longshore sediment transport.....	25
1.16	Net and gross longshore transport.....	26
1.17	Cross-shore transport in the nearshore.....	27
1.18	(a) Parameters used in the sediment budget estimation, (b) Sediment transport pathways in a coastal cell.....	29
1.19	(a) Schematic of an equilibrium profile, (b) Profiles out of equilibrium..	30
1.20	(a) Classification of beach types, (b) Nomogram showing the contribution of wave height, sediment size, wave period and beach type.	32
1.21	Schematic illustration of sorting processes.....	36
1.22	Study area extending from the Neendakara inlet in the south to the Kayamkulam inlet in the north, SW coast of India.....	38
1.23	Google image of the study area showing the mining sites.....	39
3.1	(a) Directional WRB, (b) DWRB deployed off Chavara, Kollam at 22 m water depth.....	94
3.2	Locations of deployment wave rider buoy and automatic weather station at Chavara coast.....	95
3.3	Typical mooring layout for a directional wave rider buoy for shallow waters.....	97

3.4	AWS: (a) wind speed and direction sensor (RM Young) and (b) data logger (Campbell Scientific) installed in the beach at Ponmana, Chavara coast (c).....	98
3.5	(a) Bathy-500 Echo-sounder (Ocean Data Equipment Corporation, U.S.A.), (b) 33/210 KHz dual frequency transducer.....	99
3.6	(a) Ceeducer Pro echo-sounder (Bruttour International Ltd., Australia), (b) 200 KHz hydro survey transducer.....	99
3.7	Global positioning system (a) operational principle, (b) GPS receiver (Trimble Juno SB).....	100
3.8	(a) Dumpy level and staff (Leica Geosystems) used for the beach profile survey, (b) Beach profile measurement at the Chavara coast.....	101
3.9	(a) Sediment traps attached to the housing, (b) Deployment of sediment traps offshore of Chavara.....	101
3.10	(a) & (b): Van Veen grab (KC Instruments, Denmark) used for nearshore surficial sediment sampling, (c) Surficial sediment samples collected from the nearshore of Chavara using the grab.....	102
3.11	Piston Corer: (a) principle of operation, (b) piston corer being lowered in the offshore of Chavara for sediment coring.....	103
3.12	Wind definition according to nautical convention.....	105
3.13	Sector covered for bathymetric survey; the shore-normal transects along which soundings were made are also shown.....	106
3.14	The beach profile stations and coastal structures along the Neendakara-Kayamkulam sector.....	109
3.15	Typical beach profile stations: (a) south of Kayamkulam breakwater (NK-1), (b) Srayikkadu (NK-5) and (c) Vellanathuruthu mining site (NK-6).....	110
3.16	Sediment sampling points in the beach and the innershelf of the Neendakara-Arattupuzha coast. Since the data on sedimentology pertaining to the area north of Kayamkulam inlet would be helpful in understanding the sediment dynamics and the heavy mineral distribution, the sampling locations have been extended upto Arattupuzha.....	112
3.17	Piston Corer being lowered for collection of sediment core from offshore of Chavara coast.....	113
4.1	Monthly wave roses off Chavara coast during January-December 2014..	122
4.2	Percentage occurrence of significant wave heights measured off Chavara coast during January-December 2014.....	123
4.3	Percentage occurrence of peak wave periods measured off Chavara coast during January-December 2014.....	123
4.4	Percentage occurrence of wave directions (^o N) measured off Chavara coast during January-December 2014.....	124
4.5	One-dimensional spectrum of wave measured off Chavara coast during (a) non-monsoon and (b) monsoon period of January-December 2014....	125
4.6	Frequency-Direction spectrum of wave measured off Chavara coast during January-December 2014.....	126
4.7	Monthly wind roses for Chavara coast during January-December 2014..	126

4.8	Percentage occurrence of wind speeds at Chavara coast during January-December 2014.....	127
4.9	Percentage occurrence of wind direction ($^{\circ}$ N) at Chavara coast during January-December 2014.....	127
4.10	Measured beach profile at Srayikkadu during January 2014 - January 2015.....	128
4.11	Calculated beach volume change from the measured beach profiles at Srayikkadu during January 2014 - January 2015.....	128
4.12	Cumulative volume change at Srayikkadu during January 2014 - January 2015.....	129
4.13	Measured monthly shore normal at Srayikkadu during January - December 2014.....	129
4.14	Measured offshore wave direction, shore normal and calculated breaker wave angle off Srayikkadu during January - December 2014.....	130
4.15	Estimated surf similarity parameter (ξ_0) (after Galvin 1968) off Srayikkadu during January - December 2014.....	131
4.16	Monthly maximum longshore current at Srayikkadu estimated by using LITDRIFT module of LITPACK and by Littoral Environmental Observation (LEO).....	137
4.17	Monthly LST in the surf zone at Srayikkadu computed using Kamphuis formula, CERC formula and LITDRIFT module of LITPACK.....	138
4.18	Comparison of computed longshore sediment transport in the surf zone with and without wind using LITDRIFT module at Srayikkadu.....	139
4.19	Monthly LST in the innershelf at Srayikkadu estimated by using LITDRIFT module of LITPACK. The case for 'no wind' is also presented to highlight the significant influence of wind in the LST in the innershelf unlike the surf zone.....	140
4.20	Beach profiles at Srayikkadu simulated using LITPROF for one year....	145
4.21	Validation of the cross-shore transport using the beach volume from the measured beach profile and simulated beach volume from the LITPROF cross-shore profile during January - December 2014 for Srayikkadu (Note: No beach during May to July).....	146
4.22	Monthly cross-shore sediment transport at Srayikkadu estimated by using LITPROF module of LITPACK during January - December 2014.	147
4.23	Annual cross-shore sediment transport at Srayikkadu estimated by using LITPROF module of LITPACK during January - December 2014.....	148
5.1	Sediment sampling points in the beach and the innershelf of the Neendakara-Arattupuzha coast.....	154
5.2	Spatial distribution of mean sediment size in the innershelf during the pre-monsoon.....	158
5.3	Spatial distribution of sediment mean size in the innershelf during the monsoon.....	159
5.4	Spatial distribution of sediment mean size in the innershelf during the post-monsoon.....	161
5.5	Heavy mineral concentration at MWL of beaches of different locations during the pre-monsoon, monsoon and post-monsoon seasons.....	163

5.6	Distribution of heavy mineral concentration in the surficial sediment samples during the pre-monsoon period.....	164
5.7	Distribution of heavy mineral concentration in the surficial sediment samples during the monsoon period.....	165
5.8	Distribution of heavy mineral concentration in the surficial sediment samples during the post-monsoon period.....	166
5.9	Down-core variation in heavy mineral content at different stations of Neendakara-Arattupuzha coast.....	171
5.10	Satellite imagery (Source: Google image) and snapshots showing erosion immediately north of Kayamkulam breakwater and accretion towards south of the breakwater.....	177
6.1	Monthly beach profiles during (a) 2010-2011, (b) 2012, (c) 2013, (d) 2014 and (e) 2015 at Station NK-1.....	181
6.2	Monthly beach profiles during (a) 2010-2011, (b) 2012, (c) 2013, (d) 2014 and (e) 2015 at Station NK-5.....	183
6.3	Monthly beach profiles during (a) 2010-2011, (b) 2012, (c) 2013, (d) 2014 and (e) 2015 at Station NK-6.....	184
6.4	(a-c) Beach volume change from June 2010 to December 2015: (a) NK-1, (b) NK-5 and (c) NK-6.....	185
6.5	Cumulative beach volume change (m^3/m) during the period of July 2010 to December 2015 for stations NK-1, NK-5 and NK-6 along the Neendakara-Kayamkulam coastal sector.....	185
6.6	Scatter plot of beach volume v/s beach width calculated from beach profiles for the stations (a) NK-1, (b) NK-5 and (c) NK-6.....	187
6.7	Short-term shoreline change along the northern sector of the Chavara coast during 2014.....	189
6.8	Short-term shoreline change along the northern sector of the Chavara coast during 2015.....	190
6.9	Long-term shoreline change along the Chavara coast during different time periods starting from 1968.....	193
6.10	First three eigen functions for the beach profiles at station NK-5: (a) spatial and (b) temporal dependence.....	196
6.11	Definition sketch for shoreline change calculation according to 1-line theory.....	197
6.12	Baseline orientation used in the LITLINE module of LITPACK.....	198
6.13	Alongshore discretization used in the LITLINE module of LITPACK....	198
6.14	Simulated and measured shoreline along the Neendakara-Kayamkulam coastal sector for the years (a) 2006, (b) 2010 and (c) 2015.....	202
6.15	Simulated shoreline along the Neendakara-Kayamkulam coastal sector for the year 2015 superimposed on satellite image (Google image) for the (a) northern sector near to Kayamkulam inlet and (b) Ponmana mining site.....	203
6.16	Simulated shoreline for the years 2001-2006 (a) at mining site and (b) south of Kayamkulam inlet. The simulation was performed (i) without incorporating breakwaters and groins and (ii) by providing zero sink i.e. no mining.....	204

6.17	Simulated shoreline for the years 2006, 2010, 2015, 2018 and 2022 (a) at the mining site and (b) south of Kayamkulam inlet. The simulation was performed with the influence of breakwaters, groins and seawall.....	205
6.18	The simulated shoreline for the selected sectors of the Chavara coast for the years 2006, 2010, 2015, 2018 and 2022. The measured shoreline for the year 2000 which is the baseline for the simulation is also shown in the figure.....	206
6.19	Shoreline evolution simulated for the Chavara coast for different years (2000, 2006, 2010, 2015, 2018 and 2022): (a) south of Kayamkulam inlet and (b) Vellanathuruthu-Ponmana mining site. The simulated shorelines are superimposed on the Google image for January 2016.....	207
6.20	Comparison of bathymetry of the innershelf of the Chavara coast during the years 2000, 2005 and 2010.....	208
6.21	Shift in isobaths at different locations of the Chavara coast as observed in the isobaths of (a) 10 m, (b) 14 m and (c) 20 m.....	209
6.22	Satellite images (Google images) of the Ponmana-Vellanathuruthu mining site during 2003 - 2015 showing the ruins of the old seawall at the mining site and two newly constructed groins during 2013.....	212
6.23	Google images of the coastal sector immediately south of Kayamkulam inlet: (a) 2005, (b) 2012, (c) 2013 and (d) 2015. The old and new groins constructed along the coastal stretch is marked in the figure.....	214
6.24	Google images of the north central sector of Chavara coast: (a) 2005, no groins are available; (b) 2012, no groins are available; (c) 2013, a groin field of 4 nos. is seen and (d) 2015, another groin field consisting of 7groins is added.....	215

SYMBOLS / NOTATIONS

English Symbols

A	Non-dimensional parameter used in CERC formula
A_s	Shape parameter for the cross-shore profile
C	Wave celerity in shallow water
C_o	Wave celerity in deep water
C_d	Drag coefficient (1.2×10^{-3})
C_g	Group velocity in shallow water
C_{go}	Group velocity in deep water
C_{gx}	Group velocity in x direction
C_{gb}	Breaking wave group speed
$C(z)$	Suspended sediment concentration
d	Water depth
d_b	Breaker depth
d_{50}	Median grain size of the sediment
D	Particle diameter; Grain size
D_B	Berm height
D_C	Depth of closure
D_{eq}	Wave energy dissipation per unit volume
$D(f, \theta)$	Directional spreading function
E	Wave energy in shallow water
E_o	Wave energy in deep water
E_m	Momentum exchange coefficient
E_{diss}	Dissipated power per unit area
$E(f)$	1-D frequency spectrum
f	Frequency
f_p	Peak frequency
g	Acceleration due to gravity
h	Height from the bottom
h_{act}	Height of the active cross-shore profile
H	Wave height in shallow water
H_o	Wave height in deep water
H_b	Breaker wave height
H_I	Incident wave height
H_R	Reflected wave height
H_{mn}	Data matrix
H_{max}	Maximum wave height
H_{rms}	Root mean square wave height
H_s	Significant wave height

H_{mo}	Significant wave height estimated based on the zeroth order moment of the wave spectrum
H_o/L_o	Wave steepness
I_1, I_2	Einstein integrals
I	Identity matrix
I_l	Immersed weight transport rate
k	Wave number
k_s	Bed roughness
K	Calibration parameter used in CERC formula
K_D	Dimensionless coefficient for longshore current velocity
K_s	Shoaling coefficient
K_r	Refraction coefficient
K_R	Reflection coefficient
L	Wave length
L_o	Offshore wave length
m	Foreshore slope
m_b	Bottom slope up to two wave lengths offshore of the breaker line
m_o	Zeroth order spectral moment
m_n	n^{th} order spectral moment
m_1	First order spectral moment
m_2	Second-order spectral moment
P	Porosity of sediment (typically 0.4)
P_L	Longshore component of wave energy flux
q_s	Suspended sediment transport
q_b	Bed load transport
q_x	Longshore sediment transport component
q_y	Cross-shore sediment transport component
Q_c	Cross-shore sediment transport rate
Q_l	Longshore sediment transport rate
$Q_{l \text{ Net}}$	Net longshore sediment transport rate
$Q_{l \text{ Gross}}$	Gross longshore sediment transport rate
Q_b	Fraction of breaking / broken waves
Q_p	Spectral peakedness parameter
Q_{sou}	Source/sink term expressed in volume/ Δx
Q_{vol}	Total immersed volume in m^3/year
r	Rank of the matrix
Re	Reynolds number
S_{xx}	Normal radiation stress component
S_{yy}	Transverse component of the radiation stress
S_{xy}	Shear component of the radiation stress
t	Time
T	Wave period
T_p	Peak wave period
T_z	Zero crossing period

T_{m01}	Mean wave period estimated based on the order of the moment of the wave spectrum
T_{m02}	Zero crossing period estimated based on the order of the moment of the wave spectrum
T_o	Length of record
u	Cross-shore component of flow velocity
U_{10}	Wind speed at 10 m above mean sea level
U_{max}	Peak sediment velocity at the bed
U_t	Shear velocity
$U(z)$	Flow velocity
$U_i; V_i$	Eigen functions
v	Longshore current velocity
w_s	Sediment dimensionless fall velocity (Settling velocity)
x	Long-shore position
X	Measured value
y	Offshore distance from the shoreline
$y(x)$	Coastline position
y_{intl}	Initial coastline position
Y	Simulated value
z	Vertical co-ordinate
z_b	Bed level
$Z_{b,m}$	Measured bed level
$Z_{b,s}$	Simulated bed level
$Z_{b,0}$	Initial bed level
$\Delta Z_{b,m}$	Error of the measured bed level

Greek Symbols

α_o	Wave approach angle
α_b	Wave breaker angle
α_{CN}	Crank-Nicholson factor
α_d	Dissipation factor
β	Beach slope angle
γ	Breaker index (ratio of wave height to water depth at breaking)
γ_1, γ_2	Breaker wave parameters
Γ	Diagonal matrix
λ_i	Eigen values
θ	Mean wave direction
θ'	Effective Shields parameter
θ_o	Wave direction in deep water
θ_c	Critical Shields parameter
θ_{br}	Breaker angle with respect to shore normal
θ_{bs}	Angle of breaking waves to local shoreline
θ_t	Shields entrainment function

ε	Spectral width parameter
ν	Alternative spectral width parameter
ξ_0	Surf similarity parameter
π	Constant (= 22/7)
μ	Viscosity of the fluid
η	Surface level elevation
ρ	Density of fluid/sea water
ρ_w	Density of water
ρ_a	Density of air
ρ_s	Density of sand
δ	Volumetric measurement error
τ	Wind stress
τ_b	Bed shear stress due to longshore current
τ_b'	Effective shear stress
τ_{cur}	Driving forces due to coastal current
τ_t	Threshold mean bed stress
τ_w	Driving forces due to wind
ω	Angular frequency
Ω	Dimensionless parameter indicating beach state
ϕ	Base two logarithmic scale used to describe the grain size distribution of sediment
Φ_b	Bed load solid discharge per unit width
Δx	Alongshore discretization step

ABBREVIATIONS / ACRONYMS

Avg.	Average
deg.	Degree
Lat.	Latitude
Long.	Longitude
Ltd.	Limited
w.r.t.	With respect to

AWS	Automatic Weather Station
ADCP	Acoustic Doppler Current Profiler
ASCAT	Advanced Scatterometer
ASTM	American Section of the International Association for Testing Materials
BM	Bench Mark
BSS	Brier Skill Score
BW	Breakwater
CC	Correlation Coefficient
CEM	Coastal Engineering Manual
CERC	Coastal Engineering Research Centre
CESS	Centre for Earth Science Studies
CMS	Coastal Modelling System
CTD	Conductivity Temperature Depth
CVI	Coastal Vulnerability Index
DHI	Danish Hydraulic Institute
DWRB	Directional Wave Rider Buoy
EOF	Empirical Orthogonal Function
FFT	Fast Fourier Transform
FTCS	Forward in Time - Central in Space
GENESIS	GENERALized model for SIMulating Shoreline change
GIS	Geographic Information System
GPS	Global Positional System
GSI	Geological Survey of India
HM	Heavy Mineral
HWL	High Water Line
HTL	High Tide Level
IOD	Indian Ocean Dipole
IREL	Indian Rare Earths Limited
INCOIS	Indian National Centre for Ocean Information Services
JONSWAP	Joint North Sea Wave Project
KMML	Kerala Minerals and Metals Limited
LEO	Littoral Environmental Observations

LITPACK	Littoral Processes and Coastline Kinetics
LSC	Longshore Current
LST	Longshore Sediment Transport
LTC	Long-Term Configuration
LTL	Low Tide Level
MOA	Multi-purpose, Offshore and Adjustable
MWD	Mean Wave Direction
MWL	Mid Water Line
MSL	Mean Sea Level
N	North
NW	North West
NNW	North North West
NCESS	National Centre for Earth Science Studies
NMEA	National Marine Electronics Association
OSW	Offshore Spectral Wave Model
PWD	Predominant Wave Direction
PCA	Principal Component Analysis
PSU	Public Sector Undertaking
PM	Pierson-Moskowitz
PP	Poly Propylene
RMAE	Relative Mean Absolute Error
RMSE	Root Mean Square Error
ROMS	Regional Ocean Modeling System
SC	Sediment Cell
SD	Standard Deviation
SoI	Survey of India
SPM	Shore Protection Manual
SSC	Suspended Sediment Concentration
SSE	South South East
SSW	South South West
SE	South East
SW	South West
SWL	Still Water Line
SMC	Summer Monsoon Current
SVD	Singular Value Decomposition
T-S	Travancore-Shoranur
WL	Water Line
WGS	World Geodetic System
WMO	World Meteorological Organization
WRB	Wave Rider Buoy
WSW	West South West
WICC	West India Coastal Current

LIST OF PUBLICATIONS FROM THE THESIS

Journal Papers

1. Prasad, R., Sheela Nair, L., Kurian, N.P. and Prakash, T.N., 2016. Erosion and heavy mineral depletion of a placer mining beach along the southwest coast of India: Part I– Nearshore sediment transport regime. *Natural Hazards* 83, 769–796, doi: 10.1007/s11069-016-2368-z.
2. Prakash, T.N., Varghese, T.I., Prasad, R., Sheela Nair, L. and Kurian, N.P., 2016. Erosion and heavy mineral depletion of a placer mining beach along the southwest coast of India: Part II– Sedimentological and mineralogical changes. *Natural Hazards* 83, 797–822, doi: 10.1007/s11069-016-2350-9.
3. Prasad, R., Sheela Nair, L., Kurian, N.P., Prakash, T.N. and Varghese, T.I., 2016. Erosion and heavy mineral depletion of a placer mining beach along the southwest coast of India: Part III– Short and long term morphological changes. *Natural Hazards* 83, 823–847, doi: 10.1007/s11069-016-2346-5.

Conference Proceedings

1. Prasad, R. and Sheela Nair, L., 2012. Numerical modelling of shallow water wave characteristics off a monsoon dominated coast. *Proceedings of National Conference on Hydraulic and Water Resources (HYDRO - 2012)*, IIT Bombay, India, 7th and 8th December 2012, pp. 1715–1722.
 2. Sarathraj, E.K., Prasad, R. and Badarees, K.O., 2013. Efficient utilization of wave power at Kollam coast of Kerala. *Proceedings of 25th Kerala Science Congress*, Technopark, Trivandrum, India, 29th January - 1st February 2013, 1, pp. 444–446.
 3. Sarathraj, E.K., Prasad, R., Sheela Nair, L., Reji Srinivas and Balakrishnan Nair, T.M., 2013. Influence of wind on wave climate along Kerala coast, southwest coast of India. *Proceedings of HYDRO - 2013 International Conference*, IIT Madras, India, 4th and 6th December 2013, pp. 206–211, ISBN 978-93-80689-18-0.
 4. Suresh, T., Sheela Nair, L. and Prasad, R., 2015. Wave climate studies along the Kerala Coast. *Proceedings in the 27th Kerala Science Congress*, Alapuzha, Kerala, India, January 2015, pp. 62–63, ISBN 81-86366-88-1.
-

CHAPTER 1

INTRODUCTION

1.1 General

Coastal areas are one of the most dynamic zones that are continuously changing due to natural and human induced processes. The natural processes inducing dynamics in the coastal zone are the hydrodynamic processes such as waves (which are the dominant energy source), currents, tides and wind. The hydrodynamic processes interact with the sediment causing sediment transport in the beach and innershelf area. Depending on the net transport of sediments, morphological changes of beach and innershelf takes place. In addition to the natural processes, anthropogenic activities also cause sediment imbalance in the coastal zone thereby contributing to morphological changes. The study of sediment dynamics in the coastal waters and its modelling are thus vital in understanding the driving forces of the beach-innershelf morphological changes which is essential for suggesting remedial measures for coastal erosion problems faced by the coast.

1.2 Coastal Zone

Coastal zone is a dynamic zone where the interaction of the sea and the land processes occurs and is under the continuous influence of non-linear hydrodynamic forces. Wave action is the most active phenomenon in the coastal zone along with the influence of the astronomical tide. Wind-induced currents also play an active role in this zone. The action of the wind waves and the resultant nearshore circulation brings out the most significant changes to a beach. Large volume of sediments is carried along the shore by wave-induced currents. The coastal zone extends to the continental shelf break towards offshore and first major change in topography towards onshore (Fig. 1.1) and the coastal zone is divided into four major subzones viz. Coast, Shore, Shoreface and Continental shelf (CEM, 2002).

1.2.1 Coast

The coast can be defined as a strip of land of indefinite width that extends from the coastline inland as far as the first major change in topography. This inland boundary

is marked by Cliffs, frontal dunes, or a line of permanent vegetation. The maximum reach of storm waves is the seaward boundary of the coast.

1.2.2 Shore

The shore extends from the low water line to the normal landward limit of storm wave effects, i.e., the coastline. Where beaches occur, the shore can be divided into two zones: backshore (or berm) and foreshore (or beach face). The foreshore extends from the low water line to the limit of wave uprush at high tide. The backshore is horizontal while the foreshore slopes seaward.

1.2.3 Shoreface

The shoreface is the seaward dipping zone that extends from the low water line offshore to a gradual change to a flatter slope denoting the beginning of the continental shelf. The continental shelf transition is the toe of the shoreface. Its location can only be approximately marked due to the gradual slope change. Although the shoreface is a common feature, it is not found in all coastal zones, especially along low energy coasts or those consisting of consolidated material. The shoreface can be delineated from shore perpendicular profile surveys or from bathymetric charts. The shoreface, especially the upper part, is the zone of most frequent and vigorous sediment transport.

1.2.4 Continental shelf

The continental shelf is the shallow seafloor that borders most continents. The shelf floor extends from the toe of the shoreface to the shelf break where the steeply inclined continental slope begins. It has been common practice to subdivide the shelf into inner-, mid-, and outer zones, although there are no regularly occurring geomorphic features on most shelves.

1.3 Coastal Processes

Coastal processes can be defined as the set of mechanisms that operate along a coastline, bringing about various combinations of erosion and deposition that in turn influence the geomorphic form and evolution of the coast. The coastal zone is constantly under the action of hydrodynamic processes such as waves, wind, tide and currents. They combine to produce different sediment transport processes which eventually lead to distinctive coastal landforms. Anthropogenic activities such as the

construction of coastal structures will modify the coastal processes and thereby affect the local sediment dynamics. A few of the important coastal processes are detailed in the following sections.

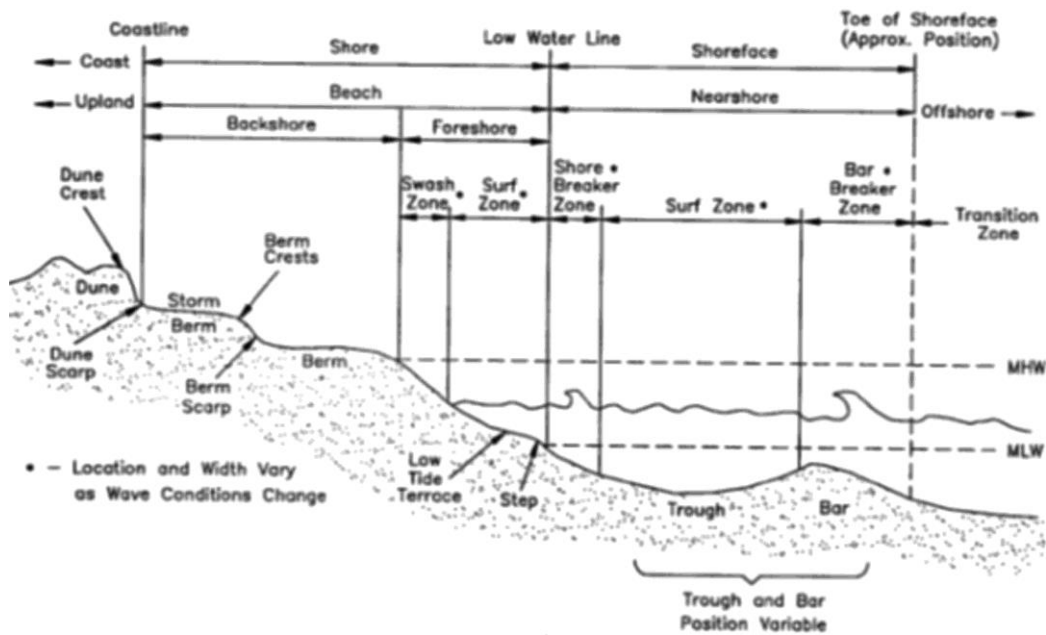


Fig. 1.1 Different zones and features of the coastal zone (Source: CEM, 2002)

1.3.1 Waves

Ocean waves are generated primarily by the influence of wind acting on the air-sea interface and other wave forms such as internal waves, edge waves, tides etc. exists on the oceanic surface. Waves play a major role in the coastal processes and sediment dynamics of any region. They are complex owing to its non-linearity and non-sinusoidal nature. Further, it consists of groups of waves of different characteristics in heights, periods and directions occurring simultaneously at a point. The water particle motion is in the closed circular orbit for each wave period then the waves are considered to be oscillatory in nature, which can be explained by linear wave theory. For the waves that are not purely oscillatory but periodic can be explained by finite amplitude wave theory. The surface waves are classified into wind seas and swells. The wind seas are short-period waves generated by the influence of local wind, whereas swells are long-period waves that have moved out from the generating area. The seas are short-crested and irregular waves having period in the range of 3-10 s. The swells are regular long-crested waves having the period greater than 10 s and can travel a large distance without much loss of energy. The action of longshore currents

generated by breaking waves is primarily responsible for the sediment transport in the nearshore region extending through foreshore upto the berm.

The particle orbital geometries undergo transformation when a wave propagates from deep to shallow water which is shown in Fig. 1.2. The orbital motions are circular throughout the water column in deep water ($d/L > 1/2$) and the orbital diameter decreases with depth (d) and die out at a distance of $L/2$ (where L is the wavelength). In transitional to shallow water ($d/L < 1/2$), the orbits reach the bottom and become elliptical in shape and the particles follow a reversing horizontal path at the bottom.

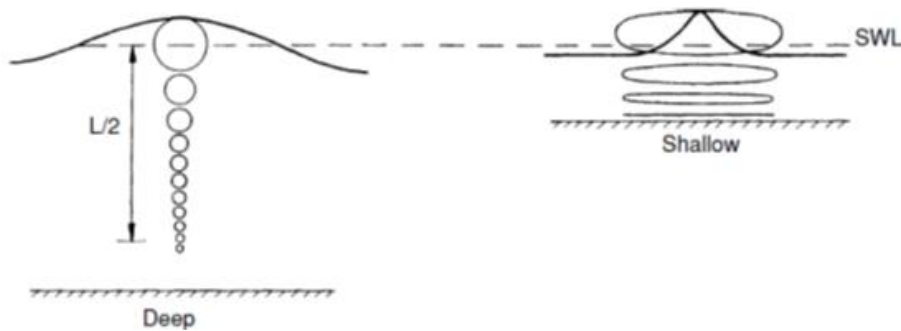


Fig. 1.2 Particle orbits in the deep and shallow waters (Source: Sorensen, 2006)

The speed at which a wave propagates is termed as the wave celerity (C) or phase velocity. The celerity can be related to wavelength and period by $C = L/T$, since the distance travelled by a wave during one wave period (T) is equal to one wavelength (L).

The expression for the celerity to wavelength and water depth is given by

$$C = \sqrt{\frac{gL}{2\pi} \tanh\left(\frac{2\pi d}{L}\right)} \dots\dots\dots(1.1)$$

where g is the acceleration due to gravity. This expression indicates that waves with different periods travel at different speeds and is termed as the dispersion relation.

The above equation can be written in terms of period (T) as

$$C = \frac{gT}{2\pi} \tanh\left(\frac{2\pi d}{L}\right) \dots\dots\dots(1.2)$$

The values $2\pi/L$ and $2\pi/T$ are called the wave number (k) and wave angular frequency (ω) respectively. The expression for wavelength as a function of depth and wave period can be written as

$$L = \frac{gT^2}{2\pi} \tanh\left(\frac{2\pi d}{L}\right) = \frac{gT}{\omega} \tanh(kd) \dots\dots\dots(1.3)$$

An approximate expression for estimating wavelength is given by Eckart (1952)

$$L = \frac{gT^2}{2\pi} \sqrt{\tanh\left(\frac{4\pi^2 d}{T^2 g}\right)} \dots\dots\dots(1.4)$$

Waves are classified based on the relative depth criterion d/L . If water depth $d > L/2$, then $\tanh(2\pi d/L) \approx 1$, then deep water wave celerity (C_o) is given by

$$C_o = \sqrt{\frac{gL_o}{2\pi}} \dots\dots\dots(1.5)$$

where L_o is the deep water wave length.

When the relative water depth becomes very less (i.e. very shallow waters; $d < L/20$), $\tanh(2\pi d/L) \approx (2\pi d/L)$, then the shallow water wave celerity (C) is given by

$$C = \sqrt{gd} \dots\dots\dots(1.6)$$

Thus when wave travels in very shallow water, wave celerity depends only on water depth.

1.3.1.1 Wave transformation

When waves propagate from deep water into shallow water environments, the effects of bathymetry begin to transform the wave direction and amplitude. The different transformation processes are shoaling, refraction, diffraction, reflection, wave breaking, dissipation due to bottom friction and percolation etc. The general equation to estimate wave transformation is the radiative transfer equation and is represented as

$$\frac{\partial E(x,y,t,f,\theta)}{\partial t} + \nabla \cdot [C_g(x,y,f) E(x,y,t,f,\theta)] = S_w + S_n + S_D + S_F + S_P \dots\dots\dots(1.7)$$

where the first term on the left hand side of the above equation represents the temporal rate of change of the spectrum, 2nd term represents the propagation of wave energy, S_w is the wind input, S_n represents the redistribution of wave energy between different wave components that arise from non-linearities of the waves, S_D represents dissipation due to breaking, S_F represents losses due to bottom friction, and S_P represents losses due to percolation. Processes that lead to the transformation of waves as they propagate to the shallow water are described in the following sub-sections.

Shoaling

The term shoaling is used to describe the propagation of waves from deep water to shallow water depths and change in the wave profile is caused by the change in water depth. When waves moves into the shallow waters, the wave characteristics change, i.e wave celerity decreases leads to a decrease in wave length, wave height or steepness increases, but the period remains constant. In the intermediate waters, an increase in the group velocity occurs resulting in a decrease in wave energy, and consequently a decrease in wave height. In shallower depths the group velocity decreases resulting in a rapid increase in wave height. This processes of change in wave height and wave length due to change in velocity of propagation is called shoaling. The changes in wave height during shoaling can be obtained from wave energy flux, i.e.

$$EC_g = E_0C_{g0} \dots \dots \dots (1.8)$$

where E and E₀ are the wave energy in shallow and deep water respectively, C_g and C_{g0} are the shallow and deep water wave celerity.

Applying the linear wave theory

$$C_g = nC \dots \dots \dots (1.9)$$

$$n = \frac{1}{2} \left[1 + \frac{2kd}{\sinh(2kd)} \right] \dots \dots \dots (1.10)$$

Also the ratio of the wave height H at an arbitrary depth to the deep water wave height H₀ is given by

$$\frac{H}{H_0} = \sqrt{\frac{E}{E_0}} \dots \dots \dots (1.11)$$

or

$$\frac{H}{H_0} = \sqrt{\frac{1}{2n} \frac{C_0}{C}} = K_s \dots \dots \dots (1.12)$$

where K_s is called the shoaling coefficient.

Refraction

Refraction is the processes by which an obliquely approaching wave train bends on entering shallow water and tends to align with bottom contours. The portion of the wave in the deeper water will move faster than the portion in shallow water. This

causes the wave crest to bend towards the alignment of bottom contours. Thus the slowing down and bending of waves when waves moves from deep to shallow water is called refraction and the refracted waves break in a line almost parallel to the shore. Fig. 1.3a & b shows the refraction along a straight beach with parallel bottom contours and refraction along an irregular shoreline. The refraction processes is analogous to the refraction of light which is explained by Snell's law.

$$\frac{\sin \theta}{c} = \frac{\sin \theta_0}{c_0} = \text{Constant} \dots \dots \dots (1.13)$$

where θ and θ_0 are the wave direction in shallow and deep water respectively, C and C_0 are the wave celerity in shallow and deep water respectively. A continent formula to represent both the effects of wave shoaling and refraction is

$$H = H_0 K_s K_r \dots \dots \dots (1.14)$$

$$K_s = \sqrt{\frac{C_{g0}}{C_g}} \dots \dots \dots (1.15)$$

$$K_r = \sqrt{\frac{\cos \theta_0}{\cos \theta}} \dots \dots \dots (1.16)$$

where H_0 is the deep water wave height, K_s is the shoaling coefficient, K_r is the refraction coefficient.

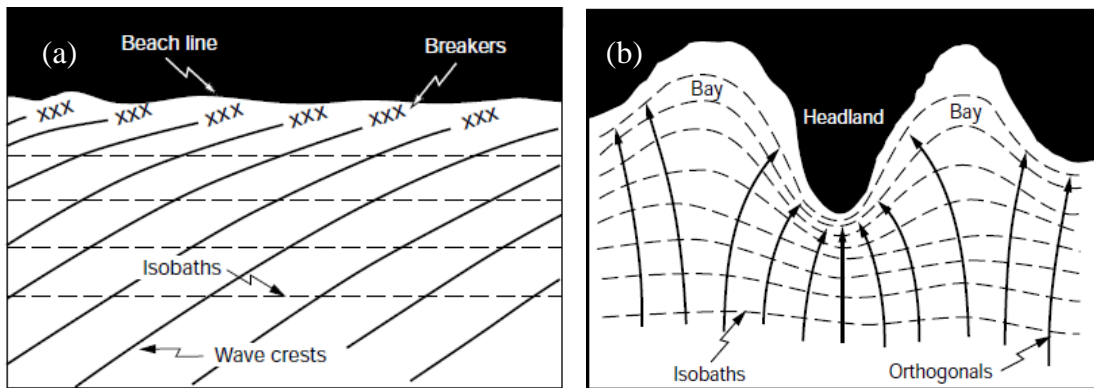


Fig. 1.3 (a) Refraction along a straight beach with parallel bottom contours, (b) Refraction along an irregular shoreline (Source: WMO, 1998)

Diffraction

Diffraction is the processes by which wave energy is transferred laterally along a wave crest. This occurs in response to rapid changes in underwater topography, around a headland, island or a breakwater (BW) (Fig. 1.4a & b). The crest wise

changes in wave height lead to change in wave direction, causing the waves to turn into the shadow zone.

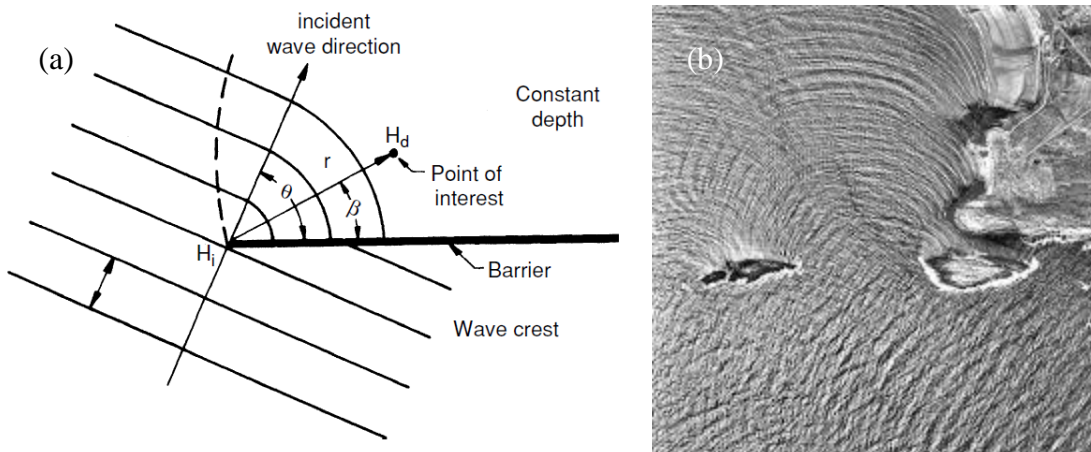


Fig.1.4 (a) Definition sketch for wave diffraction, (b) diffraction around an island (Source: Sorensen, 2006)

Reflection

Total or partial reflection occurs when waves propagate into a solid object such as breakwaters, seawall, cliff, steep beaches etc. The fraction of wave energy reflected will be large in the case of vertical hard structures. The reflection will be comparatively less for permeable structures or gentle slopes. The degree of wave reflection is defined by the reflection coefficient K_R and is given by

$$K_R = \frac{H_R}{H_I} \dots\dots\dots(1.17)$$

where H_R and H_I are the reflected and incident wave heights respectively (CEM, 2002).

Wave breaking

When the waves propagate into shallow water, the steepness increases due to increase in wave height and decrease in wave length. The wave crest becomes narrower, peaked and the waves become unstable and break. In other words as the water depth decreases the crest particle velocity increases and the wave celerity decreases leading to instability and breaking. The wave breaking process is extremely non-linear and the breaking equation for any water depth is given by

$$\frac{H}{L} = \frac{1}{7} \tanh\left(\frac{2\pi d}{L}\right) \dots\dots\dots(1.18)$$

where H is the wave height. For deep water, the limiting steepness equation reduces to

$$\frac{H_0}{L_0} = \frac{1}{7} = 0.142 \dots \dots \dots (1.19)$$

This occurs when the crest angle is equal to 120° indicating that the maximum wave height in deep water is limited to 1/7th of the wave length. In shallow water the wave heights are limited by water depth and is given by

$$\frac{H}{L} = \frac{1}{7} \left(\frac{2\pi d}{L} \right) \dots \dots \dots (1.20)$$

or

$$\frac{H}{d} = 0.9 \dots \dots \dots (1.21)$$

From the modified Solitary wave theory, Munk (1949) derived several relationships relating breaker height H_b , breaker depth d_b , un-refracted deep water wave height H_0 , and deep water wave length L_0 and is given by

$$\frac{H_b}{H_0} = \frac{1}{3.3 \left(\frac{H_0}{L_0} \right)^{1/3}} \dots \dots \dots (1.22)$$

and

$$\frac{d_b}{H_b} = 1.28 \dots \dots \dots (1.23)$$

or

$$\gamma = \frac{H_b}{d_b} = 0.78 \dots \dots \dots (1.24)$$

where γ is the breaker index which is the ratio of breaker height to breaker depth and is non-dimensional.

Breaker types have been classified into spilling, plunging, collapsing and surging (Fig. 1.5) depending on the steepness and beach slope (CEM, 2002). In spilling breaker, the wave crest becomes unstable and cascades down the shoreward face of the wave producing a foamy water surface. This occurs for waves of high steepness over gently sloping nearshore zones. Plunging breakers occurs for waves of medium steepness in moderately sloped nearshore zones, where the crest of the wave curls over the shoreward face and falls into the base of the wave, resulting in high splash. In surging breakers, the crest remains unbroken and the front face of the wave advances up the beach with minor breaking. This type of breakers occurs in a very steep shoreface and relatively low wave steepness. Collapsing breakers are intermediate

between plunging and surging. Here the crest remains unbroken while the lower part of the shoreward face steepens and then falls, producing irregular and turbulent water surface.

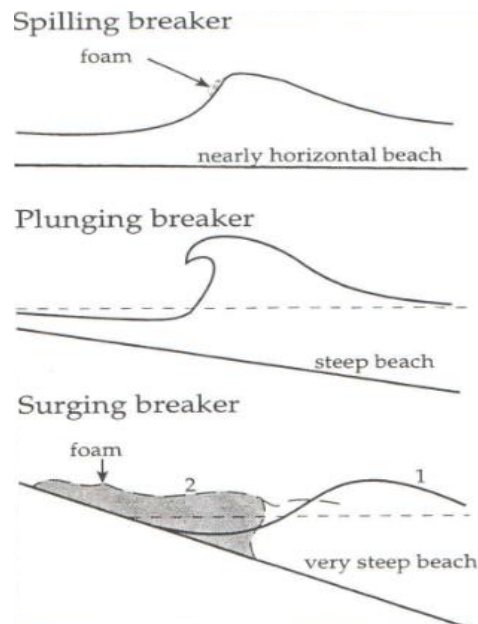


Fig. 1.5 Classification of wave breaking on the beach

Dissipation due to bottom friction

In accounting for shoaling and refraction it is assumed that there is no loss of energy at the bottom and the energy is conserved between the wave orthogonals. Energy dissipation with a reduction in wave height can occur due to bottom friction on the seabed. In bottom friction an unsteady oscillatory boundary layer develops near the bottom as the water particle motion in a wave interact with the still bottom. The bottom dissipation is more pronounced for long period high waves propagating over shallow waters of gentle bottom slope.

Dissipation due to percolation

Percolation is another form of wave energy dissipation. The wave induced fluctuating pressure distribution on the bottom will cause water to percolate in and out of the bottom, if the bottom is permeable to a sufficient depth. Thus the wave energy is dissipated.

1.3.1.2 Radiation stress

Radiation stress is the depth integrated and wave averaged excess momentum fluxes due to the presence of waves (Longuet-Higgins and Stewart, 1964). As the wave

travel across the ocean surface they also transfer momentum in the direction of travel. The momentum can be considered as a net flux of mass between wave trough and crest associated with the wave propagation. In the non-breaking zone of ocean, this net flux is related to the wave amplitude in a non-linear function. In the surf zone, this flux is substantially larger than outside consisting of two parts, non-breaking and roller. A change in the momentum flux causes wave forces to act on the fluid affecting the mean water motion and levels. Radiation stresses are responsible for setup, setdown and longshore current in the nearshore.

The radiation stress for a wave propagating in the x-direction (S_{xx}) is given by

$$S_{xx} = \frac{\rho g H^2}{8} \left(\frac{1}{2} + \frac{2kd}{\sinh 2kd} \right) = \bar{E} \left(2n - \frac{1}{2} \right) \dots \dots \dots (1.25)$$

where ρ is the density of the fluid, g is the acceleration due to gravity, H is the wave height, k is the wave number, d is the water depth, \bar{E} is the average wave energy and the subscript xx denotes the x-directed momentum flux across a plane defined by $x = \text{constant}$.

The flow of y-momentum i.e. momentum parallel to the wave crests across a plane defined by $y = \text{constant}$ is given by

$$S_{yy} = \frac{\rho g H^2}{8} \left(\frac{kd}{\sinh kd} \right) = \bar{E} \left(n - \frac{1}{2} \right) \dots \dots \dots (1.26)$$

S_{xx} and S_{yy} are the normal radiation stress component and transverse component of the radiation stress respectively. Also the shear radiation stress components S_{xy} (the flow of x-momentum across the plane $y = \text{constant}$) and S_{yx} are both zero.

In deep water the normal radiation stress components becomes

$$S_{xx} = \frac{\bar{E}}{2}, S_{yy} = 0 \dots \dots \dots (1.27)$$

In shallow water the equation becomes

$$S_{xx} = \frac{3\bar{E}}{2}; S_{yy} = \frac{\bar{E}}{2} \dots \dots \dots (1.28)$$

If a wave is propagating at an angle to the specified x direction, the normal, transverse and shear radiation stress components become

$$S_{xx} = \bar{E} \left[n(\cos^2 \theta + 1) - \frac{1}{2} \right] \dots \dots \dots (1.29)$$

$$S_{yy} = \bar{E} \left[n(\sin^2\theta + 1) - \frac{1}{2} \right] \dots\dots\dots(1.30)$$

$$S_{xy} = \frac{\bar{E}}{2} n \sin^2\theta = \bar{E} n \sin\theta \cos\theta \dots\dots\dots(1.31)$$

where θ is the angle between the direction of wave propagation and the specified x direction.

1.3.1.3 Wave spectrum

A wave record may be decomposed by means of harmonic or Fourier analysis into a large number of sinusoidal waves of different frequencies, directions, amplitudes and phases. Each frequency and direction describes a wave component, and each component has an associated amplitude and phase. A 3-dimensional sea surface is spectrally represented by frequency-directional spectrum $E(f,\theta)$. This represents the variance distributed in the frequency f and direction θ and can be multiplied by ρg to obtain the wave energy (Komen et al., 1994). The advantage of this representation is that it tells us in what direction the wave energy is moving. The directional spectrum describing the angular distribution of wave energy at respective frequencies is given by

$$E(f, \theta) = E(f) D(f, \theta) \dots\dots\dots(1.32)$$

where the function $D(f,\theta)$ is a dimensionless quantity which is known as the directional distribution or the directional spreading function. $E(f)$ is the 1-dimensional frequency spectrum and is obtained by integrating the associated directional spectra over θ and can be determined from a time series measurement in a single point.

$$E(f) = \int_0^{2\pi} E(f, \theta) d\theta \dots\dots\dots(1.33)$$

Thus a wave spectrum tells us what frequencies have the significant energy content. Fig. 1.6a & b shows the Variance density spectrum and two-dimensional frequency-direction spectrum respectively.

The spectrum of the sea surface does not follow any specific mathematical form and under certain wind conditions the spectrum has a specific shape. A series of empirical expressions can be used to fit the spectrum of the sea surface elevation and are called as parametric spectra viz. Pierson-Moskowitz (PM) spectrum, JONSWAP spectrum etc. The PM spectrum is a single parameter spectrum (Pierson and Moskowitz, 1964).

This spectrum is used as a model for a fully developed sea, an idealized equilibrium state reached when duration and fetch are unlimited.

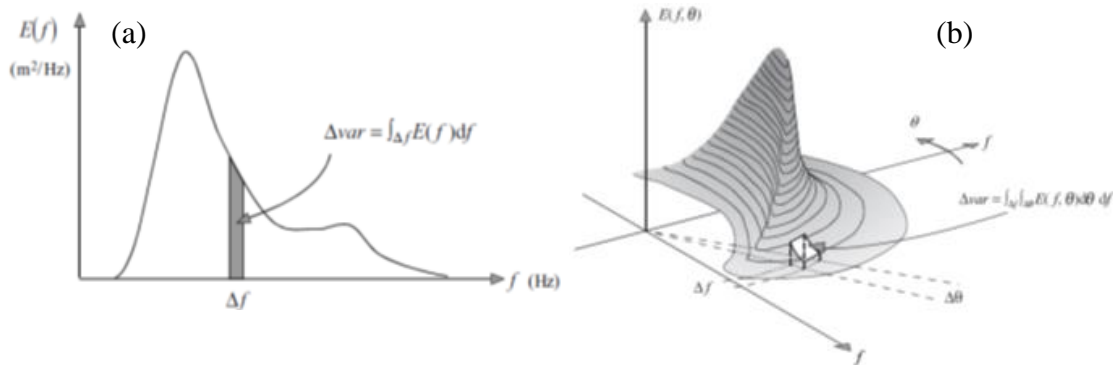


Fig. 1.6 (a) Variance density spectrum, (b) Two-dimensional frequency-direction spectrum (Source: Holthuijsen, 2007)

Hasselmann et al. (1974) made observations during the Joint North Sea Wave Project (JONSWAP), gave description of wave spectra growing in fetch-limited conditions, i.e. where wave growth under a steady offshore wind was limited by the distance from the shore. This spectrum is often used to describe waves in a growing phase. The basic form of the spectrum is in terms of the peak frequency (f_p) rather than the wind speed. Typical Pierson-Moskowitz and JONSWAP spectrum is shown in Fig. 1.7.

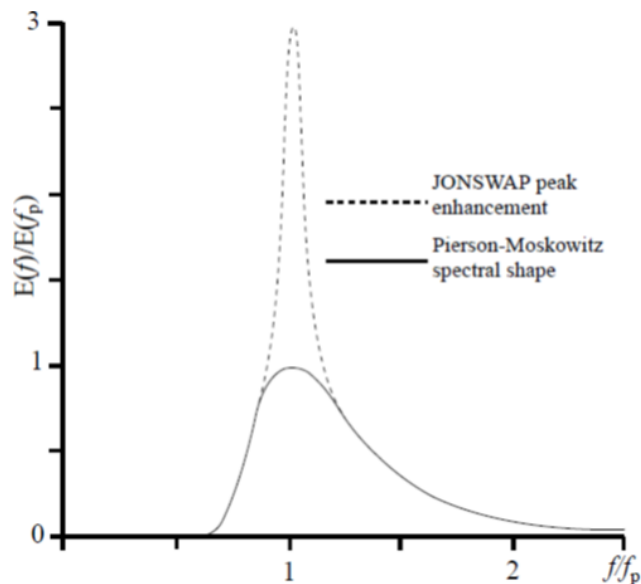


Fig. 1.7 Typical Pierson-Moskowitz and JONSWAP spectrum (Source: WMO, 1998)

1.3.2 Currents

Ocean currents are the movement of water in response to prevailing wind patterns and density variations in the ocean. Currents in the coastal waters are equally important

like waves as far as the coastal processes and sediment transport are concerned. Currents in the coastal zone can be part of the general circulation, local wind driven or tide driven. Wave driven currents confined to the nearshore zone are generally not included under the coastal currents. Currents being translatory in nature unlike waves, transport sediments both as bed load and suspended load in the alongshore and cross-shore directions.

1.3.2.1 Wind-induced current

The wind stress blowing over the ocean causes transfer of momentum from the wind to the ocean, giving rise to gravity surface waves and surface currents. The wind stress (τ), the frictional force per unit area, acting on the sea surface is given by the expression

$$\tau = \rho_a C_d U_{10}^2 \dots \dots \dots (1.34)$$

where U_{10} is the wind speed at 10 m above mean sea level, ρ_a is the density of air (1.22 kg/m^3) and C_d is the drag coefficient (typically 1.2×10^{-3}). The wind stress depends on the wind speed, roughness of the sea surface and prevailing atmospheric conditions. The effect of the wind stress at the ocean surface is transmitted downwards as a result of internal friction caused by the turbulent flow of the water.

When wind blows across the ocean surface, the upper most layer of the water begins to move and this is deflected by the Coriolis effect. The speed of the current induced by the wind decreases exponentially with the depth and the direction of the surface current makes an angle of 45° with the wind direction, to the right (left) in the northern hemisphere (southern hemisphere). This deviation angle increases with depth and the simultaneous decrease of the speed and increase of the deviation angle with depth forms to the Ekman spiral (Fig. 1.8). The mean motion and the transport in the Ekman layer (Ekman transport) take place at a right angle with the wind direction, to the right (left) in the northern hemisphere (southern hemisphere). Strong currents are produced when wind drives surface water into gulfs, through narrow straits or in and out of estuary entrances. The effect of wind is very much important in the sediment transport process, since wind-induced current velocity increases with the wind velocity and becomes much larger than the wave-induced current velocity.

1.3.2.2 Wave-induced current

The wave-induced current system which is also referred as nearshore current (Horikawa, 1988) include longshore currents, shoreward directed currents (mass transport) and rip currents. This system of circulation that recirculates water in the nearshore is also termed as cell circulation (Komar, 1976).

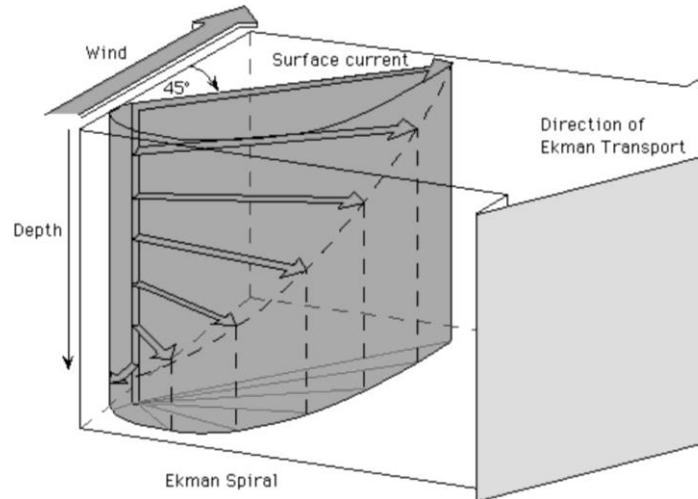


Fig. 1.8 Ekman spiral and Ekman transport direction
(Source: Trujillo and Thurman, 2010)

Longshore current

Longshore currents are generated due to waves breaking at an angle to the shoreline. The mechanism primarily responsible for generation of longshore currents is the alongshore component of radiation stress due to oblique wave breaking. The speed of the longshore current increases with increasing wave height and increasing angle between the wave crest and the shoreline. The shape of coastline, beach face slope, nearshore profile, and presence of sand bars significantly influence the distribution of longshore currents.

Galvin (1963) estimated the mean longshore current velocity over the surf zone by

$$v = K_D g m T \sin(2 \alpha_b) \dots \dots \dots (1.35)$$

where K_D is a dimensionless coefficient depending solely on the geometry of the breaking wave which is taken as 1 (Galvin, 1987), g is acceleration of gravity, m is the foreshore slope, T is the wave period, and α_b is the breaker angle (angle between the breaking wave crest and the shoreline).

Longshore currents can be explained by utilizing the radiation stress concept (Longuet-Higgins, 1970), where the alongshore component of radiation stress is equated with the bottom frictional resistance developed by the longshore current. A modified form of the Longuet-Higgins equation for longshore current velocity, based on calibration with field data, is given by the SPM (1984) and is given as

$$v = 20.7 m \sqrt{gH_b} \sin(2 \alpha_b) \dots \dots \dots (1.36)$$

where v is the average longshore current velocity across the surf zone, m is the bottom slope in the surf zone, H_b is the wave breaker height, and α_b is the wave breaker angle (Fig. 1.9). Then maximum current velocity is typically in the surf zone just inside of the breaker line. If there is a sustained alongshore wind, the wind stress acting on the surf zone can accordingly modify the wave-induced current.

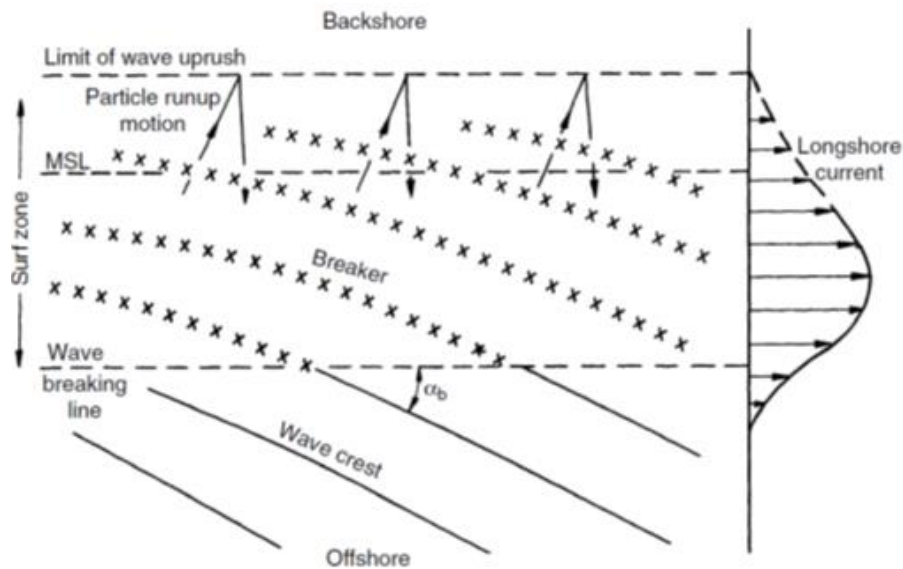


Fig. 1.9 Wave-induced longshore current (Source: Sorensen, 2006)

Rip current

Rip currents are narrow and intense offshore directed currents in the nearshore zone, which flows perpendicular to the shoreline. These currents are caused by water moving down slope (away from beach) as a result of wave setup and are fed by a system of longshore currents. Rip currents can arise with a regular spacing along the beach and are not a permanent phenomenon. The rip channel may be generated under a combination of favorable hydrodynamic conditions and may migrate along the open beach. A rip current is able to transport large volume of water and sediments towards offshore which induces morphological exchange between surf zone and the offshore.

From the Fig. 1.10a, it can be seen that the converging feeder currents are the base of the rip current followed by a narrow rip neck where the current is stronger and finally the rip head, where the flow diverges and dissipates. The slow mass transport, the feeding longshore current and the rip current together form a cell circulation system in the nearshore zone (Fig. 1.10b).

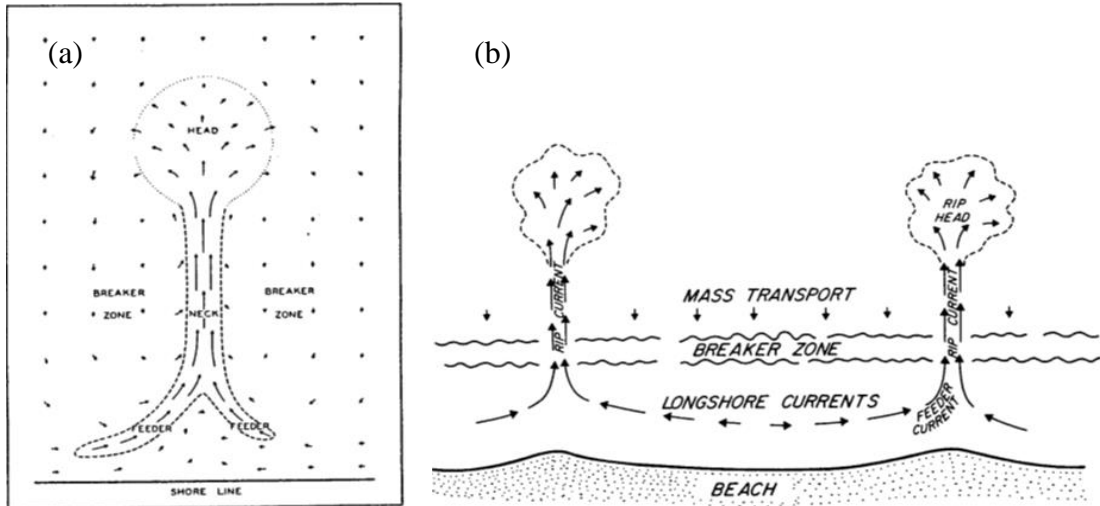


Fig. 1.10 (a) Rip current and associated current vectors (Source: Shepard et al., 1941), (b) Nearshore circulation system including rip currents (Source: Komar, 1976)

1.3.2.3 Tidal currents

Tides are the periodic motion of the ocean waters due to changes in the gravitational forces of the Moon and the Sun on the rotating Earth. The influence of tides on the coast depends on the tidal range, which determines the zone over which wave action can operate. According to the vertical tidal range the coast may be micro-tidal, meso-tidal, macro-tidal or mega-tidal. The beaches on micro-tidal coast are mostly wave dominated.

Tidal current is the periodic horizontal flow of water accompanying the rise and fall of the tide. Tidal currents may be semidiurnal, diurnal, or mixed type corresponding to the type of tide at the place. These currents in the coast are uni-directional and are primarily directed alongshore. In an enclosed water body, the tide generating force pushes water mass towards upstream during flood cycle and drains out during the ebb cycle. Currents associated with these cycles are known as flood and ebb currents. In the open ocean, tidal currents usually perform a rotary motion due to the coriolis force over a tidal period, with constantly changing magnitude and direction. In the northern hemisphere the direction of current is clock wise and completes one rotation along an

elliptical path in 12 hrs 24 min for semi-diurnal tide and 24 hrs 40 min for diurnal tide.

Tidal currents do not cause beach erosion or accretion, but they carry sediment along the coast in the nearshore zone. In the areas with large tidal ranges, the tidal current may be strong enough to transport sediment and they can operate in depths where wave orbital motion is quite weak. In the case of micro-tidal coast the tidal currents are generally significant only in the vicinity of tidal inlets and estuaries.

1.3.3 Beach Erosion / Accretion

Beach erosion is part of a cyclic process during which beach material is carried away by wave action, tidal currents, littoral currents or other similar processes, the counterpart being 'beach accretion'. A beach is said to be eroding when loss of sediment exceeds the material supplied into the system. Normally, there is an annual/seasonal balance between erosion and accretion, resulting in a net zero loss of beach. But in some cases when one of these processes dominates net erosion or accretion occurs. Significant net erosion of beach may lead to subsequent erosion of the coast, which then becomes alarming.

Causes for erosion can be both natural and man-induced. Natural causes of erosion are those which occur as a result of the response of the beach to the forces of nature. Man-induced erosion occurs due to the impact of human interventions on the natural system. The natural processes causing erosion includes storm waves, currents, tides, wind, etc. The man-made factors include construction of coastal structures viz. groins, breakwater (BW), jetties, seawall etc., construction of dams, interruption of littoral drift due to man-made entrances, beach sand mining, dredging of inlet, channel entrances and offshore dumping of the dredged materials.

Accretion is the processes of accumulation of sand or other beach material due to the natural action of waves, tides, wind and longshore currents and by the construction of shore protection structures like groins and breakwaters. Long-period waves such as swells plays a significant role in the seasonal beach building processes by transporting the eroded material from the offshore to the shore.

1.3.3.1 Coastal structures contributing to erosion/accretion

Beach-innershelf morphological changes are induced along the coastal sector by the construction of coastal structures. The coastal structures are classified into shore

protection structures and structures constructed for the development of port and harbor facilities. Shore protection structures include seawalls, groins etc. and the latter category includes jetties, breakwaters etc. The effect of coastal structures will be mainly on the sediment transport regime and the effect may even extend down drift for a few kilometers.

Seawalls

Seawalls are hard structures constructed parallel to the shoreline in order to protect the land adjoining the shoreline from intense wave action. The height of the seawall is designed to be such that no water overtops the structure. The main disadvantage of this structure is the toe erosion which induces steeper bottom profiles. Thus larger waves have a direct impact on the structure which causes structural instability.

Groins

Groins are constructed perpendicular to the shoreline extending towards offshore and are usually straight and narrow structures. Groins are intended to reduce shoreline erosion by controlling the rate of alongshore / littoral drift of beach material. The erosion is retarded by depositing the sediments in the up-drift side which however is accompanied by erosion in the down-drift side of the groins (Fig. 1.11a). The functional design of the groins is the determination of length, spacing, height, alignment and type of groin which reduces the beach erosion to an acceptable degree. Usually a series of groins of different length is used for the shore protection measures (Fig. 1.11b).

Breakwater

Breakwaters are constructed towards offshore in order to dissipate the incoming wave energy. This provides calm environment when it is used for the port/harbor development. The effect of the shore connected breakwater is same as that of groins, which creates accretion in up-drift side and erosion in the down-drift side. Breakwaters are of different types viz. fixed, detached, submerged and floating breakwaters. The choice of selecting the appropriate breakwaters depends upon the normal water depth, coastal hydrodynamics and sediment transport of the selected coastal sector.

Jetties

Jetties are shore connected structures constructed perpendicular to the shore and extending towards offshore. They are classified into solid structures and piled or open type jetties. Jetties can act similarly as breakwater with similar erosion/accretion pattern.

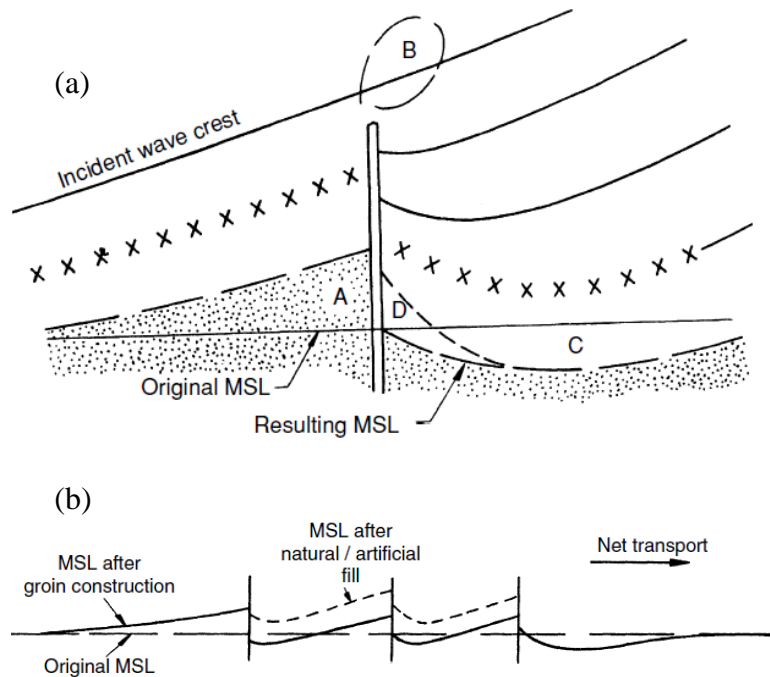


Fig. 1.11 (a) Shore response to perpendicular structure, (b) series of shore perpendicular structures (Source: Sorensen, 2006)

1.3.3.2 Other anthropogenic factors contributing to erosion

Any anthropogenic activity that takes away sediments or cuts off sediment supply to the beach can trigger beach erosion. Examples are damming of rivers, beach/river sand mining, dredging and offshore dumping of the dredged materials. Beach sand mining, either to extract rare minerals which are of commercial value or for construction purposes which is illegal, causes erosion. Due to mining the sand is lost directly from the system which leads to a deficit sand budget. Removal of beach sediments has the opposite effect of beach nourishment.

1.4 Sediment Dynamics

The dynamics of the beach and nearshore sediments is driven by the wave transformation and consequent breaking waves combined with horizontal and vertical patterns of currents associated with nearshore circulation cell. The sediment dynamics

in the nearshore zone involves both longshore and cross-shore components depending on the direction of transport. The measurement and computation / estimation of the surf zone sediment transports are very much complicated. The transport at any point is a vector with both cross-shore and longshore components of varying magnitudes (CEM, 2002). Even though both the transports are interrelated to each other, it is considered separately for the sake of simplicity. The longshore transport is generated by wave-induced longshore currents whereas cross-shore transport is associated with the orbital motion of the wave and innershelf currents. The components of the sediment transport are shown in Fig. 1.12.

The threshold flow velocity for the initiation of sediment motion by oscillatory flow over a level bed of sediment is given by

$$U_{\max} = \sqrt{8 \left(\frac{\rho_s}{\rho} - 1 \right) g d_{50}} \dots \dots \dots (1.37)$$

where U_{\max} is the peak sediment velocity at the bed, ρ_s is the density of sediment, ρ is the density of fluid, g is the acceleration due to gravity and d_{50} is the median sediment size (SPM, 1984). The maximum near-bottom velocity for non-breaking waves according to small amplitude wave theory (Thornton and Krapohl, 1974; Grace, 1976) is given by

$$U_{\max} = \frac{\pi H}{T \sinh\left(\frac{2\pi d}{L}\right)} \dots \dots \dots (1.38)$$

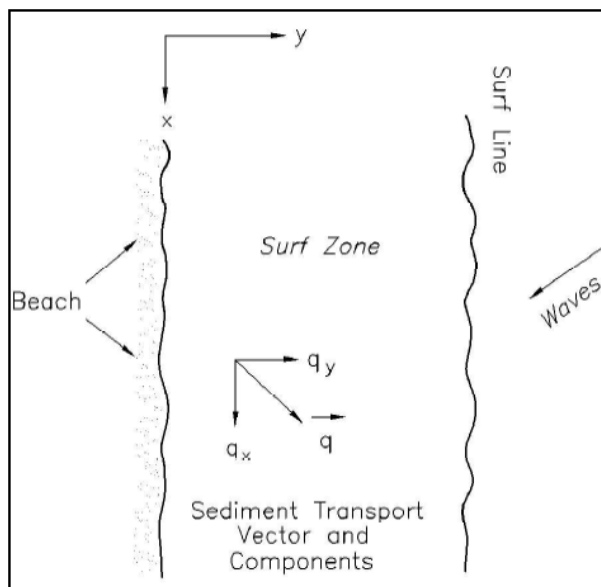


Fig. 1.12 Longshore (q_x) and cross-shore (q_y) sediment transport components (Source: CEM, 2002)

1.4.1 Modes of sediment transport

The sediment transport modes in coastal waters are classified into two viz. bed load and suspended load transport. Sediments are transported in the form of bed load and suspended load when the bed shear stress exceeds a critical value. For bed load transport, the basic modes of particle motion are sliding, rolling and saltation (Fig. 1.13). Under high energy conditions, a third mode of transport namely sheet flow is also identified.

1.4.1.1 Bed load transport

In bed load transport, the grains are very close to the sea bed and moves by sliding, rolling and saltation. The bed load transport occurs when the sea bed is more or less flat without any sand ripples and less suspension of sediments. Here the sediment particles move along the bed surface, frequently by impacting each other. During sliding, the particles remain in continuous contact with the bed and as they move, to and fro tilting take place. Rolling grains are in continuous contact with the bed as they move. Saltation refers to the transport of sediment particles in a series of irregular jumps and bounces along the bed. The sliding and rolling are prevalent during the slower flows, while saltation during faster flows.

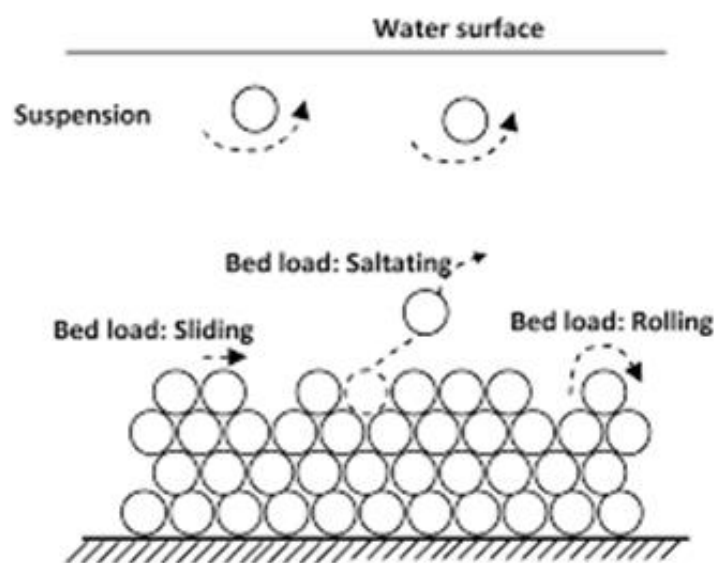


Fig. 1.13 Modes of sediment transport showing sliding, rolling and saltation
(Source: URL: <http://serc.carleton.edu/48147>)

Meyer-Peter and Mueller (1948) introduced a reliable empirical bed load transport formula based on flume experiment with uniform particles and particle mixtures. Based on data analysis, a relatively simple formula was obtained.

$$q_b = 8\sqrt{(\theta' - \theta_c)} \dots \dots \dots (1.39)$$

$$\theta' = \frac{\tau_b'/\rho}{\left(\frac{\rho_s}{\rho} - 1\right)g d} \dots \dots \dots (1.40)$$

where θ' is the effective Shields parameter, τ_b' is the effective shear stress and θ_c is the critical Shields parameter.

Bed load is expressed as the intensity of solid discharge, and this can be written in non-dimensional form (Yalin, 1977) as

$$q_b = \frac{\Phi_b}{\sqrt{\left(\frac{\rho_s}{\rho} - 1\right)gD^3}} \dots \dots \dots (1.41)$$

where Φ_b is the bed load solid discharge per unit width in m^2/s and D is the particle diameter.

1.4.1.2 Suspended load transport

In the suspended mode of transport, the sediments are carried above the bed by the turbulent eddies of water. Fine materials such as silt and clay having low settling velocities are lifted to a higher level, whereas for the coarser material such as sand, the height is restricted, which is closer to the sea bed. In this mode of transport, the particles follow long and irregular paths within the water until they are deposited when the flow weakens. The suspension occurs mainly due to the influence of wave motion on the bed and it is transported due to the effect of current. In other words the wave stirs up the sediments and current transports the sediments. When the value of the bed-shear velocity exceeds the particle fall velocity, the particles can be lifted to a level at which the upward turbulent forces will be comparable to or higher than the submerged particle weight. This results in random particle trajectories due to turbulent velocity fluctuations. The particle velocity in longitudinal direction is almost equal to the fluid velocity (van Rijn, 2012). The behavior of the suspended sediment particles is described in terms of the sediment concentration, which is the solid volume (m^3) per unit fluid volume (m^3) or the solid mass (kg) per unit fluid volume (m^3). Definition sketch of suspended sediment transport is shown in Fig. 1.14. The

suspended sediment concentrations decrease with distance up from the bed and the rate of decrease depends on the ratio of the fall velocity and the bed-shear velocity.

The suspended sediment transport can be calculated as

$$q_s = \int_0^h U(z) C(z) dz \dots \dots \dots (1.42)$$

where $U(z)$ is the flow velocity, $C(z)$ is the suspended sediment concentration (SSC) and z is the vertical co-ordinate. On applying Bijker's recommendation the suspended sediment transport can be written as

$$q_s = 1.83 q_b \left(I_1 \ln \left(\frac{h}{0.033 k_s} \right) + I_2 \right) \dots \dots \dots (1.43)$$

where q_b is the bed load transport, k_s is the bed roughness, h is the height from the bottom and I_1 and I_2 are Einstein integrals.

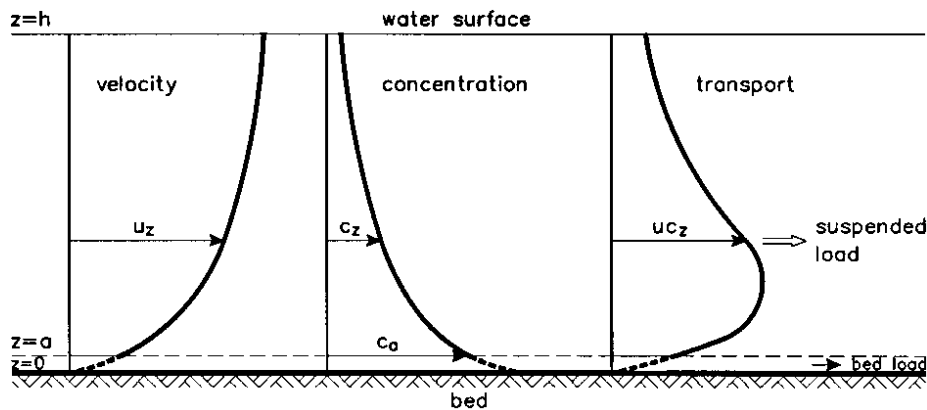


Fig. 1.14 Definition sketch of suspended sediment transport (Source: van Rijn, 2012)

1.4.1.3 Sheet flow

In the sheet flow, the sand moves in a very thin layer near the sea bed whereas in the bed load transport only the surface grains are under motion. The motion is intense enough so that the bottom boundary layer is fully turbulent. The sheet flow condition prevails only during high energy conditions and has a large effect on the overall sediment transport in a region.

1.4.2 Longshore sediment transport

The longshore transport is one of the important nearshore processes that control beach morphology including erosion, accretion and stable nature of the beach. A reliable computation/estimation of this transport is essential for solving various coastal engineering problems. When wave breaks obliquely to the coasts, longshore currents

are generated which in turn result in the movement of the sediment along the coast, referred to as longshore sediment transport or littoral transport (Fig. 1.15). The actual volume of sediment involved in the transport is termed as littoral drift. The longshore transport comprises of both bed load and suspended load transport modes. It is difficult to measure both these modes separately. The longshore transport consists of both positive transport for one or more seasons and negative transport for the remaining months in a year. This transport can be quantitatively expressed as net transport, which is the sum of both positive and negative components in a year. The gross transport is the sum of the magnitudes of the transport during the entire period.

The rate of the longshore sediment transport can be expressed as volume transport rate (Q_l) or immersed weight transport rate (I_l) and their relation is given by

$$Q_l = \frac{I_l}{(\rho_s - \rho) g (1 - P)} \dots \dots \dots (1.44)$$

where P is the sediment porosity (typically 0.4). Also the longshore transport rate can be calculated based on the energy flux method and is given as

$$Q_l = \frac{K}{(\rho_s - \rho) g (1 - P)} P_L \dots \dots \dots (1.45)$$

or

$$Q_l = K \left(\frac{\rho \sqrt{g}}{16 \sqrt{k} (\rho_s - \rho) (1 - P)} \right) H_b^{\frac{5}{2}} \sin(2\alpha_b) \dots \dots \dots (1.46)$$

where P_L is the longshore component of wave energy flux or power, K is the calibration parameter (typically 0.39, when using significant wave height), α_b is the breaker wave angle relative to shoreline and H_b is the breaker wave height.

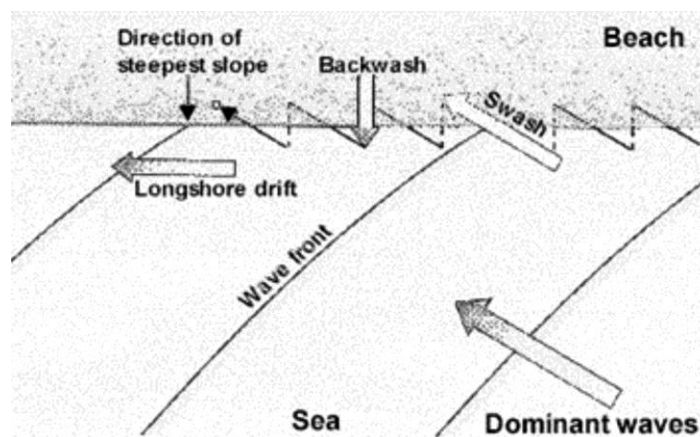


Fig. 1.15 Longshore sediment transport
(Source: http://www.southwestcoastalgroup.org/cc_how_intro.html)

The net longshore sediment transport rate or time averaged transport is calculated since the longshore sediment transport is a fluctuating quantity (CEM, 2002) and is given by

$$Q_{l\text{Net}} = \bar{Q}_l = \frac{1}{T_0} \int_0^{T_0} Q_l(t) dt \dots \dots \dots (1.47)$$

The gross longshore transport rate is given by

$$Q_{l\text{Gross}} = \frac{1}{T_0} \int_0^{T_0} |Q_l(t)| dt \dots \dots \dots (1.48)$$

where T_0 is the length of record (often taken to be greater than one year). The net transport rate is either positive or negative but the gross transport is always defined positive (Fig. 1.16).

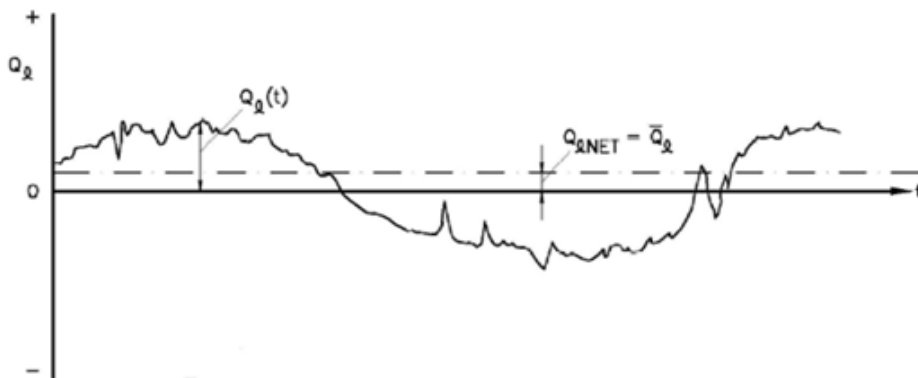


Fig. 1.16 Net and gross longshore transport (Source: CEM, 2002)

1.4.3 Cross-shore sediment transport

Cross-shore transport is a result of water motion due to the waves. The transport encompasses both onshore and offshore transport and is a result of the water motions due to waves and undertow (Fig. 1.17). The onshore transport occurs during periods of swell waves and offshore transport dominates during storm conditions. The transport is contributed by both bed load and suspended load transport and hence the complete understanding of cross-shore transport is complicated. The transport is predominantly due to sediment in suspension within the surf zone. The physical processes responsible for cross-shore transport in the surf zone are incident waves, infra-gravity waves, rip currents, and near-bed seaward return flows (Mei and Liu, 1977; Roelvink and Stive, 1989). The incident wave causes shoreward transport whereas the interactions of incident waves with infra-gravity waves and with mean

offshore flows causes offshore transport (Guza and Thornton, 1985; Huntley and Hanes, 1987).

The local time averaged sediment transport rate can be described using the basic equation given by

$$Q_c = \frac{1}{t} \int_0^{h+\eta} \int_0^t C(z, t) u(z, t) dt dz \dots \dots \dots (1.49)$$

where Q_c is the cross-shore sediment transport rate, t is the time over which average is defined, $(h+\eta)$ is the surface level elevation relative to bed level, $C(z)$ is the suspended sediment concentration (SSC), u is the cross-shore component of the flow velocity and z is the vertical co-ordinate.

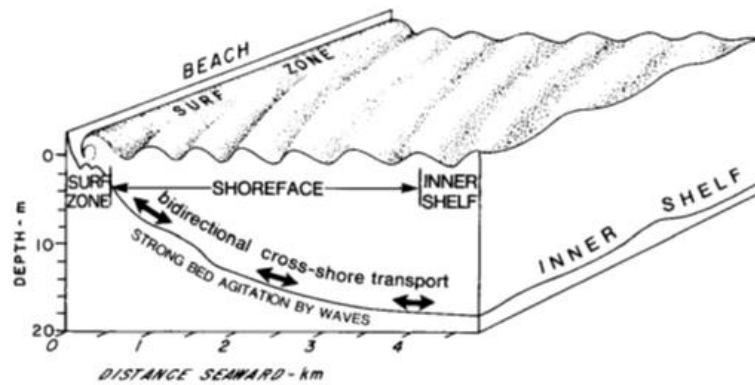


Fig. 1.17 Cross-shore transport in the nearshore (Source: Wright et al., 1991)

1.5 Sediment Budget

The sediment transport pattern/process of a coast is dependent on the hydrodynamic forces viz. waves, currents, tides and wind which vary both temporally and spatially. The changes in beach and innershelf morphology are in turn influenced by the sediment transport process. Sediment budgeting involves making assessment of the sedimentary contributions (credits) and losses (debits) (Hume et al., 1999), and equating these to the net gain or loss (sediment balance) in a given beach compartment or littoral cell. Budgeting technique can be applied to understand the sediment sources, sinks, transport pathways and magnitudes for a selected region and within a defined period of time.

According to (Rosati, 2005), the sediment budget is a balance of volumes (or volume rate of change) for sediments entering (source) and leaving (sink) a selected region of the coast, and the resulting erosion or accretion in the coastal area under consideration. The equation as expressed by Rosati is

$$\sum Q_{\text{Source}} - \sum Q_{\text{Sink}} - \Delta V + P - R = \text{residual} \dots \dots \dots (1.50)$$

where Q_{source} and Q_{sink} are the sources and sinks respectively to the control volume, ΔV is the net volume change within the cell, P and R are the amounts of material placed in and removed from the cell respectively, residual represents the degree to which the cell is balanced (residual = 0, for a balanced cell). Fig. 1.18a gives the schematic representation of the sediment budgeting parameters and Fig. 1.18b gives sediment transport pathways in a coastal cell.

Table 1.1 shows the ledger of sediment budget. The major sources in the sediment budget includes the longshore sediment transport into the cell, sediment transport from rivers, accretion of the beach, placement of the beach fill and dredged material etc. The sinks include the longshore sediment transport out of the cell, erosion of the beach, dredging and mining of the beach/nearshore and losses to a submarine canyon. Quantifying these sources and sinks being rather difficult, it is imperative that detailed collection of site specific hydrodynamic and sedimentological data and also numerical model studies are undertaken to assess the different sources and sinks while carrying out beach sediment budgeting studies. Thus sediment budget can be used for two purposes; first to analyse the present situation, and second, using the present conditions, to predict the coastal changes either due to any construction or due to natural conditions.

Table 1.1 Ledger of sediment budget (Source: Hume et al., 1999)

Credit	Debit
<ul style="list-style-type: none"> • Longshore transport into the area • Onshore transport • River/estuary input • Wind transport onto the beach • Beach nourishment • Sea cliff erosion • In-situ shell production • Dune/ridge erosion 	<ul style="list-style-type: none"> • Longshore transport out of the area • Offshore transport • Estuary infilling • Wind transport away from the beach • Sand extraction • Deposition in canyons • Solution and abrasion • Dune/ridge formation

1.6 Beach States

Beach is defined as the zone of unconsolidated material that extends landward from the low water line to the place where there is a marked change in material or

physiographic form, or the line of permanent vegetation (SPM, 1984). The equilibrium beach profile and beach state classification are described in the following sections.

1.6.1 Equilibrium beach profile

The dynamic balance of the constructive and destructive forces acting on the beach is represented by the equilibrium beach profile and imbalance will arise if there is any change in the acting forces. Gravity is the most important destructive force, since it tries to make the equilibrium profile horizontal. High turbulence level in the surf zone acts as an additional destructive force. The constructive force is due to the onshore shear stress at the bottom that results from non-linear form of shallow water wave (Dean and Dalrymple, 2001). Schematic of the equilibrium profile is shown in Fig. 1.19a & b.

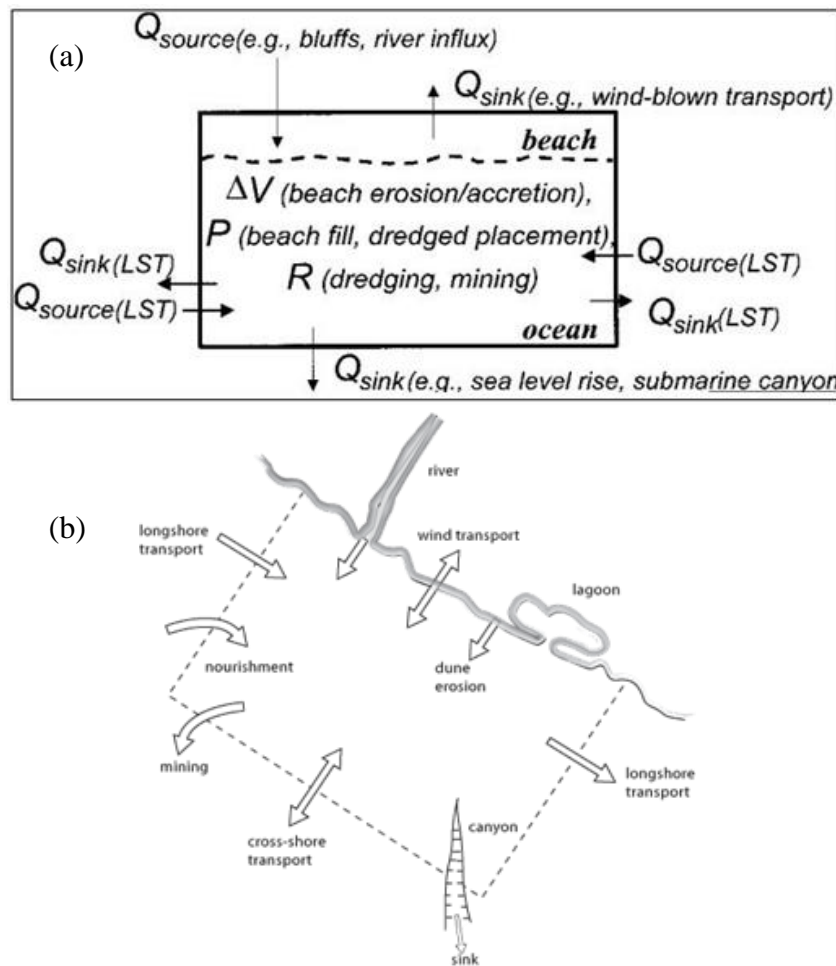


Fig.1.18 (a) Parameters used in the sediment budget estimation (Source: Rosati, 2005), (b) Sediment transport pathways in a coastal cell (Source: http://www.conscienceeu.net/what_is_coastal_erosion_and_when_is_it_a_problem/index.htm)

A sediment of given size will be stable in the presence of a particular level of wave energy dissipation per unit volume (D_{eq}) and can be expressed in terms of wave energy conservation as (Dean, 1977)

$$D_{eq} = \left(\frac{1}{d}\right) \frac{d}{dy} (EC_g) \dots \dots \dots (1.51)$$

where E is the wave energy, C_g is the group velocity of the wave, d is the water depth and y is the offshore distance from the shoreline. Again D_{eq} is assumed to be a function of sediment size or equivalent sediment fall velocity, then the above equation can be re-written in terms of simple power rule (Brunn, 1954) as

$$h(y) = A_s y^{2/3} \dots \dots \dots (1.52)$$

where y is the offshore distance from shoreline, h is the depth at the offshore distance (y) and A_s is the shape parameter of the profile which depends on the stability characteristics of the bed material and is given as

$$A_s = \left(\frac{24}{5} \frac{D_{eq}}{\rho g^{3/2} \gamma^2}\right)^{2/3} \dots \dots \dots (1.53)$$

where D_{eq} is the wave energy dissipation rate, ρ is the density of sea water, g is the gravitational acceleration and γ is the ratio of wave height to water depth at breaking. Another approximation by Moore (1982) ignores the disturbance effect of wave energy and defines the shape parameter in terms of fall velocity and can be written as

$$A_s = 0.067 (w_s)^{0.44} \dots \dots \dots (1.54)$$

where w_s is the fall velocity of the sediment.

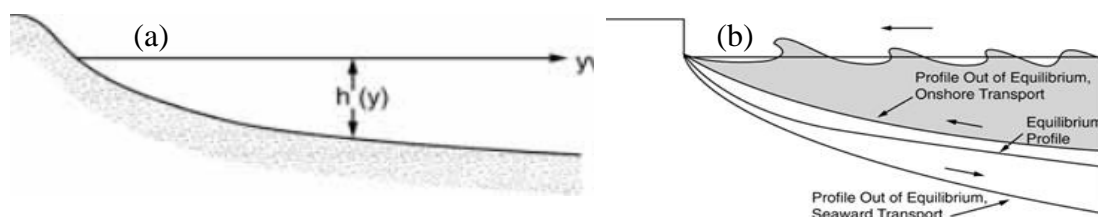


Fig. 1.19 (a) Schematic of an equilibrium profile (Source: Dean and Dalrymple, 2001), (b) Profiles out of equilibrium

1.6.2 Beach classification

According to Short (2006), the beaches are classified into wave dominated, tide dominated and tide modified (depending on the tidal range) beaches. Depending on the incident wave height, wave period and sediment characteristics, wave dominated

beaches can be classified into reflective, intermediate and dissipative beaches. The beach state at a particular location can be found by using the dimensionless fall velocity parameter Ω (Dean, 1973), which is defined as

$$\Omega = \frac{H_b}{w_s T_p} \dots \dots \dots (1.55)$$

where H_b is the breaker wave height, w_s is the sediment fall velocity and T_p is the peak wave period.

Each beach state can be classified based on the parameter Ω and if $\Omega < 1$, then the beach state is reflective; intermediate if $1 < \Omega < 6$ and dissipative state if $\Omega > 6$. All the beach state is characterized by peculiar morphodynamic features in terms of both cross-shore profile and plan-form features (Short, 1999; Benedet et al., 2004). The classification of beach states is shown in Fig. 1.20a, and nomogram showing the contribution of wave height, sediment size, wave period and beach type is shown in Fig. 1.20b.

1.6.2.1 Reflective beach

The reflective beaches ($\Omega < 1$) are characterized by low wave heights (< 0.5 m), longer wave periods and medium to coarse grained sediment. The beach face is relatively steep ($5 - 20^\circ$) with constant wave reflection. i.e. the waves break by surging at the beach base with a strong backwash which is typical of reflective beach. Low sediment transport mostly as bed load and no bar formation and or surf zone present in this beach state.

1.6.2.2 Intermediate beach

The intermediate beaches ($1 < \Omega < 6$) are characterized by medium wave heights (0.5 - 2.5 m), moderate period, and composed of fine to medium grained sand. The beaches are normally seen along open coast having plunging to spilling breakers and surf zone upto 100 m width, with one or two bars which are normally intercepted by strong nearshore circulation with rip-current. The beach comprises of rhythmic shoreline features (beach cusps), high degree of shoreline mobility and moderate rates of backshore transitioning. Intermediate beaches are subdivided into four distinct types viz. longshore bar-trough, rhythmic bar and beach (crescentic bars), transverse bar and beach, ridge and runnel (or low tide terrace) (Benedet et al., 2004).

1.6.2.3 Dissipative beach

The dissipative beaches ($\Omega > 6$) are characterized by high waves (> 2.5 m) and beaches composed of fine grained sediments with a low gradient swash of approximately 1° , where the reflectivity of the waves is very low. A wide surf zone of 300 - 500 m having at least two bars, flat topography of the berm-beach face, and multiple spilling breakers are present in the case of dissipative beach. The waves normally break at the outer bar first and subsequently on the inner bar thereby efficiently dissipating their energy as they move across the surf zone.

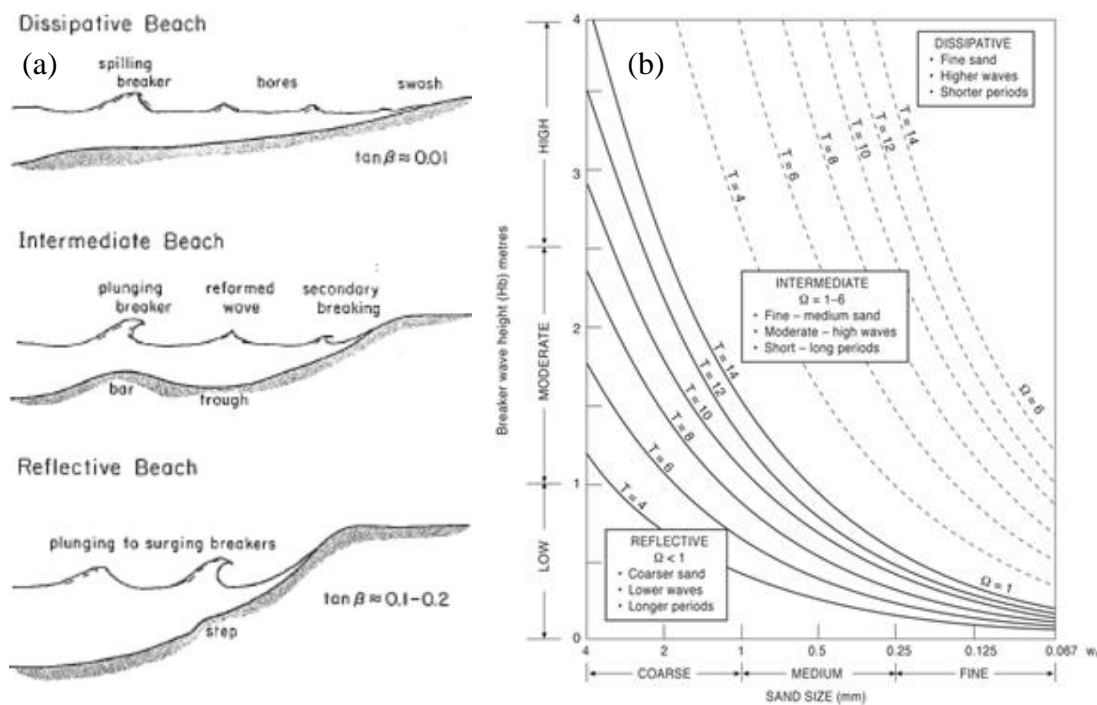


Fig. 1.20 (a) Classification of beach types, (b) Nomogram showing the contribution of wave height, sediment size, wave period and beach type (Source: Short, 1999)

1.7 Beach Placers

A placer may be defined as a deposit of residual or detrital mineral grains in which a valuable mineral has been concentrated by natural processes. The beach placers are the fruitful part of the beach and are called as black sand deposits too wherever they are black in colour due to abundance of ilmenites. The beach placers are the significant sources of heavy minerals such as ilmenite, magnetite, chromite, monazite, rutile, zircon, garnet etc. These concentrations of minerals can be commercially exploited through beach sand mining.

1.7.1 Formation of placers

The primary processes involved in the formation of placers are weathering of rocks bearing heavy minerals in the hinterland regions of the coast, their transportation to the coast by rivers and streams and finally their concentration by physical processes of grain sorting. The processes responsible for the formation of beach placers are the selective sorting by the waves and currents, which concentrates the valuable minerals according to their densities, sizes and shapes. Higher concentrations of the heavy minerals are formed under moderate to high energy environment. The influence of latitudinal and seasonal effect on the beach placer is also to be taken into account while studying their formation. Other factors that have contributed in the formation of placer deposits are the coastal geomorphology, neo-tectonics and continental shelf morphology.

1.7.2 Sorting processes

The processes of sorting depend on the densities, sizes and shapes of the sediment grains and thus provide the opportunity for sorting particles according to differences in their respective properties. Komar (1989) delves into the process of formation of beach placers and comes out with four different types of sorting processes viz. settling equivalence, selective entrainment, transport sorting and shear sorting (Fig. 1.21a-d).

1.7.2.1 Settling equivalence

Settling equivalence was the earliest proposed process of sorting which is based on the equivalence of the settling velocities of the sediments in the fluid medium. According to this concept, the denser and smaller particles would have the same settling rates as the larger but lower density particles (Komar, 1989). In other words the sediment of higher density will be finer and vice-versa. The settling equivalence is quantified based on the Stokes law based on the settling velocity given as

$$w_s = \frac{1}{18} \frac{1}{\mu} (\rho_s - \rho) g D^2 \dots\dots\dots(1.56)$$

where w_s is the settling velocity, μ is the viscosity of the fluid and D is the grain diameter. For two spherical grains of different diameters and densities, equivalence of their settling velocities is given by

$$\frac{D_1}{D_2} = \sqrt{\frac{(\rho_{s2} - \rho)}{(\rho_{s1} - \rho)}} \dots\dots\dots(1.57)$$

where sub-scripts 1 and 2 refers to the individual minerals.

1.7.2.2 Selective entrainment

The process of selective grain entrainment by current happens when the deposits consists of particles of mixed densities and sizes. In general, the heavy minerals are finer in size, while the lighter minerals are coarser. The larger grains are more exposed to the physical factors in comparison with the smaller grains. Thus the current entrains the lighter grain and transport the same leaving behind the heavy grains due to their higher density and lower exposure to the flow. Based on the laboratory flume experiments, the two dimensionless parameters involved in this processes are Shield entrainment function and Reynolds number given by

$$\theta_t = \frac{\tau_t}{(\rho_s - \rho)gD} \dots\dots\dots(1.58)$$

$$Re = \frac{\rho U_t D}{\mu} \dots\dots\dots(1.59)$$

where θ_t is the Shields entrainment function, τ_t is the threshold mean bed stress exerted by the current, Re is the grain Reynolds number and U_t is the shear velocity (Komar, 1989).

1.7.2.3 Transport sorting

The grain sorting during transport (i.e. transport sorting) is the most complex sorting process, where the grains are carried along by a flowing fluid at a differential rate. The transport sorting involves both bed load and suspension transport that depends on different grain properties and other sorting processes such as settling and selective entrainment. The transport sorting occurs in wave field and combined wave-current field in the cross-shore direction due to the asymmetry in wave profile and wave orbital velocity in shallow waters. Both heavier and lighter grains are transported due to the larger shoreward velocity under the crest. But the lighter grains are only transported back by the low offshore velocity under the trough leading to the net transport of heavy grains towards the shore (Komar, 1989).

1.7.2.4 Shear sorting

The alternate layers of light and heavy sands are formed in the vertical section of the beach due to the shear sorting processes. The dispersive pressure depends on the diameter and density of individual grain, on the total concentration and the rate of

shear. When grains of mixed sizes are sheared, the coarser grains tend to move upward to the zones of lower shear, while the finer grains move downwards towards the bed where the shear is minimum. This results in the formation of a layer with reverse grading by size. The heavy sands are found at the base of the layer due to their smaller size when compared with the lighter grains. This is the process of shear sorting.

The grain-dispersive equivalence is based on the Bagnold's analysis of grain-dispersive pressures. According to this analysis, at any single horizon within a sheared concentration, particles of equal dispersive pressure will reside together and the balance is given by

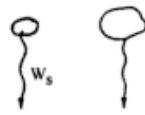
$$\frac{D_1}{D_2} = \sqrt{\frac{\rho_{s2}}{\rho_{s1}}} \dots\dots\dots(1.60)$$

where the sub-scripts 1 and 2 denotes the mineral pairs, D is the grain size and ρ is the density of the mineral. An inverse relationship between grain size and density is seen such that a heavy mineral particle will be smaller than an associated light mineral. It is also possible that by repeatedly shearing the sand as the beach face is cut back, the heavy particles would be driven progressively downward and concentrated. The larger size and less dense grains rise to the surface of the shear zone and is transported away (Komar, 1989).

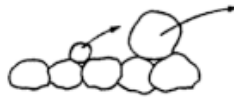
1.8 Background of the Study

The Neendakara–Kayamkulam coastal sector of length 22 km located in the southwest coast of India is world famous for its rich placer (black sand) deposits. This coastal stretch popularly known as the Chavara coast is subjected to rampant beach sand mining because of its heavy mineral resources. Since 1930, the Indian Rare Earths Ltd. (IREL) and its predecessor companies have been engaged in beach sand mining along the Chavara coast for the extraction of heavy minerals. In view of the erosion observed along the coast and the possible role that beach sand mining might be playing as alleged by the local population, CESS was requested by the IREL in 1999 to take up a study to address the various issues, and more importantly to come out with recommendations on sustainable mining volumes. Intensive hydrodynamic, sedimentological and sediment budgeting studies were carried out by CESS in consultation with ASR Ltd. during the period of 1999-2001 and sustainable mining

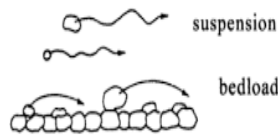
volumes were recommended for the coast (Rajith, 2006; Black et al., 2008; Hameed et al., 2007; Prakash et al., 2007).



(a) Settling Equivalence



(b) Entrainment Equivalence (Selective Entrainment)



(c) Transport Equivalence (Transport Sorting)



(d) Dispersive - Pressure Equivalence (Shear Sorting)

Fig. 1.21 Schematic illustration of sorting processes (Source: Komar, 1989)

However the scenario changed considerably since 2000. The Kerala Minerals and Metals Ltd. (KMML), another Public Sector Undertaking (PSU) situated at Chavara entered the scene with large scale mining of beach sand along the coast. Two breakwaters have been constructed at Kayamkulam inlet during the period 2000–2007, to facilitate the Kayamkulam fishery harbour, which can significantly affect the sediment transport regime of the coast. The heavy mineral concentration in the beach sediments of this coast which was reported to have had values upto 100 % in 1995 (Kurian et al., 2001) and 80 % in 2000 (Kurian et al., 2002) depleted drastically as was evident from the estimates of IREL (2010). This in turn affected the commercial viability of beach sand extraction by the IREL and KMML. There were also reports of intensification of erosion along the coast and kinking of shoreline at mining sites (Rajith et al., 2008) which certainly can be considered as a shoreline stability issue needing immediate attention.

Thus the reported depletion of heavy mineral content in the beach sediments and the drastic beach morphological changes offered an interesting topic which has remarkable societal implications for research under this Ph.D. programme. The present investigation is undertaken in this background to understand the mechanisms that manifest these drastic changes. The investigation taken up in 2010 was partly sponsored by the IREL.

1.9 Aim and Objectives

The investigation has been taken up with the following aim and objectives:

- Study the sediment dynamics and beach processes of the Neendakara-Kayamkulam coast through field observations and numerical modelling techniques
- Estimate the short- and long-term morphological changes in the beach and innershelf using multi-date data
- Estimate the short- and long-term changes in the heavy mineral content of the beach and innershelf sediments
- Decipher the beach-innershelf morphological changes and heavy mineral depletion with reference to the hydrodynamics and other forcing factors

1.10 Study Area

The study area is a 22 km costal stretch located along the southwest coast of India, extending from the Neendakara inlet in the south to the Kayamkulam inlet in the north. This coastal sector which is situated in the Kollam district of the southern state of Kerala in India is popularly known as the Chavara coast (Fig. 1.22). It is a barrier beach bound by the Lakshadweep Sea in the west and the Travancore - Shoranur Canal (T-S Canal) in the east. This is a micro-tidal coast with a climatic regime dominated by southwest monsoon and has a moderate wave energy level (Baba and Kurian, 1988; Kurian, 1989). Waves are the principal hydrodynamic force driving the coastal processes of this coast. Hameed et al. (2007) have reported a maximum significant wave height of 3.8 m in the nearshore waters of this coast. The wave climate is dominated by swells from as far away as the southern Indian Ocean during the non-monsoon period and the seas from northwest Arabian Sea during the monsoon (Hameed et al., 2007). They have also reported predominance of southerly

flows in the innershelf. The wave-induced longshore currents are predominantly northerly (Black et al., 2008)

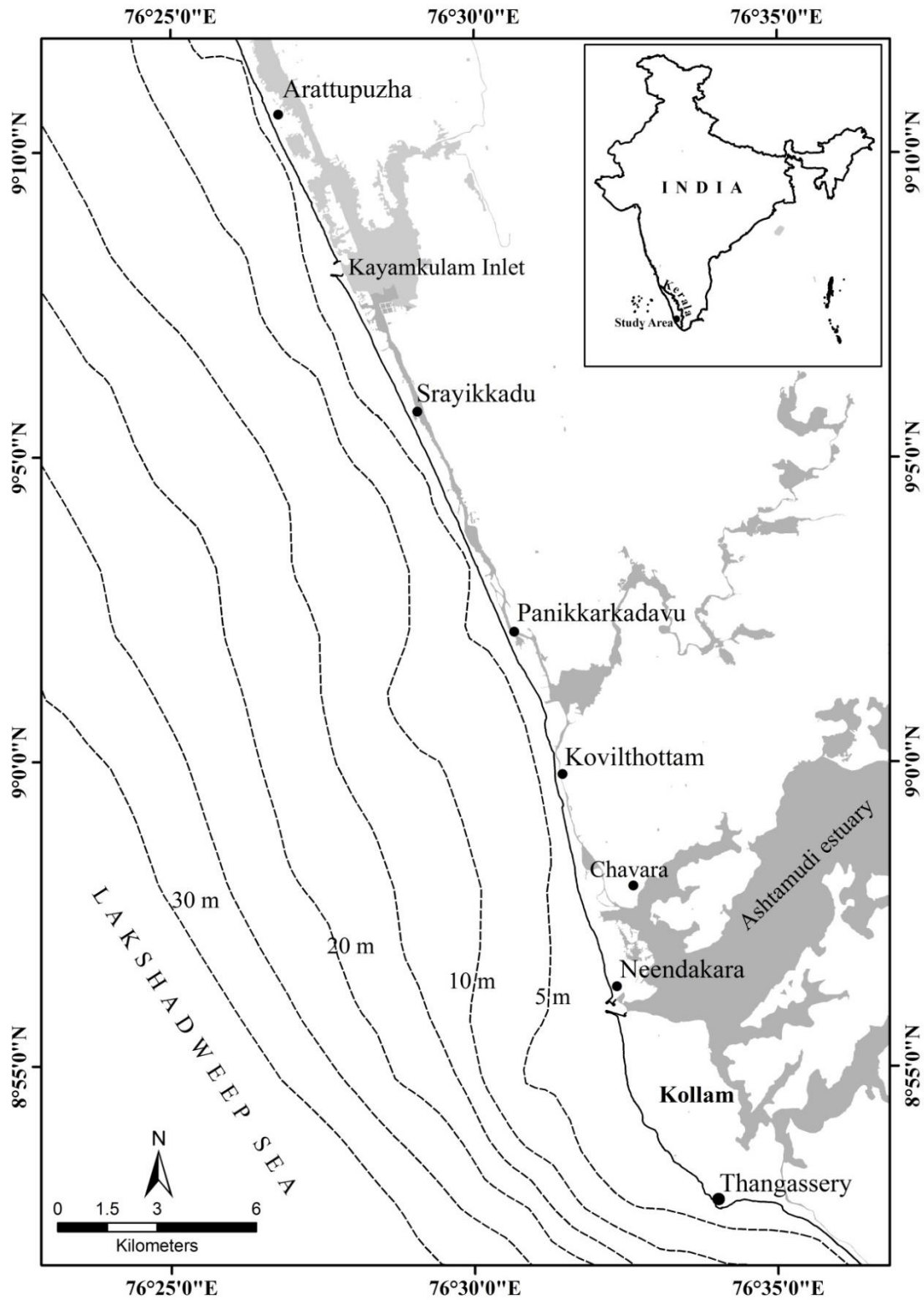


Fig. 1.22 Study area extending from the Neendakara inlet in the south to the Kayamkulam inlet in the north, SW coast of India

The Chavara coast in general has an orientation in the SSE-NNW direction. The coast exhibits significant variation in the orientation along the southern and northern parts with noticeable dents at the mining sites of Vellanathuruthu–Ponmana and Kovilthottam due to caving in of the shoreline (Fig. 1.23). The southern part of the coastal stretch from the Neendakara inlet to the Vellanathuruthu mining site is oriented 345° N while the northern sector is 334° N. Further south of the Neendakara inlet, at the Thangassery headland, there is a sharp change in the shoreline orientation from 350° to 290° N with steeper bathymetry towards south (Baba and Kurian, 1988). The continental shelf of Chavara coast is of moderate slope with the 20, 50 and 100 m isobaths at approximate distances of 7, 26 and 54 km respectively from the shoreline.

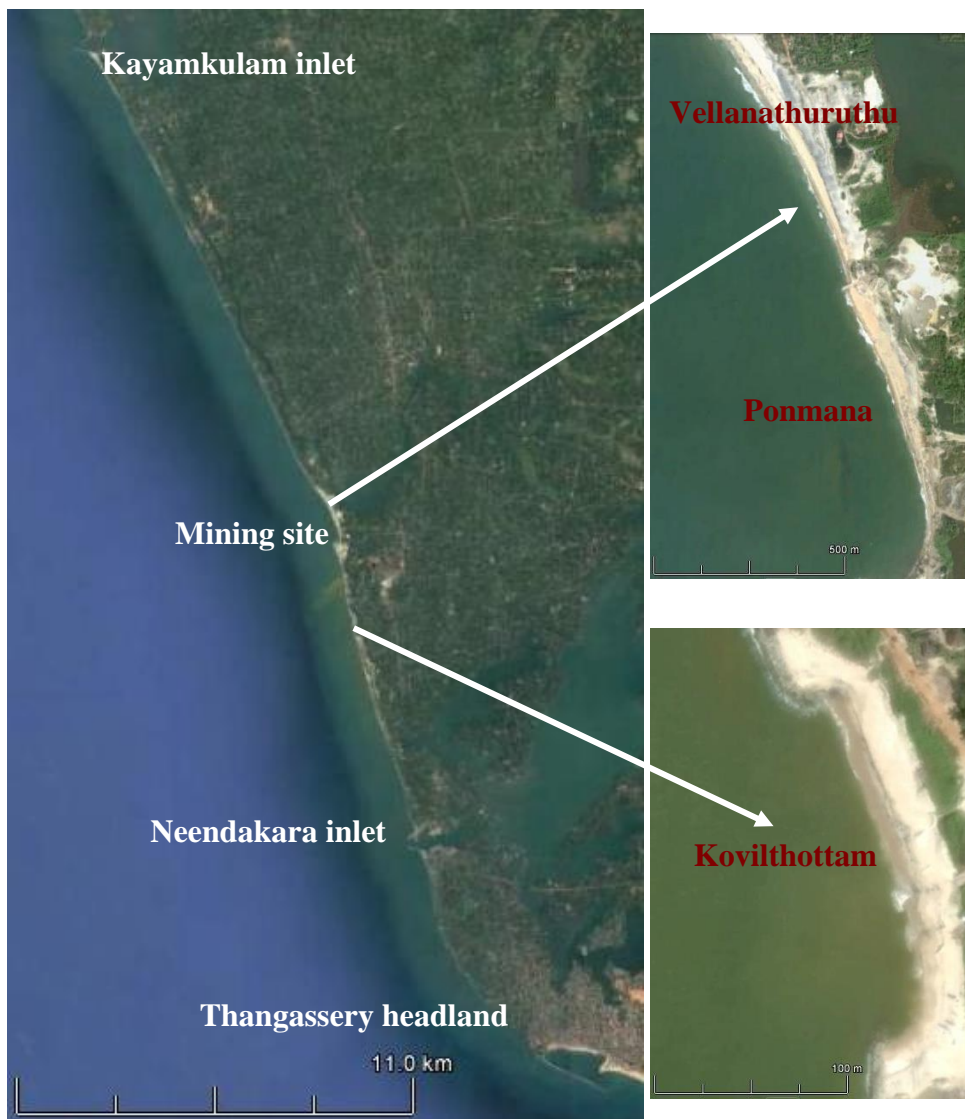


Fig. 1.23 Google image of the study area showing the mining sites

The bathymetry profile is characterized by a steep shore-face gradient of about 0.01 at 5 m depth and a much lower gradient of 0.003 in the innershelf at about 20 m depth. The Kallada River which debouches into the sea through the Ashtamudi estuary at the Neendakara inlet is the major riverine system along this coast. Till a couple of decades back, the Kallada River used to discharge a substantial quantity of sediment into the Ashtamudi estuary (Prakash and Prithvi Raj, 1988), but over the years the quantity has reduced drastically due to excessive river sand mining, reclamation at various locations and also construction of dams across the river (Black and Baba, 2001).

The whole coastline is protected by seawalls (rock) except for the sand extraction sites of IREL and KMML and the ‘fishing gaps’ left to facilitate landing/launching of country crafts of fishermen. The beach morphology of the Chavara coastal stretch has become very complicated in recent years due to a multitude of factors of which anthropogenic activities like the beach and river sand mining, construction of hard rubble mounted structures like breakwaters, groins and seawalls play a major role. Breakwaters are present at both the inlets to facilitate the fishing harbours. The Neendakara inlet which forms the southern boundary of the coastal stretch has two breakwaters of 610 m (southern) and 380 m (northern) constructed during the period 1963–1967 as part of port construction. Similarly, at the northern boundary (i.e. at Kayamkulam inlet) there are two breakwaters of lengths 720 m (southern) and 485 m (northern) constructed during 2000–2007 to facilitate the Kayamkulam fishery harbour. Thus the breakwaters at both the inlets extend beyond the depth of active sediment transport except during extreme conditions like storm. Hence it can be anticipated that the sediment transport within the coastal stretch bounded between the two inlets at Neendakara and Kayamkulam is more or less self-contained as it forms a well-defined sediment cell (SC) according to the SC concept proposed by van Rijn (1997a). In addition to these breakwaters, there are 26 groins of varying dimensions constructed during the last 5 years to address various issues of which shore protection is the most important.

1.11 Structure of the Thesis

The thesis embodies the results of the investigation carried out for realizing the objectives of the study. The thesis comprises of seven Chapters.

The first Chapter presents an introduction to the topic of research, background of the study, description of the study area and objectives of the study.

A comprehensive review of literature relevant to the field of research viz. coastal hydrodynamics, nearshore sediment transport, heavy mineral content and beach-innershelf morphological changes, both in the global and Indian scenario, is presented in the second Chapter. The identified gaps relevant to the Indian scenario are also presented.

The data collection and the methodology adopted for the study are presented in the third Chapter. The field data collection involved measurement of nearshore waves, wind, monthly beach profiles, monthly shoreline, and collection of seasonal beach and innershelf surficial sediment and innershelf core sediment samples. The numerical models / empirical formulae used for the study are discussed in this chapter. The methodology followed for the geo-spatial analysis of beach profiles and shoreline change and laboratory analysis of the sediment samples are also detailed in this chapter.

The fourth Chapter encompasses the results of studies on the nearshore sediment transport regime. The longshore and cross-shore sediment transport rates estimated by adopting the bulk formulae of CERC and Kamphuis, and processes based numerical model LITPACK are presented. The computed results are discussed with reference to the beach volume change data from field observations.

In Chapter 5, the results of studies on the reported heavy mineral depletion of the beach and innershelf of the Chavara coast are presented. Comparison of field data on heavy minerals from the present study with the past data confirmed the depletion in the heavy mineral concentration in the beach and innershelf of this coast. The factors responsible for the depletion in heavy mineral content are brought out by integrating the information on coastal processes, sediment budget and anthropogenic factors including beach sand mining.

The short- and long-term morphological changes in the beach and innershelf are presented in the sixth Chapter. The analysis of the multi-dated data for the past several decades showed an overall retreat of the shoreline and a relative deepening of the innershelf. Numerical modelling of the shoreline evolution using the LITLINE module of the LITPACK numerical modelling system corroborated the field

observations. The observed changes in the beach–innershelf morphology are analysed with respect to the nearshore sediment transport regime and the anthropogenic factors, and the causative factors for the morphological changes identified.

The Chapter 7 gives an overall summary of the present work with major findings and conclusions with the recommendations for the future work.

The references cited in the chapters are listed at the end of the thesis.

CHAPTER 2

REVIEW OF LITERATURE

2.1 Introduction

This chapter encompasses a detailed account of the review of literature carried out related to the topic of investigation viz. Sediment Dynamics, Heavy Mineral Depletion and Morphological Changes of a Placer Mining Beach of SW Coast of India. The review of literature was intended to give a status of research in the field, both in the global as well as national scenario. In addition to getting to know the emerging trend in research, the review has helped in fine tuning the methodology adopted for the work. It was also helpful in consolidating and integrating the results of the investigation and arriving at the conclusions. The review is divided into 4 themes related to the topic of work as below:

- Coastal hydrodynamics
- Nearshore sediment transport
- Beach placers
- Beach-innershelf morphological changes

The identified gaps relevant to the SW Indian coast are also presented in this Chapter.

2.2 Coastal Hydrodynamics

A review of literature pertaining to the coastal hydrodynamics and their causative factors is carried out in this section. The review comprises of observational, experimental, computational and numerical modelling studies relating to coastal hydrodynamics.

2.2.1 Global scenario

Shemdin et al. (1980) investigated the wave transformation mechanisms in finite depth waters and they examined percolation, bottom motion, shoaling and refraction along with wave-wave interaction and bottom friction. Cavaleri and Rizzoli (1981) described a wind wave forecasting model for shallow water areas. The model includes wave generation, refraction and shoaling with breaking and bottom friction. Komen et al. (1984) considered the energy transfer equation for well-developed ocean waves under the influence of wind. The conditions for the existence of an equilibrium

solution in which wind input, wave-wave interaction and dissipation balance each other was studied by them. They observed that for equilibrium spectra, the input, dissipation and non-linear transfer source functions are all significant in the energy containing range of the spectrum.

Goda (1991) developed a random wave breaking model which was applied for the computation of longshore currents. Also empirical formulation of the maximum speed and distribution of longshore currents has been made. Yang (1993) calculated the breaking wave spectra and radiation stress from a wide band breaking wave model in order to study the mean water surface in shallow water and to compute the wave set up and set down of random waves on the surf zone. van Rijn and Wijnberg (1996) developed a probabilistic model to describe the propagation and transformation of individual waves.

The role of bottom friction dissipation in predicting wind waves is assessed by Johnson and Kofoed-Hansen (2000) with a third-generation numerical wind wave model by using shallow water measured data from Vindeby, Denmark. They modeled the bottom friction dissipation source term by using the linearized bottom friction formulation which contains a dissipation coefficient that depends on wave and sediment properties. The study shows that during strong wind conditions, it is better to use the Charnock parameter (a constant) as 0.015 and variable bottom dissipation formulation was used to obtain a good agreement between measured and calculated significant wave height. Edge wave propagation on a straight beach with a perpendicular coastal structure is analyzed by Baquerizo et al. (2002). The reflection and transmission of the edge wave by the structure is considered by assuming the width of structure is much smaller than the alongshore wave length. The solution to the problem is obtained by a mode matching method including the head loss at the structure. Splinter and Slinn (2003) studied the behaviour of the time dependent low frequency along-shore currents generated by oblique wave incidence in the surf zone and is examined using a non-hydrostatic, phase-averaged, three-dimensional (3-D) numerical model. Also the model solves the Navier-Stokes equations with a Large Eddy Simulation sub-grid scale closure model on a curvilinear (σ -coordinate) grid. Simulations of alongshore currents are forced using two cross-shore distributions of momentum input. A time domain Boussinesq model for nearshore hydrodynamics is utilized to simulate surface waves and longshore currents under laboratory and field

conditions by Chen et al. (2003). The model results give insight into the spatial and temporal variability of wave-driven longshore currents.

Tai-Wen Hsu et al. (2006) developed an analytical theory for the wave setup and setdown induced by obliquely incident waves. The wave setup and setdown are found to decrease as wave obliquity increases. Moeini and Shahidi (2007) used third generation spectral models (SWAN and MIKE 21 SW) for the prediction of wave parameters. Both models were forced by temporally varying wind and the results show that the average scatter index of SWAN is about 16 % for H_s and 19 % for T_p ; while the average scatter index of MIKE 21 SW is about 20 % and 13 % for H_s and T_p , respectively. The inconsistency between the results of the models was found to be due to differences between the wind input parameterizations. Both the models were also evaluated for the prediction of wave direction and it was found that MIKE 21 SW results are slightly more accurate than those of SWAN model. Jun Tang et al. (2008) studied the propagation of irregular water waves and irregular breaking wave induced nearshore currents. This has been numerically studied based on parabolic mild slope equation and nearshore currents model. The wave radiation stresses exerted on currents have been calculated based on variables in the parabolic mild slope equation, and nearshore wave-induced currents have been numerically simulated. Different partitioning techniques and methods to identify wind-sea and swell are investigated, addressing both 1D and 2D schemes (Portilla et al., 2009). It was found that the steepness method systematically overestimates swell, while the PM method is more consistent, although it tends to underestimate swell.

Hwang et al. (2012) found that the swell–sea separation frequency should be placed between the swell and wind sea peak frequencies rather than at the wind sea peak frequency. A spectrum integration method generalised from the wave steepness method is obtained for wind-sea and swell separation of the 1D wave spectrum. Numerical modelling studies were conducted by Yang et al. (2014) for the nearshore restoration in the Skagit river estuary, Washington, USA, using a three-dimensional unstructured grid. A set of parameters were defined to quantify the hydrodynamic response of the nearshore restoration, such as inundation area, duration of inundation, water depth and salinity of the inundated area. The maximum water level near the site was estimated with consideration of extreme high tide, wind-induced storm surge, significant wave height and future sea-level rise based on numerical model results and

coastal engineering calculation. The hydrodynamic impacts of the Nador lagoon, Morocco, due to tidal waves using numerical modelling were studied by Jeyar et al. (2015). Here the two-dimensional, depth-averaged hydrodynamic model based on shallow water equations is solved with triangular mesh by the application of finite volume method. The model was calibrated and validated with observed data and water levels, tidal currents and wind effects within the lagoon were predicted by using this calibrated model.

2.2.2 Indian scenario

Dattatri et al. (1979) studied the height and period distributions for waves off Mangalore harbour by utilising measured wave data off Mangalore harbour on the west coast of India. Diwan et al. (1985) studied the wave climate of the Indian coast based on the real time data acquired from the wave gauges deployed along the selected locations. Vethamony and Sastry (1985) observed multi-peaked wave spectra at a single location during a period of 30 hr in the Bay of Bengal. Major spectral peaks were identified by them, and spectral energy has been assigned to each peak based on which significant wave height was estimated. Baba (1986) computed the wave transmission coefficient over a submerged breakwater (BW) and found that Goda's method is the simplest and most suitable. The influence of the length of record and sampling interval on the wave spectral estimate were studied by Baba et al. (1986) and it was concluded that the sampling interval has to be as short as possible to get better results. Hameed et al. (1986) computed the longshore current velocity by using Longuet-Higgins and Komar's model and found that the longshore velocity estimated by Komar's model provided values comparable to the measured.

Baba (1987) calculated the wave power potential off four locations of the south west coast of India and found that the annual average wave power ranges between 0.7 and 10.9 kW/m, with Trivandrum recording the highest and Tellicherry the lowest. Kurian and Baba (1987) and Kurian (1987) studied the spatial variations in the intensity of waves along the south-west coast of India. From their study it was established that the bottom slope controls the bottom dissipation processes which in turn decide the wave intensity along this coast. The characteristics of wave climate along the south-west coast of India have been brought out by Baba and Kurian (1988). Their study shows a maximum wave height of 6.02 m and H_s of 3.4 m at Valiathura, near Trivandrum. A decrease in the nearshore wave intensity is observed at Alleppy and at Tellicherry

further north with a maximum H_s of 2.58 m and 1.60 m respectively. Shallow water wave characteristics off Valiyathura, southwest coast of India were studied by Thomas (1988) using measured data for the period of 1980-1984. He observed that the waves were always greater than 0.5 m during the measurement period. The breaker period was 11 to 12 s during March and April and the breaker direction was 210° and 225° except during June-August, when the direction was 230 and 240° . Longshore currents were northerly except for the three monsoon months of June-August.

Harish (1988) observed that the maximum breaker height generally showed a peak during June-July as observed at Valiathura, Alleppey and Calicut. He found that the breaker period varied from 10 s during active monsoon to 15 s during the calm season. He also observed that the longshore current direction was predominantly southerly during the active monsoon season and the pattern of longshore current during fair season was different on both sides of the pier at Tellicherry. The wave climatology and littoral processes at Alleppey were studied by Hameed (1988), where the maximum wave height recorded was 3.8 m during the monsoon period. The significant wave height recorded during the monsoon and non-monsoon seasons are 3 m and 1.4 m respectively. The wave periods during monsoon are 8-9 s and 9-11 s during fair season. A model was proposed by Kurian et al. (1985) and Kurian (1989) for the prediction of shallow water wave heights. Hameed (1989) proposed a simple 2-parameter PMK spectral model which simulates the shallow water wave spectra as good as the 5-parameter TMA spectral model. The marginal distribution of individual wave height is found to follow the depth limited model by Gluhovskii. The model by Tayfun is found to simulate the joint distribution of zero-crossing wave heights and periods.

Chandramohan et al. (1991) studied the wave characteristics of the Indian coast based on the ship recorded data over 19 years (1968-1986) and the data were compared with measured waves at two locations viz. Kakinada on the east and Bombay high on the west coast. The ship borne observations are slightly higher than the measured data off Kakinada. Based on finite amplitude wave theory, a software has been developed for numerical refraction study by Chandramohan et al. (1994). They incorporated wave attenuation due to shoaling, bottom friction, bottom percolation and viscous dissipation. Sajeev et al. (1997a) conducted numerical wave refraction studies from

which the spatial and temporal variation in wave height and its distribution along the Kerala coast was obtained. Also the convergence and divergence of wave energy was found to induce non-uniform distribution of wave heights during the monsoon period.

Jose (2000) studied the convergence/divergence pattern of wave energy based on wave refraction and their interaction with the beach sediments. Srinivas and Dinesh Kumar (2002) analysed the sea level data at Cochin and Beypore ports on the southwest coast of India to understand the tidal and non-tidal variations. At both the locations they observed a large spring-neap variation and monthly variation in the semi-diurnal forcing. The amplitudes of most of the tidal constituents are slightly larger at Beypore than at Cochin. The annual cycles of non-tidal sea level at both the locations are similar. Kurian et al. (2004) has made a review of the hydrodynamic regime of the SW coast of India elucidating the salient characteristics of this monsoon dominated coast. The maximum deep water wave height of 8.95 m is recorded during the peak monsoon. The peak wave period is lower during June - August due to the proximity of the coast to the generating zones in the Arabian Sea. The SSW directions dominate the wave climate except during the intense southwest monsoon conditions when westerly waves dominate. Sanil Kumar and Anand (2004) determined the mean wave direction (MWD) by using first order Fourier coefficients and the principal wave direction by second order Fourier coefficients. Comparison is also made on wave directions at four locations in the west and east coasts of India. Study shows that at all locations, the mean and principal wave directions for frequencies ranging from 0.07 to 0.25 Hz co-vary with a correlation coefficient (CC) of 0.99 but at lower and higher frequencies, difference between the parameters is large. Also the average difference in the sea and swell directions is around 39° .

Jignesh et al. (2005) makes use of the concept of wave age in estimating ocean wave period from space borne altimeter measurements of backscattering coefficient and significant wave height. Introduction of wave age allowed better accounting of the difference between swells and sea waves. Using two years (1998 and 1999) data of TOPEX/Poseidon altimeter and ocean data buoy observations in the Indian Ocean, coefficients were generated for wave period, which were subsequently tested against data for the years 2000 and 2001. The results showed the wave period accuracy to be of the order of 0.6 s. MIKE 21 offshore spectral wave model (OSW) taking into account of wind-induced wave growth, non-linear wave-wave interaction, wave

breaking, bottom friction and wave refraction was used by Vethamony et al. (2006) for the improvement in wave prediction by using NCMRWF winds blended with MSMR winds. The wave periods clearly indicate that waves during June - September are generated by monsoon wind forcing, and dominated by 'wind waves'.

Hameed et al. (2007) studied the waves off Chavara, southwest coast of India, over a period of 2 years which showed that the waves during monsoon are characterized by higher heights, shorter periods, and are confined to westerly directions. The wave characteristics during monsoon indicate proximity of generating area to the west coast. The pre-monsoon and post-monsoon waves are characterized by lower heights and higher periods with the direction being more southerly. Waves arrive from a wider range of generating areas during the fair weather periods, particularly during the pre-monsoon months. Sanil Kumar et al. (2007) separated sea and swell from deep and shallow water locations from the measured data. The study shows that the conditions in the deep water are influenced by swell with 62 %, whereas in the shallow water, wind seas dominate for 68 % of the period. Also the mean swell direction was 168° at deep water and 187° at shallow water. The spectral characteristics of shallow water waves along the Indian coast with $H_s > 2$ m are examined by Sanil Kumar and Ashok Kumar (2008). From their study it was found that the value of JONSWAP parameters increases with H_s and mean wave period and decreases with spectral peak period.

Muraleedharan et al. (2009) used field and model wave data to study the wave period distribution and found that the zero crossing and average wave period distribution follow the Gamma distribution. They estimated the average of one-third and one-tenth highest wave periods (T_s) from Erlang distribution are in accordance with the values computed from recorded buoy and numerical coastal wave model wave period data. Aboobacker et al. (2009) calculated the spectral and statistical wave parameters obtained from the measured time series wave data off Paradip, east coast of India during May 1996 - January 1997 and were analysed along with MIKE 21 spectral wave model results. Frequency-energy spectra during extreme events are single peaked, and the maximum energy distribution is in a narrow frequency band with an average directional spreading of 20° . Spectra for other seasons are multi-peaked, and energy is distributed over a wide range of frequencies and directions.

The wave growth characteristics during the onset of summer monsoon in a swell dominated open ocean at a location off the west coast of India at 14 m water depth are studied by Sanil Kumar et al. (2010). Their study reveals that about 67 % of the measured waves are due to the swells arriving from south and south-west and the balance was due to the seas from south-west to north-west. Also the wave age of the measured data indicates that the measured waves are young sea with presence of swells. Significant wave height and other wave conditions were studied by Suresh et al. (2010) for a location of 20 m water depth off east coast of India during monsoon and they separated the wind-sea and swell components from the measured data. It was observed that the sea-state is dominated by swells arriving from south-east to south. Also the wave age shows the presence of young sea with significant occurrence of swell. Wave energy distribution along Gangavaram, east coast of India has been carried out by Prasad et al. (2010) using a wave refraction model, which computes refraction coefficient, shoaling coefficient, breaker heights and breaker energies. Higher wave energy pattern is observed in the region to the south of the port during all seasons. Complex wave conditions exist due to rocky headlands and promontories towards north of the port and as a result wave breaking transpires at deeper depths. They also concluded that the wave energy is amplified along the coast during storm conditions.

Wave data collected off Goa along the west coast of India has been subjected to spectral analysis, and swell and wind sea parameters have been estimated by separation frequency method by Aboobacker et al. (2011). According to them, swells dominate Goa coastal region not only during southwest monsoon (93 %), but also during the post-monsoon (67 %) season. Also, the numerical simulations carried out by them reproduced the swell characteristics in the Indian Ocean, and from the model results potential swell generation areas were identified. Sanil Kumar et al. (2011) measured the waves at 15 m water depth in the northern Arabian Sea during the summer monsoon for a period of 45 days and their results shows that the significant wave height varied from 1.1 to 4.5 m with an average value of 2.5 m. About 75 % of the wave height at the measurement location is due to the swells arriving from the south-west and the remaining is due to the seas from south-west to north-west. Wave age of the measured data indicates that the waves in the nearshore waters of northern Arabian Sea during the summer monsoon are swells with young sea.

Sajiv Philip et al. (2012) examined the interannual and seasonal variations in nearshore surface wave parameters over a period of three years using measured wave data at 9 m water depth off Honnavar, west coast of India. They observed H_s upto 4.3 m during the summer monsoon with an average value of 1.7 m. Predominant wave spectral energy density was within 0.05–0.25 Hz and directional spreading was narrow for high waves. Sanil Kumar et al. (2012) studied the wind wave spectra at three shallow water locations (Malpe, Honnavar and Karwar) along the 200 km stretch of the state of Karnataka using measured data from wave rider buoys.

Seasonal and annual variations in wave data controlled by the local wind system such as sea breeze and land breeze, and long period waves were studied by Glejin et al. (2013a) using wave data collected off Ratnagiri, west coast of India, during May - April 2012. The waves were classified into short waves ($T_p < 8$ s), intermediate waves ($8 < T_p < 13$ s), and long waves ($T_p > 13$ s) based on peak period (T_p) and the percentages of occurrence of each category were estimated. The study shows that the wind sea domination is observed during the calm pre-monsoon season and swell domination during the rough SW monsoon season. The variation in the presence of swells and wind seas during the post-monsoon season depends upon the cyclonic activity occurring in the Arabian Sea. Glejin et al. (2013b) examined the presence of the summer shamal swells using wave data off Ratnagiri, west coast of India, during the period of 2010 and 2011 supported by wind data from Automatic Weather Station (AWS), Advanced Scatterometer (ASCAT) and NCEP. Their study identified the presence of swells that originate from the summer shamal winds in the Persian Gulf and reach Ratnagiri during 30 % of the summer shamal period. The average occurrence of summer shamal swells is approximately 22 % during the southwest monsoon period. An increase in wave height is observed during June and July at Ratnagiri due to the strong summer shamal event. Rashmi et al. (2013) studied the co-existence of wind seas and swells along the west coast of India during non-monsoon season using the wave data for different years. They observed diurnal variation in wave parameters along the central west coast of India i.e. off Goa and Ratnagiri. This is due to the interaction of multidirectional waves (both wind seas and swells) of varying magnitudes and frequencies. Also under local wind condition, the interaction between wind sea and swell dominates and thereby the multimodal state reduces to unimodal state.

Using wave data from the directional wave rider buoys, Anoop et al. (2014) studied the reflected surface gravity waves from the shoreline and quantified the reflected swells in the frequency band between 0.045–0.12 Hz from the west and east coast of India based on the spectral wave data. The reflected waves were quantified by using reflection coefficient and ratio of the reflected and incident spectral energy. They also analyzed the influence of the seasons, cyclone, relative depth, land/sea breeze, tides and tidal current on the reflected waves. The results show that the reflection coefficient decreases with increase in relative depth off west coast of India and seasons have large impact on the reflection coefficient. Also the reflection coefficient was low during the cyclone period. Samiksha et al. (2014) analyzed the wind, wave and current data off Ratnagiri, west coast of India to study the wind-wave-current interaction during shamal event. During these events, the current data shows a distinct change in direction and increase in speed. They concluded that the waves which propagate from NW and the current which flows towards north oppose each other which results in the intensification of currents off Ratnagiri. Anoop et al. (2016) investigated the influence of the Indian Ocean Dipole (IOD), on the wave climate of the eastern Arabian Sea. Winds from the northern Arabian Sea get modified and cause inter-annual variability in the wave climate over the eastern Arabian Sea. This is due to the IOD induced changes in equatorial sea surface temperature and sea level pressure.

When compared to waves, literature on coastal currents along the coastline of India is relatively scarce. Sarma and Rao (1986) and Sanil Kumar et al. (1989) studied the measured wind induced current spanning over a short period. The circulation off west coast of India during the southwest monsoon was studied by Shetye et al. (1990) and their results show that the circulation off the west coast of India during southwest monsoon season is weak, and is dynamically similar to the wind-driven eastern boundary currents. Sahu et al. (1991) studied the coastal currents off Mangalore and observed a maximum speed of 60 cm/s during November and a minimum of 5-9 cm/s during February. Shenoi and Antony (1991) used moored array of current meters and measured currents for a period of three months off Goa. They observed that the mean flow was towards south during May and March and it was towards north in November. Stramma et al. (1996) measured the currents off south-west India at 8° N during the SW monsoon period by using ADCP and CTD and observed that the upper

the upper ocean between 75° E and 76° 52' E near the south Indian shelf was governed by a northward flow with a subsurface velocity maximum of 25 cm/s at about 100 m depth. Prasada Rao et al. (1996) studied the pre-monsoon current off Cochin using the data collected from different depths and observed a southerly current in near-surface and north-westerly currents in sub-surface. Shankar and Shetye (1997) studied the circulation pattern of the north Indian Ocean during northeast and southwest monsoon. Bruce et al. (1998) observed that the anticyclonic circulation during northeast monsoon consists of multiple eddies. Shetye (1998) observed that the West India Coastal Current (WICC) flows northward during November - February and southward during April - September. He concluded that the currents in the North Indian Ocean basin are primarily due to Equatorial Rossby and Kelvin waves and Coastal Kelvin waves.

By using the ship drift data, winds, Ekman drift and geostrophic currents derived from altimetry and hydrography and also by using numerical models, the monsoon currents in the north Indian Ocean was studied by Shankar et al. (2002). They found that the monsoon currents are seasonally reversing. The Summer Monsoon Current (SMC) flows eastward during the summer monsoon and the Winter Monsoon Current flows westward during the winter monsoon. Kurian et al. (2005) and Hameed et al. (2007) studied currents along the south-west coast of India and the results showed a seasonal change with stronger currents during monsoon and weaker currents during fair weather. The alongshore components of the currents are mostly much stronger than the cross-shore flows. The current pattern is mostly diurnal although a semidiurnal signal is also seen. The diurnal activity is mostly wind-induced. In the monsoon season, the dominant direction is southerly to southwesterly, whereas during the pre-monsoon and post-monsoon it varies between northwest and southeast. Kurian et al. (2007) based on the current measurements carried out in the innershelf of Kayamkulam-Munambam sector of the southwest coast of India concluded that the dominance of monsoon forcing, as seen in the case of waves, is not seen in the distribution of innershelf currents. They observed that the southern locations of Mararikulam and Thrikunnappuzha shows strong southeasterly movement during pre-monsoon while the monsoon and post-monsoon seasons record sluggish movements.

2.3 Nearshore Sediment Transport

The literature pertaining to sediment transport regime comprises of observational, experimental, computational and numerical modelling studies. A review of the global and Indian scenario for both the longshore and cross-shore sediment transport is carried out in this section.

2.3.1 Global scenario

Field measurements of wave and current parameters in the surf zone of El Moreno Beach and Silver Strand Beach, California and the resulting longshore transport of sand have been made by Komar and Inman (1970). The direction and flux of wave energy were measured from an array of digital wave sensors placed in and near the surf zone. Quantitative measurements of the longshore sand transport rate were obtained from the time history of the center of gravity of sand tracer. The measurements have been used to validate two models for the prediction of the longshore transport rate of sand. From field measurements in the west shore of Lake Michigan, Lee (1975) showed that the longshore currents were linearly related to the longshore momentum flux of incident waves at the breaker line. Also, the longshore sediment immersed weight transport rate is found in terms of the longshore wave energy flux per unit length of beach.

Fredsoe et al. (1985) studied the suspended sediment distribution in the combined wave-current motion, where the motion close to the bed is sufficiently strong. Laboratory and field measurements were compared with the theory. The longshore sediment transport was studied by using sediment transport models in the surf zone by Deigaard et al. (1986). They analyzed the transverse distribution of the longshore sediment transport on a coast with bars and validated using field measurements. An energy related littoral sand transport rate formula is presented by Kamphuis et al. (1986), based on extensive laboratory tests and a set of known field data and calculated the mass transport rate.

Quick and Ametepé (1991) considered the radiation stress principles and found that the cross-shore transport and slope determines the longshore stress levels, the longshore velocity and intensity of longshore transport. Quick (1991) estimated the onshore-offshore sediment transport on beaches by considering the time averaged behavior of a control volume and derived theoretical relationship which specify the

beach slope in terms of the incident wave attack and beach material properties. Wright et al. (1991) examined the mechanisms responsible for onshore and offshore sediment fluxes across the shoreface zone seaward of the surf zone using three years of field data in the southern part of the Middle Atlantic Bight at a depth ranging from 7 - 17 m. They found that the mean flows dominated and caused offshore fluxes during the storm event and contributed significantly to onshore and offshore fluxes during fair weather. Numerical model for the steady state profile of the longshore current induced by regular, obliquely incident, breaking waves was studied by Caviglia (1994). A rapid convergent numerical algorithm is described for the solution of the governing equation. The present model for longshore current computations was combined with some of the known formulae for predicting sediment transport distribution.

Larson and Kraus (1995) utilized compatible spatial and temporal scales for calculating the sediment transport and morphological changes. The calculations are made at different scales, showing the assumptions and approximations. The main conclusion from their study is that calculations at different scales can be related and reconciled if limitations in prediction of initial and boundary conditions and in the fluid forcing are recognized. Aagaard and Greenwood (1995) utilized the field measurements of near-bed current velocities and sediment concentrations within a barred nearshore environment and showed a large flux coupling at far infragravity frequencies ($< 0.005 \text{ Hz}$). In the presence of strong longshore currents upto 30 % of the longshore and 65 % of the cross shore suspended sediment transport can be attributed to far infragravity oscillations. While the former was always directed with the longshore current, the latter was variable in direction both spatially and temporally. van Rijn (1997a) developed a sand budget model, which describes the sand volume change in each compartment of the central coastal zone of Holland. A 2DV mathematical model representing the hydrodynamic (waves and currents) and sand transport processes in a cross-shore profile was used to compute the yearly-averaged transport rates in various profiles along the coast at depths of 20 and 8 m and in the surf zone. This sand budget model has been calibrated using the yearly-averaged sand volume changes derived from bathymetry data collected during the period 1964-1992.

Masselink and Hughes (1998) measured flow velocity and sediment transport of the swash zone and showed that the sediment load displayed a strong relationship with

the time averaged velocity. Wang et al. (1998) measured the total rate of longshore sediment transport by using streamer traps at 29 locations along the southeast coast of the United States and the Gulf Coast of Florida. The rate was also measured simultaneously by short-term impoundment at Indian Rocks Beach, west-central Florida. Their results show that the transport rates measured by the streamer traps and the short-term impoundment along low-wave energy coast were considerably lower than the rates predicted by empirical formulae. The linear relationship between wave energy flux factor and the total rate of longshore sediment transport contained in the commonly used CERC predictive formula is supported by the streamer trap measurements. Also a lower value of the empirical coefficient, 0.08 instead of the 0.78 recommended by the SPM (1984), was determined by the trap data for low-energy coasts.

The LST rates near the village of Duck, North Carolina, U.S. during storm period was measured and analyzed by Miller (1999). Comparisons of measurement results with predictions using CERC formula shows that the predicted rates were higher or lower than the measured suggesting that an additional term may be required for short term predictions during storm events. They studied the cross-shore distribution and LST rates during storm events. The total longshore sediment transport rate in the surf zone was measured by Wang and Kraus (1999) at a temporary groin installed at Indian Rocks Beach, west central Florida. Updrift accumulation and downdrift erosion mass balance was obtained, which were subjected to further analysis. Magnitudes of the transport rates were considerably lower than the predictions by CERC formula. Comparable or greater uncertainty in K-values exists for calibrating the predictive formulas. They concluded that K-value is not a constant and that other factors may enter, such as breaker type, turbulence intensity, and threshold for sediment transport.

The skill of six well known formulae developed for calculating the LST was evaluated by Bayram et al. (2001). The van Rijn formula was found to yield the most reliable predictions over the range of swell and storm conditions. The Engelund–Hansen formula (Engelund and Hansen, 1967) worked reasonably well, although with large scatter for the storm cases, whereas the Bailard–Inman formula (Bailard and Inman, 1981) systematically over-estimated the swell cases and under-estimated the storm cases. The formulas by Watanabe and Ackers–White (Ackers and White, 1973) produced satisfactory results for most cases, although the former over-estimated the

transport rates for swell cases and the latter yielded considerable scatter for storm cases. Bijker formula (Bijker, 1967) systematically over-estimated the transport rates for all cases. It is to be noted that the coefficient values in most of the employed formulas were based primarily on data from the laboratory or from the river environment. They concluded that re-calibration of the coefficient values with reference to the field data from the surf zone will improve their predictive capability.

Onshore directed suspended sediment fluxes and associated nearshore bar migration were observed by Aagaard et al. (2002) during the field experiments on a gently sloping beach on the Danish North Sea coast. The field measurements of suspended sediment flux obtained during three experiments on two different beaches viz. Skallingen located on the Danish North Sea coast and Staengehus on the north coast of Zealand, Denmark, is used to parameterize the observed fluxes. A non-dimensional sediment flux index is formulated which describes the tendency towards net onshore or offshore transport. This index is found to depend upon the undertow velocity, the incident wave skewness and the cross-correlation between orbital velocity and sediment concentration. Formulation of suspended sediment transport across bars is obtained by linking the flux index with a parameterization of the sediment concentration in the water column. This formulation predicts a tendency for onshore directed sediment transport due to incident waves on gently sloping beaches. Temporal and spatial variations of surf zone currents and suspended sediment concentrations were investigated by Wang et al. (2002b). Both currents and sediment concentrations exhibit great temporal and spatial variations in the surf zone. Sediment concentration decreased very rapidly upward through the water column across most of the surf zone. Elfrink and Baldock (2002) reviewed the dominant hydrodynamic forcing and resulting sediment transport mechanisms in the swash zone.

Pritchard and Hogg (2003) described a mathematical model of suspended sediment transport on an intertidal mudflat under cross-shore tidal currents. A Lagrangian formulation was employed to obtain periodic solutions for the sediment transport over idealized bathymetries. Shah Alam Khan (2003) studied the beach profile evolution in a wave tank and found that the transport rate gradually diminishes offshore from the wave break point. The effect of density variations of the sediment on coastal sediment transport has been studied in a wave flume experiment by Koomans and de Meijer (2004). Two types of sands with an equal grain size distribution but with different

densities (heavy minerals and quartz) have been used. The experiments show that the presence of heavy minerals in the sediment results in reduced erosion on the beach face. Kobayashi and Lawrence (2004) examined the cross-shore sediment transport processes under breaking solitary waves on a fine sand beach based on laboratory experiments. The beach was exposed to positive solitary waves and again to negative solitary waves after re-building of the beach. The positive solitary wave plunged violently near the shoreline and suspended a considerable volume of sand. The strong downrush followed by the large run-up results in the erosion on the foreshore. But the negative solitary wave collapsed against the seaward flow induced by the free surface slope of the negative wave and caused less sediment suspension. This generates weak downrush following small run-up results in the deposition on the foreshore. This study indicates the importance of the initial wave profile for swash sediment dynamics and the capacity of a single wave in causing noticeable beach profile changes.

Masselink et al. (2005) conducted field measurements of water depth, flow velocity and suspended sediment concentration made at three fixed locations across the high tide swash and inner surf zones of a dissipative beach. Suspended sediment concentrations, loads and transport rates in the swash zone were almost one order of magnitude greater than in the inner surf zone. Also the suspended sediment transport flux measured in the swash zone was related to the bed shear stress through the Shields parameter. Karambas (2006) estimated the sediment transport rate in the swash zone using a Boussinesq model coupled with a porous flow model in order to incorporate the infiltration-exfiltration effects. Also the depth-integrated transport equation for suspended sediment is solved. Turker and Kabdas (2007) studied the effect of wave climate and grain size characteristics in the definition of transport rate parameter and thus witness their influence on the parameter. Smaller transport rate value gives a longer elapsed time before equilibrium is attained on the beach profile. Bayram et al. (2007) has developed an expression to find out alongshore sediment transport. The model assumes breaking waves mobilize the sediment and move it by current. Dean number is also used for this expression and is well suited for practical applications in coastal areas, as well as for numerical modeling of sediment transport and shoreline change in the nearshore.

Masselink et al. (2008) conducted field investigation on a macrotidal beach of Truc Vert, France, with intertidal bar morphology. They quantified the cross-shore

sediment transport rates and beach response by using four different ways viz. net transport from bed-level changes, measured suspended sediment fluxes, sediment fluxes associated with migrating wave ripples, total load transport predicted using Bailard model (Bailard, 1981). The qualitative agreement between the different measures are excellent under all recorded wave conditions, with onshore (offshore) sediment transport and beach accretion (erosion) observed under low-to- moderate (high) wave conditions. Longshore sediment transport in the surf zone on Galveston Island, Texas, was studied by Rogers and Ravens (2008) and they developed a new technique involving optical instruments to measure transport rates and the results are compared with CERC formula. Measured sediment transport rates ranges from 86,000 to 231,000 m³/year. CERC formula gave sediment transport rates significantly greater than the observed values.

Pham Thanh Nam et al. (2009) developed a two-dimensional numerical model of nearshore waves, currents, and sediment transport. Good agreement between computations and measurements was obtained with regard to the cross-shore variation in waves, currents, mean water elevation, and sediment transport in the nearshore and swash zone. The model can be used for predicting morphological evolution in the nearshore due to waves and currents. Field measurements of LST were undertaken by Esteves et al. (2009) on barred and non-barred beaches in Brazil, Denmark and Portugal. Measurements and predictions of vertical suspended sediment concentration profiles and cross-shore hydrodynamic parameters were then combined in a new semi-empirical model (LT-MOD) for prediction of LST which they compared with predictions using bulk LST formulae. The results show that LT-MOD gave more accurate predictions than existing bulk LST formulae. Laboratory studies were conducted by Smith et al. (2009) to investigate the importance of wave height, period and breaker type on total rate of LST and the cross-shore distribution of LST. The well-known bulk formulas viz. CERC, Kamphuis, Readshaw were compared with the accurately measured total LST rates. Several K-values were used with the CERC formula, including the recommended value of 0.39. The recommended K-value and most of the calculated K-values over predicted the measured total LST rates. But the method that includes parameters to indicate the breaker type gave good estimate of LST rate. The Kamphuis equation, which includes wave period and beach slope that in turn influences wave breaking, also compared well with the measurements. The

CERC formula gave excellent results if K was calibrated with measured data. They also concluded that the transport in the breaker zone was influenced by breaker type and wave height was the dominating factor and is independent of wave period. The swash zone transport showed a dependence on wave height, period, and beach slope.

Walton and Dean (2010) presented the concept of littoral drift rose (LDR) for the improvement in understanding of longshore sediment transport and consequent shoreline processes in areas with gradually varying offshore bathymetry, where the deep water wave climate is reasonably uniform. The stability of the shoreline using LDR, and development of LDR from one wave component of given magnitude and direction are discussed in the paper. The magnitude and direction of littoral drift throughout a region can be interpreted from limited measured, calculated, or observed data. Investigation of the cross-shore sediment transport process by wave induced current was carried out in the laboratory environment by Mahalder and Navera (2010). This study provides information regarding the process of sediment transport due to wave in the cross-shore direction due to varying water depth and wave parameters in the laboratory. They observed that the changes of bed level depend on water depth and wave period greatly as well as the wave height.

Cartier and Hequette (2011) estimated the LST on sandy barred macro-tidal beaches of Northern France using sediment traps. They showed that LST increased with both wave height and mean flow. No relation was found with wave angle which is probably due to the influence of tidal currents that interact with wave-induced longshore currents. Cross-shore variation showed that sediment fluxes were higher on the middle to lower beach. This can be explained by a decrease in tidal flow velocity towards the upper beach as well as wave-energy dissipation over the beach and intertidal bars. LST direction appeared to be controlled by both incoming wave and tidal current direction. Appendini et al. (2012) estimate the potential LST along the northern coast of the Yucatan Peninsula. The waves were characterized using a 12 year (1997-2009) deep water wave hindcast data (WAVEWATCH III) as forcing for the spectral wind-wave numerical model (MIKE 21 SW). The simulated time series of significant wave height, peak period, and direction are compared against in-situ measurements at 10 m water depth. LST is assessed by using LITDRIFT model. A net westward potential LST is found along the entire coast, ranging between 20,000 and

80,000 m³/year. The potential erosion and deposition areas are identified based on the sediment transport gradients.

Mil-Homens et al. (2013) studied the predictive skill of the most commonly used bulk LST formulas viz. CERC (SPM, 1984), Kamphuis (Kamphuis, 1991) and Bayram (Bayram et al., 2007). The calibration coefficients in these three formulas are improved using a least-squares optimization algorithm which has improved the predictive skill of all the three formulas. The improved formula is verified by using the statistical methods of bootstrapping and cross-validation, and the improved Kamphuis formula performs best, followed by the improved Bayram formula. Aagaard (2014) conducted field measurements of suspended sediment load and cross-shore transport on the lower shoreface. This is used to derive a model for sediment supply from the lower to the upper shoreface at large spatial and temporal scales. The results showed that both suspended sediment load and cross-shore sediment transport scale with the grain-related mobility number, which ranged upto $\psi \approx 1000$ in the measurements. A one year long simulation of sediment transfers between the lower and the upper shorefaces on a natural beach compares well with transport rates estimated from long-term bar migration patterns and aeolian accretion on the same beach.

van Rijn (2014) studied the longshore transport of sand, gravel and shingle using field and laboratory data. Numerical model CROSMOR (van Rijn, 1997b, 1998) was used for the estimation of cross-shore and LST. This has been used to determine the effects of wave period, grain size, beach/surf zone slope and type of waves (wind waves or swells). The longshore transport was found to be proportional to wave height to the power 3.1 ($\approx H^{3.1}$), to grain size to the power -0.6 ($\approx d_{50}^{-0.6}$) and to beach slope to the power 0.4 ($\approx \tan \beta^{0.4}$). Based on the results, a new expression for longshore transport of sand, gravel and shingle beaches with grain sizes between 0.1 and 100 mm has been derived by them. The cross-shore distribution of long-term average LST rate on a sandy beach exposed to waves with various directionalities was investigated by Kuriyama and Sakamoto (2014). They developed a process based one-dimensional model to simulate the cross-shore distributions of LST rate in the nearshore at 2 hour intervals for 15 years at the Hasaki coast of Japan. The simulation results showed that although the direction of average total LST rate was southward, the direction of predominant LST near the shore was northward. This was caused by the cross-shore

distribution of average LST rate that was northward near the shore, but southward away from the shore. Northward transport was dominant when the longshore sediment transport developed only near the shore owing to relatively small waves. Sediment transport in the southerly direction takes place when the transport developed both near and away from the shore owing to relatively large waves. The results indicates that the evaluation of the cross-shore distribution of LST rate is crucial for gaining a better understanding of LST on a sandy beach exposed to waves with various directionalities. Barbaro et al. (2014) proposed an expression for the calculation of the LST, including the effect of the spectral shape associated with the free surface displacement. The expression for LST is derived theoretically by using the wave flux approach combined with the spectral representation of the wave field propagating to the coast. The reliability of the proposed formula is assessed by utilizing the field data. They showed that the proposed LST formula is capable of reducing the large over estimations associated with the LST calculation and of reducing scattering between calculated and the measured LST rates.

2.3.2 Indian scenario

Reddy (1979) examined the wave condition and sediment transport nature in the Mormugao harbour area and found high waves from west-southwest direction during the southwest monsoon. Also the offshore sediment transport appears to be directed towards north or north-west due to the combined influence of currents and waves.

Prasannakumar et al. (1983) computed the volume of littoral sediment transport at 2 m depth contour along the Munambam - Andhakaranazhi coastal sector for waves approaching the shore from 200° to 300° with periods varying from 6 to 14 s. They estimated that about 9 million m^3 of material drifted towards south annually between Munambam and Vypeen and about 7 million m^3 of material drifted towards south between Fort Cochin and Andhakaranazhi. Variations in the alongshore drift of littoral sediments in the area between Azhikode and Vypeen was studied by Prasannakumar (1985). The study shows that the littoral drift values are higher during rough weather season than the fair weather season. Murty and Veerayya (1985) studied the longshore currents at selected locations along the Goa and Kerala coast over a period of 5 years and observed high variability in the current speed and direction. Chandramohan and Rao (1986) computed the LST using different empirical formulas along Visakhapatnam coast.

LST rates near Visakhapatnam Port have been estimated using an energy flux method by Sarma and Reddy (1988). They found that the direction of littoral drift is from south to north during the period March to October, when the wave directions are between SE and S, and from north to south during the period November to February when the wave directions are between ENE and E. The net drift is northwards and is by far the most dominant for this coast. The beach and shoreline changes were critically examined in relation to the littoral drift. Prakash and Prithvi Raj (1988) studied the seasonal longshore transport direction utilising the textural parameters of the foreshore sediments along a 41 km stretch of the Paravur-Purakkad coast in Kerala. The seasonal grain-size variation and sediment budget along the coast were also examined. Prithvi Raj and Prakash (1988) studied the textural parameters of surficial sediments in the innershelf of Kerala, between Kuzhipalli and Chawghat (Chavakkad), to delineate probable sediment transport trends. The study delineates the transport trends both in onshore as well as offshore directions in sectors where fluvial action is prevalent. The onshore transport only occurred in the sector devoid of fluvial influence. The LST shows a strong northerly sediment movement beyond 20 m depth and movement in north and south directions at shallower depths. They concluded that the movement of sediments in shallower portions of the shelf is influenced by the interaction of waves, currents, and fluvial processes.

Mcdougal and Hudspeth (1989) studied the longshore current on natural beaches having an equilibrium profile. Their study shows that the location of the maximum longshore current moves closer to the shore as the planar beach face width decreases. A narrower beach face results in the maximum sediment transport being closer to the shore. Total sediment transport rates are also a function of the planar beach face width and this suggests that longshore transport rates are modulated by the tidal elevation. LST rates for the south Indian coast from Allur to Cochin and for Sri Lanka were estimated from ship reported wave data for the period of 1968 - 1986 (Chandramohan et al., 1990). Annual gross sediment transport is high ($1.5 - 2 \times 10^6 \text{ m}^3$) along the coasts of north Tamilnadu and south Kerala. The annual net transport is southerly along the west coast of India and predominantly easterly along the east coast. Prasanna Kumar et al. (1990) examined the wave-induced nearshore circulation and sediment exchanges between two littoral cells along Vypeen and Chellanam. Southerly littoral

currents are observed during most of the year and they presented a conceptual model in order to explain the sediment movement along the two littoral cells.

Chandramohan and Nayak (1991) developed an empirical sediment transport model for the Indian coast on longshore energy flux equation and estimated an annual gross sediment transport of 1.5 - 2 million m^3 along the south Kerala coast. Nayak and Chandramohan (1992) and Chandramohan and Nayak (1992) developed an empirical sediment transport model based on longshore energy flux equation. The study indicates that annual gross sediment transport rate is high ($1.5 \times 10^6 \text{ m}^3$ to $2 \times 10^6 \text{ m}^3$) along the coasts of Orissa, north Tamilnadu, south Kerala and south Gujarat. The transport is comparatively low ($0.5 \times 10^6 \text{ m}^3$ to $1 \times 10^6 \text{ m}^3$) along the south Tamilnadu coast. Also the direction of annual net transport is towards north along the east coast and towards south along west coast. Chandramohan et al. (1993a) studied the sediment transport along the South Maharashtra coast and estimated that the longshore sediment transport at Ratnagiri, Ambolgarh and Vengurla were 0.12, 0.19 and 0.05 million m^3 respectively towards south. Chilka lake inlet mouth is exposed to high annual littoral drift of about $1 \times 10^6 \text{ m}^3$ and the inlet mouth was observed to migrate about 500 m northward during the period of one year study (Chandramohan et al., 1993b). Measurement of daily longshore currents indicated that the predominant LST across the mouth is towards north throughout the year. Revichandran et al. (1993) calculated the vertical profiles of suspended sediment concentration, current velocity and salinity carried out in the Azhikode estuary and studied the shoaling and siltation in the harbour region.

Jayappa (1996) studied the longshore currents and sediment transport along the beaches of Manglore for a period of one year and found that average longshore current velocity was high and net sediment transport was towards south. Jose et al. (1997) studied the longshore transport at three different locations with varying littoral characteristics along the SW coast using the wave energy flux method. They observed the highest transport of 2.9 million m^3 at Vizhinjam and the lowest value of 0.07 million m^3 at Chavara. Jena and Chandramohan (1997) studied the sediment transport near the Peninsular tip of India based on monthly measurement of littoral environmental data and beach profiles. They estimated that the annual gross longshore sediment transport rate was 0.9 million m^3/year and the annual net transport rate was 0.3 million m^3 towards west. Sajeev et al. (1997b) studied the longshore

transport characteristics of the Kerala coast using Walton's equation and found that the net drift was southerly during monsoon periods and northerly during other seasons. The annual net transport was southerly at all the stations except at Trivandrum, Alleppey and Nattika.

The longshore current and sediment transport along Kannirajapuram coast, Tamilnadu were studied by Sanil Kumar et al. (2000). The predominant direction of transport was northerly from March to November and southerly from December to February. They calculated that the annual gross transport was 0.46 million m³ and annual net was 0.44 million m³/year towards northeast. Kunte and Wagle (2000) carried out the study to determine the dynamics of littoral transport along the west coast of India. The study indicates that though the littoral drift is variable, bi-directional and season dependent, long-term net littoral drift along west coast of India is southwards. Chandramohan et al. (2001) studied the littoral drift sources and sinks along the Indian coast and found that rivers were the major sources for the littoral drift and the annual discharge of sediments to the sea along the Indian coast was about 1.2×10^{12} kg. Sanil Kumar et al. (2001) studied the nearshore processes along Tikkavanipalem Beach using wave rider buoy data. They estimated the longshore currents and longshore sediment transport rate considering the sea and swell waves separately using the CERC formula. The difference between the gross sediment transport rates estimated based on the Longuet-Higgins and Galvins equation was around 6 %. The sediment transport estimated using Walton's equation shows that average annual gross transport was 0.371 million m³ and the average annual net transport (towards northeast) was 0.173 million m³.

Sanil Kumar et al. (2002) calculated the longshore sediment transport rate in Nagapattinam coast using CERC formula and found that the average annual gross transport was 0.448 million m³ and the average net transport (towards south) was 0.098 million m³. Measurements of the longshore sediment transport rate along the surf zone at a 4 km long beach on the central west coast of India were made over a 4 month period by Sanil Kumar et al. (2003). Both lateral and vertical distributions of the sediment transport rate were measured with traps deployed on a line spanning the surf zone. The measured average gross transport was 726 m³/day and during 69 % of the time, the transport was northerly, and in the remaining period, it was direct towards south. Sediment transport along the Mangalore coast was estimated by using

MIKE 21 sediment transport module by Babu et al. (2003). The results show that the offshore sediment movement is dominant only in monsoon season due to higher wave activity and in non-monsoon periods the onshore movement is pre-dominant. The net longshore sediment transport is negligible, according to them (0.22 million m³/y), along this coast and the direction is southerly in all the seasons. Sanil Kumar et al. (2006) studied the coastal processes along the Indian coastline using measured data on waves and currents. They calculated that the gross sediment transport rate was about 1million m³/year along south Kerala and south Orissa coasts.

A closed sedimentary circulatory system described as a “step-ladder” was identified by Black et al. (2008), on the basis of observation and numerical modelling off Kerala coast. According to them, dynamic sediment equilibrium on a regional scale is maintained by an annual net northerly sediment flux in the nearshore zone, driven by wave-induced currents. This is balanced by a net southerly flux on the innershelf, but driven instead by wind-induced currents which transport the wave-induced suspended sediment. The two counter-directional shore parallel sedimentary pathways are linked by cross-shore bridging transport. Singh et al. (2008) employed neural network and genetic programming which, according to the authors, produce better results for the estimation of littoral drift. Numerical models were developed by Kurian et al. (2009) to simulate the wave and sediment transport regime of the innershelf of the south-central Kerala coast. The net annual longshore sediment transport is southerly in the innershelf and northerly in the surf zone. These counter directional transports are linked by seasonally reversing the cross-shore transports. Stable beaches prevail in the locations where the longshore and cross-shore transport balances. Erosion/accretion patterns are noticed in the locations where the sediment transports are not balanced.

Beach width data for a period of 5 years (1993–1998) was categorized and analysed in relation to the seasons by Suresh et al. (2011) to have an understanding of the coastal processes over a 50 km long coast west of Cape Comorin along the southwest coast of India. The study area was affected partially by the great Indian Ocean tsunami and the field measurements are used to validate a finite difference based numerical model employing the empirical formulation of Larson and Kraus (1989). The nearshore wave climate was derived by adopting the MIKE 21 Parabolic Mild Slope module. The prediction from the numerical model revealed that the average onshore-offshore transport varies from about 50 to 200 m³/m/year width of the beach. Shanas and Sanil

Kumar (2014) examined the variation in the LST estimate using four well known formulae and the sensitivity of the wave parameters on LST determination. The study was conducted along the Kundapura coast, central west coast of India. They showed that the net LST was towards north for most of the time (non-monsoon period), whereas the LST was towards south during the monsoon season. According to the authors, the influence of breaker height was more during the non-monsoon period whereas during the monsoon period, breaker angle shows more influence on LST. The annual net LST estimated for the region are 0.36, 0.30, 0.16 and 0.26 million m³ based on the CERC, Walton and Bruno, Kamphuis and Komar formulae respectively.

Based on waves measured at 9 m depth, nearshore wave transformation was simulated using REFDIF-1 numerical model (Kirby and Dalrymple, 1994) and the nearshore breaker parameters were estimated at two micro-tidal beaches along central west coast of India (Honnavar Coast) by Sajiv Philip et al. (2014). Longshore current and LST rates were computed by using semi-empirical equations from the breaker parameters. Predominant direction of LSTR is observed towards north during pre-monsoon and post-monsoon, and towards south during monsoon. The sensitivity analysis of LST estimate shows that coastal inclination is the prominent factor in determining LST than incident wave angle. Wave-induced Longshore Sediment Transport (LST) of the Dhanushkodi sandspit located southeast of Rameshwaram, India was studied by Gowthaman et al. (2015). The study was based on data collected simultaneously in the Gulf of Mannar and Palk Bay using directional wave rider buoys. They have used numerical modelling to calculate the nearshore wave climate and estimated LST using three different formulae. This estimated LST are again compared with the numerical model LITDRIFT module of LITPACK. The net sediment transport along the Gulf of Mannar coast at Dhanushkodi indicates that the predominant direction of transport is south-eastward and is 0.3, 0.28, 0.23 million m³ based on the CERC, Walton & Bruno and Kamphuis formulae, respectively. The numerical model studies based on the LITLINE module of LITPACK showed that, during the 2010-2015 period, the sand spit along Dhanushkodi grew by 65 m due to the net southeastward LST along the Gulf of Mannar coast.

2.4 Beach Placers

2.4.1 Global scenario

Swift et al. (1971) examined the sediments of the North Carolina-Virginia coast in order to determine the genesis of the coastal sands. They concluded that strong mineralogical gradient exist across the study area and the heavy mineral distribution along this coast is due to the in-situ fractionation of the substrate generated by shore face retreat.

Barrie (1980) presented the quantitative heavy mineral distribution, the individual mineral threshold values and heavy mineral enrichment of the Bristol Channel. The differential mineral transport of heavy minerals, according to him, depends upon the hydraulic conditions of unidirectional and oscillatory flow. Such a model can be used to explain the development of heavy mineral enrichment found on the open, high energy beaches and in the areas of local tidal current enhancement. Luepke and Clifton (1983) analyzed the heavy mineral distribution of Willapa Bay, Washington which indicated a dominance of two mineralogic assemblages. The distribution of heavy mineral suggest that the sand discharged from the Columbia River, is borne north by longshore transport, and carried into the bay by tidal currents. Komar and Wang (1984) considered the important grain sorting mechanisms such as selective entrainment and differential transport. They found that the grain density and size are the important parameters for placer formation. The higher densities and finer grain sizes of heavy sands require greater entrainment flow stress. This result in lower transport rates compared with the light minerals.

Best and Brayshaw (1985) studied the flow separation in the alluvial channels that occurs due to abrupt changes in the bed geometry. This generates a region of high bed shear stress that can entrain heavy minerals, and a region of low velocity that is a preferred site for the deposition of denser particles. They found that significant concentrations of heavy minerals are formed by the flow separation processes. Peterson et al. (1986) studied the beach segments enriched by heavy minerals which are located between Cape Lookout and Cape Perpetua, Oregon. Beach face retreat in the winter of 1982-83 exposed underlying placers containing the economic minerals. The highest concentration of placer minerals occurs in an area of maximum shoreline curvature. Slingerland and Smith (1986) from their study of the occurrence and

formation of water-laid placers have provided valuable contributions in the grain scale processes. Komar (1989) makes a review of the physical processes of mineral sorting and dynamic equivalence. He categorises the sorting processes under waves and currents to fall under four different types viz. settling equivalence, selective entrainment, transport sorting and shear sorting.

Morton and Smale (1990) assessed the effects of transport and weathering processes on heavy mineral suite from the Cascade-Martyr river system, Westland, New Zealand. Weathering processes on the floodplain does not affect the heavy mineral suites during the transit. Coarse sediment movement takes place during floods and they will not reside for extensive periods on the floodplain. They concluded that neither mechanical abrasion nor weathering has a marked effect on the heavy mineral suites in this river system. Pujos et al. (1990) studied the distribution of the heavy minerals of the continental shelf sands off French Guiana. He concludes that the heavy minerals provide an excellent tool for the reconstruction of paleo-environments. In order to test the spatial distribution and temporal variability of beach heavy minerals, five beach zones from the backshore out to the breaker zone were sampled by Isla (1991). The heavy minerals dominate to the backshore and light minerals are more abundant in the submerged zones. Seasonal changes are shown by the lighter of the heavy grains. Li and Komar (1992) used laboratory flume experiments to study the processes of selective entrainment of grains from sands of mixed sizes and densities. A minimum threshold stress for the entrainment of intermediate grain sizes of mixed size sediments exists while higher threshold stresses are required for the movement of both smaller and coarser size fractions. Frihy and Komar (1993) analysed the shoreline positions from the beach profile surveys along the coastline of the Nile Delta during 1971 to 1990. Associated with the longshore sediment movement, there is a selective transport of different minerals according to their densities and grain sizes, with the light minerals having the highest advection rates and the dense minerals having the lowest rates.

Frihy et al. (1995) collected sediment samples along 34 beach profiles spanning along the 240 km length of the Nile Delta in order to examine the sorting patterns of heavy minerals that develop during cross-shore and longshore sediment transport. Factor analysis of the heavy mineral contents shows that two mineral factors or groups results from sorting due to the contrasting densities and sizes of the grains. The spatial

distributions of these two factors reflect the grain-sorting patterns of the heavy minerals which coincide with the general trends of shoreline erosion versus accretion. Nine types of heavy mineral have been found by Liu (1999) in the fluvial sediments of the Ordovician Natal Group, South Africa. These heavy minerals are concentrated mainly in the Eshowe and Inanda Formations of the succession. Grain size analysis shows that heavy mineral rich beds are composed mostly of fine to medium size sand and are better sorted than the host rocks. Roy (1999) studied the heavy mineral sand provinces of southeastern Australia. He found that a number of fractionating mechanisms that concentrate heavy minerals operates during marine transgressions and under highstand conditions to produce different types of beach placers.

Sorting and concentration of heavy minerals along the coast between Gadani and Phornala, Baluchistan, Pakistan are studied by Chaudry et al. (2002). Sediment samples from different intertidal zones between Gadani and Phornala were collected for grain size analysis and petrographic/petrological study. They studied the variations in grain size and mineral assemblage in the intertidal zones. Beach sand sediments from 33 stations along the Susanoglu coast in Mersin, Turkey were collected and heavy metals were analyzed by Yalcin (2009). To determine the source of heavy metals (natural and anthropogenic), simple and multivariate statistical analyses were applied. According to factor analysis three factors were determined viz. natural process factor, anthropogenic factor and intermediate factor.

Heavy minerals of twenty sediment samples of Schirmacher Oasis, east Antarctica, have been studied for their textural characteristics, abundance and provenance determination by Srivastava et al. (2010). The high concentration of specific minerals of metamorphic origin reveals high-grade metamorphic terrain as the primary source.

2.4.2 Indian scenario

Rao (1957) surveyed the east coast of India, extending from Vasishta Godavari river in the south to Vamsadhara river in the north. They studied the beach configuration and concentration of heavy minerals along this coastal stretch. The concentration of well-sorted heavy mineral sands, according to him, is effected by beach erosion and beach regression. Siddiquie and Mallik (1972) studied the mineralogy of selected samples from the innershelf of Mangalore, India. Trend-surface analyses of distribution of the heavy minerals were made to determine the various factors

controlling the mineral distribution pattern in the area. The mineral distribution in this area is mainly the result of dynamic interaction of process and response elements.

Wagle et al. (1989) studied the coastal features of the central west coast of India from Bombay to Goa by using aerial photographs. Beach samples collected from high tide and low tide levels were analyzed to obtain the heavy mineral content. Impact of lithology, coastal geomorphology and drainage on the concentration of heavies was established in their study. In aerial photographs, beach sands show white, greyish white, dark grey and black tone depending upon the percentage of the black sand. Mineralogical study indicated that the heavy mineral percentage varied from 0.4 to 98.64 %.

The placer mineral concentration on the beaches at Chavara, Kerala, India is studied by Prakash et al. (1991). The rivers in the southern Kerala transport higher amounts of radioactive elements than the larger Kallada River due to higher radioactive minerals in the hinterland rocks. They concluded that the seasonal longshore current pattern and the coastal configuration played a major role in the alongshore distribution of minerals. Shankar et al. (1996) used rock magnetic properties to obtain estimates of heavy mineral contents of placers from the SW coast of India. Their study showed that magnetic susceptibility and other magnetic properties show strong correlations with heavy and opaque mineral contents. As one or more types of magnetic minerals are invariably present in placers, magnetic properties may be used as a proxy for heavy and opaque mineral contents, according to the study.

Prakash (2000) examined the surficial sediment samples from the innershelf off Quilon, SW coast of India for the sediment type, placer distribution and titanium content. A major portion of the innershelf of this coast is covered with sands and silty clays. The total heavy mineral content in the shelf varies from 1 to 12 %. Their study shows a high percentage of heavy mineral in the sandy sediments and titanium content is higher in the southern shelf. The distribution of heavy minerals and titanium in the innershelf indicates net sediment movement towards the northern shelf region, where rich concentrations of placer minerals occurs along the coast. Kurian et al. (2001) studied the spatial and temporal distributions of heavy minerals of Chavara and Manavalakuruchi along the southwest coast of India. The concentration of heavy minerals along the mid-tide line of the beaches is considerably higher in monsoon than during non-monsoon period. The study brings out the dominant role of wave

over the coastal current in the transport of sediment, and the heavy sand is less easily moved than the white sand. During the monsoon season, winnowing of the white sand from the eroded beach takes place, leaving heavies at the beach. During post-monsoon, the erosion ceases and the swell waves dominates which brings more-easily entrained white sand towards the beach. Thus there is a reduction in the beach enrichment during non-monsoon periods.

Angusamy et al. (2004) studied the two different zones of enrichment of placer deposits namely, Kanyakumari-Kuttankuli and Kallar-Vaippar along the southern coast of Tamil Nadu. The heavy mineral assemblages of the two zones were similar to each other. According to the study, the northerly currents in the Gulf of Mannar must have transported and deposited the heavy minerals due to the inflection of coastline, and down warped basinal structure. Hegde et al. (2006) studied the heavy minerals of the Honnavar beach, Karnataka, central west coast of India. The study indicates that the heavy mineral suite has been derived from the hinterland and the river Sharavati brings these minerals. The heavy minerals appear to be reworked and derived from the offshore/palaeo-beach and brought out by combined action of alongshore current from south and waves to the present beach.

Prakash et al. (2007) studied the suspension and enrichment of the heavy sands at Chavara, south-west coast of India. The results indicate that there is an enrichment of heavy sand on the beach face which is initiated during the erosive events. Evidence was obtained for the arrival of bimodal coarse populations to the beach during post-monsoon and loss of quartz sands during stormy monsoon periods. Due to the influence of swells during post-monsoon and under the influence of wave asymmetry, shore-ward migration of denser sands is observed. The magnetic fractions of ilmenite from the beach placer deposit of Chavara, southwest India have been studied for mineralogical and chemical composition by Nair et al. (2009). Chavara deposit represents a highly weathered and relatively homogenous concentration. The ilmenite from Chavara is compared with that from the Manavalakurichi deposit of similar geological setting and provenance. The lower ferrous iron oxide and higher TiO_2 contents highlight the advanced state of alteration of Chavara. This is also evidenced by the relatively higher $\text{Fe}^{3+}/\text{Fe}^{2+}$ ratio compared to Manavalakurichi ilmenite.

The heavy mineral deposits of the coastal sediments in the south Maharashtra stretch were studied by Gujar et al. (2010). The area is a narrow submergent coastal plain

lying between the Achara and Gad Rivers. The heavy mineral concentration shows an increasing trend from north to south. The observed variations in the heavy mineral distribution are due to the differences in the sediment supply, specific gravity and oceanographic processes, all of which result in a selective sorting of the sediments. Chandrasekar et al. (2010) studied the placer formation in the beaches between the Kallar and Vembar River mouths on the southeast coast of India which are rich in placer mineral deposits. Their study reveals that density sorting plays a very crucial role in the concentration of placer minerals in this region. Also the economically viable heavy mineral deposits are governed by the presence of the source rock being in close proximity, topography, climate, and coastal processes.

Heavy mineral analysis was carried out for the beach and fore dune sediments along 60 transects of Nizampatnam - Lankavanidibba, Andhra Pradesh, east coast of India by Reddy et al. (2012). The sectors nearer to the river mouth contain high concentration of high specific gravity heavy minerals than sectors away from the river mouth. They concluded that the redistribution of heavy minerals is controlled by creek dynamics, longshore currents, size and specific gravity of the heavy minerals. The study of heavy mineral placer deposits of the coastal sediments in Bhimunipatnam stretch from Chapala Uppada to Annavaram in the south of Visakhapatnam, Andhra Pradesh was carried out by Rao et al. (2012). They observed that the concentration of heavy minerals is more in dunes than in the beach sediments. The heavy mineral concentration shows an increasing trend from south to north. The observed variations in the distribution of heavy minerals are mainly due to differences in the sediment supply, sorting and oceanographic processes all of which results in a selective sorting of the sediments.

Anooja et al. (2013) studied the provenance and depositional history of the heavy mineral placers in the coastal lands of Kollam district, SW India. According to them, the heavy mineral residues of the upper estuarine zones are generally garnet bearing and are of alluvial origin while sediments in the lower estuary are garnet-free and are derived from the nearby littoral zones during the tidal processes. Dinesh Kumar et al. (2014) has studied the nearshore sediment transport that controls the placer mineral depletion at Manavalakurichi, India. Their analysis shows the landward shift of 10 and 20 m contours by about 35-100 m. They concluded that the removal of sand from

the high energy zones would eventually lead to sediment starvation situations and depletion of placers in the adjacent beaches.

2.5 Beach - Innershelf Morphological Changes

The beach and innershelf morphological changes are very much linked to the sediment dynamics in the beach-innershelf system. Extensive studies are available on beach morphological changes, though those on innershelf morphological changes are relatively less. Also, studies integrating the beach-innershelf morphological changes with sediment dynamics are relatively less. A review of the literature on observational, laboratory and numerical modelling studies pertaining to beach-innershelf morphological changes and the role of hydrodynamic, geomorphological and sedimentological characteristics in the observed morphological changes is carried out in this section.

2.5.1 Global scenario

Frihy (1988) adopted the method of air-photographic analysis to detect erosional and accretional changes along the coast of Nile Delta, Egypt. The aerial photographic analysis is applied to three unstable coastal zones viz. the Rosetta, Damietta promontories and the Burullus-Baltim sector. This study reveals that highest erosion occurs in the outer margin of both Rosetta and Damietta promontories. The estimated highest rate of erosion during the 28 year period of study is 114, 9 and 31 m/year respectively, at Rosetta, Baltim and Damietta sectors. The morphometry of the coastline along the Egyptian Mediterranean has been studied by Smith and Abdel-Kader (1988) from the analysis of satellite images. Landsat images acquired in 1973, 1978 and 1984 were compared with topographic maps from the 1930's and other historical references to the shoreline. They showed that the coastal erosion is a serious problem along the Egyptian Mediterranean Coast and it is localized at specific areas. These areas have undergone slow to moderate erosion as a result of natural decrease of the River Nile flow and due to the increased number of structures across the Nile.

Observations of long-term shoreline change and bathymetry on the inner continental shelf off the northern Nile Delta are compared by using two bathymetric maps of closely spaced soundings from 1919/22 and 1986 (Frihy et al., 1990). The changes are depicted from the analyses of 40 bathymetric profiles upto a depth of 30 m, extending about 30 km from the shore. The profiles are compared in terms of changes in water

depth, shift in bottom contours and volumetric changes in bottom sediments from which the areas of erosion and accretion are identified. These changes are generally due to long-term sediment movement in which most of the accreted sands come from eroded promontory tips as well as from offshore sources. Statistical correlation analysis indicates that areas of potential erosion and accretion are not related to sediment texture, slope and water depth. Anctil and Ouellet (1990) assess the potential sedimentological impacts of an innershelf sand extraction near the Iles-de-la-Madeleine archipelago, in the central Gulf of St. Lawrence, Canada. They found that modifications to the wave refraction patterns due to bathymetry changes are the dominant criterion. Excavations through dredging operations are then designed to limit these modifications in such a way as the resulting littoral drift changes are kept within bound specified after the local sediment budget.

Morton et al. (1993) adapted the technique of Global Positioning System (GPS) surveying to beach monitoring activities. Both the GPS and conventional beach surveying was conducted, and a new beach monitoring method employing kinematic GPS surveys was devised. This new method involved the collection of precise shore-parallel and shore-normal GPS positions from a moving vehicle. Results show that the GPS measurements agree with conventional shore-normal surveys at the 1 cm level. The application of GPS surveying techniques combined with the refinement of appropriate methods for data collection and analysis provides a better understanding of beach changes, sediment transport, and storm impacts. Nearshore coastal sand mining and its adverse effect on coastal environment of Pakiri-Mangawhai sand system, New Zealand was examined by Hilton and Hesp (1996). The results indicate that the nearshore - innershelf boundary is about 25 m isobath at Pakiri and no significant sediment transport occurs beyond this depth. This weak recovery of the Pakiri-Mangawhai coast following severe erosion in 1978 is attributed to the consequence of sand mining. They conclude that there is a high risk in nearshore coastal sand mining which will adversely affect the coastal processes and landforms.

Jackson (1999) studied the erosion/accretion of sand beaches and evaluated the performance of the criteria that predict beach erosion and accretion due to wave-induced cross-shore sediment movement. Relations based on small scale laboratory and field data were evaluated for predicting erosion or accretion of the study area. Larson et al. (1999a) presented theoretical models to determine the equilibrium profile

shape under breaking and non-breaking waves. These models produced equilibrium profile shapes of power type with the power typically in the range 0.15-0.30.

The logic and benefits of offshore coastal protection structures are addressed by Black (2001). Offshore reefs have three important "MOA" qualities (Multi-purpose, Offshore and Adjustable), which makes these structures more versatile and adaptable than sea walls, breakwaters or groins. High quality computer modelling, field datasets on surfing reef behaviour and advances in construction technology make these elegant and scientifically complex coastal protection solutions achievable. Makota et al. (2004) used remote sensing data and GIS to quantify shoreline change in Kunduchi shoreline off the Dar es Salaam coast, Tanzania. The study has revealed that during 1981–2002, more erosion took place in the northern part of the creek while deposition took place in the southern part. Between 1981 and 1992, about 2.04 ha were eroded from the northern part of Kunduchi–Manyema creek. This area has increased to more than 2.60 ha by 2002. van Lancker et al. (2004) studied the beach and nearshore area of Teignmouth, U.K. The sedimentological and morphological investigations of the intertidal and nearshore area were carried out. Sediment mobility is high during fair weather conditions owing to the strong jet like current flows associated with the presence of the narrow estuary mouth. The influence of waves and associated longshore currents cannot be neglected as they form the link between different sedimentary environments.

Miler and Dean (2004) developed a shoreline change model and calibrated/evaluated with several sets of high quality field data. The model represents the shoreline response to cross-shore processes only, requiring wave and water-level data as input. A quantitative method for evaluating the significance of changes to coastal processes that result from offshore sand mining is introduced and applied at three borrow site locations along the east coast of U.S.A. by Kelley et al. (2004). The temporal variations in wave climate and longshore sediment transport are evaluated relative to average annual conditions. They suggested a criterion for accepting or rejecting a potential borrow site, which is based on a range of one-half standard deviation (SD) about the mean.

Elsayed et al. (2005) investigated the stability of the Rosetta Promontory shoreline on the Nile Delta over the period 1988-95. The effect of the revetments constructed between 1986 and 1991 on the western and eastern parts of the promontory is a major

concern in this study. The results from the modelling are compared with those computed from beach profile data. The study shows that the shoreline along Rosetta Promontory is still unstable and that the revetments have not been efficient enough to stop the erosion. Long-term and short-term average rates of shoreline change were calculated along the Gulf of Mexico, United States by comparing three historical shorelines (1800, 1930, 1970) with an operational mean high water shoreline derived from LIDAR (light detection and ranging) surveys by Morton et al. (2005). For the Gulf of Mexico region, rates of erosion are generally highest in Louisiana along barrier island and headland shores associated with the Mississippi delta. Erosion is rapid along some barrier islands and headlands in Texas, whereas barrier islands in Mississippi are migrating laterally. Highest rates of erosion in Florida are generally localized around the tidal inlets. The sub-tidal dynamics of the Bahia Blanca Estuary, Argentina was studied by Cuadrado et al. (2005). The effect of a breakwater on currents and circulation was assessed by using bathymetric and side-scan sonar records, sedimentology, and tidal current measurements. They observed that different modes of transport occur on either sides of the breakwater. The longshore transport is the principal mode on the eastern side and tidal transport is predominant on the western side.

The shape parameter helps in determining the shape of equilibrium beach profile in terms of offshore distance and water depth (Turker and Kabdas, 2006). The shape parameter represents the effect of all the environmental factors involved in beach profile formation, such as wave climate and sediment properties. The morphological evolution of Sao Miguel beach, north coast of Ilheus - Bahia - Brazil, was studied by the measurements of beach profiles associated with granulometric analysis of beach sediments by Nascimento and Lavenere-Wanderely (2006). The result shows that the beach continues quite susceptible to the erosion in most of the coastline except for the first sector of the beach. Southern Monterey Bay, in the U.S. was the most intensively mined shoreline, where the sand is removed directly from the surf zone during the period from 1906 to 1990 (Thornton et al., 2006). They assessed the impact of sand mining and for this erosion rates along an 18 km range of shoreline during the times of intensive sand mining (1940–1990) are compared with the rates after sand mining ceased (1990–2004). Long-term erosion rates vary from about 0.5 m/year at Monterey to 1.5 m/year in the middle of the range, and then decrease northward. They

concluded that the erosion events are episodic and occur when storm waves coincides with high tides.

Ozolcer and Komurcu (2007) studied the effects of various groin parameters (length and spacing) and wave parameters (wave height, wave period and wave angle) on the accretion of the area protected by straight groin by both physical and numerical models. They found good agreement in the results of physical and numerical models. Also they compared the results of the numerical model GENESIS (Hanson and Kraus, 1991) with field data that were obtained by depth sounding at Carsibasi coasts, Trabzon Province, Turkey. The coastal erosion in the area of Kizilirmak River mouth, Turkey was examined using physical and numerical models by Kokpinar et al. (2007). A shore protection structure system, based on the results of the physical model tests were developed and implemented at the site. A one-line model was also applied for this part of the shoreline to study the problem mathematically. Observations in the field shows that the erosion was completely controlled one year after the completion of the shore protection structures. The construction of a deep water harbour jetty near Nouakchott, Mauritania significantly modified the southward longshore transport, causing severe shoreline recession (Elmoustapha et al., 2007). The UNIBEST (Delft Hydraulics, 1993) numerical model was used to study the impact of this structure and to assess the future shoreline evolution. The results, validated by field measurements, indicate that the shoreline evolution rate has undergone a 10-fold increase after harbour construction, with significant accretion to the north and severe erosion to the south of the harbour.

Mwakumanya and Bdo (2007) studied the spatial and temporal changes in beach morphology along the Nyali-Bamburi beaches in Mombasa, Kenya. The study was undertaken by analyzing the grain size distribution and the effect of the hydrodynamic conditions on the beach. They observed that beach morphology was rapidly changing with time along the shoreline and these changes were attributed to the wave and sediment characteristics. They concluded that the steep-sloping beaches were associated with strong wave energy and coarse sediments. But gently-sloping beaches were of fine, well-sorted, and positively-skewed sediments, with relatively less strong waves. Farris and List (2007) observed a strong correlation between shoreline change and sub-aerial volume change, both spatially and temporally. About 50 % of the variability in volume change is explained by the variability in shoreline change and

concluded that shoreline change is a useful proxy for sub-aerial volume change. The stability of the shoreline on the eastern side of the Rosetta promontory on the Nile Delta coast was studied by Elsayed and Mahmoud (2007). Numerical models developed by the DHI were used to calculate wave transformation from deep water to the nearshore region, compute littoral drift, and predict shoreline evolution along the eastern side of the Rosetta promontory. The results generated by the shoreline evolution model show that, in the case of applying no structures, the maximum retreat of the shoreline along the east part of the promontory is estimated to be 1405 m after 20 years. The minimum shoreline retreat along the east side of the Rosetta promontory was achieved with a system of five groins spaced at 800 m.

Birben et al. (2007) conducted experimental and numerical studies on the effect of offshore breakwater parameters (length, distance and gap) and wave parameters (height, period and angle) on sediment accumulation ratio. They concluded that the distance between breakwaters and shoreline is one of the most important factors on the variation of sediment accumulation ratio for offshore breakwaters. Another factor affecting sediment accumulation ratio is the breakwater length. The gap between the breakwaters is ascertained to have less effect on sediment accumulation ratio than the other parameters. Sediment transport inside and outside a permeable submerged breakwater was examined in the laboratory experiment combined with numerical computation by Tsujimoto et al. (2007). The study shows that the amount of sediment deposited in the breakwater decreased gradually from offshore to onshore side during the experiment, but decreased rapidly in the numerical computation. They reproduced the surface profile over the submerged breakwater.

Requejo et al. (2008) proposed a new long-term beach evolution model and is based on an analytically integrated sediment conservation equation and beach profile evolution model. The beach profile evolution model redistributes the sediment supplies or losses along the beach profile. A new formulation for the dependency between wave height and period on coastal erosion has been developed by Callaghan et al. (2008) and this includes the physical wave steepness limitation. Kroon et al. (2008) studied the seasonal, yearly and decadal (long-term) behavior of the coastal morphological features, which is derived from field data by using advanced statistical techniques. The methods proved to be useful for extracting characteristics of coastal sedimentary features concerning length scales and temporal scales. The success of the

statistical analysis strongly depends on the total size of the data set characterized by the specific spatial coverage, spatial resolution, temporal resolution, and overall length in time. The data sets from Argus video systems often meet these requirements and are of major importance for the formulation of conceptual behavior models. Payo et al. (2008) describes a procedure for calculating the uncertainty associated with the prediction of the evolution of a stretch of beach in terms of probability. The simulation of possible sequences of storm events was developed on the basis of oceanographic data records as well as empirical orthogonal functions (EOF). They presented a case study based on the evolution of an initially straight beach, where a rectangular tapered fill had been constructed. The beach is located upshore of a groin perpendicular to the coastline, and had blocked all longshore sediment transport. For this analysis, a one-line model with time-dependent boundary conditions and a non-homogeneous diffusion coefficient was utilized.

Vaselali and Azarmsa (2009) studied the influence of the breakwater constructed in the fishing port of Pozm Bay located in the northern part of the Oman Sea. The sediment movement has been studied using numerical model before and after the construction of the breakwater. Kim and Lim (2009) conducted field measurements during the mining operations in Kyunggi Bay, Korea to develop sediment parameters and source conditions for a three-dimensional sediment transport model. This was built on the Regional Ocean Modeling System (ROMS). The resulting vertical and horizontal distribution of sediment shows encouraging agreement with the field data. The resulting depositional patterns suggest that only the coarser size classes (500 and 250 μm) particles remain close to the mined site, while finer size classes are widely dispersed.

Davidson et al. (2010) forecasted seasonal to inter-annual shoreline change by using an empirical one-dimensional model which is calibrated and tested using five years of weekly video-derived shoreline data from the Gold Coast, Australia. A simple linear trend forecast of the shoreline position was used as a baseline for assessing the performance of the model. The model performance relative to this baseline prediction was quantified by several objective methods, including cross-correlation (r), root mean square (RMS) error analysis and Brier Skill tests. Hanson et al. (2010) adopted a mathematical approach and numerical model to simulate beach and dune changes. This was in response to the cross-shore processes of dune growth by wind and dune

erosion by storms, and by gradients in longshore sand transport that will alter the shoreline position. The numerical model is applied to examine the consequences of groin shortening at Westhampton Beach, Long Island, New York, as an alternative for providing a sand supply to the down-drift beach. Results indicate that the sand will be released over several decades as the shoreline and dune move landward in adjustment to the new equilibrium condition with the shortened groins. Adegoke et al. (2010) carried out a time series analysis of recent changes in the Niger Delta Coastline of Nigeria using Satellite Imagery. Landsat TM images of 1986 and Landsat ETM+ of 2003 both covering the Niger Delta area were used for this study and the images were processed using ERDAS Imagine and GIS operations. The results show that the coastline erosion was dominant over accretion.

The Coastal Modelling System (CMS) captured several key spatial trends of morphological change, at a dual-inlet system, the Johns Pass and Blind Pass system in West-Central Florida (Wang et al., 2011). They computed a sedimentation volume of 32,000 m³/year in the dredge pit at the updrift side of Blind Pass, which correlates well with the measured value of 35,000 m³/year. This shows that the calculated net longshore sediment transport rates are accurate. The rate of shoreline change for the Areao-Poco da Cruz beach in the Aveiro sandy barrier (northwest of Portugal) and the Furnas beach (southwest of Portugal) is computed by Baptista et al. (2011) based on global positioning system (GPS) in differential mode, which is a high resolution survey method. The spatial rate of the shoreline change is assessed by utilising the developed algorithms. Shoreline is monitored by using a land vehicle (motor-quad) in wide straight coastal stretches and by using an on-foot simplified version to survey small and more irregular stretches. The system-inherent errors are within the centimeter level (< 0.05 m) in both the modes of operation.

van Rijn (2011) explores the coastal cell concept to deal with coastal erosion by identifying and analysing the sediment volumes accumulated in large-scale and small-scale coastal cells at various sites. Mechanisms causing chronic erosion and episodic erosion related to coastal variability are identified. The effectiveness of soft and hard remedial measures for sandy beaches is assessed based on laboratory, field and modelling experiences. Hanson and Kraus (2011) reviewed the 25-plus year history of significant developments of the GENESIS (Hanson and Kraus, 1991) shoreline response model. This has been done in a consistent way, based on thorough literature

reviews, beta testing, comparison to beach behavior, and quality control. The challenges have been not only to represent the features themselves, but to be consistent to the basic assumptions of shoreline modeling theory.

Lopez-Ruiz et al. (2012) analysed one-line model to explain the formation and evolution of shoreline undulations on circular or elliptic curvilinear coasts. The model takes into account the variation of the surf zone width stemming from the convergence and divergence of the waves propagating over a conical bathymetry with a small radius of curvature. The alongshore sediment transport varies with the angle formed by the wave crests and the coastline, as well as with surf zone width and sediment grain size. This model was applied to the shoreline undulations observed at the mouth of the River Guadalquivir (Gulf of Cadiz, Spain) and those at El Puntal Spit (Cantabrian Sea, Spain). Plomaritis and Collins (2013) studied the interaction between macro-tidal currents and offshore breakwaters along with the resulting bed load transport processes over a spring–neap cycle along the west Sussex coastline, south coast of England. They concluded that in order to correctly predict the morphological evolution under the influence of coastal protection schemes, the tidal processes have to be studied in addition to the wave processes.

Baptista et al. (2014) compares the performance of two shoreline evolution models Long-term Configuration (LTC) and GENESIS (Hanson and Kraus, 1991) for forecasting the shoreline position scenarios for decadal temporal scales. The models were then calibrated with observed waves from the wave rider buoy, and shorelines acquired within a 5 km stretch. LTC overestimate the retreat rates, which are 30 % higher than the observed retreat, while GENESIS underestimates the retreat rates i.e.70 % lower retreats. Biria et al. (2014) predicted the sediment transport in the vicinity of submerged groin and compared with non-submerged groin. This study was focused on a part of the coast at Dahane Sar Sefidrood, Guilan Province, Iran, where critical coastal erosion has been occurred. The simulations were designed using a one-line model which can be used as a first approximation of shoreline prediction in the vicinity of groin. The result from the study show that submerged groin is an efficient way to control the sediment and beach erosion without causing severe environmental effect on the coast. Columbus Bay, located on the south-western peninsula of Trinidad, experiences high rates of coastal erosion and hence three makeshift sandbag groins were installed in the northern part of this Bay to arrest the coastal erosion

problem (Darsan and Alexis, 2014). Beach profiles were conducted at eight stations to determine the change in beach widths and beach volumes along the bay. Beach width and volume changes were determined from the profiles. A generalized shoreline response model GENESIS (Hanson and Kraus, 1991) was applied and simulated a 4 year model run. Results indicate that there was an increase in beach width and volume at five stations located within or adjacent to the groin field.

McCall et al. (2015) observed that the process-based hydrodynamic model XBeach-G can be applied to predict storm impacts on pure gravel beaches. Also the model is capable of reproducing the type of morphodynamic response of the barrier well in qualitative and quantitative sense (BSS = 0.75), with higher skill for more energetic storm conditions. Rosetta inlet, Egypt suffers from coastal problems represented in shoreline erosion, and siltation inside the inlet (Masria et al., 2015). Their study investigates different alternatives of hard and soft measures attempting to find an optimal solution for these problems (erosion and accretion) to enhance the stability of the Rosetta promontory. The interference of groins with the coastal dynamics and sediment transport was studied by Guimaraes et al. (2016), and was used to improve the numerical modeling capacity to simulate the groin impact. They compared the performance of physical and numerical studies on evaluating the evolution of updrift cross-shore profile geometry and shoreline position after the construction of a groin.

2.5.2 Indian scenario

The interaction between beach topography and wave forces in the presence of seawalls was investigated by Murty et al. (1979). The study shows that some of the structures along the Kerala coast help in stabilising the beaches at certain locations and others are responsible for severe erosion.

Murty and Varadachary (1980) discussed the profile variations of the Valiathura beach near Trivandrum using measured data. The beaches are in the stable equilibrium and well defined erosion/accretion processes are repeated every year. Varma et al. (1981) studied the erosion/accretion of the Trivandrum beach of about 2.4 km during the period of 1976-1977. From their study, they conclude that shoreline recession takes place along this coast during the two monsoons seasons and maximum erosion is noticed during the months of July-August (south-west monsoon period). Sheno and Prasannakumar (1982) identified areas of possible erosion and accretion

along the shoreline from Andhakaranazhi to Azhikode on the Kerala coast. According to their study, the coastline showed an erosional tendency under the influence of waves approaching from 220° and 240° and an accretional tendency under the influence of waves from 280° and 300°.

Mallik et al. (1987) studied the erosion-accretion scenario of the coastal zone of Kerala and carried out beach profiling at 5 km intervals along the 560 km stretch of the Kerala coast during the pre- and post-monsoon seasons. Beach volume changes were calculated at each profile station, and the erosional and accretional trends for the entire coastal tract were found out. Total erosion along 55 stations is 1276 m³/m, and accretion is 626 m³/m, with a net erosion of 650 m³/m. Beach profile and longshore current data measured bi-monthly for a year were analysed by Samsuddin and Suchindan (1987) to understand the relationship of the longshore current to the beach erosion and accretion phenomena in the northern Kerala coast. Their study indicates that the longshore current activity can be linked with a depositional phase dominated by northerly current; a transitional phase with perceptible erosion showing reversal in current direction; and an erosional phase dominated by a southerly current. The intensity of the longshore current and the rates of erosion and accretion are directly related.

Thomas (1988) studied the erosion/accretion processes along the beach of Valiathura, southwest coast of India. The result shows that the beach is in equilibrium due to the cyclic erosion/accretion processes and erosion is mainly due to monsoonal wave attack. The dominating mode of sediment transport that causes beach morphological changes is the on-shore-offshore transport. This study established relationship between various stages of beach development, parameters of beach profiles like beach slope and prevailing wave and current parameters. The littoral processes along the Alleppey coastal sector, southwest India was studied by Hameed (1988) using nearshore wave data, LEO data and beach profiles for the period 1981-1984. The results show that the beach profiles reach the highest level during the pre-monsoon months and reach their nadir during July. It is also observed that the beach has advanced with an accretion of about 30-60 m³/m of sand and attained dynamic equilibrium by the end of the year 1982. Kurian (1988) studied the littoral processes along the Calicut coast, southwest India. The study reveals that the beach undergoes considerable seasonal changes in accordance with the nearshore wave characteristics.

The groin effect of the pier and other man-made features also influence the beach dynamics. The northern stretch of the beach responds more or less in a uniform manner and the southern stretch shows considerable variance. The beach processes along the Tellicherry coast, further north of Calicut is studied by Harish (1988). From this study, it is observed that the beach development along this coast is controlled by the offshore stack and the tombolo behind it, in addition to the wave-related processes. Maximum change in the beach occurs along the southern sections of the beach. Also the erosional trend of the beach is established by using the empirical eigen function analysis.

Samsuddin et al. (1991) observed for the north Kerala coast that the obliquely approaching swell waves generate northerly longshore currents during non-monsoon seasons which are favorable for the accretion of beaches. Also the foreshores in the accreted zones are gentler and are characterized by finer sediments. Hanamgond and Chavadi (1993) studied the erosional and accretional behaviour of Aligadde Beach, Uttara Kannada District, west coast of India. Monthly measurements of beach profiles over a period of three years (1988-1991) disclose spatial as well as temporal changes in beach configuration in response to different environmental processes. Empirical Orthogonal Function (EOF) analysis and volume changes have been compared to understand the on-offshore sediment movement. Their study revealed that the beach morphology undergoes cyclic seasonal changes in response to the changing wind and wave climate in three distinct phases viz. major erosional phase during May-August, accretional period during fair weather, and minor erosional phase during December-February.

Sajeev et al. (1996) estimated the mean grain size distribution under different environmental conditions along the Kerala coast. Their results show considerable spatial variation in the mean grain size in the range of 0.14-0.96 mm. Sreekala et al. (1998) studied the long-term erosional/accretional trend along the Kerala coast by using the satellite imageries (IRS-1A) and aerial photographs for the year 1990, and the survey of India toposheets of 1967. They identified the sectors undergoing erosion/accretion and classified as low erosion/accretion zone for the shoreline change upto 100 m, moderate zone for the change between 100 m and 200 m, and high for the change above 200 m. They concluded that about 148 km of the coastline which also includes some areas protected by seawalls was under erosion and 304 km under

accretion. This study also shows that about 30 km of the coast comes under high erosion category and 21 km of the coast shows high rate of accretion.

Mishra et al. (2001) studied the wave breaker characteristics, sediment budget and beach profiles along an 11 km stretch of an open-coast port which was constructed at Gopalpur, east coast of India. Monthly beach profile changes revealed that during the SW monsoon the entire coast is affected by heavy erosion and the coastline recedes by about 30-40 m. Erosion/deposition take place intermittently from October, however deposition was the dominant feature. Analysis of multi-date satellite data indicates loss of 1836 ha of land during 1976–2001 along the Godavari deltaic coast (Hema Malini and Rao, 2004). A decrease in the sediment load from an annual average of 145.26 million tons in 1971–79 to 56.76 million tons during 1990–98 is observed by them. This is attributed to construction of dams which diminished the vertical accretion at the delta and the sea level rise led to the shoreline retreat. The study indicates that the problem may compound in future causing irreparable damage to this important deltaic ecosystem.

Multi-temporal satellite data has been used by Hanamgond and Mitra (2007) for determining coastal erosion/accretion, identifying beach ridges and tectonic influence at Karwar coast, central west coast of India. The study shows that the coast has experienced net erosion during the 13 years of observation. The net erosion is of 661.86 and 924 hectares during 1989-2000 and 2000-2003 respectively. This study indicates that the erosion of land was dominant during 2000-2003 which could be mainly due to the human interference. Jayakumar et al. (2008) studied the changes in the beach profiles, longshore currents, breaking wave characteristics in the surf zone at selected locations along the Tamil Nadu coast after the tsunami event of December 2004. The post-tsunami observations were compared with the earlier studies to establish the variations in the littoral environment. They observed that the shoreline receded by about 20 m and backshore was built-up by about 0.5 m at most of the locations of the coast. Rajith et al. (2008) studied the erosion/accretion pattern along the Chavara coast, southwest coast of India based on a monitoring of the coast for a period of 5 years starting from 1999. They concluded that in addition to the natural hydrodynamic forces, anthropogenic activities like sand mining and construction of seawalls/breakwaters have also contributed to the beach erosion/accretion along the coast. They also concluded that the impact of sand mining is not felt on the beach

when the mining is within an optimum level, equivalent to the natural replenishment from offshore.

Foreshore morphodynamic processes in the vicinity of the Sharavati estuary at Honnavar, central west coast of India, were studied by Hegde et al. (2009) based on the wave refraction analyses, sediment characteristics and foreshore morphological changes. Nearshore coastal processes and wind largely control shore-face modification of the beaches to the south of the river mouth. The islands in this region modify the geomorphic processes of beach to the north of the river mouth. Northerly drift prevailing during the post-monsoon season favours spit growth across the river mouth, whereas the southerly drift during December to February is responsible for erosion to the north of the river mouth. Westerly wave approach during March-April leads to the development of littoral cells in the vicinity of river mouth that provides stability to the beach. Manimurali et al. (2009) analysed the multi-temporal satellite images of Indian Remote Sensing Satellites from 1998 to 2005 to monitor the coastal environment of Paradip, east coast of India. The resultant coastal vector maps were used to estimate the geomorphological changes and shifting of the shoreline position. The shoreline maps were compared with the 1973 Survey of India toposheets to estimate the changes which have occurred in the region. They estimated a net increase in shoreline length of about 7.26 km and a net loss of beach area of 15.6 km² between 1973 and 2005.

A study of the beach erosion/accretion processes during south-west monsoon and its numerical modelling is attempted by Shamji et al. (2010) for a micro-tidal high-energy beach. The model LITPROF of the LITPACK software of DHI is found to simulate well the beach morphological changes by adjustment of the calibration parameters. The integrated cross-shore transport computed across the profile, using the model shows high erosion in the beach face coupled with an equivalent accretion in the offshore. Detailed investigations were taken up by Gujar et al. (2011) to analyse the volumetric and morphologic variations of the beaches between Pirwadi and Sarjekot of South Maharashtra, central west coast of India. They studied the seasonal topographic profiles for the period from October 2004 to December 2005. The results shows a number of erosional hotspots along this coastal sector which may be due to the influence of rip currents, wave dynamics, variable coastal configuration, beach gradient etc. Qualitative and quantitative studies on changes of coastal

geomorphology and shoreline of Karnataka, west coast of India have been carried out using toposheets of Survey of India and satellite imageries (IRS-P6 and IRS-1D) by Vinayaraj et al. (2011). Changes during 30 year period are studied at each selected station. Their study indicates that gradual erosion is observed at Karwar spit along the northern side of the Kali river mouth, the spit at the southern side of the Sharavathi river mouth and at some regions of Kundapur.

Cross-shore beach profiles and textural characteristics of foreshore sediment were analyzed by Udhaba Dora et al. (2012) for understanding an annual cycle of intertidal beach dynamics at Devbag, Karwar, Karnataka. The field observation on beach dynamics during February 2008 to February 2010 showed both erosion and accretion. The net result over an annual cycle was the sediment accretion. They proposed that the short-term beach erosion along the Devbag shoreline can be minimized by increasing the beach width through beach nourishment. Mohanty et al. (2012) studied the impact of groins on the beach morphology and shoreline change along the Gopalpur Port, east coast of India. Their study shows the impact of groins with erosion and deposition in the beaches on the north and south of the groin respectively. The rate of deposition on the south beach is much faster than the rate of erosion on the north, which is estimated from the analysis of beach volume, beach width, and beach area.

Roy Chowdhury and Sen (2013) studied the shoreline changes of the Sagar island which is a miniature form of Ganga-Brahmaputra delta. This area faces severe erosion both by natural and anthropogenic activities and the increasing rate of coastal erosion plays an important role in the shoreline change. Chandrasekar et al. (2013) classified the vulnerable risk zones of the southern tip of India using shoreline change analysis and coastal vulnerability index (CVI). The shoreline change analysis has been carried out by automatic image analysis techniques using multi-temporal Landsat data during the year of 1973, 1992, 2000 and 2006. The result shows remarkable erosion along the coastal sector. The CVI index was also established by them. The beach profile data from Ovari to Kanyakumari beach, south east India has been analysed by using empirical orthogonal function (EOF) analysis (Saravanan et al., 2013). They identified the characteristic patterns of temporal and spatial variations in the sediment volume of the beaches. The result shows that variation in the beach sediment volume is determined by interaction between the biennial and seasonal exchanges. Evaluation

of coastal erosion and accretion processes along the southwest coast of Kanyakumari, Tamil Nadu was carried out by Kaliraj et al. (2013) using multi-temporal Landsat satellite images from 1999 to 2011. The long-term coastal erosion and accretion rates have been calculated for the periods between 1999 and 2011. The subsequent short-term changes were performed during 1999–2000, 2005–2006 and 2010–2011. The long-term coastal changes indicate that the net erosion rate is higher on the coasts of Kanyakumari, Kovalam, Manavalakurichi, Mandaikadu, and Thengapattinam. Coastal beaches, beach ridges, and marine terraces are predominantly disturbed by the hydrodynamic processes including wave action, littoral current, and intervention of littoral drift by the artificial coastal structures.

The processes of shoreline morphological changes from Veli to Varkala along Thiruvananthapuram coast are analyzed using numerical models by Noujas et al. (2014). Shoreline changes, nearshore processes and beach characteristics along this sector are studied through extensive field observations. The data is used to calibrate and validate sediment transport and shoreline change models for this coast. Sediment transport and shoreline changes are simulated using different modules of LITPACK model and the calibration of the model is done with field observations. The result shows that the beach sediments get deposited on southern side of the breakwater and bypassed sediment gets deposited at the inlet mouth. The study by Udhaba Dora et al. (2014a) describes short-term dynamics of inter-tidal sedimentary environment at beaches along the micro-tidal coast of Karwar, west coast of India. Correlation is established between cross-shore morphodynamics and textural characteristics of surface sediments. The sedimentary environment is examined for a complete annual cycle using monthly collected cross-shore profiles and sediment samples. The beach dynamics along with the propagation of south-west and west-south-west waves towards the coast significantly exhibit a dominance of northward sediment transport with the existence of a northerly longshore current. Foreshore morphology and morphodynamics were examined by Udhaba Dhora et al. (2014b) to identify stability of two micro-tidal sandy beaches, Kundapura and Padukare, along the Karnataka coast, west coast of India during three annual cycles from March 2008 to March 2011. The net observation at both sites exhibits slow rate of sediment accretion followed by non-uniform sediment erosion and accretion processes. Study revealed that the beaches are not favorable for recreational activity because of their narrow width and

steeper slope. During summer monsoon, the absence of backshore zone at Padukare makes it more vulnerable to erosion than Kundapura beach.

Shoreline change mapping on 1:25,000 scale for the entire Indian coast based on multi-date satellite data in GIS environment has been carried out by Rajawat et al. (2015) for 1989–1991 and 2004–2006 time frame. The results show that 3829 km (45.5 %) of the Indian coast is under erosion, 3004 km (35.7 %) is getting accreted, while 1581 km (18.8 %) of the coast is more or less stable in nature. The analysis shows that the Indian coast has lost a net area of about 73 sq. km during 1989–1991 and 2004–2006 time frames. Sand mining along Ponmana coast, Kerala and land reclamation along Mumbai, Maharashtra are crucial, which alters the sediment dynamics and triggers coastal erosion. This information has been used by them to prepare a Shoreline Change Atlas for the Indian Coast. Mohanty et al. (2015) studied the shoreline movement at Gopalpur, Odisha, east coast of India and found shoreline advance towards sea (deposition) on the south and shoreline retreat (erosion) on the north of Gopalpur Port. The rate of deposition is higher as compared to the erosion. Beach width and volume changes also corroborate well with the above observations. The impacts due to the construction of groins and breakwaters were also analyzed.

2.6 Salient Conclusions from the Literature Survey Relevant to the SW Indian Coast

The coastal sector of south-west coast of India has maximum beach width during fair weather period and minimum during the monsoon. Waves approaching the coast are mostly swell waves during fair weather, and sea waves during the peak monsoon periods. The beach erosion is observed during the monsoon period due to the effect of steep waves, and the beach gets recovered during the fair weather period due to the action of swell waves. The highest wave height and shortest wave period are observed during the peak monsoon (June-July) and lowest wave height and longest wave period during the fair weather period. In general, the longshore currents are northerly during fair weather period and southerly during peak monsoon periods. The innershelf currents are predominantly southerly irrespective of the seasons but need not be strong during monsoon as in the case of waves.

There are several studies on estimation of longshore sediment transport (LST) for the surf zone of different coastal locations. The LST is commonly computed by using

bulk formulas. Estimation of cross-shore sediment transport is rather scanty. Numerical modeling is emerging as an important tool for analyzing and studying sediment dynamics in the coastal zone. It is to be noted that the local wind data are not being incorporated which is crucial while doing the numerical modeling of nearshore processes. Fine grid bathymetry also is critical in getting the desired accuracy in simulations using numerical models.

Studies on erosion/accretion scenario of different locations of the coastline are several, but integration of the results of such studies with the sediment transport regime through numerical modelling is lacking in many cases. Most of the studies point to the occurrence of erosion at many coastal locations which till recently were stable and the role of anthropogenic factors as causative factors in such cases is quite evident.

CHAPTER 3

DATA AND METHODOLOGY

3.1 Introduction

Nearshore hydrodynamics are highly non-linear and the physical processes behind this can be analyzed by utilizing the data collected from the field programmes and also by establishing the numerical modelling systems. The observational data are of immense importance in order to understand the actual coastal processes. Deployment/retrieval of equipments in the offshore and sediment sampling were the most challenging tasks under the field programmes. The field programmes undertaken during the period 2010-2014 included the measurements of wind, wave and littoral environmental parameters in addition to beach profile survey and shoreline mapping. Seasonal sediment sampling from the beach, surf zone and innershelf and collection of sediment cores from innershelf were meticulously carried out. Bathymetric survey was carried out in the study area during the fair weather period of April 2010 by using a shallow water echo-sounder integrated with GPS using HYPACK hydrographic software and bathymetric chart prepared. Collation of secondary data was also taken up simultaneously. The methods adopted in the field data collection, data processing and numerical computations are detailed in the following sections.

3.2 Instruments Used

The instruments used for the field data collection includes the wave rider buoy, automatic weather station, echo-sounder, global positioning system, dumpy level, sediment traps, grab sampler and piston corer. The descriptions of the instruments utilized in the data collection are detailed below.

3.2.1 Wave rider buoy

The wave data for the study were obtained from the Directional Wave Rider Buoy (DWRB) DWR-Mk III of 0.9 m diameter, manufactured by M/s Datawell bv, The Netherlands, which measures the wave parameters such as height, period and direction (Fig. 3.1). The buoy was deployed off the Chavara coast (Fig. 3.2) jointly by the Indian National Centre for Ocean Information Services (INCOIS) and National Centre for Earth Science Studies (NCESS) for the real-time validation of Ocean State Forecast issued by the INCOIS. The DWRB consists of a heave-pitch-roll sensor

(Hippy - 40), a 3-axes flux-gate compass and two fixed X and Y accelerometers. The accelerometers are placed on a gravity stabilized platform and this platform is formed by a disk, which is suspended in the fluid within a plastic sphere placed at the bottom of the buoy. Two vertical coils are wound around the plastic sphere and one small horizontal coil is placed on the platform. The pitch and roll angles are determined by measuring the coupling between the fixed coil and the coil on the stabilized platform. The result of the measurement gives the sine of the angles between the coil axis and the horizontal plane. The components of the earth's magnetic field in the direction of the x- and y-axis and the direction of z-axis are measured by means of a fluxgate compass.

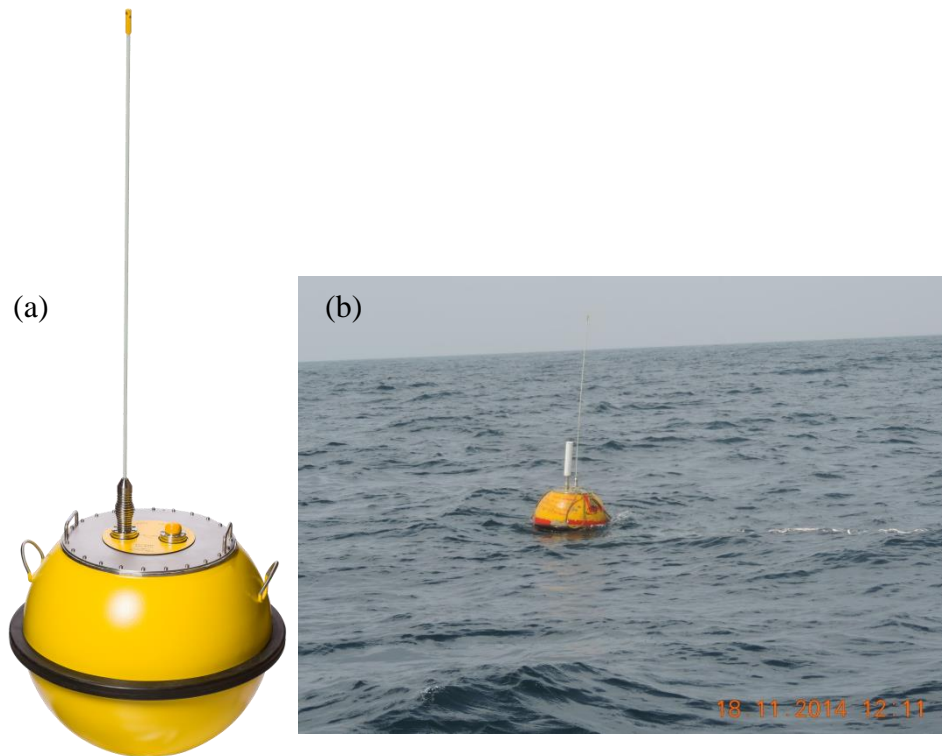


Fig. 3.1 (a) Directional WRB, (b) DWRB deployed off Chavara, Kollam at 22 m water depth

The three accelerometers measure the vertical, north and west accelerations of the buoy. The vertical accelerometer yields the measurement of wave height. All these accelerations are then digitally integrated twice to get displacements (elevations) and filtered to a high frequency cut-off at 1.5 Hz, by applying a low-pass filter. The filtered sensor outputs are then sampled and transformed to north, west and vertical accelerations all at a rate of 3.84 Hz. The direction measurement is based on the translation principle, where the horizontal motions of the buoy instead of wave slopes

are measured and this motion is correlated with the vertical motion of the buoy (Datawell, 2009). The specification of the wave rider buoy DWR-MKIII is shown in Table 3.1.

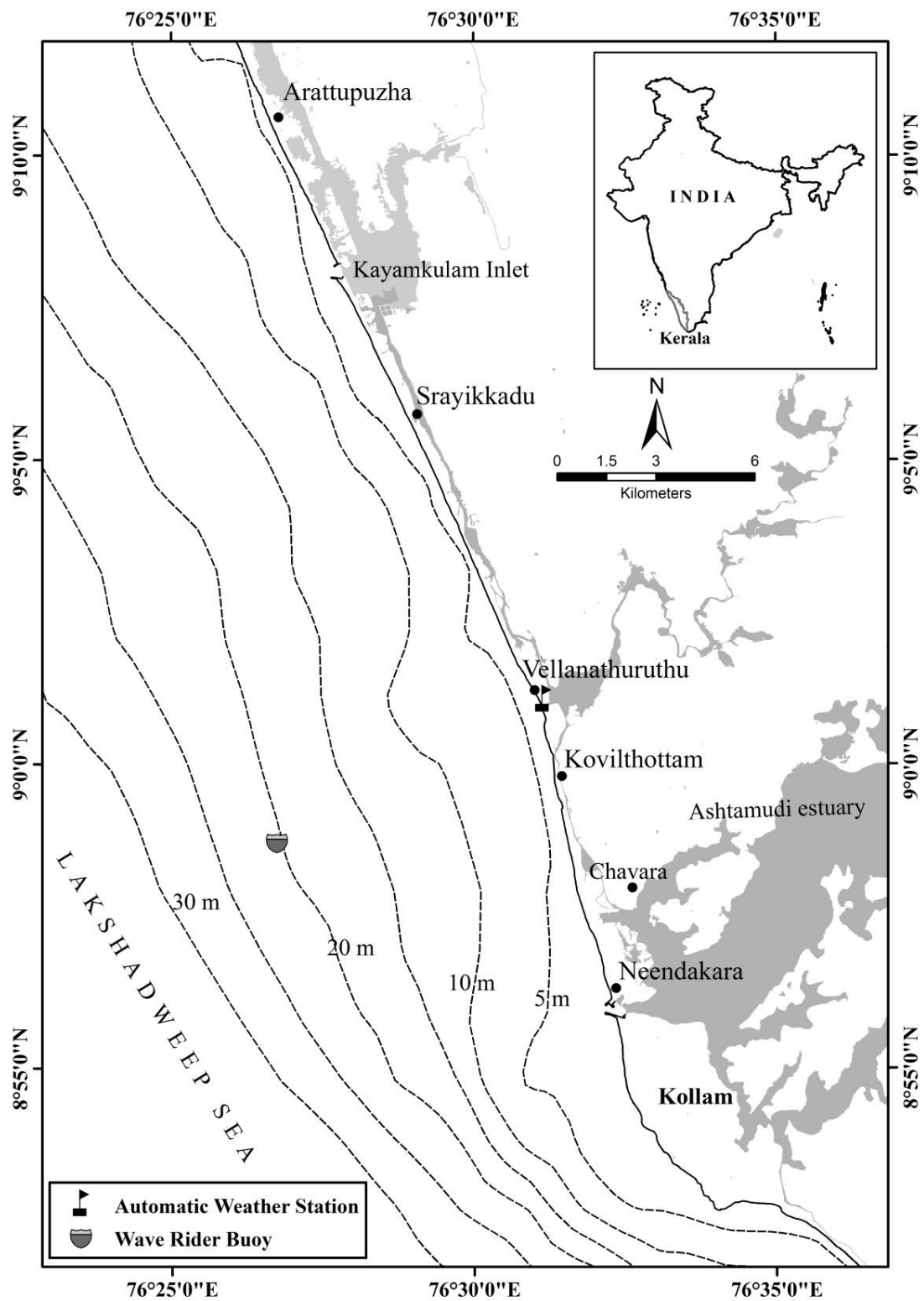


Fig. 3.2 Locations of deployment of wave rider buoy and automatic weather station at Chavara coast

The complete system consists of the Directional Wave rider, Directional Wave rider Receiver RX-C and a personal computer running the software Waves-21 for display and data storage. The signals from the buoy deployed in the sea are transmitted in 27.705 MHz that is picked up by the antenna of the receiving station and processed by RX-C receiver and the computer. The buoy has a transmitter of range upto 50 km.

Mooring system

The mooring assembly for the DWRB (Fig. 3.3) consists of:

- 1 m long stainless steel chain connected below the buoy followed by a 30 m rubber cord with a PP rope running parallel to the rubber cord (such that every 3 m length of the PP rope is tied to every 1 m length of rubber cord)
- 5 kg float (1 no.) attached to the bottom end of the rubber cord
- 25 m long bottom mooring line of 12 mm PP rope attached below the rubber cord with a sinker in the middle (1 kg weight)
- 3 kg float attached at about 5 m above the bottom end of the mooring line
- bottom chains (2 nos. of 5 m long chain for connecting the anchor weights)
- anchor weights (3 individual anchors of approximately 125 kg) at the end

*Table 3.1 Specification of wave rider buoy DWR-MKIII
(Source: Datawell, 2009)*

Parameter	Value
<i>Heave</i>	
Range	-20 to +20 m
Resolution	0.01 m
Accuracy	< 0.5 % of measured value after calibration
Period time	1.6 s to 30 s
Cross sensitivity	< 3 %
<i>Direction</i>	
Range	0 ° to 360 °
Resolution	1.5 °
Reference	Magnetic North
Buoy heading error	0.5 °
<i>Filter</i>	
Sampling frequency	3.84 Hz
HF data output rate	1.28 Hz

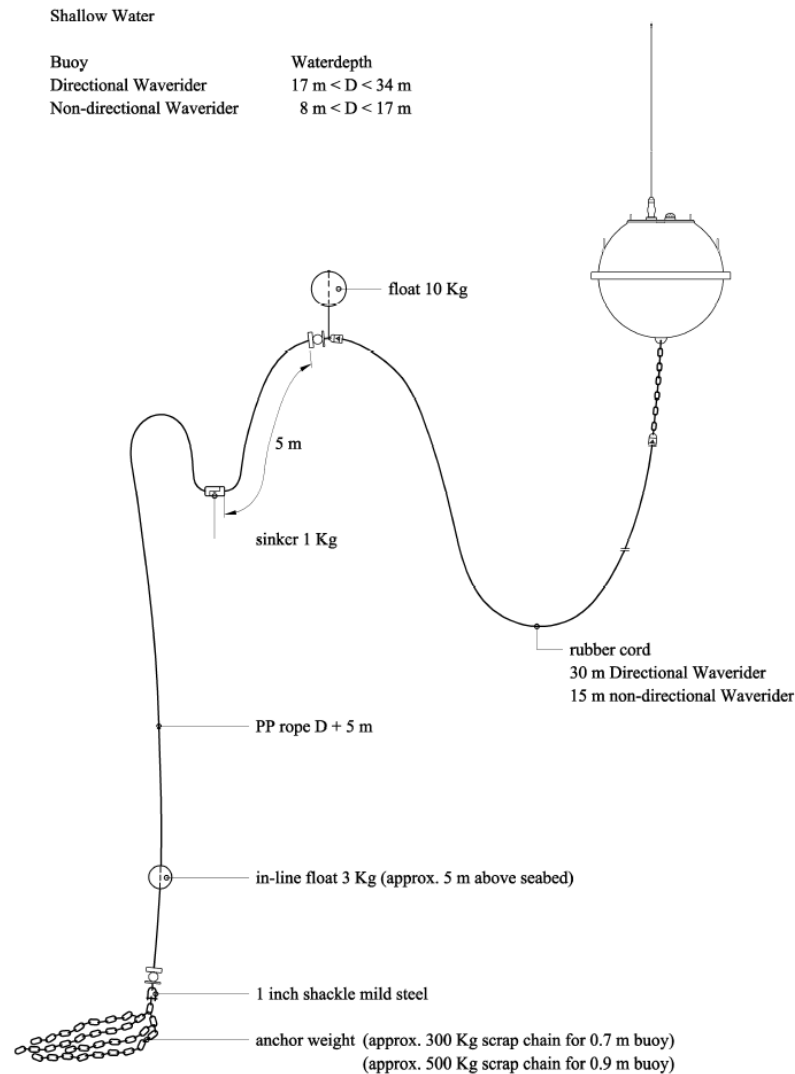


Fig. 3.3 Typical mooring layout for a directional wave rider buoy for shallow waters (Source: Datawell, 2009)

3.2.2 Automatic weather station

For collecting the coastal wind data, an Automatic Weather Station (AWS - Campbell Scientific) was used (Fig. 3.4). In this AWS, wind speed is measured with a helicoid-shaped four-blade propeller, where the rotation of the propeller produces an AC sine wave signal with frequency proportional to the wind speed. Wind direction is measured using the vane which is coupled to a 10 K Ω potentiometer and the output voltage is proportional to wind direction by applying a precision excitation voltage. The AWS was installed at a height of about 10 m above MSL on the beach at Ponmana, Chavara coast (Fig. 3.4c).

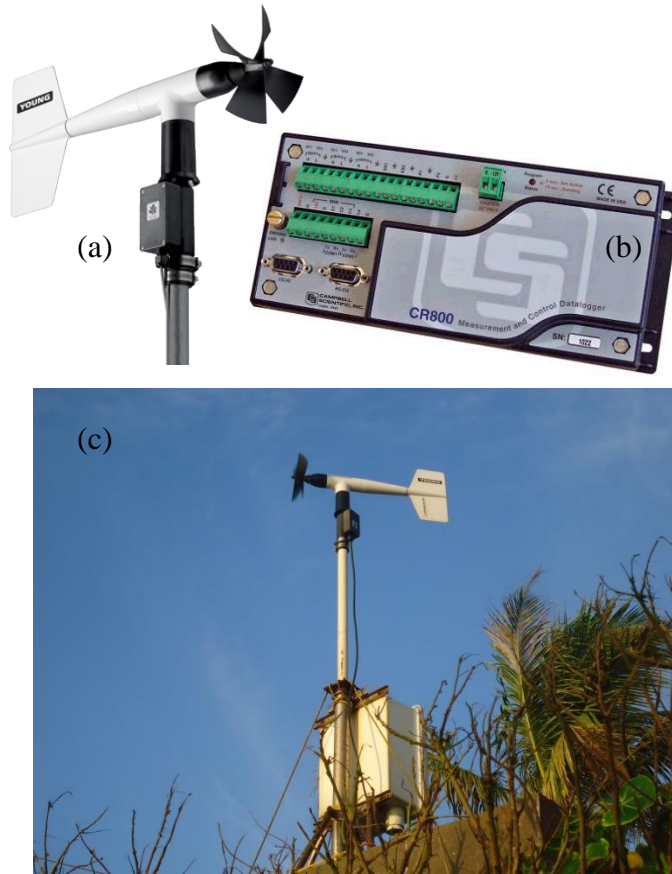
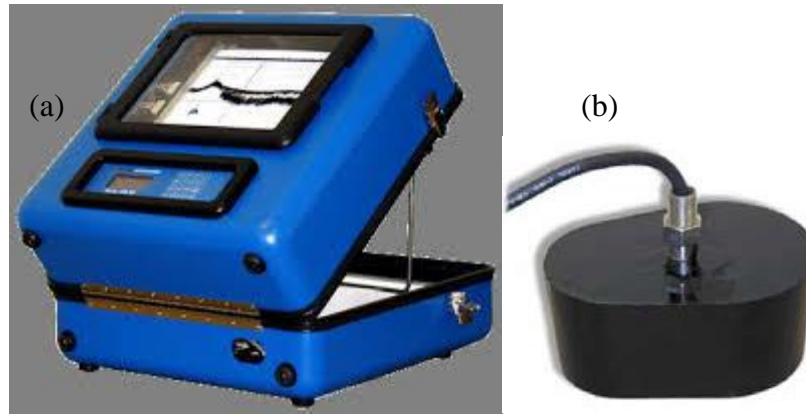


Fig. 3.4 AWS: (a) wind speed and direction sensor (RM Young) and (b) data logger (Campbell Scientific) installed in the beach at Ponmana, Chavara coast (c)

3.2.3 Echo-sounder

The echo-sounder used for depth sounding is a Bathy-500 dual frequency echo-sounder manufactured by Ocean Data Equipment Corporation, U.S.A. (Fig. 3.5). The dual frequency Bathy-500 is operating in 33/210 KHz. It provides important parameters such as depth, speed of sound and offset for draft/tide. Depth sounding data is available to external devices in digital form, via an interface and the digital depth data can be obtained in standard RS-232/422 formats or NMEA-0183. The echo-sounder was interfaced to the HYPACK software through RS-232 interface.

At shallower depths less than 5 m where the mechanized boat with Bathy-500 cannot operate, a Ceeducer Pro manufactured by Bruttour International Ltd., Australia (Fig. 3.6) was used. It comprises of an echo-sounder and GPS integrated into a single platform. The Ceeducer has a general purpose hydro survey transducer working at 200 KHz with 8° beam width for measuring the soundings and a Hemisphere Crescent SX-2 GPS for fixing the locations of sounding. The interface with Ceeducer Pro was provided by using HYPACK software.



*Fig. 3.5 (a) Bathy-500 Echo-sounder (Ocean Data Equipment Corporation, U.S.A.),
(b) 33/210 KHz dual frequency transducer*

HYPACK Software

The hydrographic survey software HYPACK (version 6.2), developed by HYPACK Inc. U.S.A. is used to integrate the received signals of GPS and soundings. This is also used for preparing the survey lines, navigation of the boat along the survey lines and processing of the data by applying the tidal and other corrections.

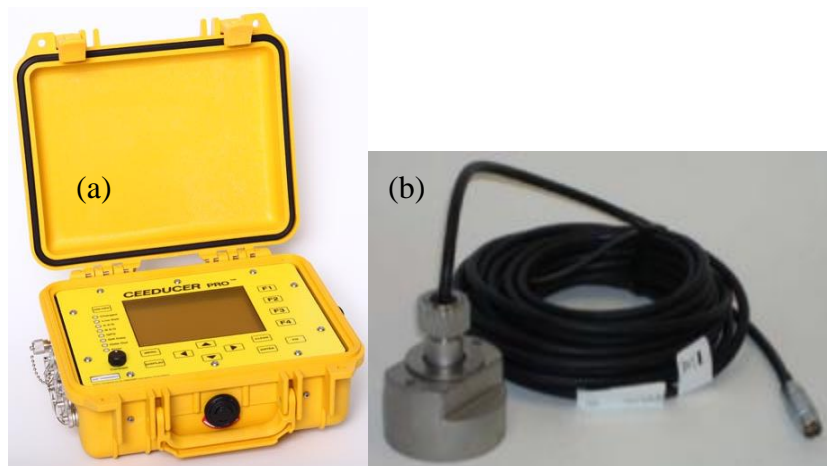


*Fig. 3.6 (a) Ceeducer Pro echo-sounder (Bruttour International Ltd., Australia),
(b) 200 KHz hydro survey transducer*

3.2.4 Global positioning system

The Global Positioning System (GPS) consists of a network of 24 satellites placed into orbit at an altitude of about 20,000 km at an inclination angle of 55° with 11 hour 58 minute period, having an orbital velocity of 3.9 km/s. A GPS receiver calculates the position on the ground based on triangulation method (Fig. 3.7) and the positioning is achieved by measuring the time taken for a signal to reach a receiver. The method of triangulation requires the receiver to know the precise time that the

signal was transmitted and received. The atomic clocks used in the satellite gives the most accurate time so that the receiver on the ground can compare the time delays between the satellite signals to compute its position anywhere on the earth. The L-band radio wave used to communicate to Earth from the satellites is effectively immune to local atmospheric conditions such as rain, storms etc. The satellites broadcast two L-band signals (L1 and L2) operating at the frequencies, L1 = 1575.42 MHz and L2 = 1227.6 MHz. Civilian GPS uses the L1 frequency band and the L2 is used for the military applications. In the present study Trimble Juno SB is utilized for position fixing related to various applications such as shoreline mapping, echosounding. This is a high sensitivity GPS receiver having a positional accuracy of about 2 - 5 m after real time differential correction. Higher positional accuracy of about 1 - 3 m is obtained by adopting post-processing techniques.

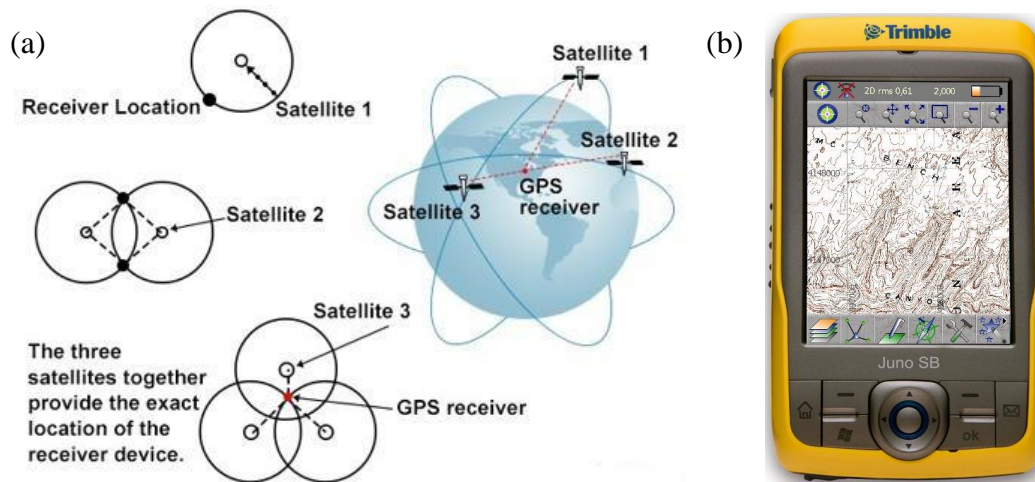


Fig. 3.7 Global positioning system (a) operational principle, (b) GPS receiver (Trimble Juno SB)

3.2.5 Dumpy level

Beach profile measurements were conducted by using the level and staff method by using a dumpy level and staff manufactured by Leica Geosystems (Fig. 3.8). These profiles taken normal to the beach gives a cross-sectional profile of the beach. A typical beach profile shows the variation of the elevation with distance from a fixed benchmark. The leveling staff used for the profile survey have a least count and accuracy of 1 cm and 0.01 cm respectively.

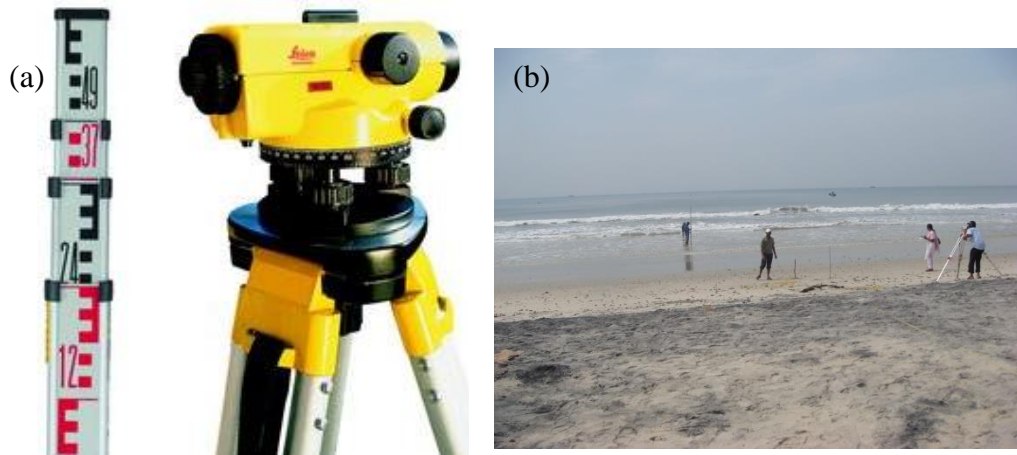


Fig. 3.8 (a) Dumpy level and staff (Leica Geosystems) used for the beach profile survey, (b) Beach profile measurement at the Chavara coast

3.2.6 Sediment traps

The sediment traps used for the study were fabricated in house using high quality PVC pipes with suitable end caps and reducers (Kurian et al., 2002). Two types of sediment traps were used for the collection of suspended sediments. The normal ones are vertical type with a height of 40 cm and diameter 9 cm for sampling suspended sediments. The other type is horizontal one which is of same diameter, but with a length of 60 cm and is used for installing at the bottom layers where there is high sediment load. Both the types have a nozzle or reducer in the top to provide a reduced opening of 4 cm for use in monsoon when there is high suspended load. The horizontal traps are at the bottom at elevations in the range of 20-30 cm and vertical traps at heights of 50, 75, 125 and 200 cm approximately (Fig. 3.9).

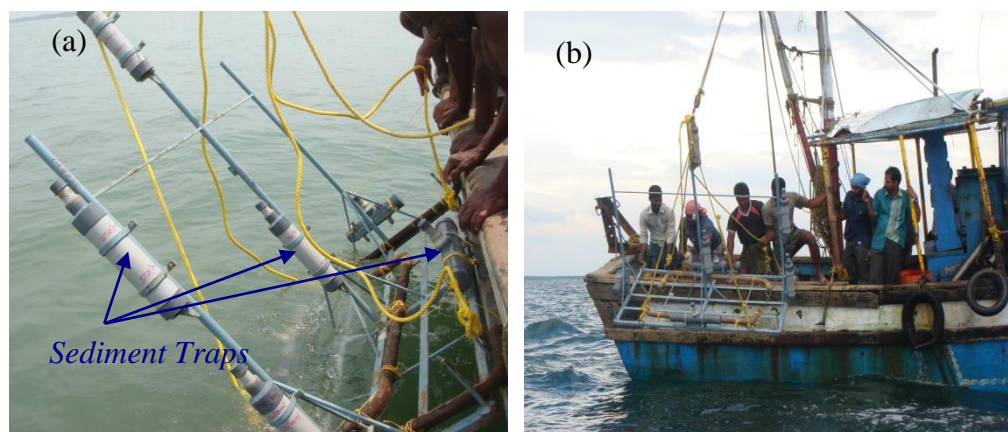


Fig. 3.9 (a) Sediment traps attached to the housing, (b) Deployment of sediment traps offshore of Chavara

3.2.7 Van Veen grab

Van Veen Grab sampler is used for collection of surficial sediments in the innershelf. The grab is of Van Veen design, made of AISI 316 stainless steel of 3 mm plate thickness having sample area of 1000 cm² and is manufactured by M/s. KC Instruments, Denmark A/S (Fig. 3.10).

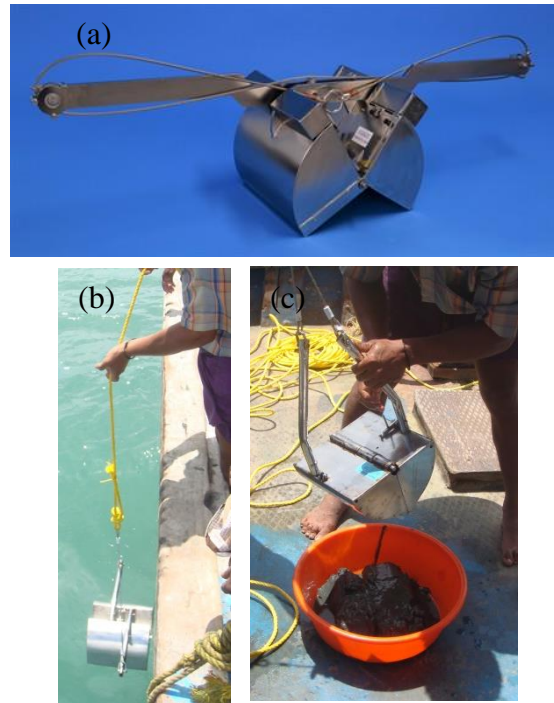


Fig. 3.10 (a) & (b): Van Veen grab (KC Instruments, Denmark) used for nearshore surficial sediment sampling, (c) Surficial sediment samples collected from the nearshore of Chavara using the grab

3.2.8 Piston corer

Sediment coring was carried out using a Piston Corer, procured from M/s. KC Instruments, Denmark A/S, which is capable of collecting undisturbed sediment cores upto 4.5 m length (Fig. 3.11). The instrument consists of a long, heavy steel tube of 1.5 m length with weight attached on top and is plunged into the sea floor to extract the undisturbed samples from the water body. To extend the length of the corer the individual steel tubes of length 1.5 m are linked using a couple device and is fastened by spikes. The piston is lowered inside the core pipe which is attached to a trigger weight called Kullenberg releasing unit.

The piston corer works like a syringe. During the lowering of Corer from the boat using davit and winch facility the Piston will be at the bottom of the pipe or just above

the core catcher. As soon as the trigger weight hits the bottom of the sea bed free fall of the coring apparatus is activated. The action of the piston creates a pressure differential at the top of the sediment column and the piston inside pulls up and sediment enters through the core catcher. The recovery of sediment depends upon the nature of sediment present (Fig. 3.11a).

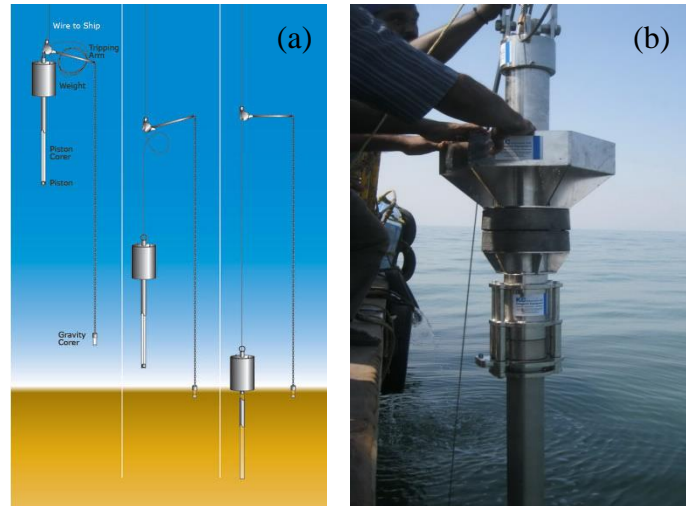


Fig. 3.11 Piston Corer: (a) principle of operation, (b) piston corer being lowered in the offshore of Chavara for sediment coring

3.3 Scheme and Methodology Followed for Data Collection

In order to understand the beach and nearshore processes, field experiment was designed and various oceanographic and sedimentological parameters measured in the offshore and beach adjoining the Chavara coast. The methodology adopted for the present study is discussed in the following sections.

3.3.1 Waves

The wave data used for the study are from the wave rider buoy deployed off Ponmana, Chavara coast as described in Section 3.2.1 at about 22 m water depth (Lat. 8° 58' 41.8" N; Long. 76° 26' 40.6" E) which is approximately 9 km from the shore. The wave rider buoy was preset for the collection of continuously recording vertical and horizontal displacement (eastward and northward) data and is obtained by double integration of the respective acceleration signal. The data was recorded for 30 minutes duration at a frequency of 1.28 Hz at every half an hour during the measurements. A total number of 256 heave samples (i.e. $N = 256$) were collected for every 200 seconds interval and FFT is applied to obtain a periodogram in the frequency range 0.033 - 0.58 Hz (i.e. 30 s - 1.7 s). The wave parameters such as significant wave

height, peak period, zero-crossing period, predominant wave direction (PWD) etc. are derived from the respective first, second or fourth order spectral moments of the wave spectrum (Datawell, 2009). The wave spectrum $E(f)$ gives the variance density at a frequency f , the n^{th} order spectral moment m_n is given as

$$m_n = \int_0^{\infty} f^n E(f) df \dots\dots\dots(3.1)$$

where $n = -1, 0, 1, 2$ etc. The wave parameters can be defined as

$$H_{m0} = 4\sqrt{m_0} \dots\dots\dots(3.2)$$

$$T_{m01} = \frac{m_0}{m_1} \dots\dots\dots(3.3)$$

$$T_{m02} = \sqrt{\frac{m_0}{m_2}} \dots\dots\dots(3.4)$$

where H_{m0} is the significant wave height, T_{m01} is the mean period, T_{m02} is the zero-crossing period, m_0 is the zeroth-order spectral moment which gives the area under the spectral density curve, represents the variance of the surface elevation processes. m_0 also represents the total energy of the waves. The first order spectral moment (m_1) gives the mean value. The second-order spectral moment (m_2) represents the variance of the wave elevation velocity.

The spectral width parameter ε is a measure of the root mean square width of a wave energy density spectrum defined as

$$\varepsilon = \sqrt{\left(1 - \frac{m_2^2}{m_0 m_4}\right)} \dots\dots\dots(3.5)$$

The fourth-order spectral moment (m_4) represents the variance of the wave elevation acceleration. An alternative spectral width parameter ν is given by Longuet-Higgins (1975) as

$$\nu = \sqrt{\left(\frac{m_0 m_2}{m_1^2} - 1\right)} \dots\dots\dots(3.6)$$

Uncertainty in the estimates of m_2 and m_4 has led to the use of another shape parameter, namely, spectral peakedness parameter, Q_p of the wave spectrum. This parameter has been introduced by Goda (1970) and is defined as

$$Q_p = \frac{2m_1 m_2}{m_0^2} \dots\dots\dots(3.7)$$

The quality of the collected data was checked thoroughly and linear interpolation technique was adopted for filling up the missing data sets obtained from the wave rider buoy. Wave rose diagrams are plotted for each month and probability of occurrence were calculated and plotted for the entire year for the wave parameters viz. significant wave height, peak period and predominant wave direction (PWD).

3.3.2 Wind

The automatic weather station was installed in the beach at a height of 10 m above the mean sea level at Ponmana, Chavara coast (Lat. $9^{\circ} 01' 2.61''$ N; Long. $76^{\circ} 31' 9.11''$ E) (see Fig. 3.4). The wind speed and direction (w.r.t north) were measured on hourly basis. The wind definition according to the nautical convention is shown in Fig. 3.12. The wind data was collected for a period of 1 year from January to December 2014 synchronous with the wave data. The collected data underwent thorough quality checks for further analysis. Wind rose plots were drawn on monthly basis along with the probability occurrence of wind speed and direction for the period of one year. In addition to this the data were also given as input to the numerical modelling for the computation of the sediment transport rates.

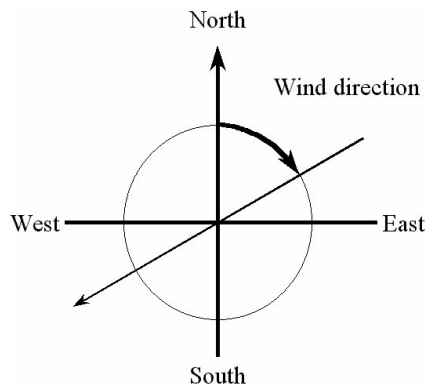


Fig. 3.12 Wind definition according to nautical convention

3.3.3 Bathymetry

Bathymetric survey of the innershelf region of the Neendakara - Kayamkulam coast covering a distance of about 22 km was carried out in the fair weather month of April 2010 along transects normal to the shore extending upto a depth of 20 m which varied from about 6 km at Neendakara in the south to 7.5 km at Kayamkulam inlet in the north (Fig. 3.13).

Prior to the start of bathymetric survey, sounding lines were generated normal to the shore at 1 km spacing using the HYPACK software selecting the reference ellipsoid WGS-84 for the survey. The survey area consisted of 28 shore normal transects at a spacing of 1 km. The survey started from the south of Neendakara inlet and ended at the north of Kayamkulam inlet. The echo-sounder and GPS were fixed in a fishing boat which was used for the survey and interfaced through the HYPACK. Offset values for the transducer depths are corrected in echo-sounder and subsequently GPS readings along with depth soundings are logged at regular intervals. HYPACK software was also used to navigate the boat along survey lines. Each transect started from around 4 m and ended at 20 m depth.

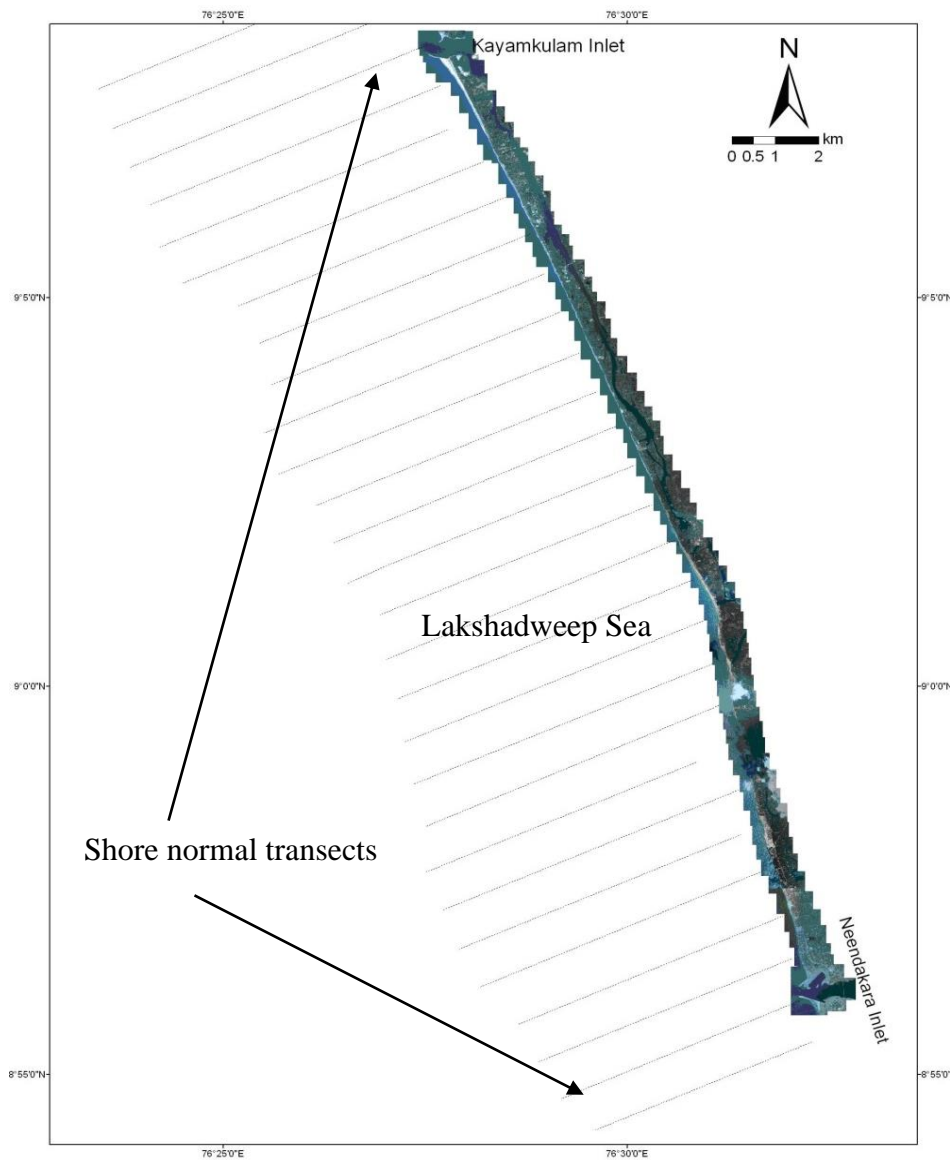


Fig. 3.13 Sector covered for bathymetric survey; the shore-normal transects along which soundings were made are also shown

The Ceeducer, fixed onto a country boat, was used to carry out soundings in the nearshore region where the fishing boat fitted with the echo-sounder was unable to sail due to shallow waters and rough seas. The survey using the Ceeducer was done in the nearshore upto 4 m isobath.

The collected data were processed using the HYPACK software. Each transect line is then processed separately to obtain the data in the required x, y, z (x-Easting, y-Northing and z-depth below MSL) format after applying tidal corrections. For applying tidal corrections the predicted tide from the MIKE C-MAP (DHI, 2007) software is used. Finally the recorded data were converted to grids and the depth contours were generated.

Collation of past bathymetric data

The bathymetric data generated as above for the year 2010 together with the data available for the years 2000 and 2005 have been used to understand the decadal changes in the innershelf morphology (Table 3.2). The bathymetric chart for the year 2000 is from the data collected by the Centre for Earth Science Studies (CESS) as part of the sediment budgeting studies carried out for the Chavara coast (Kurian et al., 2002). The 2005 bathymetric chart is again derived from the data acquired by CESS (Kurian et al., 2006b) to analyse the nearshore morphological changes soon after the December 2004 Tsunami. In order to analyse and understand the changes, the bathymetric charts for the three years were overlaid in GIS for a one-to-one comparison. The distances of the three isobaths, viz. 10 m, 14 m and 20 m from the fixed reference points on the shore at each of the pre-defined coastal locations are then measured applying the GIS tools for the years 2000, 2005 and 2010.

3.3.4 Beach profile

Beach profiles are two-dimensional vertical sections of the beach showing elevations with respect to distance from backshore and are taken usually normal to the shoreline. Beach profiling is an effective tool for accurate estimate of erosion/ accretion in short time scales. In order to understand the seasonal beach erosion/accretion pattern in the study area, monthly beach profile measurements were carried out for a period of five years commencing from June 2010. Short-term beach morphological changes are assessed by comparing these monthly measured beach profiles. For beach profile measurements, 8 stations with bench mark stones were chosen. As the coast under

study is in general an eroding one and beaches are present only in a few stretches, the stations for profile measurements were not evenly distributed along the coast as can be seen in Fig. 3.14. The profile measurements were carried out by using standard level and staff method. Permanent and stable locations were identified and fixed as bench marks for regular profile measurements. The benchmarks used in the survey were the reference stones laid by the Coastal Erosion Studies Wing of the Irrigation Department which are available throughout the coast. The beach elevations were measured from the fixed benchmark towards the low waterline at an interval of 5 m.

The stations are named NK-1 to NK-8 in the order from Kayamkulam inlet to the Neendakara inlet, which include the mining sites of Vellanathuruthu and Kovilhottam (Fig. 3.14). Snapshot of typical beach profile stations are shown in Fig. 3.15. The station NK-1 being located about 100 m south of the southern breakwater at the Kayamkulam inlet is under the influence of the breakwater with regard to sedimentary pathways. The station NK-5 is located approximately 2 km to the south of the Kayamkulam inlet and hence can be considered as a typical location which is not under the influence of any coastal structure. However, with the construction of a groin field at about 100 m south of the NK-5 station during 2014–2015 the situation has changed. NK-6 is located close to the Vellanathuruthu mining site on the northern side and is influenced by the mining operations. The measured beach profile data were processed, plotted and the beach volume changes for successive months were computed for which a computer programme developed by Hameed (unpublished) was used. The cumulative volume change for a period of five years (June 2010 - December 2015) is then calculated from the beach volume change analysis.

3.3.5 Shoreline mapping

Shoreline, which is the line of intersection of the sea level with the shore is an indicator of the erosional / accretional status of a coast. An advancement of the shoreline towards sea indicates accretion while a shoreward retreat is indicative of erosion. Sea level, being very dynamic, keeps on oscillating in time due to the hydrodynamic processes and hence the identification of shoreline is a rather complicated process. In such a complex situation of oscillating sea level one of the reference levels such as low tide level (LTL), Mean Sea Level (MSL), High Tide Level (HTL) can be taken to represent sea level. The shoreline with HTL as the reference level is discernible in the field due to the variation in the physiography,

vegetation, etc. Demarcation of shoreline is normally done using topographic maps and satellite imageries. The shoreline change being a small quantity, the long term trend in the erosion or accretion only can be estimated from the shoreline change analysis.

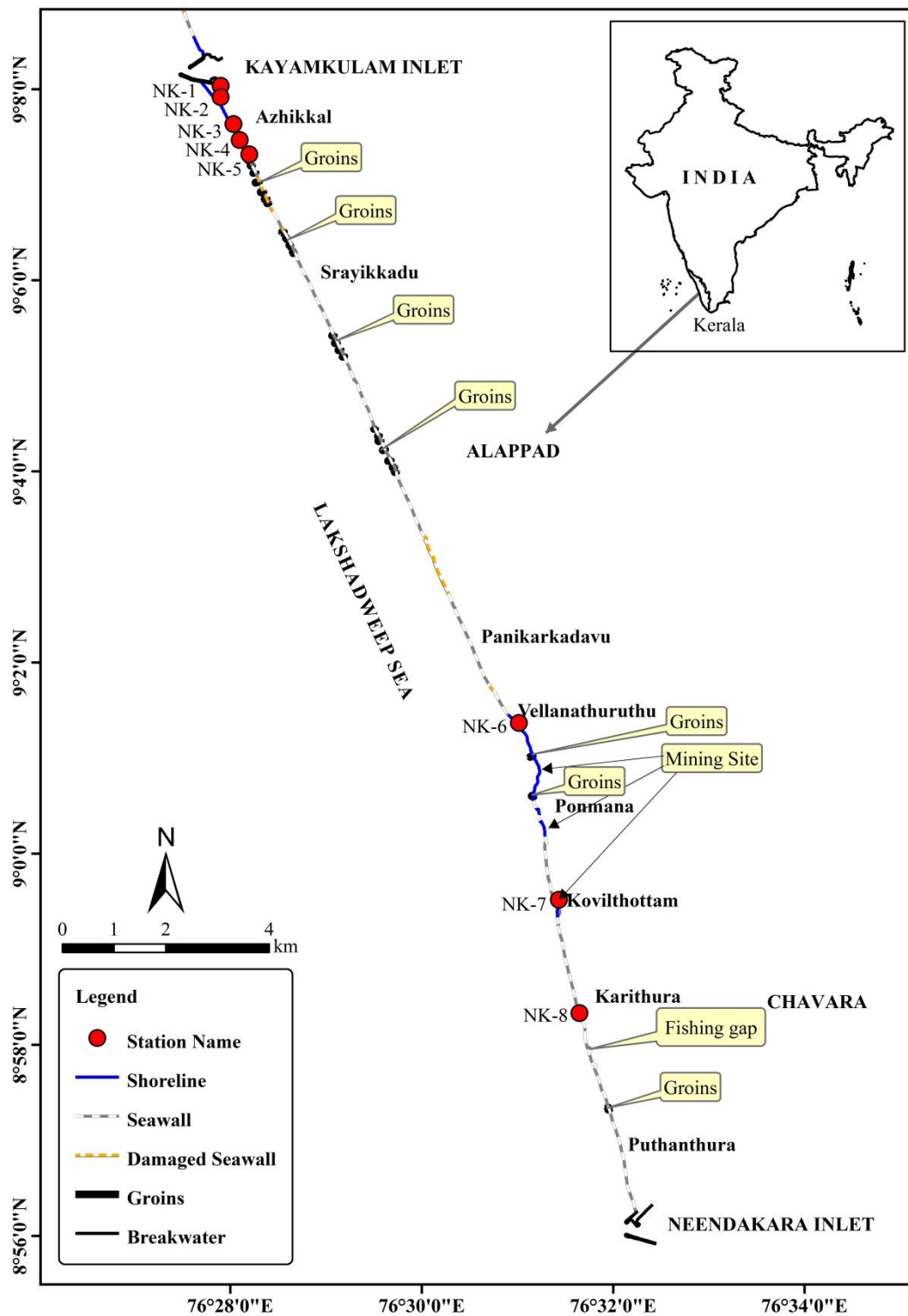


Fig. 3.14 The beach profile stations and coastal structures along the Neendakara-Kayamkulam sector



Fig. 3.15 Typical beach profile stations: (a) south of Kayamkulam breakwater (NK-1), (b) Srayikkadu (NK-5) and (c) Vellanathuruthu mining site (NK-6)

During the course of the present study, monthly shoreline mapping was done along the Chavara coast taking the mid-water level as the reference, using a Trimble Juno SB GPS for a period of five years. In addition to this the data pertaining to multi-dated toposheets of the Survey of India and satellite imageries (Table 3.2) were collated for delineating the long-term shoreline change.

Table 3.2 Bathymetry, beach profile and shoreline data used for the present study

Data	Period
Bathymetry	
(a) CESS archived data	2000, 2005
(b) measured during present study	2010
Toposheet (1:50,000)	
Toposheet (1:25,000) (Ponmana-Kayamkulam inlet sector)	1967-68
Satellite imagery	2003; 2006
Monthly field measurements (beach profile, shoreline mapping)	2010-2011; 2012; 2013; 2014 & 2015

3.3.6 Beach and innershelf sediment sampling

In order to understand the sediment characteristics, their transport and distribution, the sediment samples from several locations of the beach and nearshore area is inevitable. The locations of the sediment sampling points in the beach and in the innershelf limited to 25 m depth along the Neendakara-Arattupuzha coast are shown in Fig. 3.16. Since the data on sedimentology and mineralogy pertaining to the area north of Kayamkulam inlet would be helpful in understanding the sediment dynamics and the Heavy Mineral (HM) distribution in the study area, the sampling locations have been extended upto Arattupuzha.

Beach surficial sediment samples were collected from six locations, viz. Arattupuzha, Kayamkulam, Srayikkadu, Panikkarkadavu, Kovilthottam and Neendakara (Fig. 3.16), during the pre-monsoon, monsoon and post-monsoon periods. At each location, the beach surficial samples were collected from backshore, berm, mid water line and breaker zone and analysed for their textural and mineralogical characteristics.

Innershelf surficial sediment samples were collected along 6 transects off the beach sampling locations viz. Arattupuzha, Kayamkulam, Srayikkadu, Panikkarkadavu, Kovilthottam and Neendakara using Van Veen Grab sampler during the three seasons of monsoon (July, 2010), post-monsoon (November 2010) and pre-monsoon (April, 2011). Along each transect, the sampling was conducted at 5 m, 10 m, 15 m and 20 m water depth.

In addition to surficial samples, the sub-surface samples (cores) were also collected using piston corer from selected stations with depth ranging from 4 to 15 m (Figs. 3.16 & 3.17). Table 3.3 shows the details of sediment cores collected. The recovery lengths of cores varied from 0.6 to 1.3 m. Each of the core samples was split into two; one half was kept as archive and the other half was sub-sampled at 5 cm interval. All the sub-samples were analysed for texture and HM content.

3.3.7 Suspended sediment sampling

Two sediment trap assemblies were deployed for estimating the suspended sediment load in the coastal waters. Each sediment trap assembly consisting of 6 sediment traps (see Fig. 3.9), were deployed at 8 m (nearshore site) and 12 m depth (offshore site) during the monsoon and post-monsoon seasons of 2010 and also during the pre-

monsoon season of 2011. Table 3.4 shows the details of the sediment traps deployed at the offshore and nearshore sites of Chavara.

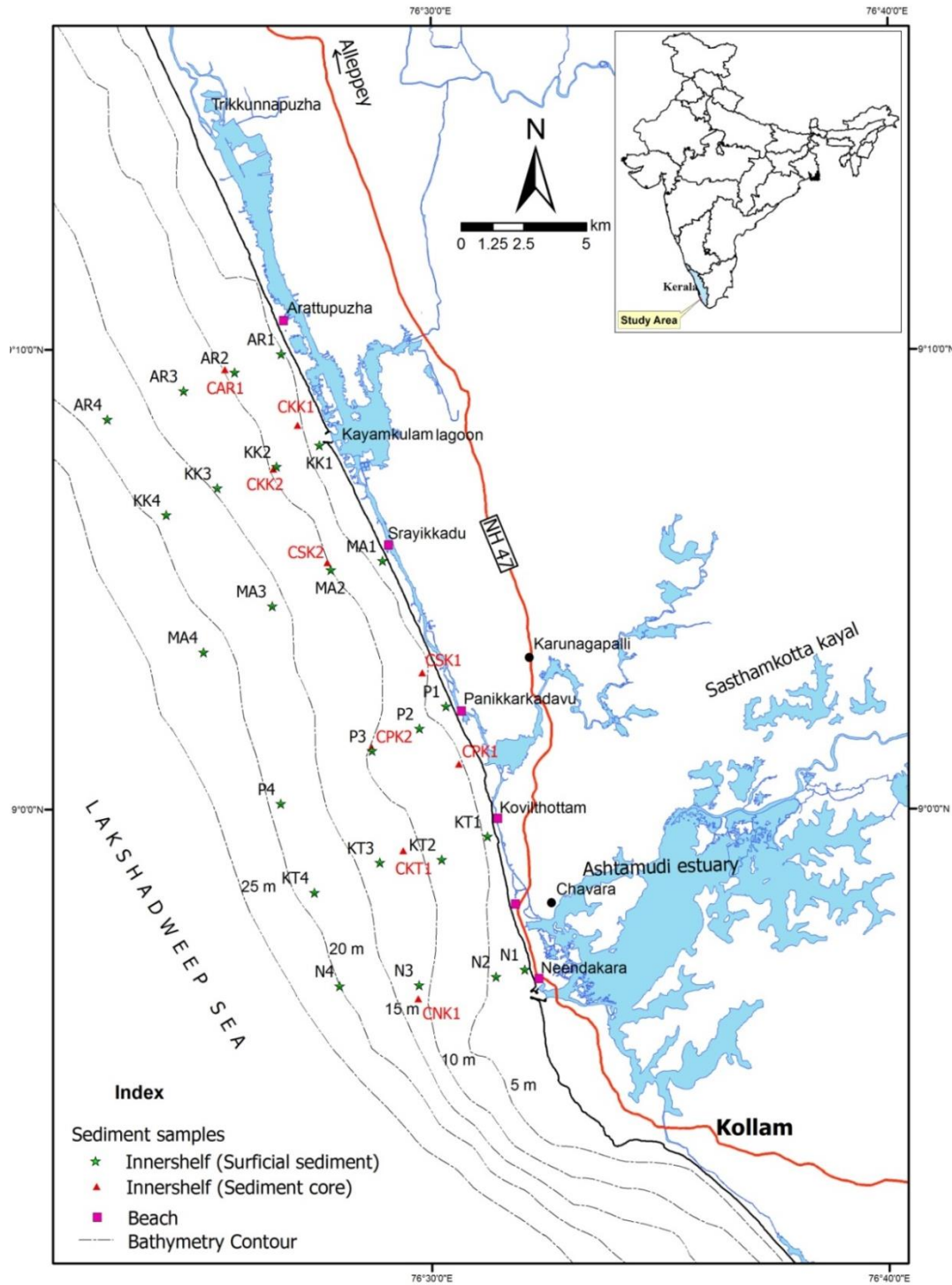


Fig. 3.16 Sediment sampling points in the beach and the innershelf of the Neendakara-Arattupuzha coast. Since the data on sedimentology pertaining to the area north of Kayamkulam inlet would be helpful in understanding the sediment dynamics and the heavy mineral distribution, the sampling locations have been extended upto Arattupuzha

Table 3.3 Details of sediment cores collected from the innershelf of Neendakara-Aratupuzha coastal sector

Sl. No.	Location (Station No.)	Latitude	Longitude	Depth (m)	Core recovery (m)
1	Neendakara (CNK1)	8° 55' 52.42"	76° 29' 42.45"	14.5	1.05
2	Kovilhottam (CKT1)	8° 59' 05.80"	76° 29' 22.81"	12.5	1.10
3	Panikarkkadavu (CPK1)	9° 01' 20.70"	76° 28' 41.17"	12.5	1.30
4	Panikarkkadavu (CPK2)	9° 02' 58.00"	76° 29' 48.00"	8.0	0.65
5	Srayikkadu (CSK1)	9° 05' 22.13"	76° 27' 43.56"	10.5	0.85
6	Srayikkadu (CSK2)	9° 05' 52.00"	76° 28' 30.00"	7.5	0.15
7	Kayamkulam South (CKK2)	9° 07' 24.00"	76° 26' 33.00"	10.5	0.55
8	Kayamkulam North (CKK1)	9° 08' 21.40"	76° 27' 05.00"	8.0	0.60
9	Aratupuzha (CAR1)	09° 09'33.84"	76° 25'29.82"	10.5	1.05



Fig. 3.17 Piston Corer being lowered for collection of sediment core from offshore of Chavara coast

3.3.8 Littoral Environmental Observations

The Littoral Environmental Observations (LEO) which include the visual observation of breaker wave parameters, longshore currents and beach characteristics were done monthly following the standard procedures (Schneider, 1981) at selected coastal locations. The breaker wave direction was measured by using Brunton compass. The breaker wave height and period were estimated visually by averaging ten consecutive significant waves. The longshore current velocity and direction were measured by

deploying neutrally buoyant float in the surf zone and measuring the distance travelled by the float in two minutes.

Table 3.4 Details of sediment traps deployed at Chavara offshore and nearshore sites

Location	Sl. No.	Trap type	Trap length (cm)	Height from bottom (cm)	Date and Time	
					Deployment	Retrieval
Monsoon Season						
Offshore Site Lat: 08°58'52.0"N Long: 76°29'45.0"E	1.	Horiz. Trap	60	22.1		
	2.	Horiz. Trap	40	29.8		
	3.	Vert. Trap	40	51.8	13/07/2010;	29/07/2010;
	4.	Vert. Trap	40	76.6	12:17 hrs.	12:50 hrs.
	5.	Vert. Trap	40	126.5		
	6.	Vert. Trap	40	200.4		
Inshore Site Lat: 08°58'58.0"N Long: 76°30'42.0"E	1.	Horiz. Trap	60	22.2		
	2.	Horiz. Trap	40	30.2		
	3.	Vert. Trap	40	51.5	23/07/2010;	29/07/2010;
	4.	Vert. Trap	40	76.4	09:49 hrs.	13:50 hrs.
	5.	Vert. Trap	40	126.7		
	6.	Vert. Trap	40	200.5		
Post-monsoon Season						
Offshore Site Lat: 08°58' 50.8"N Long: 76° 29' 47.1"E	1.	Horiz. Trap	60	22.1		
	2.	Horiz. Trap	40	29.8		
	3.	Vert. Trap	40	51.8	20/11/2010;	30/11/2010;
	4.	Vert. Trap	40	76.6	14:20 hrs.	09:05 hrs.
	5.	Vert. Trap	40	126.5		
	6.	Vert. Trap	40	200.4		
Inshore Site Lat: 08°59'00.3"N Long: 76° 30' 40.6"E	1.	Horiz. Trap	60	22.2		
	2.	Horiz. Trap	40	30.2		
	3.	Vert. Trap	40	51.5	20/11/2010;	30/11/2010;
	4.	Vert. Trap	40	76.4	11:15 hrs.	10:05 hrs.
	5.	Vert. Trap	40	126.7		
	6.	Vert. Trap	40	200.5		
Pre-monsoon Season						
Offshore Site Lat: 09° 00' 12.5"N Long: 76° 29' 37.2"E	1.	Horiz. Trap	60	22.1		
	2.	Horiz. Trap	40	29.8		
	3.	Vert. Trap	40	51.8	30/04/2011;	12/05/2011;
	4.	Vert. Trap	40	76.6	12:20 hrs.	11:35 hrs.
	5.	Vert. Trap	40	126.5		
	6.	Vert. Trap	40	200.4		
Inshore Site Lat: 09°00'39.6"N Long: 76° 30' 34.4"E	1.	Horiz. Trap	60	22.2		
	2.	Horiz. Trap	40	30.2		
	3.	Vert. Trap	40	51.5	30/04/2011;	12/05/2011;
	4.	Vert. Trap	40	76.4	11:25 hrs.	12:40 hrs.
	5.	Vert. Trap	40	126.7		
	6.	Vert. Trap	40	200.5		

3.4 Laboratory Analysis of Sediment Samples

Textural and mineralogical analyses of all the sediment samples (surface and subsurface) were carried out adopting the standard methods (Carver, 1971) to understand their spatio-temporal distribution. The laboratory analyses adopted are given in the following sub-sections.

3.4.1 Textural analysis of sediments

The most conventional and popular method for textural analysis of sediment samples is the mechanical sieve analysis, which is used for the samples comprising of sand. For clayey sediments pipette analysis is commonly adopted. If the sediments are composed of both coarse and fine particles a combination of both sieve and pipette methods are adopted.

3.4.1.1 Mechanical analysis

The sediment samples were washed thoroughly using the distilled water to remove salt content and all the shell fragments were hand-picked. The moisture in the samples was removed by drying it to 100-105 °C in the oven for at least 20 minutes. Coning and quartering method was used to obtain the representative samples. These sample are again weighed and subjected to mechanical sieving for 15 minutes in a Rotap Sieve Shaker using standard sieves (ASTM) at $1/2 \Phi$ intervals (Ingram, 1971). The fraction retained on each sieve was weighed on a single pan balance and the weight percentage was computed for further statistical analysis.

3.4.1.2 Pipette analysis

Size analysis of fine-grained sediment is usually performed by using pipette analysis. Here the particle size is estimated from the rate at which particles sink through the fluid, i.e. a predictable relationship between particle grain size and settling velocity in a fluid medium is achieved.

The textural analysis using this method was carried out following Carver (1971). For the removal of the salt content, the sediment sample of about 50 g was washed repeatedly using deionized water. To remove the calcium carbonate content, the salt free sample is treated with dilute hydrochloric acid and washed repeatedly with deionised water. To remove the organic matter content, the sample is again treated with 30 % hydrogen peroxide followed by repeated washings with deionised water.

The samples are then made into paste form by oven drying at about 40 °C for further analysis adopting the moisture replica method. Two watch glasses having samples with approximate weight of 5 g and 25 g respectively are taken according to the moisture replica method. The watch glass with 5 g is dried at 110 °C for the estimation of moisture content whereas the other watch glass with sample (25 g) is allowed to soak overnight after adding 20 ml sodium hexametaphosphate (Calgon). The soaked sample is then wet sieved through a 63 µm sieve to separate sand and mud fraction. The sand fraction (> 63 µm) retained in the sieve is dried and weighed, while the mud fraction is collected in a 1,000 ml measuring glass cylinder. This is subjected to pipette analysis to estimate the silt and clay fractions (Folk, 1980). The percentage of sand, silt and clay contents as well as statistical parameters in each of the sample are then determined using the Gradistat software (Simon, 2007). The sand-silt-clay ratios are plotted on trilinear diagram for textural nomenclature based on Shepard (1954) classification.

3.4.2 Estimation of heavy mineral content

Heavy minerals are generally concentrated in fine grade sediments. The light and heavy minerals are separated on the basis of density difference. Wet sieving of fine grained material is necessary for innershelf samples as they are composed mostly of silt and clay at varying proportions. About 20–30 g of the selected sample is wet sieved using 230 ASTM mesh and the coarser fraction separated. For removal of shell fragments, the collected fraction is treated with dilute hydrochloric acid (HCl) and washed with deionized water. Subsequently, dry sieving of the prepared samples is done to separate into fractions of medium, fine and very fine sand. Bulk samples weighing about 5–8 g each are taken for estimation of HM content using Bromoform. The total weight percentages of heavy minerals in sand fractions are calculated to get their concentration.

3.4.3 Analysis of core sample

A total of 9 core samples were collected from the innershelf along the Neeendakara - Aratupuzha sector (Fig. 3.16). As seen Table 3.3, the recovery lengths of cores varied from 0.6 to 1.30 m. Each of the core samples was split into two; one half was kept as archive and the other half was sub-sampled at 5 cm interval. All the sub-samples were analysed for texture and HM content as per the procedures given above.

3.4.4 Estimation of quantum of sediment and HM concentration in the sediment trap collections

After the retrieval of sediment traps from the sea, the samples were brought to the laboratory for analyses. All the samples from the traps were wet sieved using 0.045 mm size mesh, the washings collected, dried and weighed for the estimation of suspended sediment concentration. Further analysis to determine the sand, silt and HM contents of the suspended sediments were carried out as per Carver (1971).

3.5 Geo-spatial Analysis for Shoreline Change

Long-term trends in beach morphological changes are deduced from the shoreline change map which is a useful proxy for the identification of erosion/accretion areas (Farris and List, 2007). Shoreline change maps are prepared using multi-dated topographic sheets and satellite imageries applying digital image processing and GIS techniques, by taking numerous precautions to minimize the errors. High water lines (HWL) from the Survey of India (SoI) toposheets of 1:25,000 (1989) and 1:50,000 (1968) were taken as shorelines for the respective years. Toposheets (1:25,000) for the Ponmana to Neendakara sector (about 9 km long in the south) were not available, and hence, the comparisons with 1:25,000 are limited to the available sector (Ponmana to Kayamkulam).

Satellite imageries have been used for delineating the shoreline after 1989 and the images used are the IRS P6 LISS IV of 2007 and the Google imageries of 2003–2007. The dry beach–wet beach interface as seen in the image was taken as the HWL and the shoreline deduced accordingly. Information on shoreline changes was also collected from earlier studies carried out for the area (Prakash and Verghese, 1987; Sreekala et al., 1998; Kurian et al., 2002; Sreeja, 2005; Praveen, 2006; Thomas et al., 2010). As described in Section 3.3.5, shorelines for the period 2010-2015 were mapped using a GPS. Shoreline changes in linear distance for a few representative locations along the coast are calculated after overlaying in ArcGIS platform. The long-term beach erosion/accretion trend is then deduced from the estimated shoreline changes.

3.6 Geo-spatial Analysis for Innershelf Morphological Changes

The morphological changes in the innershelf were estimated from the bathymetry collected and collated for different years, viz. 2000, 2005 and 2010. In order to

quantify the shift in isobaths over the 10-year period, the bathymetry data for the 3 years were overlaid on ArcGIS platform. Shore normal transects of one kilometre width each were drawn from nearshore to offshore off seven locations identified for computation of the isobath shift. The isobaths of 10, 14 and 20 m were chosen for the computation of the shift, and the area enclosed by the shift of the above isobaths over the periods 2000–2005, 2005–2010 and 2000–2010 were estimated. The shift of each isobath over different time periods per unit width is also calculated for delineating the innershelf morphological changes.

3.7 Empirical Orthogonal Function Analysis

Empirical Orthogonal Function (EOF) analysis provides the most efficient method of compressing data which uses a combination of statistics and linear algebra to isolate the dominant patterns in a data set. This analysis separates spatial and temporal dependence of data to represent as a function of space and time. The beach profiles can be represented in terms of shape functions known as eigen functions and widely used to investigate patterns in the beach variations (Winant et al., 1975; Aubrey, 1979; Shenoi et al., 1987; Larson et al., 1999b). The first few eigen functions provide information on most of the data variability and this analysis uses the entire profile to describe the beach changes rather than considering just one point along the profile. Thus the variation in the beach profile configuration in terms of distance from the fixed data point and in terms of temporal changes in the profile over the period of study is represented by using the EOF analysis.

The data set is denoted by a matrix ‘ H_{mn} ’ with each of the rows containing a time series of the elevation at a particular point along the profile and each columns represents the beach profile at a particular time. The variability of the data matrix is explained in terms of few eigen functions of the matrix H_{mn} and the matrix is decomposed by using the Singular Value Decomposition (SVD) technique. Principal Component Analysis (PCA) tool box in the MATLAB software was used for the present analysis.

The data matrix H_{mn} is represented as a product of three matrices in the form

$$X_{m \times n} = \frac{H_{mn}}{(m \times n)^{1/2}} = U_{m \times r} \Gamma_{r \times r} V_{n \times r}^T \dots \dots \dots (3.8)$$

where m and n are the no. of rows and columns of the data matrix respectively, $\Gamma = r \times r$ is the diagonal matrix with diagonal elements called the singular values of H_{mn} , r is the rank of the matrix H_{mn} , The column vectors U and V are orthogonal, i.e.

$$U^T U = I, V^T V = I \dots \dots \dots (3.9)$$

where I is the identity matrix. Solving the eigen value problem from equations 3.8 and 3.9 then

$$(B - \lambda_i I) V_i = 0 \dots \dots \dots (3.10)$$

$$(A - \lambda_i I) U_i = 0 \dots \dots \dots (3.11)$$

where $B = X^T X$ and $A = X X^T$, U_i and V_i are the column vectors U and V respectively.

The values of λ_i is obtained by solving the characteristic equation $|B - \lambda_i I| = 0$ and substituting in the Eqn. 3.10 leads to a system of equations which are solved by following the standard Gaussian elimination method to obtain the values of V . Thus the eigen functions (U_i and V_i) and the eigen values λ_i are determined.

The eigen functions are ranked according to the percentage of mean square value of the data they explain. The first three eigen functions describe the major beach changes. The first eigen function explains the mean beach profile which shows similarity in its shape for all the beach profiles and provides information on beach gradients. The second eigen function represents the seasonal onshore/offshore movement and the third eigen function partly describes how the beach oscillates between a berm and bar profile.

3.8 Numerical Computations

Numerical computations are used in the present study for the estimation of longshore transport, cross-shore transport and shoreline change which involves the utilization of processes based models and bulk formulae.

Bulk formulae viz. the CERC and Kamphuis, and the process based model LITDRIFT module of the LITPACK modelling suite by the Danish Hydraulic Institute (DHI) are used for the computation of the Longshore Sediment Transport (LST). The cross-shore sediment transport was estimated by using LITPROF and the shoreline change modelling by using LITLINE module of LITPACK modelling suite. Coastline evolution was modeled by using the LITLINE module of LITPACK modelling suite.

The description of the models/formulae used along with the process of calibration and validation is given in the relevant chapters.

3.9 Summary

The methodology followed for the investigation and the methods of data collection and analysis are described in this chapter. A comprehensive field measurement and data collation programme taking care of the requirements of the study including numerical modelling was meticulously planned and implemented during the period 2010-2015. The instruments used/devised for the data collection along with the principle and scheme of measurement are detailed. Monthly beach profiles at selected stations and GPS based shoreline survey were conducted during the period 2010-2015 to study the beach morphological changes. Bathymetric survey was carried out in the month of April 2010 in the innershelf of Chavara coast along transects at 1 km interval and extending upto 20 m depth. The bathymetric chart prepared out of this survey was used in conjunction with bathymetric data collected by the CESS for the years 2000 and 2005 to understand the innershelf morphological changes. Seasonal surficial sediment sampling from the beach and nearshore, suspended sediment sampling using sediment traps from two stations in the nearshore and one-time sub-surface core sampling from selected stations in the innershelf were systematically carried out during 2010-2011. Wave data which is the most important one required for the numerical modelling studies is the year-round wave rider buoy data collected in 2014 off Chavara coast at 22 m water depth. Synchronous with the wave data, wind data at the beach site were also measured by using an automatic weather station installed at Chavara beach. Monthly littoral environmental observations which include the measurement of longshore current, breaker wave and beach characteristics were also carried out at selected coastal locations in 2014.

The methodology adopted for the sample and data analysis which included the hydrodynamic data analysis, laboratory analysis of the sediment samples, empirical orthogonal function analysis for the beach profiles and geo-spatial analysis for the beach-innershelf morphological change are presented. A brief outline of the processes based models and bulk formulae used for numerical computations are also provided. The details of the models/formulae used along with the process of calibration and validation are given in the subsequent chapters.

CHAPTER 4

NEARSHORE SEDIMENT TRANSPORT REGIME

4.1 Introduction

The stability of a beach is decided by the sediment transport processes induced by various hydrodynamic processes coupled with human-induced activities in the beach and innershelf. The sediment transport pattern/processes of a coast is dependent on the hydrodynamic forces viz. waves, currents, tides and wind which vary both temporally and spatially. The changes in beach and innershelf morphology are in turn influenced by the sediment transport processes. Reports on the caving in of the beach at the mining sites in Chavara and the alarming rate of depletion of the heavy mineral content in the beach sediment during recent years, as reported by the firms engaged in beach sand mining, have given impetus for undertaking a comprehensive study on the sediment transport regime of the nearshore of this coast. Such a study has been carried out combining field measurements with computations using different mathematical formulations. The field programmes included measurements of wind, wave, beach profiles and littoral environmental parameters and mapping of shoreline for the period of January to December 2014. The field data are discussed first followed by the computational processes and the characteristics of sediment transport regime.

4.2 Nearshore Wave Characteristics

As already discussed in Chapter 3, the data from the wave rider buoy deployed at a station of water depth 22 m off Kovilthottam (see Fig. 3.2) is used for the study. Fig. 4.1 gives the monthly wave rose plots and Figs. 4.2, 4.3 & 4.4 give the percentage occurrence plots for the various wave parameters for the whole year. The analysis shows the dominance of south-southwesterly waves with peak periods of around 11 s during the months of January-May and September-December and 9 s during the monsoon. This indicates that the coast is under the influence of swell waves during major part of the year. From the monthly wave rose plots, it can be seen that the south westerlies and westerlies dominate the peak monsoon period of June-August due to the influence of the monsoon waves generated in the Arabian Sea.

The percentage occurrence plots for H_s shows that it is in the range of 0.29 - 3.2 m. Of these about 55 % of the H_s are in the range of 0 to 1.0 m and it is mostly during the

non-monsoon periods. The percentage occurrences of H_s in the range of 1 - 2 m and > 2 m are 36 % and 9 % respectively. High wave activity is normally during the peak monsoon season and hence the percentage occurrence of waves with $H_s > 2$ m in a year is relatively low.

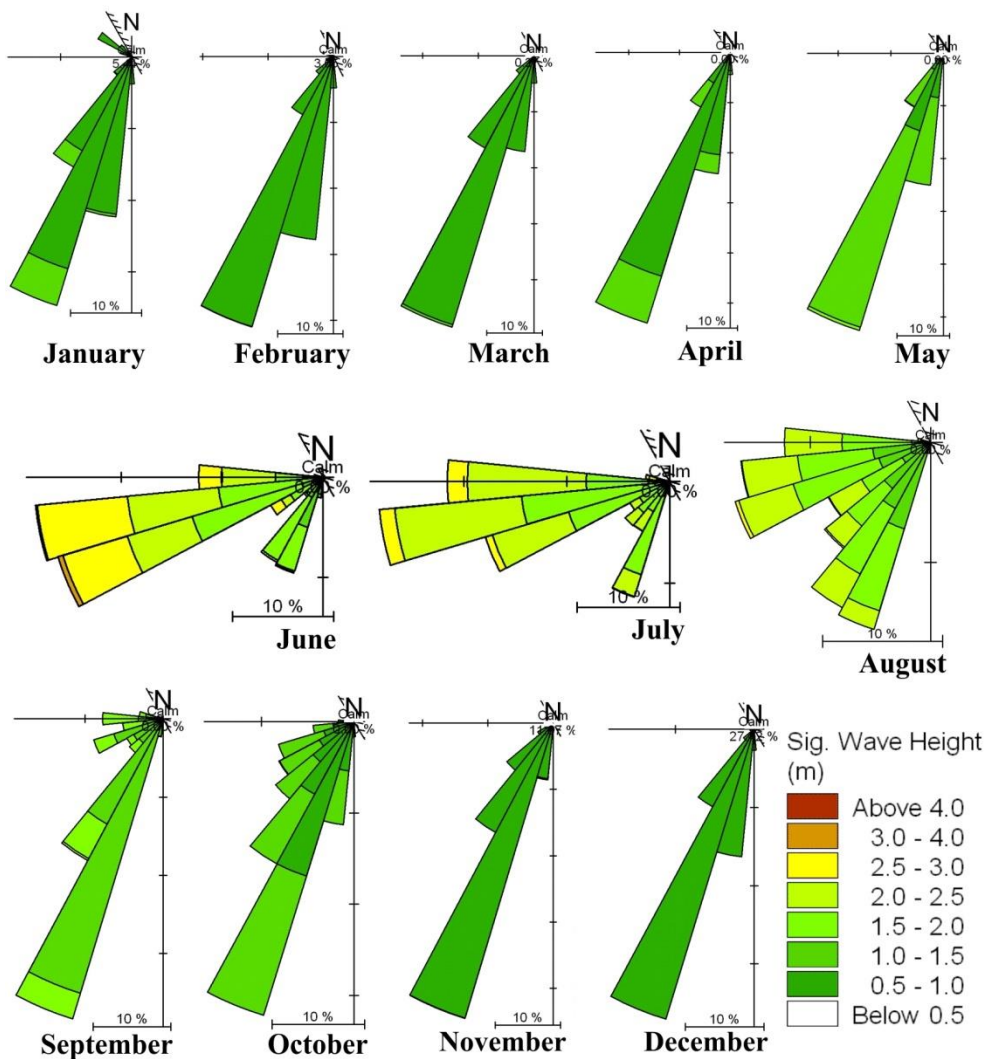


Fig. 4.1 Monthly wave roses off Chavara coast during January-December 2014

The peak wave period (T_p) is found to vary between 3 and 23 s. The percentage occurrence of T_p in the range of 3 to 10 s is only 16.7 % and this indicates the influence of local wind waves is less. In general swell waves with $T_p > 10$ s dominate with a percentage occurrence of 83.2 %.

The wave direction varies between 105 and 357° N. About 73.3 % of the waves are from the southerly to south-southwesterly (SSW) direction and this happens during the non-monsoon period which clearly shows the dominance of southerly swell

waves. For the rest of the period southwesterly (SW) to northwesterly (NW) directions dominate, indicating the influence of sea waves which are more common during the monsoon. In a nutshell, the analysis of the percentage occurrence of the measured wave parameters decipher that the coast is dominated by the influence of swell waves during the major part of the year and steep waves for a short period during the monsoon.

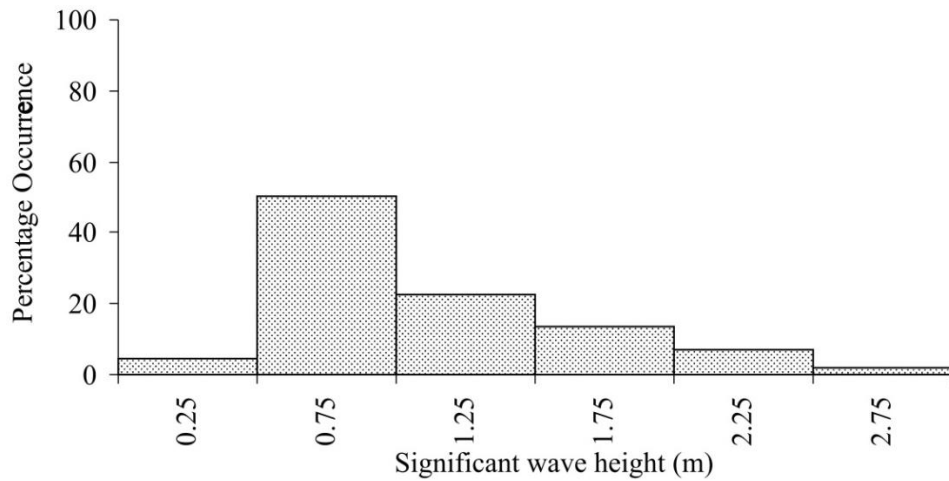


Fig. 4.2 Percentage occurrence of significant wave heights measured off Chavara coast during January-December 2014

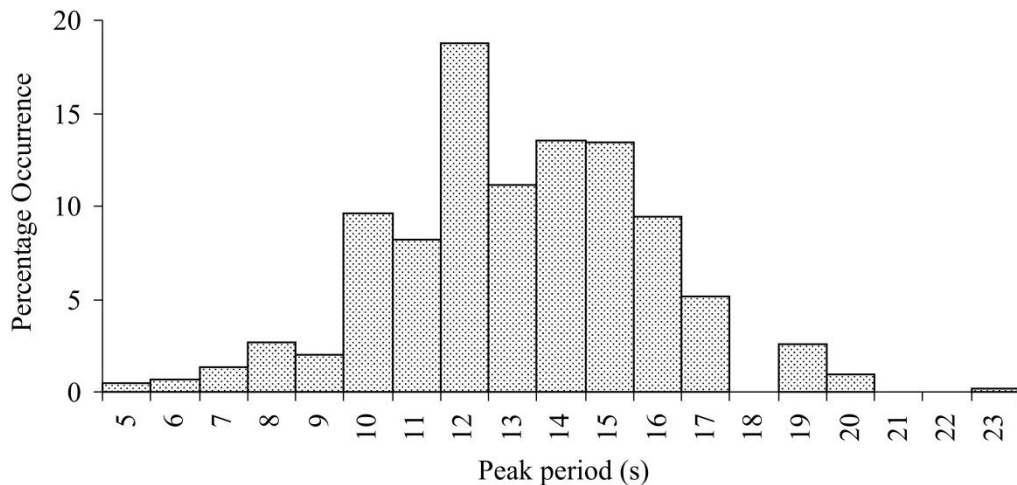


Fig. 4.3 Percentage occurrence of peak wave periods measured off Chavara coast during January-December 2014

4.2.1 Spectral analysis of waves

For the analysis, both the one-dimensional and frequency-direction spectrum data received from the wave rider buoy are considered. The analysis of one-dimension spectra shows the dominance of the swell waves as indicated by the peaks at the low frequency end of the spectrum at frequency of about 0.07 Hz (wave period of about

14 s) (Fig. 4.5a) during the non-monsoon periods. Secondary peaks are also discernable having a frequency of about 0.15 Hz (period of about 6.6 s) which shows the local wind influence. The wind wave influence is dominant during the monsoon season with the shifting of the peak frequency towards the higher frequency side of the spectrum (0.1 Hz) (Fig. 4.5b). The months of June and July shows a single peaked spectrum, which confirms the dominance of local wind waves during the peak monsoon. But during the month of August, two distinct peaks are observed with the secondary peak showing the influence of swell waves.

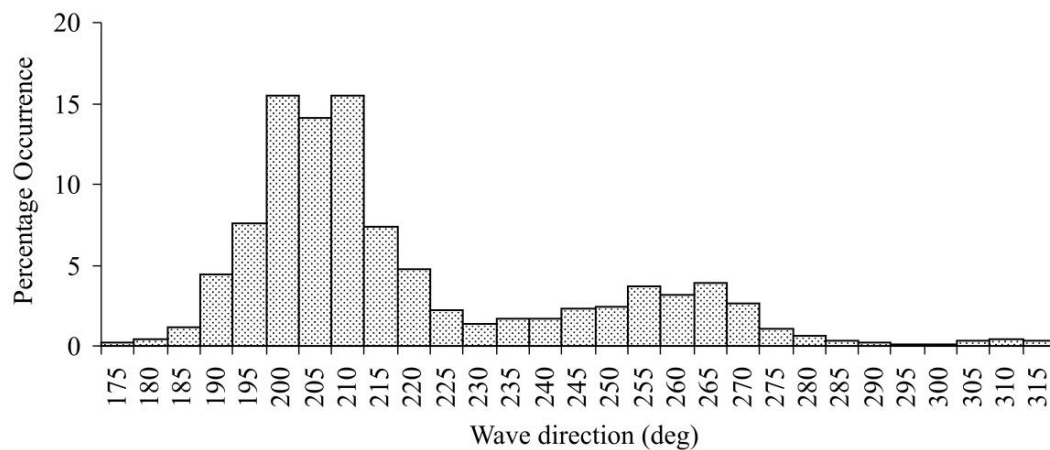


Fig. 4.4 Percentage occurrence of wave directions ($^{\circ}N$) measured off Chavara coast during January-December 2014

The information on the wave direction is not obtained from the one-dimensional spectrum which is one of its major drawbacks. The seasonal shifting of the wave directional contours is clearly observed from the frequency-direction spectrum (Fig. 4.6). During the non-monsoon periods, the direction is in the range of 200 - 240 $^{\circ}$, whereas during the monsoon period of June-September, the direction is shifted to 240 - 300 $^{\circ}$ w.r.t north. This indicates the influence of the swell waves coming from the southerly to southwesterly direction during the non-monsoon seasons and wind waves during monsoon (westerly to northwesterly direction). The shifting in the frequency towards the lower end of the spectrum during the non-monsoon and towards higher end during the peak monsoon is also observed from the frequency-direction spectrum.

4.3 Coastal Wind Characteristics

The one year wind data collected from the Automatic Weather Station (AWS) shows a maximum wind speed of 10 m/s recorded during August, with an average magnitude and standard deviation (SD) of 3 m/s and 1.5 m/s respectively. From the monthly

Wind Rose plots presented in Fig. 4.7 it can be seen that westerly and northwesterly winds dominate except during the months of February, March and December. Scattering is low during the months of June and July. The measured data being from a coastal station, daily reversal of wind due to the influence of sea and land breeze could be observed.

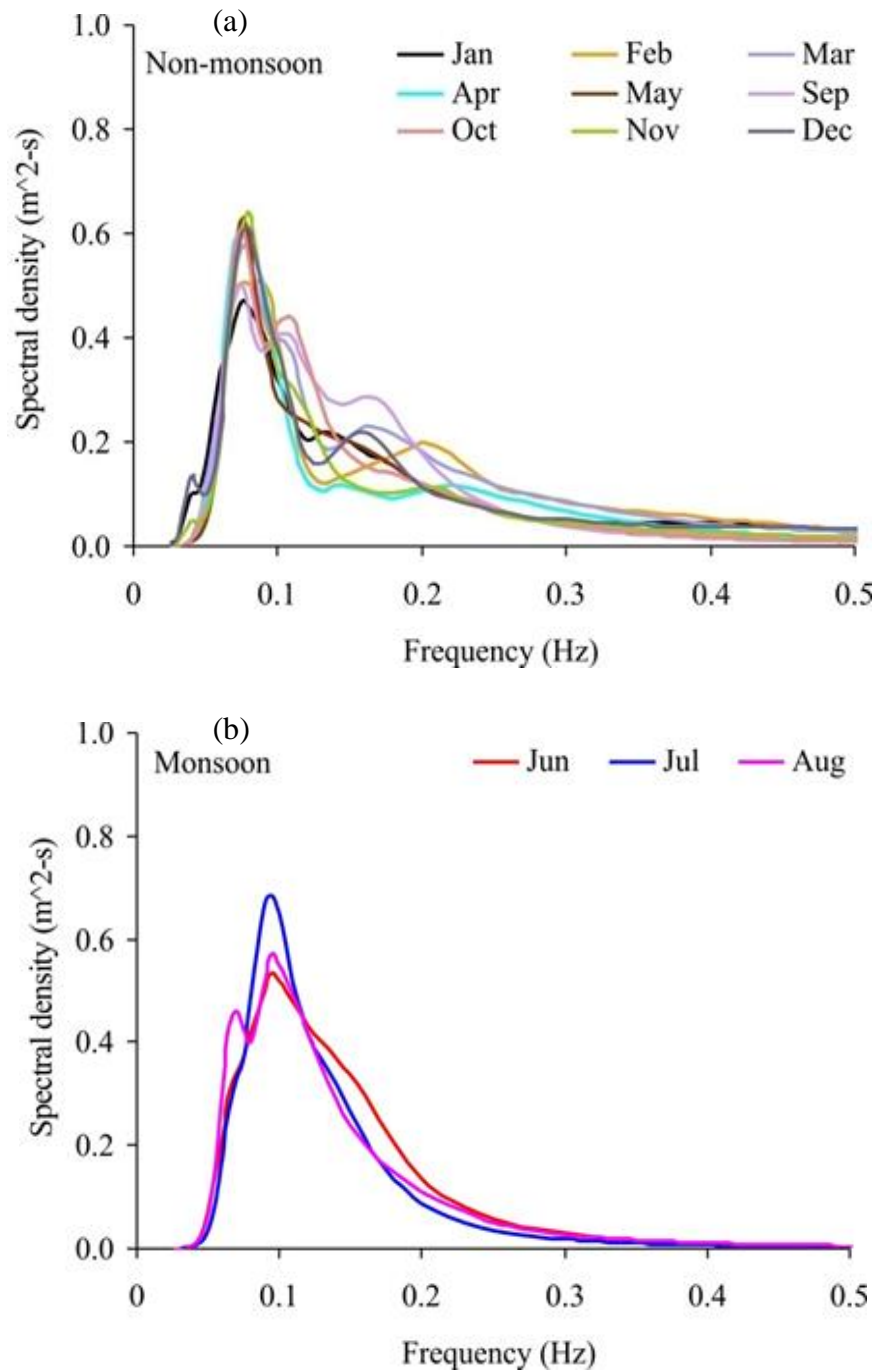


Fig. 4.5 One-dimensional spectrum of waves measured off Chavara coast during (a) non-monsoon and (b) monsoon period of January-December 2014

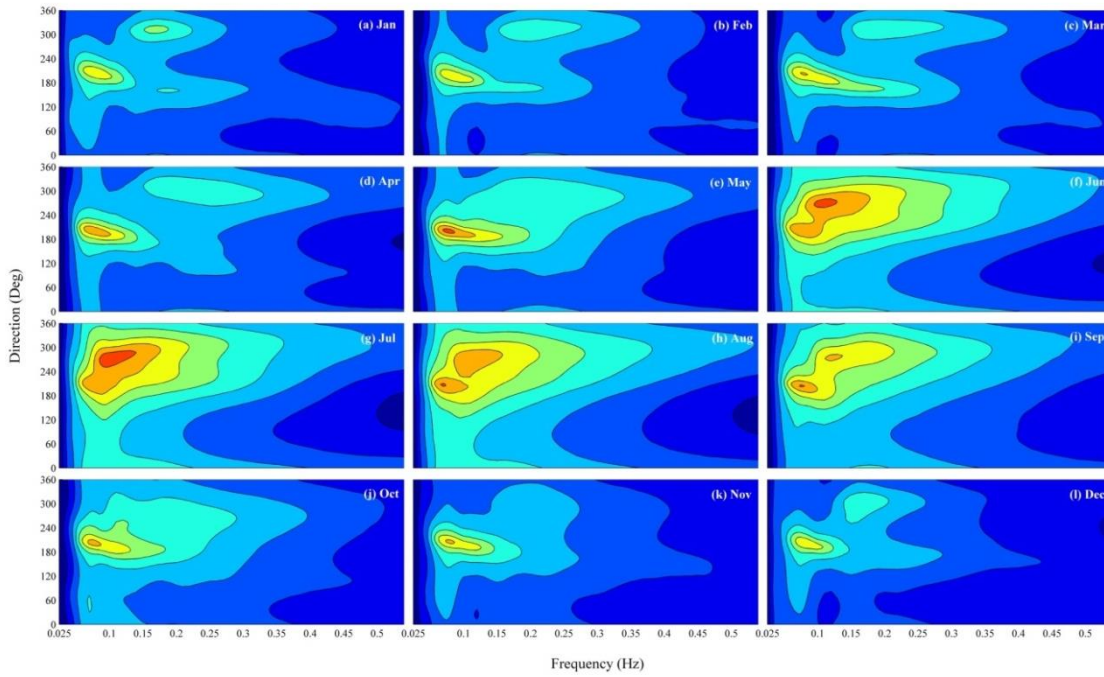


Fig. 4.6 Frequency-Direction spectrum of waves measured off Chavara coast during January-December 2014

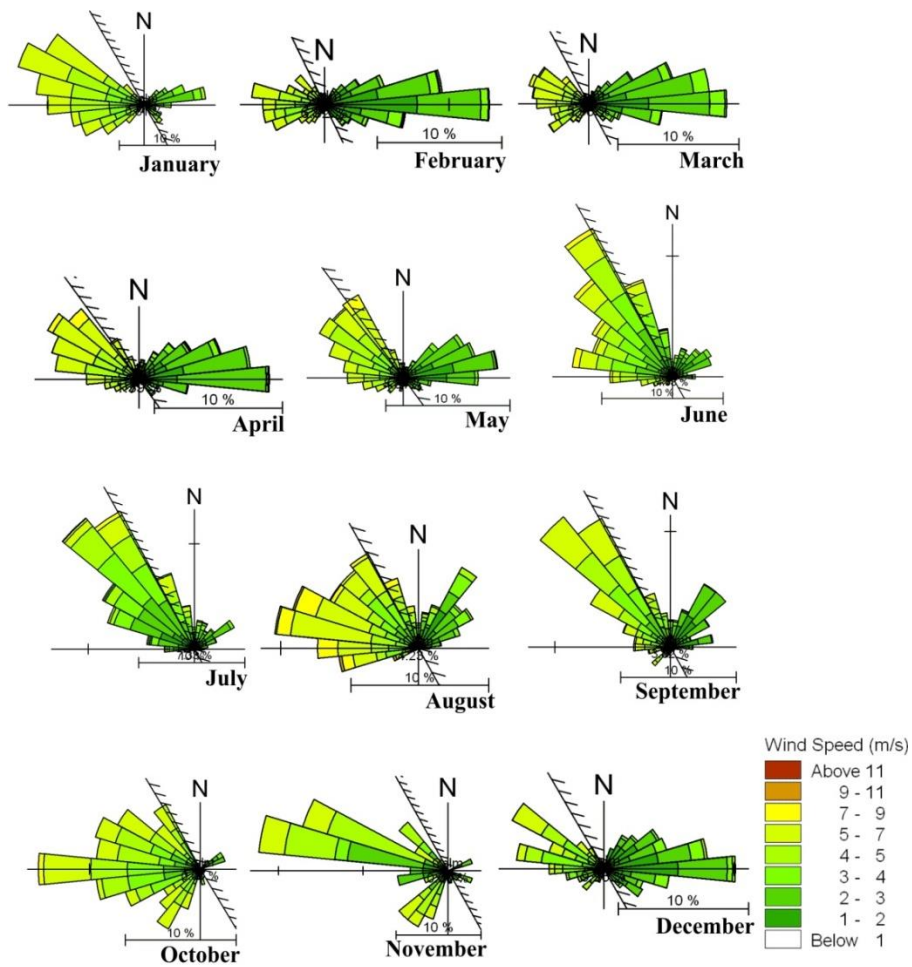


Fig. 4.7 Monthly wind roses for Chavara coast during January-December 2014

Figs. 4.8 & 4.9 show the percentage occurrence plots for the wind speed and direction recorded for 2014. The wind speeds are in the range of 0-5 m/s for 86 % of the observation period. The remaining 14 % of the wind speed falls in the range 5-9 m/s. The predominant wind directions are northwesterly (NW) to north-northwesterly (NNW) with a combined percentage occurrence of 50 %. The northeasterly winds constitute about 27 % and the remaining 23 % of the total observations comprises of southeasterlies (SE) to southwesterlies (SW).

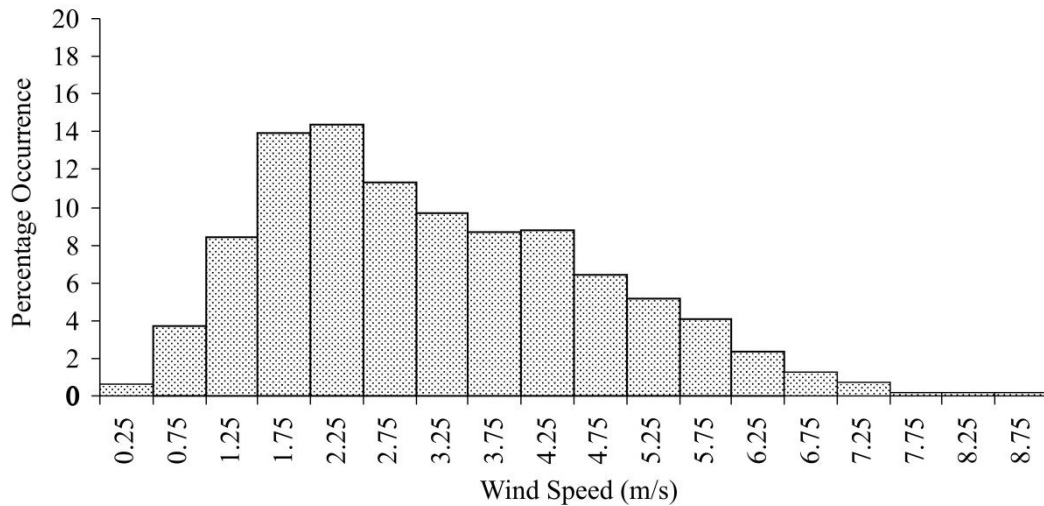


Fig. 4.8 Percentage occurrence of wind speeds at Chavara coast during January-December 2014

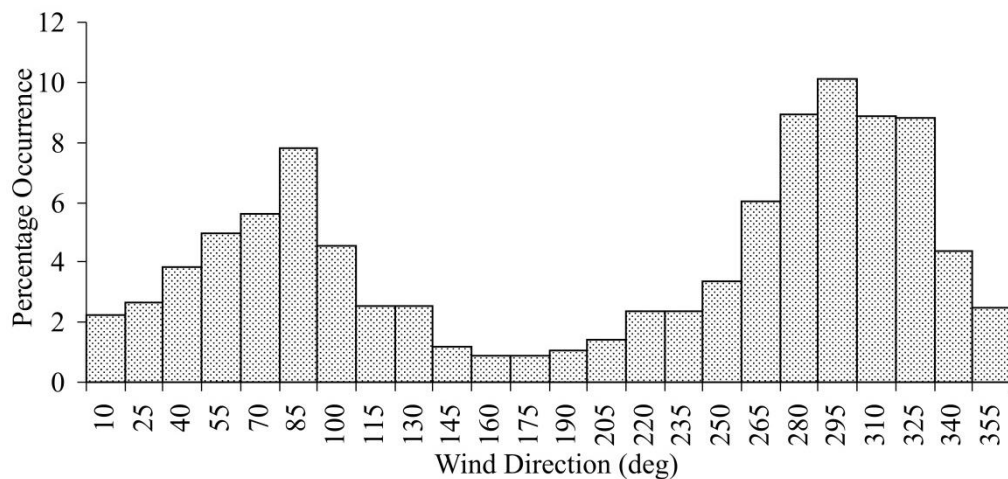


Fig. 4.9 Percentage occurrence of wind directions ($^{\circ}$ N) at Chavara coast during January-December 2014

4.4 Beach Profiles

The seasonal variation in the beach profiles at Srayikkadu (Station NK-5, see Fig. 3.14) which is the station selected for sediment transport computation is given in Fig. 4.10. The maximum beach width is observed during January and minimum in

December. During the months of May, June and July the beach was more or less completely eroded and hence no profile data is available. From the volume change (Figs. 4.11 & 4.12), it can be seen that significant accretion occurs during the months of July-August and September-October. However erosion in the subsequent period of October-January has offset the accretion made earlier and at the completion of one year (i.e. in January 2015) the beach has not regained its original profile. In general the observation is that the coastal stretch is not dynamically stable and has a negative cumulative beach volume change during the one year period indicating net eroding tendency.

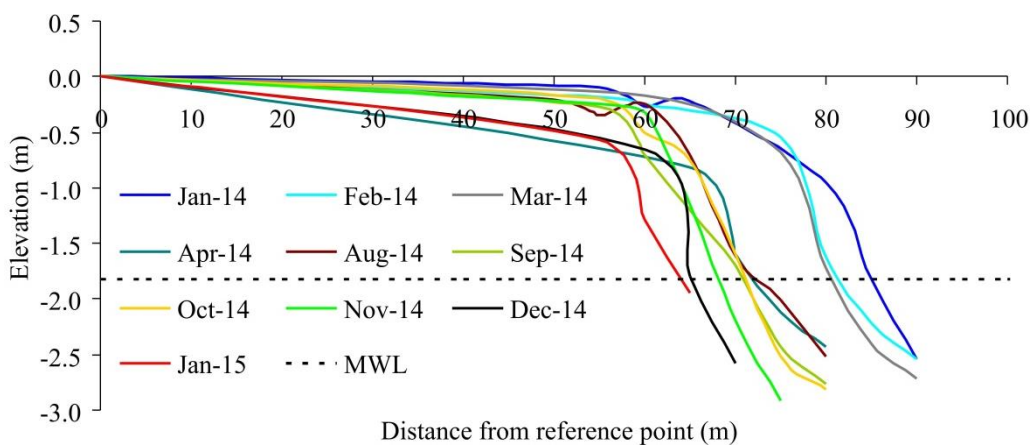


Fig. 4.10 Measured beach profile at Srayikkadu during January 2014 - January 2015

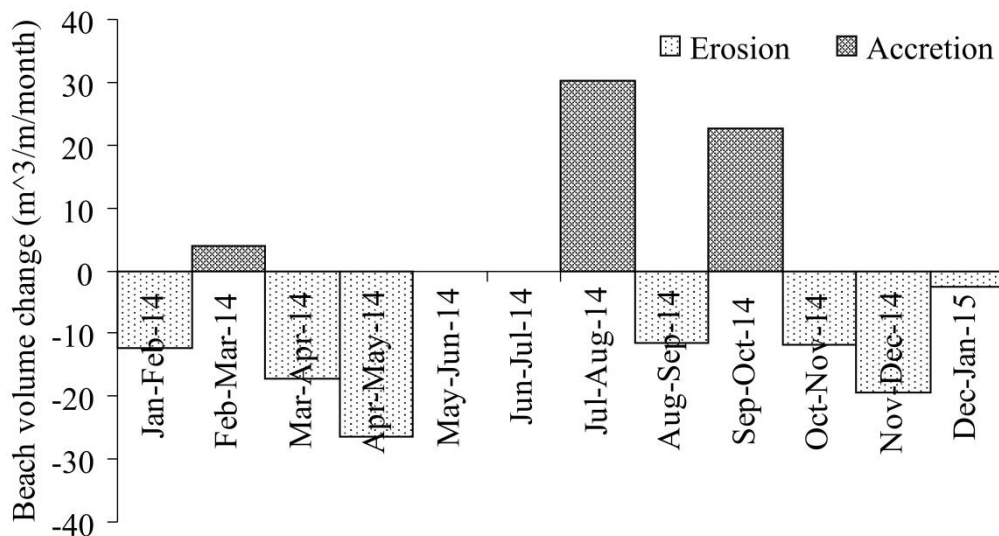


Fig. 4.11 Calculated beach volume change from the measured beach profiles at Srayikkadu during January 2014 - January 2015

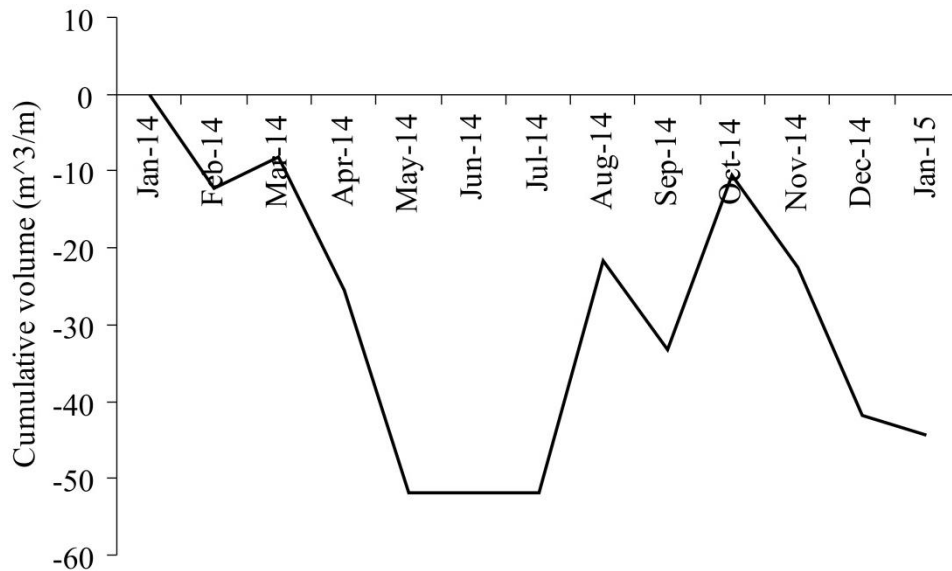


Fig. 4.12 Cumulative volume change at Srayikkadu during January 2014 - January 2015

4.5 Shoreline Orientation

Shoreline orientation which is defined as the normal to the shoreline with respect to North has been derived from the GPS measured shoreline data. The monthly shoreline orientation presented in Fig. 4.13 varies between 234° and 244° N. The computed average value during the one year observation period of January-December 2014 is around 240° with a standard deviation of 3°.

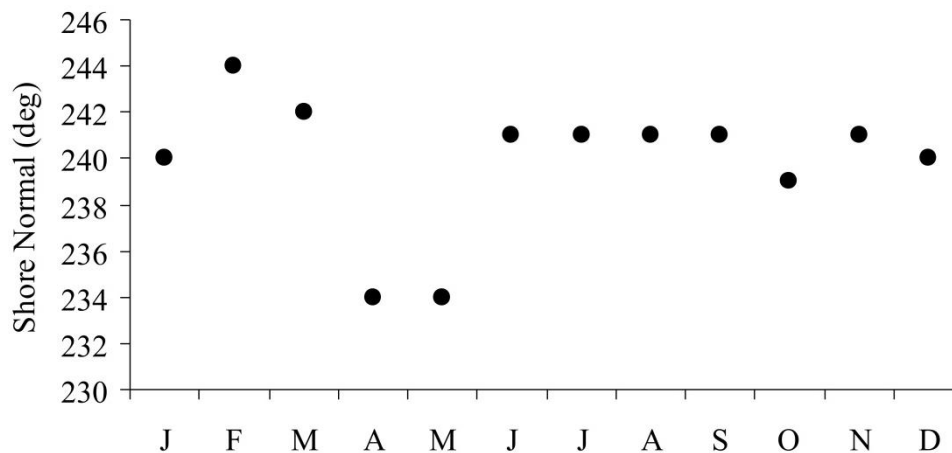


Fig. 4.13 Measured monthly shore normal at Srayikkadu during January - December 2014

4.6 Sediment Size

Sediment samples were collected during the field measurements and were analysed for their textural characteristics. The sediment characteristics are detailed in Chapter 5.

4.7 Wave Breaking and Breaker Type Estimation

Breaking of waves is the most important wave transformation phenomenon that takes place in the surf zone region and it is considered to be very complex as it depends on various parameters like the water depth, offshore wave steepness (H_o/L_o), deep water wave approach angle (α_o) and the beach slope ($\tan \beta$). To estimate the temporal variation in the breaker parameters viz. the breaker wave height, breaker wave direction and the breaker depth off the Chavara coast, the data from the offshore wave rider buoy was utilized. The breaker parameters were derived from the offshore wave data adopting standard procedures (CEM, 2002) and the variation of these parameters during the observation period of January-December 2014 are plotted in Fig. 4.14. The breaker wave angle is southwesterly to westerly during the monsoon months of June to August. Since the wave breaker angle during this period oscillates on either side of the shore normal, the wave induced longshore currents are also oscillatory. However an overall domination of southerly current and sediment transport can be seen. During the remaining months, the breaker wave angle is on the southern side of the shore normal, resulting in northerly wave induced longshore currents and northerly sediment transport.

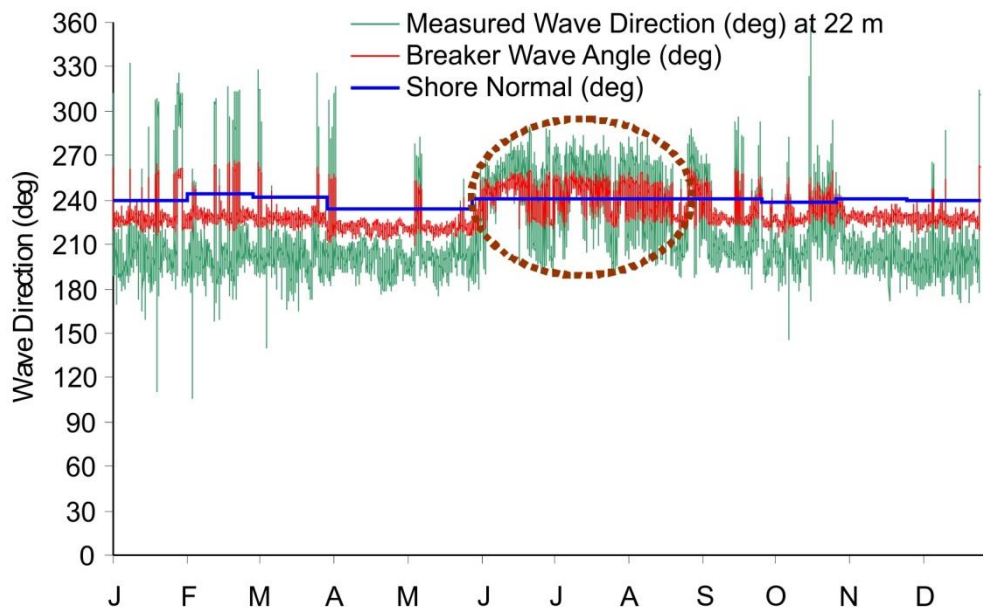


Fig. 4.14 Measured offshore wave direction, shore normal and calculated breaker wave angle off Srayikkadu during January - December 2014

Waves as they approach very shallow waters can break in four different ways - plunging, spilling, collapsing and surging - depending on the offshore wave steepness, beach slope and breaker wave height. The condition under which a particular type of

breaking occurs is attributed to the dimensionless breaker parameter ξ_0 (surf similarity parameter) (Galvin, 1968; Battjes, 1974) which is defined as given below:

$$\xi_0 = \frac{\tan \beta}{\sqrt{\frac{H_0}{L_0}}} \dots\dots\dots(4.1)$$

where $\tan \beta$ is the beach slope, H_0 is the deep water wave height and L_0 is the deep water wave length. Surging/collapsing, plunging and spilling will occur for $\xi_0 > 3.3$, $0.5 < \xi_0 < 3.3$ and $\xi_0 < 0.5$ respectively.

For studying the wave breaking phenomenon along the Chavara coast the offshore wave data is used. For determination of the breaker type the wave steepness (H_0/L_0) obtained from the one year wave data as shown in Fig. 4.1 and the beach slope from the monthly field measurements are used. The computed surf similarity parameter for the one year observation period is presented in Fig. 4.15. From the figure it is observed that plunging type of wave breaking dominates during the entire period of observation. Spilling and surging breakers are of rare occurrences in this coastal sector.

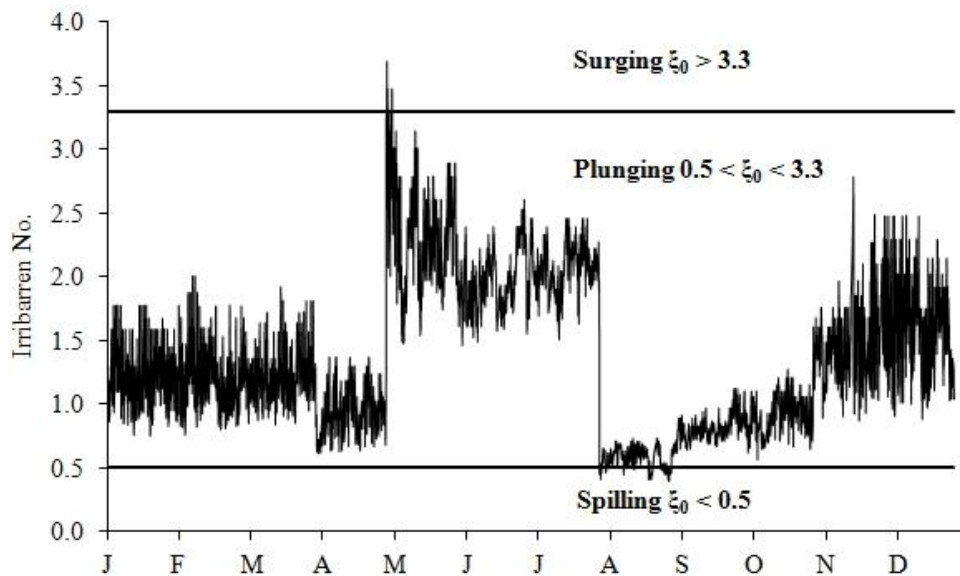


Fig. 4.15 Estimated surf similarity parameter (ξ_0) (after Galvin, 1968) off Srayikkadu during January - December 2014

4.8 Longshore Current (LSC) along the Chavara Coast

The LSC was one of the important parameters measured as part of the LEO. The monthly LSC values are presented in Table 4.1. During the fair weather months of January - April, the currents are either oscillatory or northerly with values ranging

upto 0.23 m/s. The monthly LEO data could not be collected for the months of May – July because of high wave activity. From August to December the currents are again either oscillatory or northerly with magnitudes ranging upto 0.3 m/s. The observations corroborate very well with the current directions that can be deduced from the breaker waves. As can be seen from Fig. 4.14, the breaker waves are on the southern side of the shore normal generating northerly currents during the non-monsoon months. The breaker directions are on the northern side of the shore normal during the monsoon months which can generate the southerly currents.

Table 4.1 Monthly LSC values at Srayikkadu obtained from the LEO

Month	LSC (m/s)
Jan-14	Oscillatory
Feb-14	0.13
Mar-14	0.23
Apr-14	Oscillatory
May-14	No Measurement
Jun-14	No Measurement
Jul-14	No Measurement
Aug-14	Oscillatory
Sep-14	Oscillatory
Oct-14	0.2
Nov-14	0.3
Dec-15	0.25

+ve sign indicates northerly transport. Since measurement during monsoon months are not available the southerly currents are missing

4.9 Estimation of Longshore Transport

The longshore sediment transport (LST) in the surf zone is computed by using both bulk formulas and process-based numerical models, whereas for the innershelf, the computation is based on the numerical modelling studies. The selection of an appropriate method for the computation of the LST depends on the applicability as well as adaptability of the technique for the coast and the dependence of the various parameters like the breaker wave height, wave period, nearshore slope, sediment grain size, etc. which greatly influence the sediment transport. Both the methods are discussed in detail in the subsequent sections.

4.9.1 Bulk formulae used

Bulk formulae viz. the CERC and Kamphuis are used for the computation of the longshore sediment transport and are detailed below.

4.9.1.1 CERC formula

The Coastal Engineering Research Centre (CERC) formula (SPM, 1984), which is based on field measurements, is commonly used for computing the LST rate. Accuracy of the CERC formula is believed to be only $\pm 30\text{-}50\%$ as several parameters that logically might influence the LST like the breaker type and grain size are excluded in the formula (Wang et al., 2002a; Smith et al., 2004).

The total rate of longshore transport (Q_l) according to the CERC formula (SPM, 1984), is computed using the equation

$$Q_l = (H^2 C_g)_b [A \sin(2 \theta_{bs})] \dots\dots\dots(4.2)$$

where H is the wave height, C_g is the wave group speed given by linear wave theory, the subscript b denotes wave breaking condition, θ_{bs} is the angle of breaking waves to the local shoreline, A is a non-dimensional parameter defined as

$$A = \frac{K}{16 \left(\frac{\rho_s}{\rho_w} - 1 \right) (1-P)} \dots\dots\dots(4.3)$$

where K is an empirical co-efficient, treated as a calibration parameter, taken as 0.58, ρ_s is the density of sand taken as 3000 kg/m^3 for quartz sand, ρ_w is the density of water taken as 1025 kg/m^3 for seawater and P is the porosity of sand on the bed (taken to be 0.4).

The equation used for calculating the breaker wave height for depth-limited wave breaking is given by

$$H_b = \gamma d_b \dots\dots\dots(4.4)$$

where γ is the breaker index, generally taken as 0.78 and d_b is the breaker depth.

Knowing H_b , the breaker depth (d_b) can be calculated and this in turn is used for obtaining the wave group speed using the shallow water approximation given by

$$C_g = \sqrt{g d_b} \dots\dots\dots(4.5)$$

4.9.1.2 Kamphuis formula

Kamphuis (1991, 2002) formula takes into account all the important parameters like the breaker height, breaker angle, sediment grain size, bed slope, and also the effect of swells included in the form of the peak wave period. This is particularly important for the Chavara coast as it shows the influence of swells throughout the year. The formula proposed by Kamphuis for the estimation of the LST is

$$Q_{vol} = 6.4 \times 10^4 H_{sbr}^2 T_{op}^{1.5} m_b^{0.75} d_{50}^{-0.25} \sin^{0.6} (2 \theta_{br}) \dots\dots\dots(4.6)$$

where, Q_{vol} is the total immersed volume in $m^3/year$, H_{sbr} is the breaker wave height, T_{op} is the peak wave period, m_b is the bottom slope upto two wave lengths offshore of the breaker line, d_{50} is the median grain size and θ_{br} is the breaker angle with respect to the shore normal.

4.9.2 Processes based model for the estimation of LST

LST in the surf zone and innershelf was estimated by using the LITDRIFT module, one of the major modules available in the LITPACK modelling suite, which is an integrated modelling system used for modelling of littoral processes and coastline kinetics. This is a 'stand-alone' deterministic numerical modelling system, describing the major processes in the nearshore zone. LITPACK simulates non-cohesive sediment transport driven by waves and currents, littoral drift, coastline evolution and profile development along quasi-uniform beaches. The LITDRIFT module simulates the cross-shore distribution of wave height, setup and longshore current for an arbitrary coastal profile (DHI, 2004).

4.9.2.1 Theoretical background

The longshore and cross-shore momentum balance equations are solved to give the cross-shore distribution of the longshore current and the wave setup. Wave decay due to breaking is modelled, either by an empirical wave decay formula or by a model of Battjes and Jansen (1978). According to them, the wave energy balance equation for a stationary condition is given by

$$\frac{\partial}{\partial x} (C_{gx}E) + E_{diss} = 0 \dots\dots\dots(4.7)$$

where E is the mean wave energy, C_{gx} is the group velocity in x direction, E_{diss} is the time-mean dissipated power per unit area. E and E_{diss} can be written as

$$E = \frac{1}{8} \rho g H_{rms}^2 \dots\dots\dots(4.8)$$

$$E_{diss} = \frac{1}{4} \alpha_d \rho g \frac{1}{T} Q_b H_{max}^2 \dots\dots\dots(4.9)$$

where H_{rms} is the root mean square value of wave height, ρ is the density of sea water, g is the acceleration due to gravity, T is the wave period, Q_b is the fraction of breaking or broken waves, H_{max} is the maximum wave height and α_d is the dissipation factor

which is a scale parameter that gives the amount of wave breaking. The maximum wave height is calculated by

$$H_{\max} = \frac{\gamma_1}{k} \tanh\left(\frac{\gamma_2}{\gamma_1} kd\right) \dots\dots\dots(4.10)$$

where k is the wave number, d is the water depth, γ_1 and γ_2 are the two wave breaking parameters. γ_1 controls the breaking due to wave steepness condition and γ_2 controls the breaking due to limiting water depth condition.

The major assumption in the LITDRIFT module is that uniform conditions exist along the straight coast. The shore-parallel momentum balance defined in the equation given below is used to determine the longshore current velocity profile.

$$\tau_b - \frac{d}{dy}\left(\rho E_m d \frac{dv}{dy}\right) = -\left(\frac{dS_{xy}}{dy}\right) + \tau_w + \tau_{\text{cur}} \dots\dots\dots(4.11)$$

where τ_b is the bed shear stress due to the longshore current, ρ is the density of water, E_m is the momentum exchange coefficient, d is the water depth, v is the longshore current velocity, y is the shore normal coordinate, S_{xy} is the shear component of the radiation stress, τ_w and τ_{cur} are the driving forces due to wind and coastal current respectively. The relation between u and τ_b is established by the model of Fredsoe (1984).

The LITDRIFT calculates the net/gross littoral transport over a specific design period. Important factors, such as linking of the water level and the profile to the incident sea state, are included. The input data given for defining the physical conditions of the sediment transport are the cross-shore profile, hydrodynamic data which includes the water level, wave, current and wind data. The depth of closure has been arrived at based on Hallermeier (1981). The output of the LITDRIFT module provides a detailed deterministic description of the cross-shore distribution of the longshore sediment transport for an arbitrary bathymetry for both regular and irregular sea states.

4.9.2.2 Input data

The basic input used for the LITDRIFT module are cross-shore bathymetry profile, bed roughness and grain properties (size, fall velocity and gradation), water level, wave properties (height, period and angle) and wind parameters (speed and direction). The cross-shore bathymetric profile at intervals of 1 m was extracted from the

measured bathymetry upto a depth of 10 m. Sediment characteristics estimated from the collected sediment samples from the beach and innershelf (see Chapter 5) were utilized for the calculation of the bed roughness and fall velocity. Separate model setup was used for each month starting from January to December with appropriate wave and wind characteristics. Water level for the period of simulation was extracted from the MIKE C-Map. Monthly shore normal values were measured from the GPS surveyed shoreline (Fig. 4.13). Tables 4.2 & 4.3 give the sediment characteristics of cross-shore profile and the climatic description respectively for the LITDRIFT model.

Table 4.2 Sediment characteristics of cross-shore profile used for the LITDRIFT model

Parameter	Value
Mean grain diameter (mm)	0.1 - 0.24
Fall velocity (m/s)	0.063 - 0.097
Bed roughness (m)	0.00025 - 0.0006
Geometrical spreading	1.5
Relative sediment density (kg/m ³)	2.65

4.9.2.3 Calibration and validation

The breaker wave parameters γ_1 and γ_2 are given as 1 and 0.8 respectively and the dissipation factor (α_d) is calibrated as 1 for the model according to the formulation by Battjes and Janssen (1978). For validation of the model, monthly Littoral Environmental Observations (LEO) taken at the field which includes the longshore current data was used. A comparison of the measured and computed LSC is presented in Fig. 4.16. It can be seen that the results from LITDRIFT corroborates reasonably well with the field observations. The simulated LSC for the months of May, June and July have not been validated as the monthly LEO data could not be collected because of high wave activity. The LSC computed using the LITDRIFT module shows southerly current during the monsoon months of June and July with magnitudes of 0.12 and 0.21 m/s respectively. Because of the southerly current, the sediment transport during the monsoon can be expected to be towards south. During the remaining nine months the LSC is northerly indicating a net annual northerly transport. The computed maximum LSC of 0.41 m/s is during May. The LSC computed from LITDRIFT corroborates well with the field observation.

Table 4.3 Climatic description for the LITDRIFT model

Item	Minimum	Maximum
Duration (perct. year)	0.005708	0.005708
Wave height (m)	0.21	2.28
Wave direction ($^{\circ}$ N)	-113.2	138.5
Profile number	1	1
Wave period (s)	2.8	10.7
Ref. depth, height (m)	22	22
Ref. depth, angle (m)	22	22
Mean water level (m)	-0.83	0.87
Spectral description	2	2
Spreading factor	0.5	0.5
Current speed (m/s)	0	0
Ref. no for current	0	0
Wind speed (m/s)	0.11	10.47
Wind direction ($^{\circ}$ N)	0.0	359.9
Wind friction coeff.	0.001	0.001

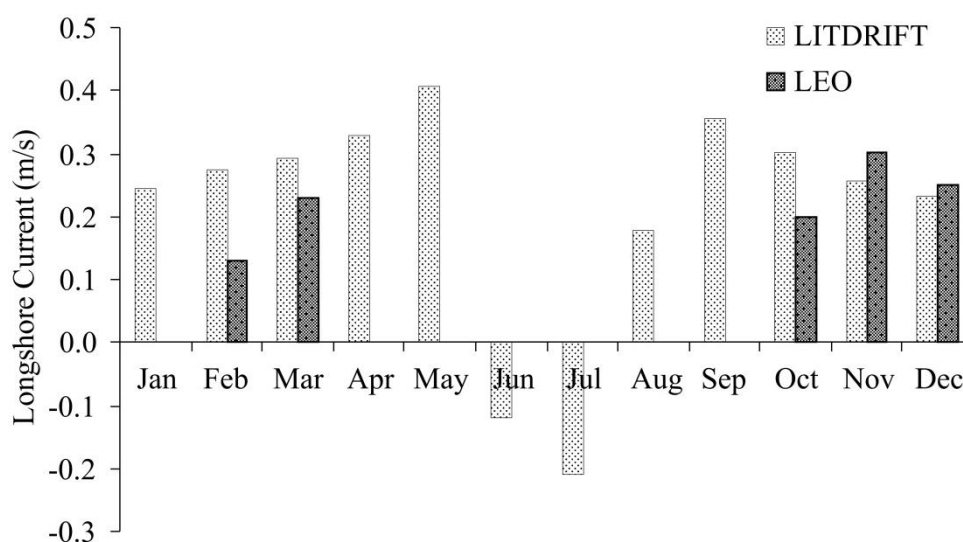


Fig. 4.16 Monthly maximum longshore current at Srayikkadu estimated by using LITDRIFT module of LITPACK and by Littoral Environmental Observation (LEO)

4.9.2.4 Surf zone longshore transport along the Chavara coast

The monthly LST computed using the three methods viz. CERC formula, Kamphuis formula and LITDRIFT module of LITPACK (Fig. 4.17 and Table 4.4) were

compared among themselves as well as with field signatures/observations to assess/ascertain the applicability of the adopted method for the Chavara coast. It is observed that the monthly directions of the LST obtained using all the three methods match throughout.

As regards the magnitude, it can be seen from the results that the monthly LST rates computed using the LITDRIFT are closer to those by the Kamphuis, while the CERC computations are exorbitantly higher than the LITDRIFT and Kamphuis throughout. The northerly transport dominates during the whole year except for the peak monsoon months of June and July. The northerly LST ranges from about 3,000 to 18,000 m³/month for the LITDRIFT, 7,000 to 24,000 m³/month for the Kamphuis and 20,000 to 110,000 m³/month for the CERC during the months of January – May and August – December. Southerly LST is observed only during June and July with the values in the range about 6,500 - 9,000 m³/month for the LITDRIFT, 15,000 - 17,500 m³/month for the Kamphuis and 165,000 - 177,000 m³/month for the CERC. Fig. 4.18 and Table 4.4 show that the inclusion of wind in the input parameters of LITDRIFT will bring about only marginal changes in the quantum of LST.

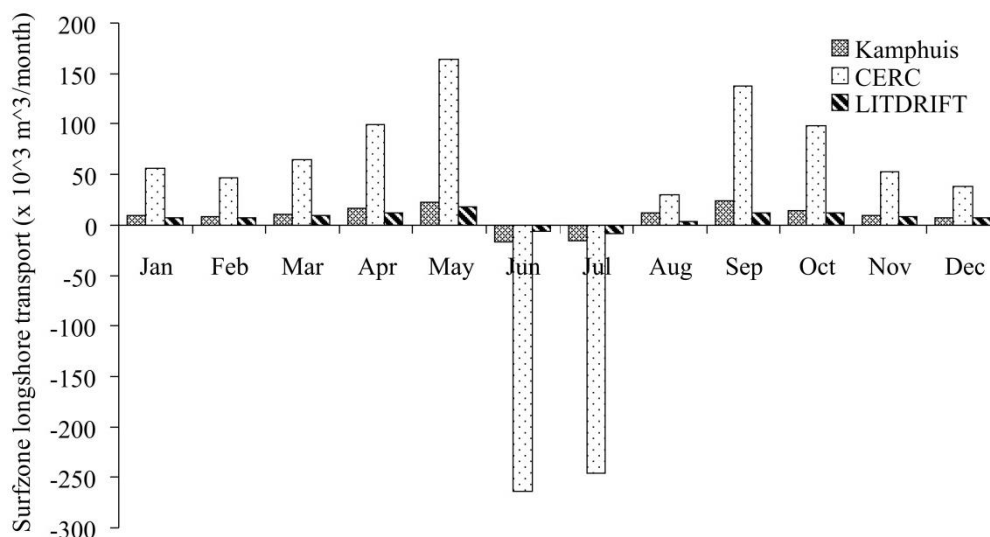


Fig. 4.17 Monthly LST in the surf zone at Srayikkadu computed using Kamphuis formula, CERC formula and LITDRIFT module of LITPACK

As expected, the gross transport obtained is very high for CERC, than the results from Kamphuis and LITDRIFT (Table 4.5). The results computed adopting the Kamphuis formula and the LITDRIFT shows reasonably good comparison with net transport values of 101,369 m³/year and 78,961 m³/year respectively, whereas the CERC formula gives exorbitantly higher values (275,513 m³/year). The values arrived at on

the basis of numerical model studies using LITDRIFT are more realistic compared to the Kamphuis method (which uses an empirical formula) as the model output is based on simulation of the site specific field processes and the effects of coastal wind and tide also have been included. The estimation of LST using the Kamphuis formula gives better results compared to that of the CERC mainly because the effect of swells, the sediment gain size and the bed slope have been considered in the sediment transport computation.

Table 4.4 Monthly LST in the surf zone at Srayikkadu computed using Kamphuis formula, CERC formula and LITDRIFT module of LITPACK

Month	Shore Normal (°N)	Kamphuis Formulae	CERC Formulae	LITDRIFT	
				(With Wind)	(No Wind)
Jan-14	240	9,932	37,586	7,301	7,675
Feb-14	244	7,730	31,066	7,272	7,444
Mar-14	242	10,977	43,002	9,090	9,326
Apr-14	234	16,251	66,599	12,130	12,679
May-14	234	22,289	110,352	17,732	18,288
Jun-14	241	-17,316	-177,677	-6,712	-6,151
Jul-14	241	-15,400	-165,406	-8,848	-8,286
Aug-14	241	12,184	19,965	3,179	3,984
Sep-14	241	23,981	92,597	12,100	12,692
Oct-14	239	14,528	65,836	11,173	11,706
Nov-14	241	9,176	35,633	8,047	8,191
Dec-14	240	7,037	25,708	6,496	6,656

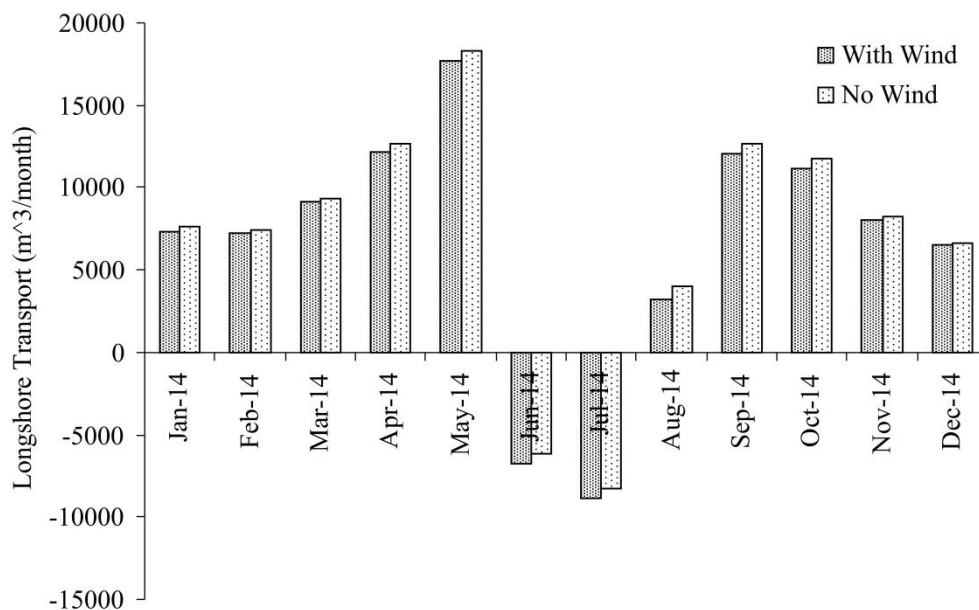


Fig. 4.18 Comparison of computed longshore sediment transport in the surf zone with and without wind using LITDRIFT module at Srayikkadu

Table 4.5 Annual longshore sediment transport in the surf zone at Srayikkadu estimated by using Kamphuis formula, CERC formula and LITDRIFT module of LITPACK

Annual surf zone longshore transport Q (m ³ /year)				
Direction	Kamphuis Formula	CERC Formula	LITDRIFT	
			With Wind	No Wind
Northerly Transport	134,085	785,737	94,521	98,641
Southerly Transport	-32,716	-510,224	-15,560	-14,437
Gross Transport	166,801	1,295,961	110,081	113,078
Net Transport	101,369	275,513	78,961	84,205

Note: -ve sign indicates southerly transport and vice versa

4.9.2.5 Innershelf longshore transport along the Chavara coast

The longshore transport computed for the innershelf between isobaths of 3 m and 10 m using the LITDRIFT module shows net southerly transport throughout the year unlike in the surf zone where the northerly transport dominates except during monsoon. The magnitude of the transport is generally high during the peak monsoon period (June-July). Also a strong correlation between the innershelf transport and the local wind conditions has been noticed as is evident from the results presented in Fig. 4.19 and Table 4.6. The computed annual innershelf longshore transport (Table 4.7) is predominantly southerly with a net magnitude 43,172 m³.

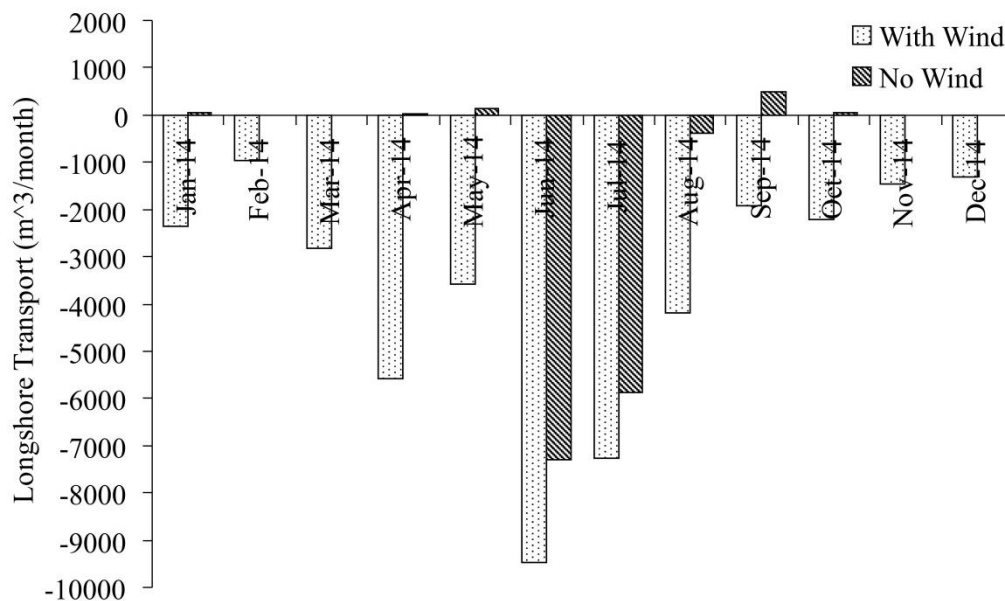


Fig. 4.19 Monthly LST in the innershelf at Srayikkadu estimated by using LITDRIFT module of LITPACK. The case for 'no wind' is also presented to highlight the significant influence of wind in the LST in the innershelf unlike the surf zone

Table 4.6 Monthly LST in the innershelf at Srayikkadu estimated by using LITDRIFT module of LITPACK

Month	Shore Normal (°N)	Monthly Innershelf longshore Transport (m ³ /month)	
		With Wind	No Wind
Jan-14	240	-2,355	48
Feb-14	244	-969	0
Mar-14	242	-2,825	0
Apr-14	234	-5,580	30
May-14	234	-3,590	132
Jun-14	241	-9,485	-7,302
Jul-14	241	-7,265	-5,868
Aug-14	241	-4,175	-381
Sep-14	241	-1,935	478
Oct-14	239	-2,227	57
Nov-14	241	-1,450	0
Dec-14	240	-1,316	0

Table 4.7 Annual LST in the innershelf at Srayikkadu estimated by using LITDRIFT module of LITPACK

Direction	Annual innershelf longshore transport Q (m ³ /year)	
	With Wind	No Wind
Northerly Transport	0	745
Southerly Transport	-43,172	-13,551
Gross Transport	43,172	14,296
Net Transport	-43,172	-12,806

4.9.3 Estimation of cross-shore transport

The LITPROF module of the LITPACK suite of programs developed by Danish Hydraulic Institute (DHI, 2004, 2008) is used for the simulation of the cross-shore profile changes under the influence of temporally varying wave conditions. The model accounts for all the important phenomena in the nearshore region such as shoaling, refraction, bed friction and wave breaking. The model is based on the assumption that the longshore gradient in hydrodynamic and sediment conditions is negligible and that the depth contours are parallel to the coastline. The offshore boundary condition for running this model is defined by specifying time varying wave conditions.

4.9.3.1 Theoretical background

The sediment transport is calculated from an intra-wave hydrodynamic model where the time evolution of the bed boundary layer is resolved. The basic equation used is the continuity equation for sediment transport given as

$$\frac{\partial z_b}{\partial t} = - \left(\frac{1}{1-P} \right) \frac{\partial Q_c}{\partial x} \dots\dots\dots(4.12)$$

where z_b is the bed level, Q_c is the cross-shore sediment transport and P is the porosity of the bed material. The LITPROF module uses a Forward in Time - Central in Space (FTCS) scheme to solve the continuity equation.

4.9.3.2 Input data

The wave parameters given as input are the root mean square wave height (h_{rms}), mean wave period and the mean wave direction. The model calculates vertical variations of turbulence, shear stress and means flow for which the effects of asymmetry of the wave orbital motion, mass flux in progressive waves, surface rollers and the wave setup are considered. For waves approaching the coast at an angle, the longshore currents are calculated from the wave induced radiation stress gradients. Table 4.2 shows the sediment characteristics of cross-shore profile used for the LITPROF model, which is same as that of LITDRIFT model. The climatic description for the LITPROF model is shown in Table 4.8.

Table 4.8 Climatic description for the LITPROF model

Item	Minimum	Maximum
Wave height (m)	0.21	2.28
Wave direction (°N)	105.5	357.2
Wave period (s)	2.8	10.7
Spreading factor (°)	6.3	79.7
Water level (m)	0	0

4.9.3.3 Calibration and validation

The main tuning parameters used for the calibration of the LITPROF model setup for a particular location, are the scale parameter and maximum angle of the bed slope. The scale parameter is a calibration factor which reflects the cross-shore exchange of momentum and it is proportional to the characteristic length scale over which the

transport is smoothed. For the present study the final values of the tuning parameters used are 30° for the maximum angle of the bed slope, 3 for the scale parameter, 0.78 and 0.8 for γ_1 and γ_2 (wave breaking factors) respectively and 0.15 for the roller coefficient (Table 4.9). The parameters are named according to the model interface. The calibration of the model is carried out by comparing the model results with that of the measured for various tuning parameters. Correlation coefficients (CC) between the simulated and measured monthly beach profiles have been calculated. In addition to this, the Brier Skill Score (BSS) which is used to assess the skills of coastal morphological models (Sutherland et al., 2004; van Rijn et al., 2003; Pender and Karunaratna, 2013) is also estimated. The BSS compares the mean square difference between the simulation and the measurement with the mean square difference between initial/baseline simulation and measurement and is defined as

$$BSS = 1 - \frac{\langle (|Z_{b,s} - Z_{b,m}| - \Delta Z_{b,m})^2 \rangle}{\langle (Z_{b,0} - Z_{b,m})^2 \rangle} \dots\dots\dots(4.13)$$

where $Z_{b,m}$ is the measured bed level, $Z_{b,s}$ is the simulated bed level, $Z_{b,0}$ is the initial bed level, $\Delta Z_{b,m}$ is the error of the measured bed level and $\langle \dots \rangle$ denotes the averaging procedure over time series. Perfect agreement with the measured and simulated values gives a skill score of 1, whereas a lower value indicates a poor/bad performance. The classification of BSS by van Rijn et al. (2003) is shown in Table 4.10.

van der Wegen et al. (2011) expressed the BSS in terms of volumetric change and is defined as

$$BSS = 1 - \frac{\langle (\Delta Vol_{simul} - \Delta Vol_{meas})^2 \rangle}{\langle (\Delta Vol_{meas})^2 \rangle} \dots\dots\dots(4.14)$$

where ΔVol is the volumetric change compared to the initial bed in m^3 , for simulated and measured quantity, $\langle \dots \rangle$ denotes an arithmetic mean or a spatial average. The measurement error can be accounted by using the extended BSS_{vr} proposed by van Rijn et al. (2003) and is defined as

$$BSS_{vr} = 1 - \frac{\langle (|\Delta Vol_{simul} - \Delta Vol_{meas}| - \delta)^2 \rangle}{\langle (\Delta Vol_{meas})^2 \rangle} \dots\dots\dots(4.15)$$

where δ denotes the volumetric measurement error in m^3 .

For this work, both the BSS estimates as proposed by van Rijn et al. (2003) and van der Wegen et al. (2011) have been used as the study involves temporal comparison of cross-shore profile and volume changes.

Table 4.9 Calibration terms used for the LITPROF model

Parameter	Value
Max. morphological time step (s)	900
Scale parameter	3
Max. bed slope (deg.)	30
Wave breaking factor (γ_1)	0.78
Wave breaking factor (γ_2)	0.8
Dissipation roller coeff.	0.15

Table 4.10 Classification of BSS (van Rijn et al., 2003; van der Wegen et al., 2011)

BSS	BSS _{vr}	Remarks
0.5-1.0	0.8-1.0	Excellent
0.2-0.5	0.6-0.8	Good
0.1-0.2	0.3-0.6	Fair
0.0-0.1	0.0-0.3	Poor
<0.0	<0.0	Bad

BSS - Brier Skill Score; BSS_{vr} - Brier Skill Score extended by van Rijn et al. (2003)

4.9.3.4 Cross-shore transport along the Chavara coast

The temporal variation in cross-shore transport across the innershelf and surf zone for a period of one year has been computed and the results are presented in Fig. 4.20. For validation of the LITPROF results the simulated monthly cross-shore profiles were compared with the monthly measured beach profile. Since the measured monthly profile measurements were limited to the portion above the Still Water Line (SWL) the validation was limited to the sub-aerial portion of the profile. The computed beach volume results are in close agreement with the computed volume from the beach profiles during non-monsoon and monsoon months except during October and November. The comparison for the months of May to July is not possible since the beach is completely eroded at this station due to the rough monsoon wave conditions. The measured beach profiles indicate an overall eroding tendency without any significant recovery even towards the end of the year (i.e. during December) and this corroborates well with the simulated beach volume computation (Fig. 4.21).

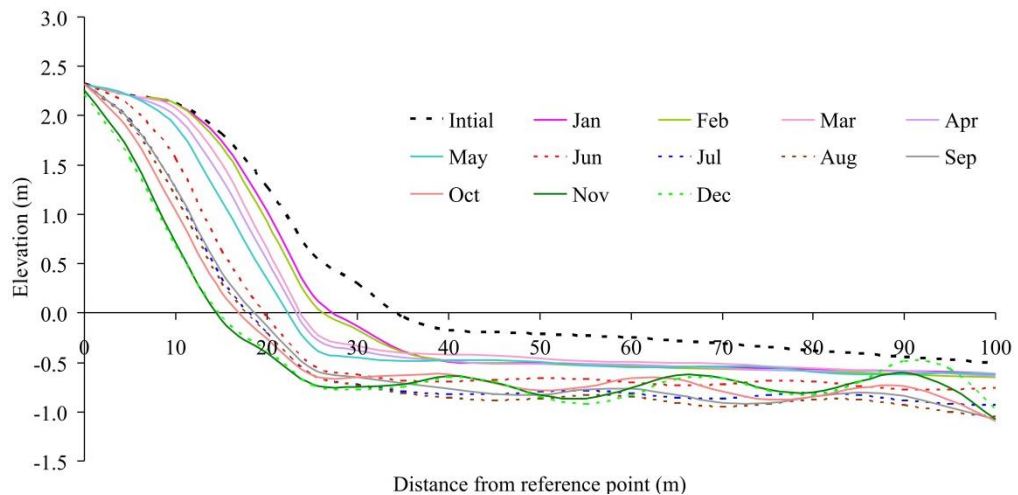


Fig. 4.20 Beach profiles at Srayikkadu simulated using LITPROF for one year

Correlation coefficients between the simulated and measured monthly beach profiles have been calculated and are presented in Table 4.11. The results show a good correlation during the entire period of observation. The Brier Skill Scores (BSS) have been estimated from the measured beach profiles and from the simulated cross-shore profile for each month during January to December 2014 (Table 4.12). As per the classification of the BSS (proposed by van Rijn et al., 2003; Sutherland et al., 2004; van der Wegen et al., 2011) Scores < 0, 0-0.1, 0.21-0.2, 0.2-0.5 and 0.5-1.0 represent 'bad', 'poor', 'fair', 'good' and 'excellent' validation of the model results respectively. Also an additional error factor was introduced in the BSS estimation by van Rijn et al. (2003) and the Scores were reclassified as BSS < 0, 0-0.3, 0.3-0.6, 0.6-0.8 and 0.8-1.0 representing 'bad', 'poor', 'fair', 'good' and 'excellent' scores respectively. In the present simulation the highest BS Scores of 0.93 and 0.92 are observed during the months of September and December respectively and the scores are considered as excellent. The BSS estimates for the remaining months indicate mixed response as is evident from the scores of 0.24 (February), 0.34 (August) and 0.45 (November) which denotes 'poor' and 'fair' validation. The negative values obtained for the BSS estimates for January, March and October show poor comparison between the measured and simulated values. This probably could be due to the changing environmental conditions that prevail during the transition periods between the high and low wave activity period (i.e. the monsoon, monsoon breaks, and non-monsoon period). It is expected that by increasing the frequency of measurements during these periods better tuning of the model results is possible during the calibration stage and the BS scores can be improved considerably.

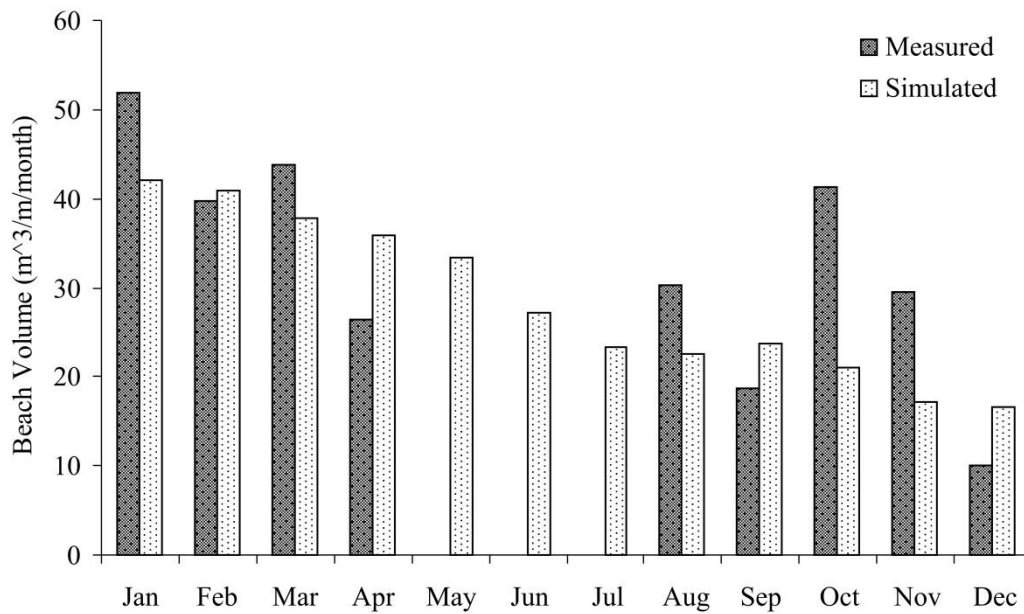


Fig. 4.21 Validation of the cross-shore transport using the beach volume from the measured beach profile and simulated beach volume from the LITPROF cross-shore profile during January - December 2014 for Srayikkadu (Note: No beach during May to July)

Table 4.11 Error estimation for the beach profiles using the measured beach profile and simulated cross-shore profile (from LITPROF) during January-December 2014

Month	*CC	*BSS _{vr}	Remarks from BSS (van Rijn et al., 2003)
Jan-2014	0.73	-0.31	Bad
Feb-2014	0.83	0.24	Poor
Mar-2014	0.82	-0.29	Bad
Apr-2014	0.99	0.83	Excellent
May-2014	#	#	-
Jun-2014	#	#	-
Jul-2014	#	#	-
Aug-2014	0.91	0.34	Fair
Sep-2014	0.97	0.93	Excellent
Oct-2014	0.92	-3.79	Bad
Nov-2014	0.89	0.45	Fair
Dec-2014	1.00	0.92	Excellent

*CC - Correlation Coefficient; *BSS - Brier Skill Score;
No beach

For validation of numerical models, the estimation of BS Scores considering the measured and simulated volume has been adopted widely by many researchers for similar studies. In the present study the BSS estimates have been made from the measured and simulated beach volume for each month from January to December 2014. A similar study has been performed by van der Wegen et al. (2011) using the

measured and modelled depositional volume. Scores indicating 'excellent' performance is observed for 7 months (February, March, April, August, September, November and December) out of the total of 9 months. The score shows 'fair' for January and 'bad' for the month of October.

Table 4.12 Estimation of BSS from the measured and simulated beach volume (from the LITPROF cross-shore profile) during January-December 2014

Month	*BSS	Remarks from BSS (van der Wegen et al., 2011)
Jan-2014	0.19	Fair
Feb-2014	0.78	Excellent
Mar-2014	0.97	Excellent
Apr-2014	0.70	Excellent
May-2014	#	#
Jun-2014	#	#
Jul-2014	#	#
Aug-2014	0.98	Excellent
Sep-2014	0.92	Excellent
Oct-2014	-1.22	Bad
Nov-2014	0.88	Excellent
Dec-2014	0.93	Excellent

*BSS - Brier Skill Score; # No beach

The BSS estimates using the measured and simulated profile and beach volume, in general, confirms the acceptability of the model. The monthly cross-shore sediment transports across the surf zone and innershelf for Srayikkadu computed using the model are presented in Fig. 4.22 and Table 4.13 and the annual cross-shore sediment transports are presented in Fig. 4.23 and Table 4.14.

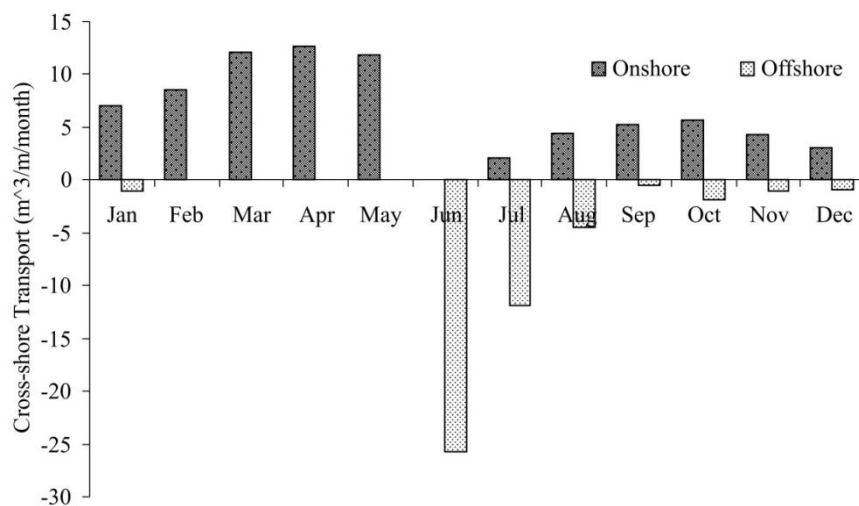


Fig. 4.22 Monthly cross-shore sediment transport at Srayikkadu estimated by using LITPROF module of LITPACK during January - December 2014

The computed values show an annual onshore and offshore transport of 77 m³/m and 47 m³/m respectively with a net annual cross-shore transport of 30 m³/m in the onshore direction. It can be seen that the onshore transport dominates during the one year simulation period.

Table 4.13 Monthly cross-shore sediment transport at Srayikkadu estimated by using LITPROF module of LITPACK during January-December 2014

Month	Cross-shore transport (m ³ /m/month)		
	Onshore	Offshore	Net
Jan-14	7.06	-1	6.06
Feb-14	8.52	0	8.52
Mar-14	12.08	0	12.08
Apr-14	12.65	0	12.65
May-14	11.88	0	11.88
Jun-14	0	-25.77	-25.77
Jul-14	2.08	-11.86	-9.78
Aug-14	4.39	-4.51	-0.12
Sep-14	5.24	-0.45	4.79
Oct-14	5.67	-1.81	3.87
Nov-14	4.37	-0.99	3.38
Dec-14	3.02	-0.92	2.1
Net (m ³ /m/year)	77	-47	30

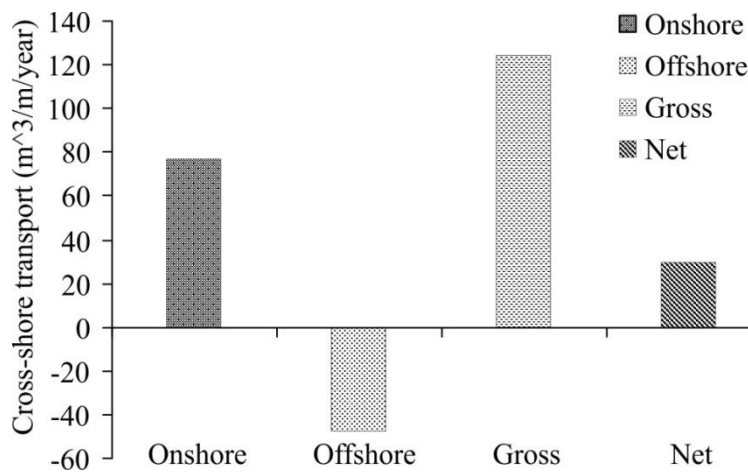


Fig. 4.23 Annual cross-shore sediment transport at Srayikkadu estimated by using LITPROF module of LITPACK during January - December 2014

4.10 Discussion

The study has brought out the nearshore sediment transport regime for a location of the Chavara coast. The LST in the surf zone has a net yearly value of about 79,000 m³ in the northerly direction whereas the transport in the innershelf is consistently

southerly with a value of about 43,000 m³. While LST in the surf zone has been estimated by various researchers for this coast (Chandramohan and Nayak, 1991; Sajeev et al., 1997b; Jose et al., 1997; Sanil Kumar et al., 2006; Black et al., 2008; Sheela Nair et al., 2015), the LST in the innershelf is estimated only by Black et al. (2008). Barring the recent works of Black et al. (2008) and Sheela Nair et al. (2015), the earlier authors have used empirical methods and the computations are based on wave data available only for short duration (seasonal observations for few days, monthly/weekly LEO observations). Thus the exceptionally high quantities and contrasting direction obtained by them [Chandramohan and Nayak (1991) _ 950,000 m³/year towards south; Sajeev et al. (1997b) _ 380,000 m³/year towards south; Jose et al. (1997) _ 360,000 m³/year towards south; Sanil Kumar et al. (2006) _ 380,000 m³/year towards south] may not be realistic. The present estimates of the LST in the surf zone (LITDRIFT ~ 79,000 m³/year; Kamphuis ~ 101,000 m³/year) works out to be closer to the net northerly LST of 125,000 m³/year computed by Black et al. (2008) for this coast. That the net surf zone longshore transport is northerly is amply clear from the huge accretion on the southern side of the breakwater at Kayamkulam inlet and the critical erosion observed on the northern side of the inlet (Kurian et al., 2012).

Table 4.14 Annual cross-shore sediment transport at Srayikkadu estimated by using LITPROF module of LITPACK during January-December 2014

Annual cross-shore transport (m ³ /m/year)	
Onshore Transport	77
Offshore Transport	-47
Gross Transport	124
Net Transport	30

As regards the LST in the innershelf, the only other work available is that of Black et al. (2008). For a 2 km width of the innershelf, they have estimated a southerly transport of 1,72,000 ± 50 % m³/year which can be considered as high. The wide difference in the computed results may have to do with the models used. Moreover, the lower value of 43,000 m³/year appear to be agreeing to the field signatures which do not support the high quantum of transport obtained by Black et al. (2008).

Except for the study by Black et al. (2008), estimates on cross-shore sediment transport are lacking for this coast. They obtained onshore and offshore fluxes of 0.201 m³/m/day and 0.437 m³/m/day respectively. Based on the assumption that onshore and offshore fluxes are predominant for 8 months and 4 months respectively

in a year, they arrived at yearly values of 49 m³/m/year and 53 m³/m/year in the onshore and offshore directions respectively. The assumption of offshore flux for 4 months in a year appears to be on the higher side as can be seen from the measured wave data in the present study. Thus there is every possibility that the onshore flux estimated by them could be on the higher side when compared to the offshore flux. The higher onshore flux obtained in the present study when compared to offshore flux appear to conform to their results.

Black et al. (2008) based on their study for the Chavara coast has concluded that the system is a closed, dynamic, and finely balanced one. They have coined the term “step ladder” for the observed dynamic equilibrium on a regional scale. However, the dynamic equilibrium which was proposed by them based on their field data pertaining to the period 1999-2001 is no more applicable to this coast. The physiographic setup of the coast has undergone tremendous change since then starting with the construction of two breakwaters at the Kayamkulam inlet in 2000 having lengths of 720 m and 485 m on the south and north of the inlet respectively. Groins numbering 26 that were constructed during the past five years also have brought in localised shoreline changes. The results of the present study confirm the absence of this dynamic equilibrium which is evident from the field data as well as the computed results. The monthly beach profiles for the year 2014 shows that the profile has not regained its original shape on completion of one year. To put it in terms of volume change, on completion of one year, the beach is in short of 44 m³/m of sand to regain its original position. While 101 m³/m is the offshore transport (volume of erosion), the onshore transport (volume of accretion) is only 57 m³/m. Considering the fact that the beach profile station (Srayikkadu) could be under the influence of excessive sand mining in the neighbourhood some amount of sand loss is expected from that account. The actual quantity of sand available for onshore transport could be reduced due to this. Hence the onshore transport observed in the field is found to be considerably less than the computed one.

The computed and observed sediment fluxes have a bearing on the mining volumes. As per the beach profile data, the yearly onshore transport is 57 m³/m. Thus the maximum sustainable mining volume from a 1 km stretch of beach can be 57,000 m³ only. As per the computed onshore sediment flux, the mining can be a much higher figure of 77,000 m³ over a one km stretch of mining site. However, it should not be

expected that the actual replenishment from offshore will be in tune with the computed one due to the reasons already mentioned.

4.11 Summary

A study of the nearshore sediment transport regime of a placer mining beach has been carried out combining field measurements with computations using different mathematical formulations. The field programmes included measurements of wind, wave, beach profiles and littoral environmental parameters and mapping of shoreline for the period of January to December 2014. The longshore sediment transport (LST) in the surf zone was computed by using both bulk formulas (CERC and Kamphuis) and process-based numerical model (LITDRIFT). The longshore (3-10 m depth excluding surf zone) and cross-shore sediment fluxes in the innershelf were estimated using the validated LITDRIFT and LITPROF models of LITPACK modelling system respectively. The model results indicate dominance of annual onshore transport over offshore transport. The net longshore transport in the surf zone is northerly while it is consistently southerly in the innershelf. The two counter-directional pathways are linked through the cross-shore transport. The domination of the computed onshore flux is actually not reflected in the observed beach volume change, probably due to the influence of excessive sand mining by the industries. The actual quantity of sand available in the innershelf for onshore transport could be reduced due to the mining. This reduction in the replenishment of sand from offshore will affect the stability of the coast.

CHAPTER 5

HEAVY MINERAL DEPLETION IN THE SEDIMENTS

5.1 Introduction

The 'Chavara placer deposit' of the Neendakara-Kayamkulam coastal sector is known for the rich concentration of heavy minerals. The commonly occurring minerals in the deposits are ilmenite, leucoxene, rutile, sillimanite, garnet, zircon, monazite, that have a specific gravity of >2.57 . This deposit is also known for high content of titanium ($>60\%$) in the ilmenite which makes it as one of the world's richest beach deposits in terms of mineral content. Heavy Mineral (HM) concentration, as high as 100 %, was reported in the beach sediments of this coast since a long time (Prakash and Verghese, 1987). Kurian et al. (2001) as part of their study conducted during 1995 had estimated high concentration of the HM in the beach sediments and observed that it was even upto 100 % during the monsoon period. Further field investigations carried out along the same coastal stretch later during 1999-2000 by Kurian et al. (2002) also indicated high concentration of heavy minerals, as much as 80 %, but at the same time reported a general reduction in the concentration of heavies at the mining site of Vellanathuruthu located in the southern sector of the coast. As per the recent estimates of IREL (IREL, 2010) there is a drastic decrease in the HM concentration in the beach sands extracted by them.

This depletion in the HM concentration over the years offered an interesting case for a detailed investigation to understand the mechanisms that manifest these changes. This chapter encompasses the results of a detailed study of the sedimentology and mineralogy of the beach and innershelf sediments of the Chavara coast delineating the factors responsible for the depletion in the HM content. While doing so sedimentological sampling has been extended to the HM-rich Arattupuzha coast, north of the Chavara coast in order to better understand the long-term changes in the HM concentration.

5.2 Textural Characteristics of Beach Sediments

For the present study surficial samples were collected along nearly shore-normal transects extending upto 20 m depth covering beach, surf zone, nearshore and offshore off six locations viz. Neendakara, Kovilhottam, Panikkarkadavu,

Srayikkadu, south of Kayakulam inlet and Arattupuzha (Fig. 5.1). The results of textural analyses of beach samples collected during the months of July and November 2010 and April 2011 representing the monsoon, post-monsoon and pre-monsoon months are presented in Tables 5.1 - 5.3.

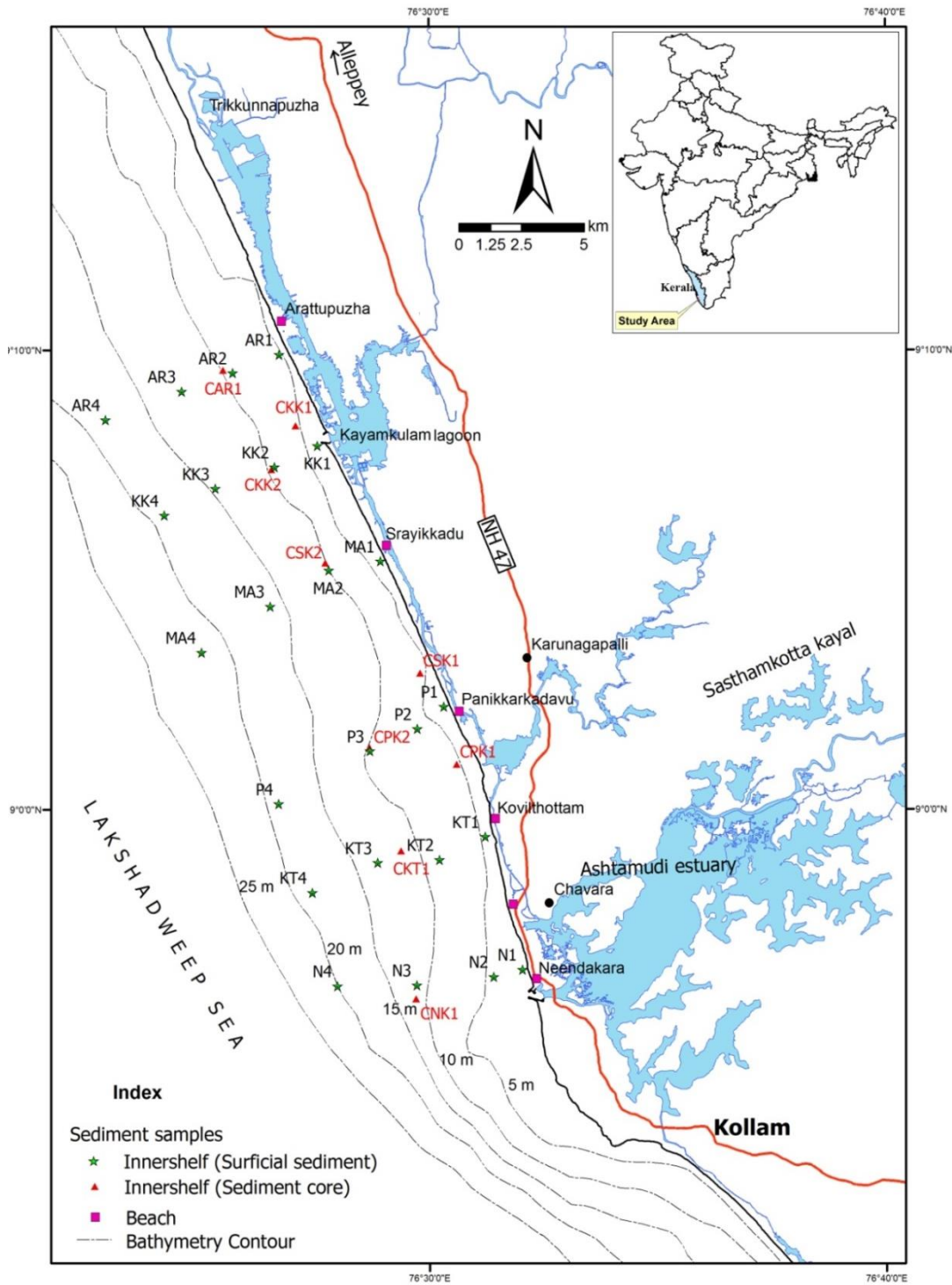


Fig. 5.1 Sediment sampling points in the beach and the innershelf of the Neendakara-Arattupuzha coast

5.2.1 Mean size

The mean grain size of a beach is a function of the incident wave energy and nature of the sand availability. The mean grain size of sediment samples collected from the beach during the pre-monsoon season were in the range of 0.10 to 0.26 mm in the breaker zone; 0.20 to 0.29 mm in the mid water line (MWL) and 0.18 to 0.28 mm in the berm indicating that the beach is mainly composed of medium to fine sand. In the breaker zone, domination of very fine to fine sand was observed except at Arattupuzha which showed the presence of medium sand.

During the monsoon the mean grain size ranged from 0.26 to 0.58 mm in the breaker zone, 0.20 to 0.39 mm in the mid water line (MWL) and 0.19 to 0.21 mm in the berm indicating that the beach is mainly composed of medium to coarse sand. The beach building processes is normally initiated during the post-monsoon period when the onshore transport of sediment takes place. During this period, the mean grain size in the breaker zone, the MWL and the berm are between 0.12 and 0.29 mm; 0.22 and 0.40 mm; and 0.18 and 0.26 mm respectively. It is also observed that the berm point at Kovilhottam location contains relatively coarser sediments (0.26 mm) compared to that of Kayamkulam and Arattupuzha (0.20 mm) samples which are predominantly of fine sediments rich in HM.

5.2.2 Sorting coefficient

The base two logarithmic ϕ (phi) scale is used here to describe the grain size distribution of the sediment. The sorting coefficient measures the amount of spread of a particle size distribution from the mean (Folk and Ward, 1957). The sorting coefficients of sediments of different locations are given in Tables 5.1 - 5.3. Majority of the sediment samples during the pre-monsoon period falls under the moderately to moderately well sorted category. The variation of sorting co-efficient at the breaker zone, the MWL and the berm are between 0.54 and 1.01 ϕ (Avg. 0.76 ϕ); 0.58 and 0.80 ϕ (Avg. 0.66 ϕ); and 0.48 and 0.79 ϕ (Avg. 0.62 ϕ) respectively, which indicates poor sorting in the breaker zone with gradual improvement towards the berm. The samples collected during the monsoon are slightly better sorted compared to that of the pre-monsoon with a slight variation in the sorting coefficient among the different locations except at Arattupuzha. At Arattupuzha coast with high concentration of HM, the sorting coefficient varies between 0.31 and 0.96 ϕ in the breaker zone indicating

poor sorting. The post-monsoon samples show a wide range of sorting characteristics with domination of moderately well sorted material. Based on the analysis of the sorting characteristics of the beach sediment samples collected from the coastal stretch from Neendakara to Arattupuzha it can be inferred that the beach samples exhibit poor sorting, progressively towards the north with the worst sorting ($>1.0 \phi$) observed to the south of Kayamkulam inlet. This further indicates that the sediments are generally of mixed type showing accretion towards the south of Kayamkulam inlet. These observations also corroborate well with the observed morphological changes which show accretion towards the south of Kayamkulam breakwater. However, at the Arattupuzha beach which is eroding and is located to the north of the Kayamkulam inlet, the sediments are better sorted with an increase in the HM concentration.

Table 5.1 Textural characteristics of beach sediment samples from different locations of the Neendakara-Arattupuzha coast during the pre-monsoon period

Sl. No.	Sample Location	Backshore		Berm		Mid Water Line		Breaker Zone	
		Mean (mm)	Sorting (ϕ)	Mean (mm)	Sorting (ϕ)	Mean (mm)	Sorting (ϕ)	Mean (mm)	Sorting (ϕ)
1	Neendakara	No Beach		No Beach		No Beach		0.10	0.69
2	Kovilhottam	No Beach		0.28	0.79	0.28	0.68	0.17	0.75
3	Panikkarkadavu	No Beach		No Beach		0.23	0.80	0.15	0.68
4	Srayikkadu	No Beach		No Beach		0.21	0.65	0.17	0.89
5	Kayamkulam	No Beach		0.19	0.59	0.29	0.58	0.12	0.54
6	Arattupuzha	No Beach		0.18	0.48	0.20	0.64	0.26	1.01

Table 5.2 Textural characteristics of beach sediment samples from different locations of the Neendakara-Arattupuzha coast during the monsoon period

Sl. No.	Sample Location	Backshore		Berm		Mid Water Line		Breaker Zone	
		Mean (mm)	Sorting (ϕ)	Mean (mm)	Sorting (ϕ)	Mean (mm)	Sorting (ϕ)	Mean (mm)	Sorting (ϕ)
1	Neendakara	No Beach		No Beach		No Beach		0.26	0.81
2	Kovilhottam	No Beach		No Beach		0.39	0.82	0.55	0.96
3	Panikkarkadavu	No Beach		No Beach		0.20	0.38	0.58	0.52
4	Srayikkadu	0.23	0.57	No Beach		No Beach		0.26	0.76
5	Kayamkulam	No Beach		0.21	0.66	0.30	1.06	0.32	0.84
6	Arattupuzha	No Beach		No Beach		No Beach		0.10	0.31

Table 5.3 Textural characteristics of beach sediment samples from different locations of the Neendakara-Arattupuzha coast during the post-monsoon period

Sl. No.	Sample location	Backshore		Berm		Mid Water Line		Breaker Zone	
		Mean (mm)	Sorting (ϕ)	Mean (mm)	Sorting (ϕ)	Mean (mm)	Sorting (ϕ)	Mean (mm)	Sorting (ϕ)
1	Neendakara	No Beach		No Beach		No Beach		0.13	0.70
2	Kovilhottam	No Beach		0.26	0.57	0.40	0.97	0.15	0.53
3	Panikkarkadavu	No Beach		No Beach		0.22	0.71	0.12	0.66
4	Srayikkadu	0.24	0.63	No Beach		0.27	0.81	0.19	0.89
5	Kayamkulam	No Beach		0.18	0.46	0.31	1.04	0.29	1.05
6	Arattupuzha	No Beach		0.20	0.48	0.35	0.76	0.17	0.57

5.3 Textural Characteristics of Innershelf Sediments

The distributions of mean size of sediments in the innershelf during the pre-monsoon, monsoon and post-monsoon seasons are presented in Figs. 5.2 - 5.4 and the data are presented in Tables 5.4 - 5.6.

During the pre-monsoon period (Table 5.4) the innershelf is carpeted by ‘sand’, ‘silty sand’ and ‘sandy silt’ types of sediments. Sand covers the major portion of the nearshore zone between Neendakara and Srayikkadu (located south of the Kayamkulam inlet) whereas clayey type of sediments is found off the Kayamkulam inlet and further north. Beyond 10 m depth, sandy silt sediments dominate. The mean size of ‘sandy’ sediments is in the range of 0.05 to 0.17 mm indicating fine to very fine type of sand. Silty type of sediment has a mean size of <0.05 mm. At 20 m water depth off the Kayamkulam inlet a patch of medium to coarse sand is encountered which has a mean size of 0.33 mm. Majority of the sandy sediments are of the moderately sorted category with a sorting coefficient of <0.70 ϕ . Silty sediments are poorly sorted with a sorting coefficient >1.0 ϕ . Based on the spatial distribution of mean size of sediment (Fig. 5.2) in the innershelf it can be inferred that the fine type of sandy sediment is dominant in the shelf of <10 m water depth between Neendakara and Srayikkadu whereas in the rest of the area clayey silt dominates.

‘Sand’, ‘silty sand’ and ‘sandy silt’ type of sediments occurs during the monsoon period (Table 5.5). Sandy sediment is dominant in the nearshore zone between Neendakara and Panikkarkadavu whereas the sandy silt and clayey silt are seen more towards Kayamkulam and further north. Beyond 10 m depth the clayey silt dominates

towards south of Srayikkadu whereas towards north the sediment becomes clayey silt and sandy silt.

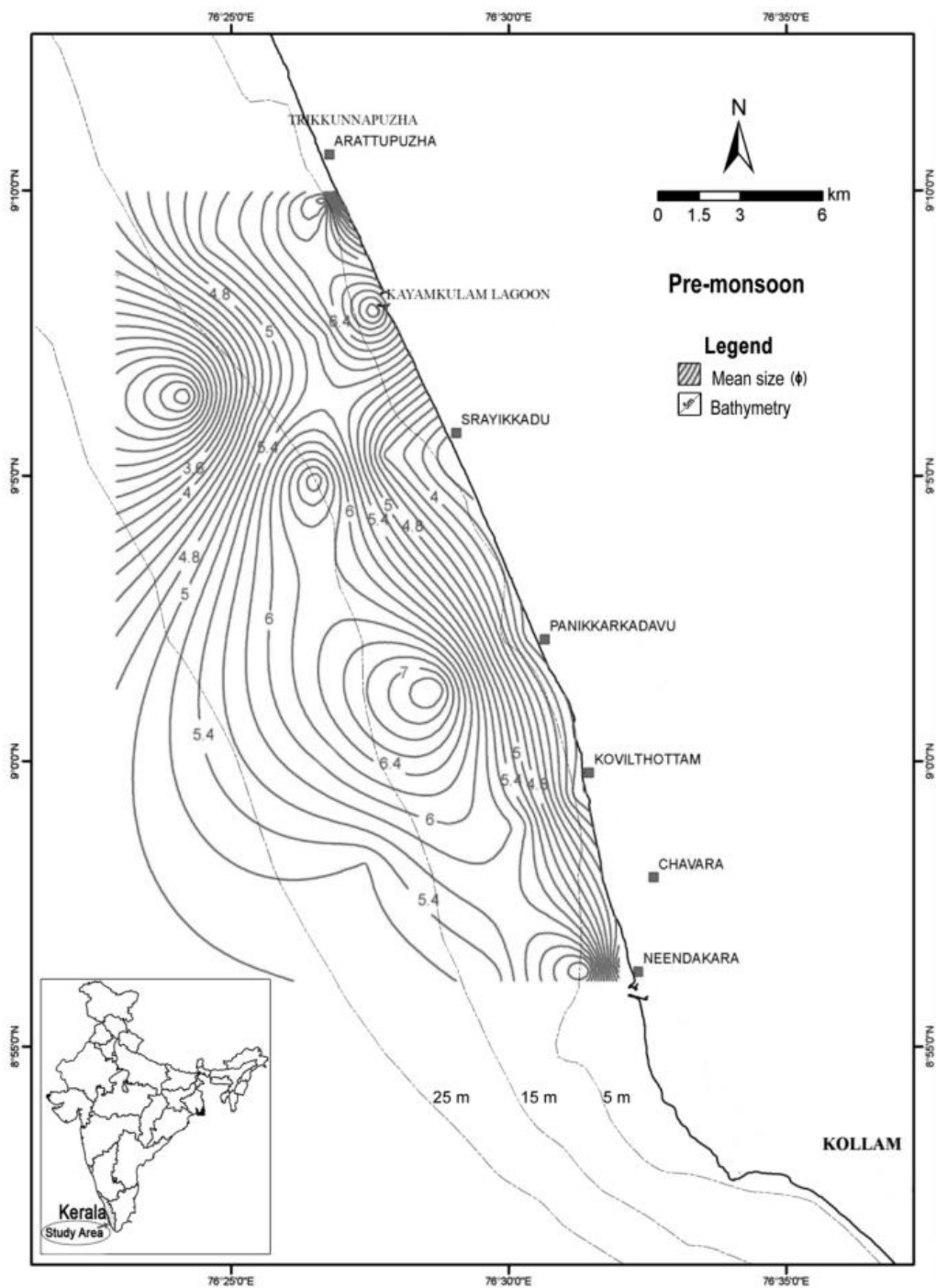


Fig. 5.2 Spatial distribution of mean sediment size in the innershelf during the pre-monsoon

The spatial distribution of mean size of sediment during the monsoon period is shown in Fig. 5.3. The mean sizes of ‘sandy’ sediments are in the range of 0.07 to 0.41 mm indicating that they are very fine to medium sand. Medium sand occurs off

Arattupuzha coast at a depth of 20 m. The mean size of silty sediment encountered is < 0.05 mm. Majority of the sandy sediments in the nearshore are well sorted compared to the area north of Srayikkadu.

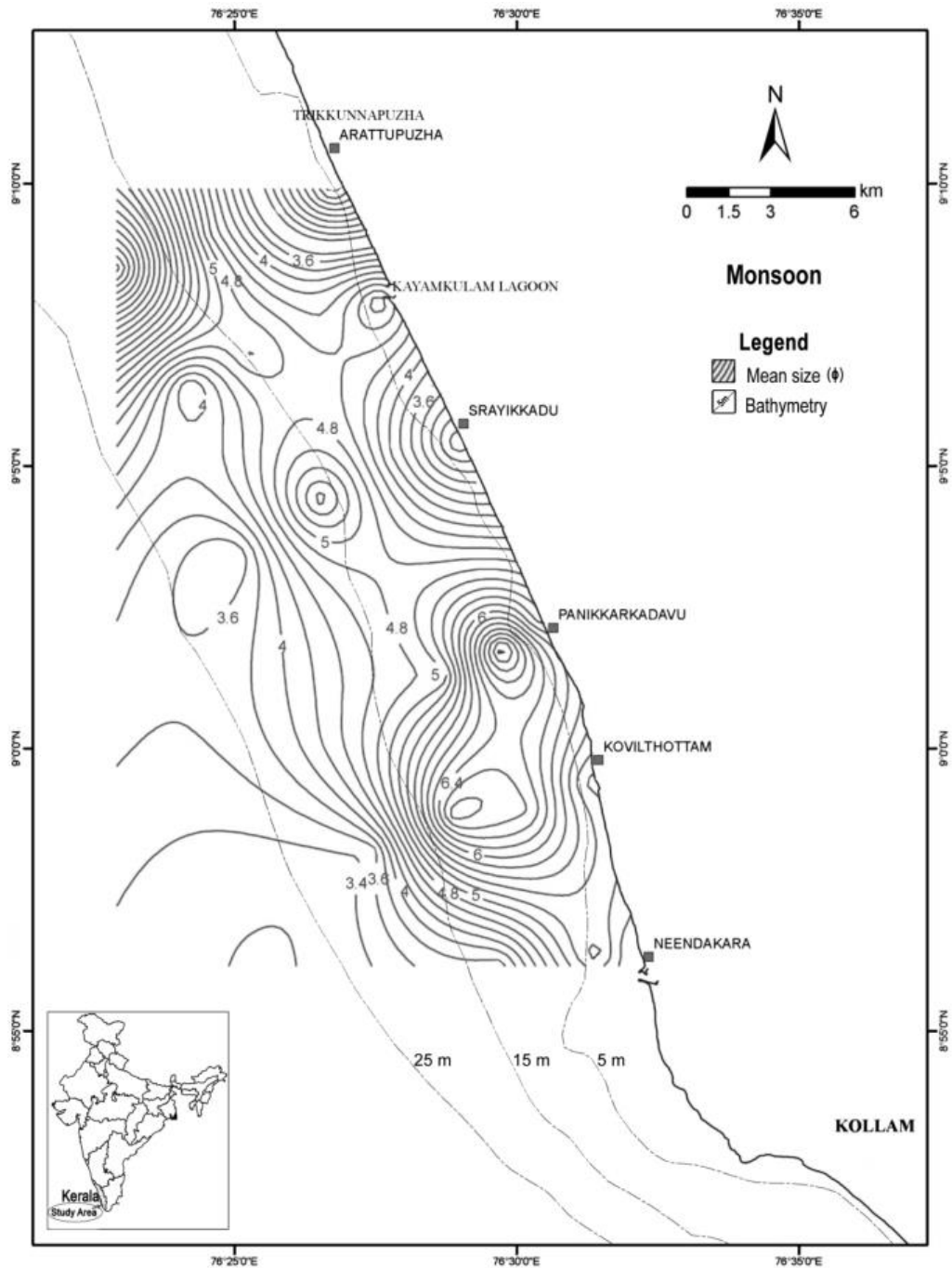


Fig. 5.3 Spatial distribution of sediment mean size in the innershelf during the monsoon

During the post-monsoon period (Table 5.6) the seabed is carpeted by a mixture of sand, silty sand, clayey silt and clay type of sediments. The study of the spatial distribution of the sediments indicates sand domination in the nearshore zone upto

Srayikkadu. But further north of Srayikkadu and also towards the offshore region, presence of fine sediments i.e., clayey silt and mud is observed. The sandy sediments are fine to medium sand type with a mean size ranging from 0.08 to 0.33 mm (3.58 to 1.62 ϕ). The mean size distribution is shown in Fig. 5.4. Silty sand have the mean size > 0.08 mm whereas the muddy sediment which is a mixture of sand, silt and clay of equal proportion have the mean size around 0.01 mm. It is noticed that majority of the sandy sediments are well sorted to moderately well sorted category whereas the fine sediments are poorly sorted.

Table 5.4 Textural characteristics of the innershelf sediments during the pre-monsoon

Sl. No.	Transect	Station No.	Depth (m)	Mean		Sorting (ϕ)	Sediment type (after Shepard, 1954)
				(ϕ)	(mm)		
1	Neendakara	N1	4.85	3.64	0.08	0.36	Sand
2		N2	9.8	6.66	0.01	2.46	Clayey Silt
3		N3	15	5.24	0.03	1.81	Silt
4		N4	20	5.06	0.03	1.98	Sandy Silt
5	Kovilhottam	KT1	3.5	3.41	0.09	0.30	Sand
6		KT2	6.3	3.57	0.08	0.44	Sand
7		KT3	11.8	5.74	0.02	2.30	Clayey Silt
8		KT4	15.2	5.98	0.02	2.46	Sand Silt Clay
9		KT5	21.3	5.18	0.03	2.03	Sandy Silt
10	Panikkarkadavu	P1	5	3.39	0.10	0.32	Sand
11		P2	10	4.93	0.03	2.27	Silty Sand
12		P3	15	7.45	0.01	2.69	Clayey Silt
13		P4	21	6.09	0.01	3.18	Sand Silt Clay
14	Srayikkadu	MA1	5	3.36	0.10	0.31	Sand
15		MA2	10	4.12	0.06	1.45	Silty Sand
16		MA3	16	7.00	0.01	2.74	Clayey Silt
17		MA4	20	5.20	0.03	3.28	Sandy Silt
18	Kayamkulam	KK1	3.5	6.92	0.01	2.69	Clayey Silt
19		KK2	5	7.49	0.01	2.80	Clayey Silt
20		KK3	10	5.67	0.02	2.29	Sandy Silt
21		KK4	15	4.57	0.04	3.08	Silty Sand
22		KK5	20	1.60	0.33	1.79	Sand
23	Arattupuzha	AR1	3.5	2.80	0.14	0.69	Sand
24		AR2	5	6.94	0.01	3.22	Clayey Silt
25		AR3	10	6.08	0.01	2.49	Clayey Silt
26		AR4	15	5.52	0.02	3.38	Sandy Silt
27		AR5	20	3.95	0.06	3.06	Sand

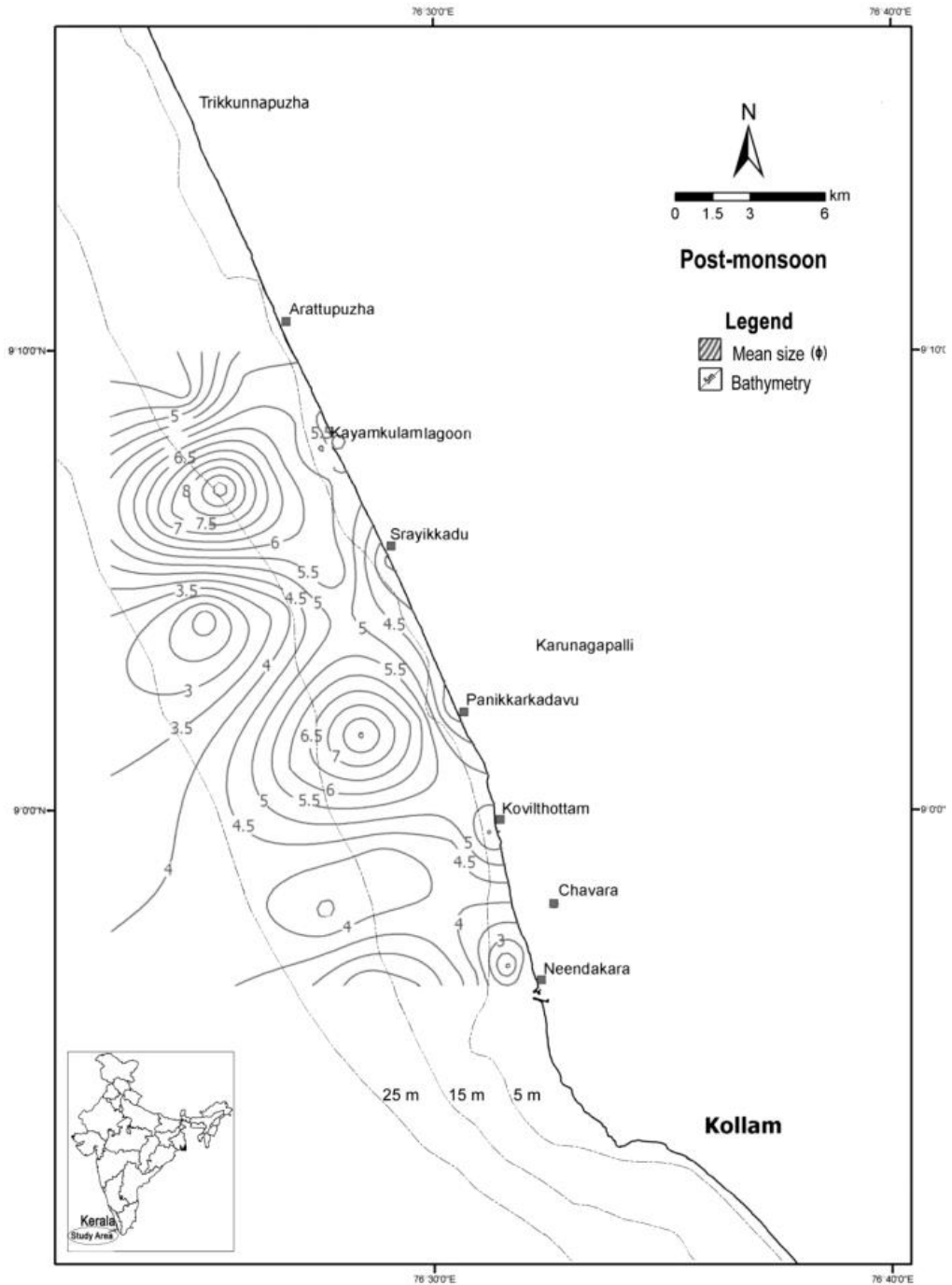


Fig. 5.4 Spatial distribution of sediment mean size in the innershelf during the post-monsoon

5.4 Heavy Mineral Distributions of Surficial Sediments

5.4.1 Beach

The distribution of HM at the mid water line (MWL) of the beaches at different locations during the three seasons is presented in Fig. 5.5. It is seen that higher concentrations are seen at Panikkarkadavu, Srayikkadu and Arattupuzha. The lowest

concentration (<1 %) is observed at Kovilthottam during the post-monsoon while the highest (83 %) is seen during pre-monsoon at Arattupuzha.

Table 5.5 Textural characteristics of the innershelf sediments during the monsoon

Sl. No.	Transect	Station No.	Depth (m)	Mean		Sorting (ϕ)	Sediment type (after Shepard, 1954)
				(ϕ)	(mm)		
1	Neendakara	N1	4.5	3.55	0.0853	0.17	Sand
2		N2	8	3.7	0.0769	0.19	Sand
3		N3	14	5.50	0.022	1.94	Silt
4		N4	21	4.77	0.037	1.71	Silt
5	Kovilthottam	KT1	6	3.46	0.0905	0.16	Sand
6		KT2	10.5	6.92	0.008	2.91	Clayey Silt
7		KT3	15	6.61	0.010	2.58	Clayey Silt
8		KT4	21	5.17	0.028	1.87	Silt
9	Panikkarkadavu	P1	6.5	4.29	0.051	1.59	Silty Sand
10		P2	9.5	4.85	0.035	2.32	Silty Sand
11		P3	15.0	7.8	0.005	2.72	Clayey Silt
12		P4	20.5	5.61	0.020	2.84	Sandy Silt
13	Srayikkadu	MA1	6	3.4	0.095	0.22	Sand
14		MA2	10	5.72	0.019	2.22	Clayey Silt
15		MA3	16	3.97	0.064	2.62	Silty Sand
16		MA4	20.5	2.64	0.161	1.02	Sand
17	Kayamkulam	KK1	6	3.78	0.073	1.78	Silty Sand
18		KK2	10	5.04	0.030	2.21	Sandy Silt
19		KK3	15	4.42	0.047	2.56	Sandy Silt
20		KK4	20	5.17	0.028	3.23	Sandy Silt
21	Arattupuzha	AR1	6.5	8.32	0.003	2.43	Clayey Silt
22		AR2	10.5	4.58	0.042	2.147	Silty Sand
23		AR3	14.5	3.05	0.121	1.81	Silty Sand
24		AR4	20.5	1.27	0.4147	0.62	Sand

5.4.2 Innershelf

The seasonal distribution of HM in the innershelf for the pre-monsoon, monsoon and post-monsoon period are presented in Figs. 5.6 - 5.8. The general distribution of HM in the innershelf indicates an increase in concentration in the nearshore zone compared to the deeper region. The seasonal HM percentage ranges from 1 to 28 % (Avg. 8.9 %), < 1 to 17 % (Avg. 6.3 %) and < 1 to 22 % (Avg. 7.6 %) during the pre-monsoon, monsoon and the post-monsoon periods respectively. Low concentrations (roughly < 5 %) are observed in the offshore at 20 m depth.

Table 5.6 Textural characteristics of the innershelf sediments during the post-monsoon

Sl. No.	Transect	Station No.	Depth (m)	Mean		Sorting (ϕ)	Sediment type (after Shepard, 1954)
				(ϕ)	(mm)		
1	Neendakara	N1	3.5	3.58	0.08	0.30	Sand
2		N2	5	1.75	0.30	1.34	Sand
3		N3	10	4.21	0.05	1.46	Silty Sand
4		N4	14.75	5.52	0.02	1.93	Silt
5		N5	20	5.96	0.02	2.42	Clayey Silt
6	Kovilthottam	KT1	3.5	3.38	0.10	0.37	Sand
7		KT2	5	3.49	0.09	0.31	Sand
8		KT3	10	4.35	0.05	1.52	Sandy Silt
9		KT4	15	6.18	0.01	2.03	Silt
10		KT5	20	5.90	0.02	2.16	Silt
11	Panikkarkadavu	P1	5	3.51	0.09	0.32	Sand
12		P2	10	6.31	0.01	2.78	Sand Silt Clay
13		P3	15	8.13	0.00	2.54	Clayey Silt
14		P4	20	6.06	0.01	2.31	Clayey Silt
15	Srayikkadu	MA1	5	3.33	0.10	0.44	Sand
16		MA2	10	6.00	0.02	2.73	Sand Silt clay
17		MA3	15	3.66	0.08	2.34	Silty Sand
18		MA4	20	1.62	0.33	0.66	Sand
19	Kayamkulam	KK1	3.5	7.42	0.01	2.88	Clayey Silt
20		KK2	5	9.38	0.00	2.13	Silty Clay
21		KK3	10	6.13	0.01	2.83	Sand Silt Clay
22		KK4	15	4.81	0.04	2.98	Silty Sand
23		KK5	20	6.30	0.01	3.95	Sand Silt Clay
24	Arattupuzha	AR1	5	4.85	0.03	3.09	Clayey Sand
25		AR2	10	4.92	0.03	2.49	Sandy Silt
26		AR3	15	2.74	0.15	2.22	Sand
27		AR4	20	3.53	0.09	2.75	Silty Sand

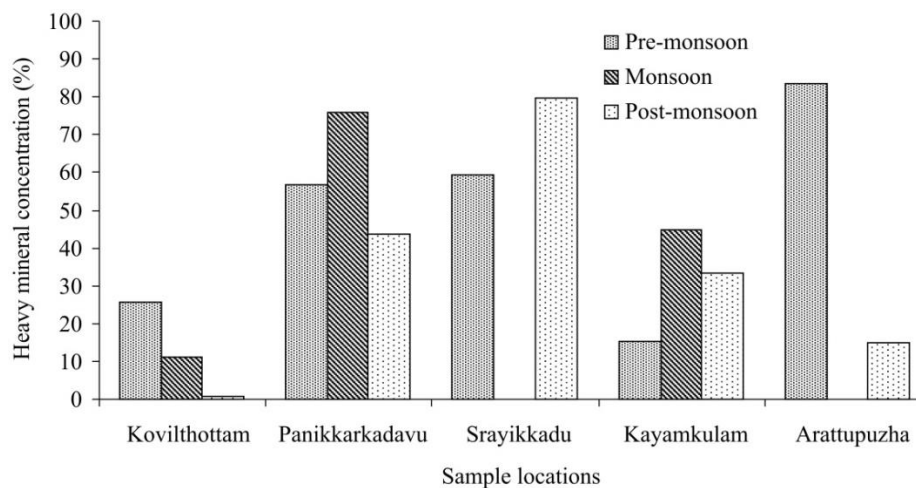


Fig. 5.5 Heavy mineral concentration at MWL of beaches of different locations during the pre-monsoon, monsoon and post-monsoon seasons

The spatial distribution of HM in the shelf during the pre-monsoon (Fig. 5.6) indicates concentrations towards the nearshore zone of Kovilthottam, Kayamkulam inlet and Panikkarkadavu. However, during the monsoon period (Fig. 5.7) the major concentration is restricted to Kovilthottam with minor ones off Srayikkadu and Arattupuzha. The innershelf bordering the Neendakara-Kovilthottam region has less HM (< 1 to 4 %) in the offshore at a depth of 20 m and the HM increases gradually to 17 % at a depth of 5 m. The nearshore region of Srayikkadu has 12 % heavies at a depth of 5 m. Towards further north a similar distribution is observed.

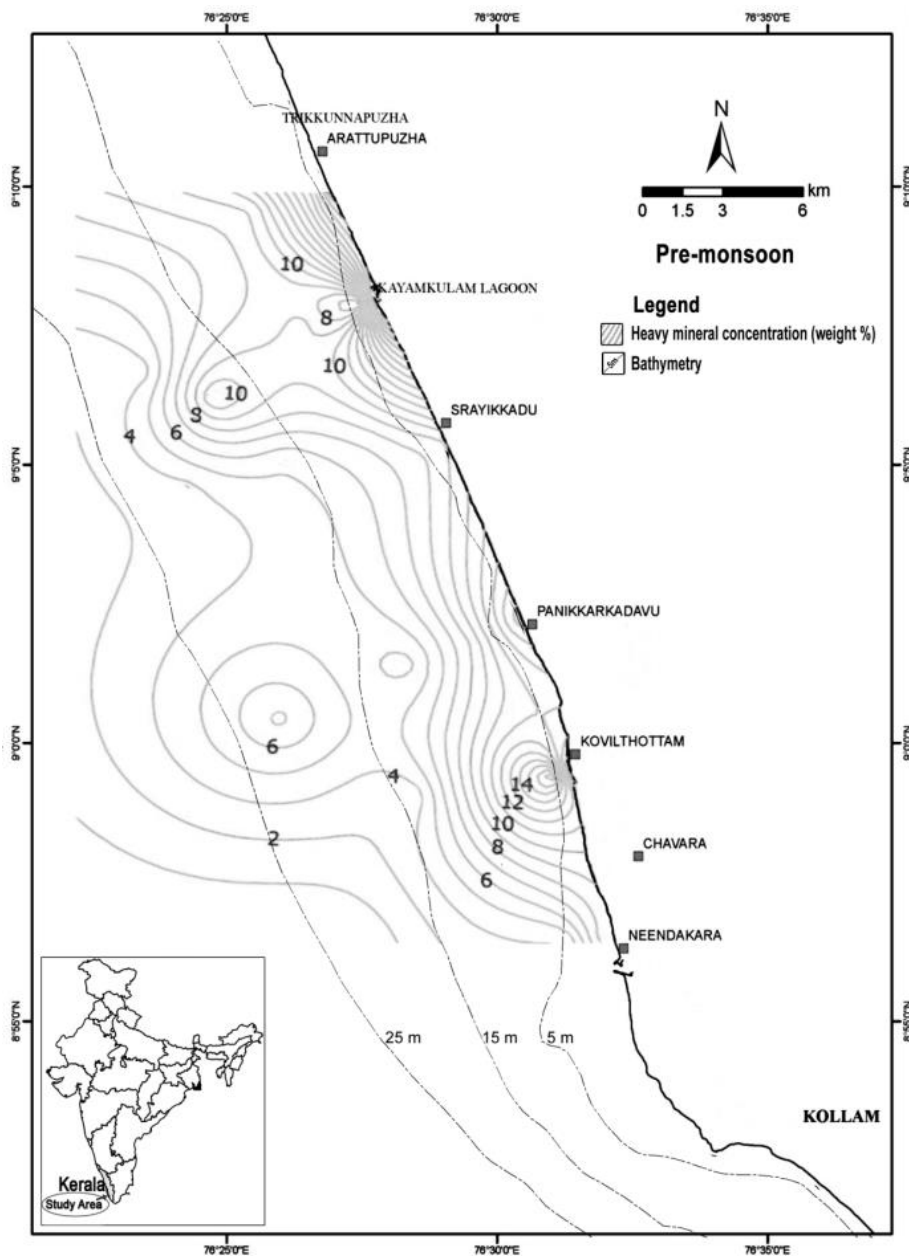


Fig. 5.6 Distribution of heavy mineral concentration in the surficial sediment samples during the pre-monsoon period

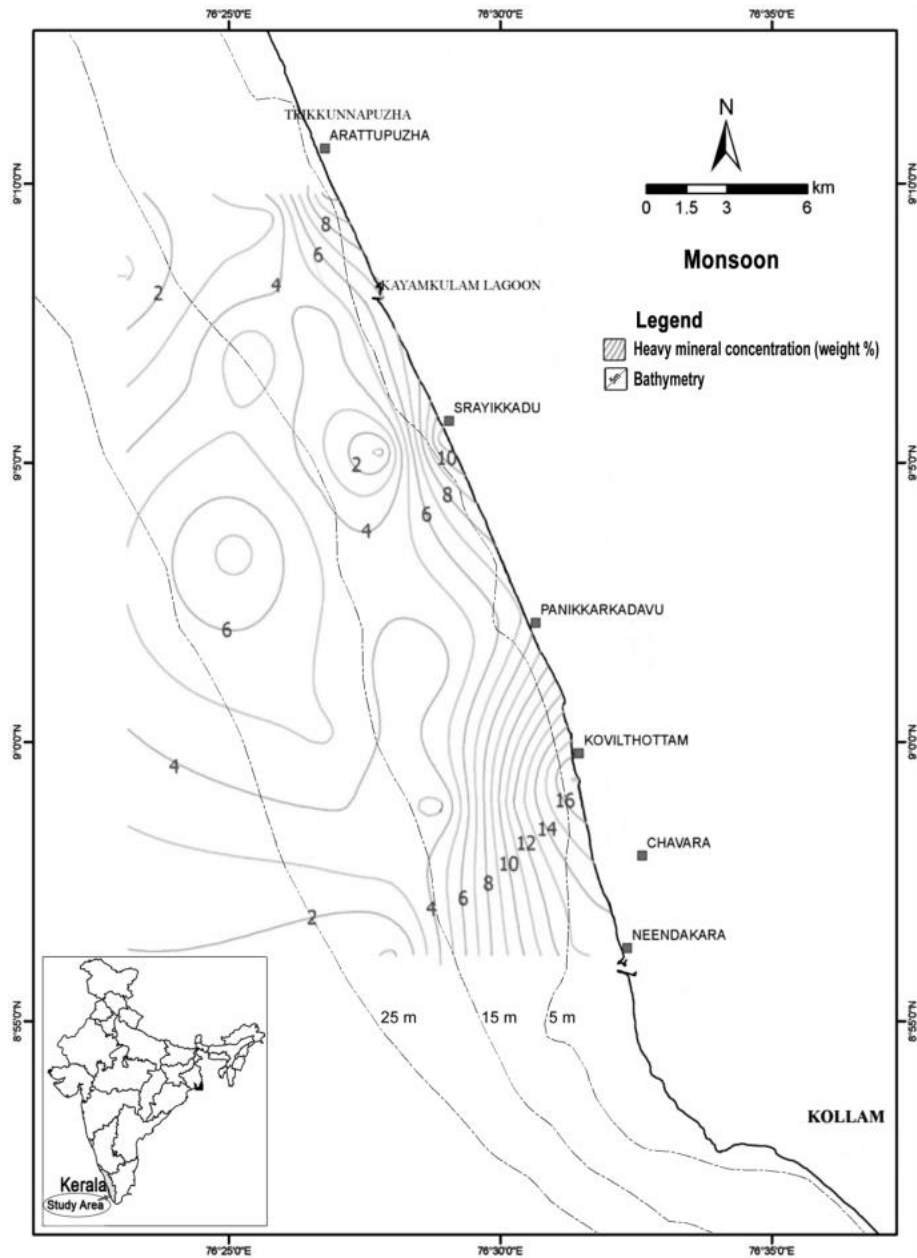


Fig. 5.7 Distribution of heavy mineral concentration in the surficial sediment samples during the monsoon period

Fig. 5.8 shows the HM distribution during the post-monsoon period. The distribution shows a prominent enrichment zone north of Kayamkulam inlet. Majority of the contour lines south of the inlet are parallel to the shoreline indicating a uniform enrichment towards shore all along the coast. Off the Arattupuzha coast a high concentration (22 %) is observed at a depth of 5 m which is much higher compared to the other locations with similar depth.

The seasonal variation of HM content in the shelf during the three seasons indicates that the concentration is focused towards the nearshore in a few locations like

Kayamkulam inlet (during pre- and post-monsoon seasons) and Kovilthottam (during all the three seasons). During the post-monsoon period there is a uniform distribution of HM in the offshore.

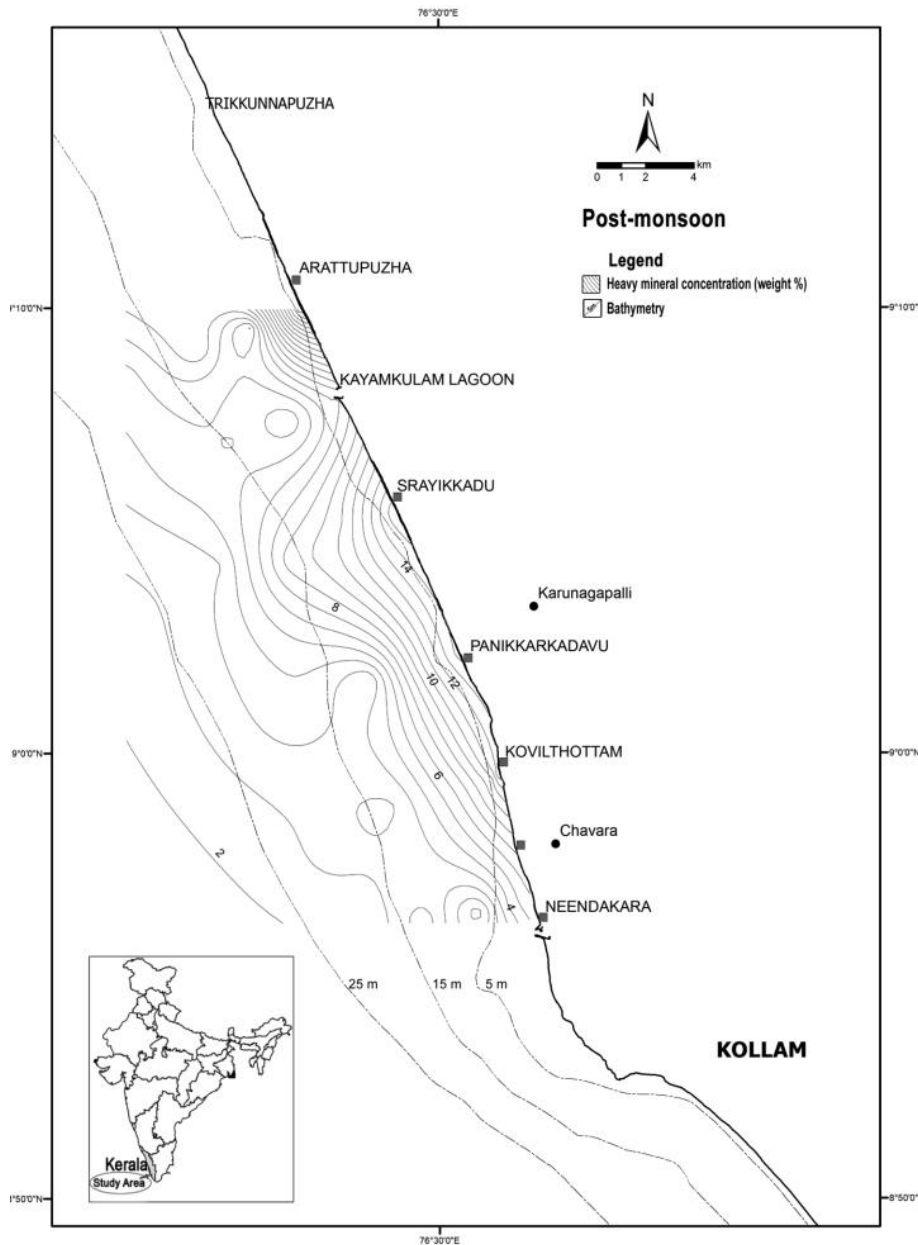


Fig. 5.8 Distribution of heavy mineral concentration in the surficial sediment samples during the post-monsoon period

5.5 Heavy Mineral Concentration in Suspended Sediment

At the nearshore site the mass of sediment trapped is highest at the bottom traps and decreases gradually upwards (Tables 5.7 - 5.9). Maximum deposition during the monsoon deployment of July 2010 is 214 g/day whereas it is 22.44 g/day during pre-

monsoon and 8.89 g/day during the post-monsoon respectively. During the monsoon deployment, the sediment deposition rates is significant even at the upper levels traps whereas during the pre- and post-monsoon deployments sediment collections are practically very less in the upper level traps. The results are in agreement with the seasonal variations in the hydrodynamic regime and the associated sediment re-suspension and transport processes (Kurian et al., 2001). The wave intensity is maximum during the monsoon causing a high amount of sediment re-suspension and a high sediment trap collections. During the other two seasons the wave intensity is relatively less causing lesser suspended sediment load and sediment trap collections.

Silt occupies a major portion of the sediment in the traps followed by clay and sand. The total HM content at the nearshore site ranges from 4.4 to 14.1 % (9 % Avg.) during monsoon, 11.9 to 16.6 % (14.5 % Avg.) during post-monsoon and 5.4 to 12 % (9.1 % Avg.) during pre-monsoon period. At the offshore site, the HM content in the trap collections is generally higher for the monsoon period when compared to the pre- and post-monsoon seasons. Overall, there is a higher suspension of heavy minerals at the nearshore site compared to the offshore. One important point to be noted is that the nearshore site shows higher percentage concentration of heavies in the traps (though not in actual quantum) during post-monsoon compared to the monsoon period. One possible explanation may be that the sorting processes dominated by the transport sorting (Komar, 1989) during the period of occurrence of long period swells as seen during post-monsoon season are effecting preferential transport of HM onshore from the offshore paleo-channel deposits (Prakash, 2000; Hegde et al., 2006).

5.6 Sub-Surface Profile of Heavy Mineral Concentration

The HM concentrations in the different sub-samples of the sediment cores are depicted in Fig. 5.9. Off Neendakara, at station CNK1 of water depth 14.5 m, the core length is 1.00 m and the HM concentration varies from 1.69 to 10.34 % with an average concentration of 5 %. The concentration gradually decreases from 6 % at surface to 2 % at a depth of 40 cm. The concentration oscillates between 2 and 4 % in the subsequent column of 30 cm thicknesses. Further down, from 70 cm there is an increase in concentration of heavies upto 10 % till the end of the core.

Table 5.7 Sediment trap collections and heavy mineral content at different levels of nearshore and offshore sites off Chavara during 23-29th July 2010

Location	Sample No.	Trap diameter (cm)	Height from bottom (cm)	Total sediments (g)	Sediments (g/day)	Heavy minerals (%)
Nearshore site at 8 m	S1	4	22.2	1322	214.36	14.10
	S2	4	30.2	1089	176.58	12.08
	S3	4	51.2	1389	225.23	6.90
	S4	4	76.2	57.25	9.28	7.91
	S5	4	126.7	1.49	0.24	4.44
Offshore site at 12 m	D1	4	22.1	38.71	2.41	12.83
	D2	4	29.8	73.03	4.55	8.61
	D4	4	76.6	16.09	1.00	3.22
	D5	4	126.5	1.57	0.09	7.03
	D6	4	200.4	9.16	0.57	5.25

Table 5.8 Sediment trap collections and heavy mineral content at different levels of nearshore and offshore sites off Chavara during 20-30th November 2010

Location	Sample No.	Trap diameter (cm)	Height from bottom (cm)	Total sediments (g)	Sediments (g/day)	Heavy minerals (%)
Nearshore site at 8 m	S1	4	22.2	88.50	8.89	16.60
	S2	4	30.2	25.08	2.52	14.65
	S3	4	51.2	4.81	0.48	13.76
	S4	4	76.2	2.37	0.23	11.85
	S5	4	126.7	1.18	0.11	13.73
	S6	4	200.5	0.75	0.07	13.70
Offshore site at 12 m	D1	4	22.1	26.36	2.69	4.62
	D2	4	29.8	9.30	0.95	3.17

Table 5.9 Sediment trap collections and heavy mineral content at different levels of nearshore and offshore sites off Chavara during 30th April to 5th May 2011

Location	Sample No.	Trap diameter (cm)	Height from bottom (cm)	Total sediments (g)	Sediments (g/day)	Heavy minerals (%)
Nearshore site at 8 m	S1	4	22.2	966	22.44	12
	S2	4	30.2	946	21.98	12
	S3	4	51.2	807	18.74	5.4
	S4	4	76.2	536	12.44	-
	S5	4	126.7	126	2.92	-
	S6	4	200.5	38	0.88	-
Offshore site at 12 m	D1	4	22.1	663	15.43	5.5
	D2	4	29.8	471	10.96	1.7
	D3	4	51.8	562	13.08	4.3
	D4	4	76.6	90	2.08	-
	D5	4	126.5	25	0.58	-
	D6	4	200.4	9	0.22	-

Along the Kovilthottam transect which is off the beach sand extraction site of IREL, the core sample from station CKT1 at a depth of 12.5 m has a length of 1.0 m. The heavy mineral concentration is less ranging from 1.7 to 5.7 % with an average of 4 %. The top 30 cm has around 4 to 6 % of heavies and then it decreases further down. However from 70 cm onwards the concentration increases and is steady at around 4 %.

At station CPK1 at a depth of 8 m off Panikkarkadavu, the sediment core has a length of 0.60 m. The HM concentration is substantially high at this station, varying from 6.03 to 13.3 % with an average of 8 %. The concentrations of heavies decrease from nearly 13 % in the top 10 cm of the core to 6 % at a depth of 30 cm. Further down there is a gradual increase upto 9 % till the end of the core. At the second station CPK2 at a depth of 12.5 m off Panikkarkadavu, the recovery of the core is high with a length of 1.30 m. Here the concentration is less ranging from 3 to 6 % with an average content of 4.7 %. This core has shown more or less steady concentration of HM throughout the core.

Further north at station CSK1 of depth 8 m off Srayikkadu, the HM varies from 5.5 to 12.7 % in the 0.70 m core with an average content of 8.8 %. The top 30 cm has high concentration and it decreases to nearly 6 % towards the bottom of the core. At station CSK2 off Srayikkadu, the recovery of core is reasonably good with a length of 0.80 m. The HM variation along the core varies from 4.9 to 11.5 % with an average of 6.8 %. High concentration (10-12 %) is noticed at the top 20 cm of the core and further down there is a sharp decrease with the concentration remaining more or less steady at around 5-6 % in the rest of the core. The distribution profile at this station is quite similar to those of stations CPK1 and CSK1.

The core recovery is rather poor at both stations CKK1 and CKK2 off the Kayamkulam inlet. The HM profile at station CKK1 of depth 8 m is notable for a high concentration of 12 % at the 30 cm level increasing from the surface value of around 5 %. Towards the end of the core, the concentration again decreases to a value of around 8 %. The HM content in the 0.60 m long core from station CKK2 of depth 10.5 m varies from 3.3 to 6.4 % with an average of 4.8 %. In the top 30 cm the HM concentration is more or less uniform with a value of around 5 %. At a depth of 40 cm the concentration is about 6 % and it gradually decreases to 4 % towards the bottom of the core.

The HM concentration at station CAR1 at a depth of 10.5 m off Arattupuzha with a core recovery of length 1.10 m varies from 5.5 to 9 % with an average value of 6.8 %. In general the vertical variation is relatively less. At top the concentration is around 7 % and decreases to 5 % at a depth of 20 cm. The sub-surface maximum seen off Kayamkulam is present here too with an increase of upto 9 % at 50 cm. Like other stations the concentration decreases further down.

In general it can be summarised that the cores from the shallower stations in the Kovilthottam-Panikkarkadavu-Srayikkadu region which are shorter than the cores from deeper stations show higher HM concentrations in the range of 11-13.5 % in the surface. The longer cores from the deeper stations on the other hand show lower concentrations from surface to deeper layers. However, the deeper station off Neendakara shows concentrations above 10 % even at the 100 cm layer.

5.7 Long-Term Change in the Heavy Mineral Concentration

An analysis of long-term changes in the HM concentration in the study area is carried out in the following sections using the data available in the literature as well as from the present study.

5.7.1 Surficial distribution

A comparison of heavy mineral concentration along the beaches of Chavara coast for the period 1981 and 2000 indicates more or less similar concentration pattern with high % of HM, as high as above 90 %. However by 2011 the situation has changed drastically. The concentration at the beach varies from <1 to 60 % (Table 5.10). In contrast the beach of Arattupuzha, north of Kayamkulam inlet shows concentration as high as 83 %. The result indicates that there is an appreciable reduction in the heavy mineral concentration in the beaches of Neendakara-Kayamkulam coast during the past one decade. The concentration in the sector north of Kayamkulam inlet has increased even upto 83 % from as low as 15 % in 1981.

Table 5.10 Long-term variation in average heavy mineral concentration in the beach samples from Chavara coast

Year	Source	Max. Concentration (%)
1981	Prakash et al. (1991)	96
1995	Kurian et al. (2001)	100
2000	Kurian et al. (2002)	100
2011	Present study	60

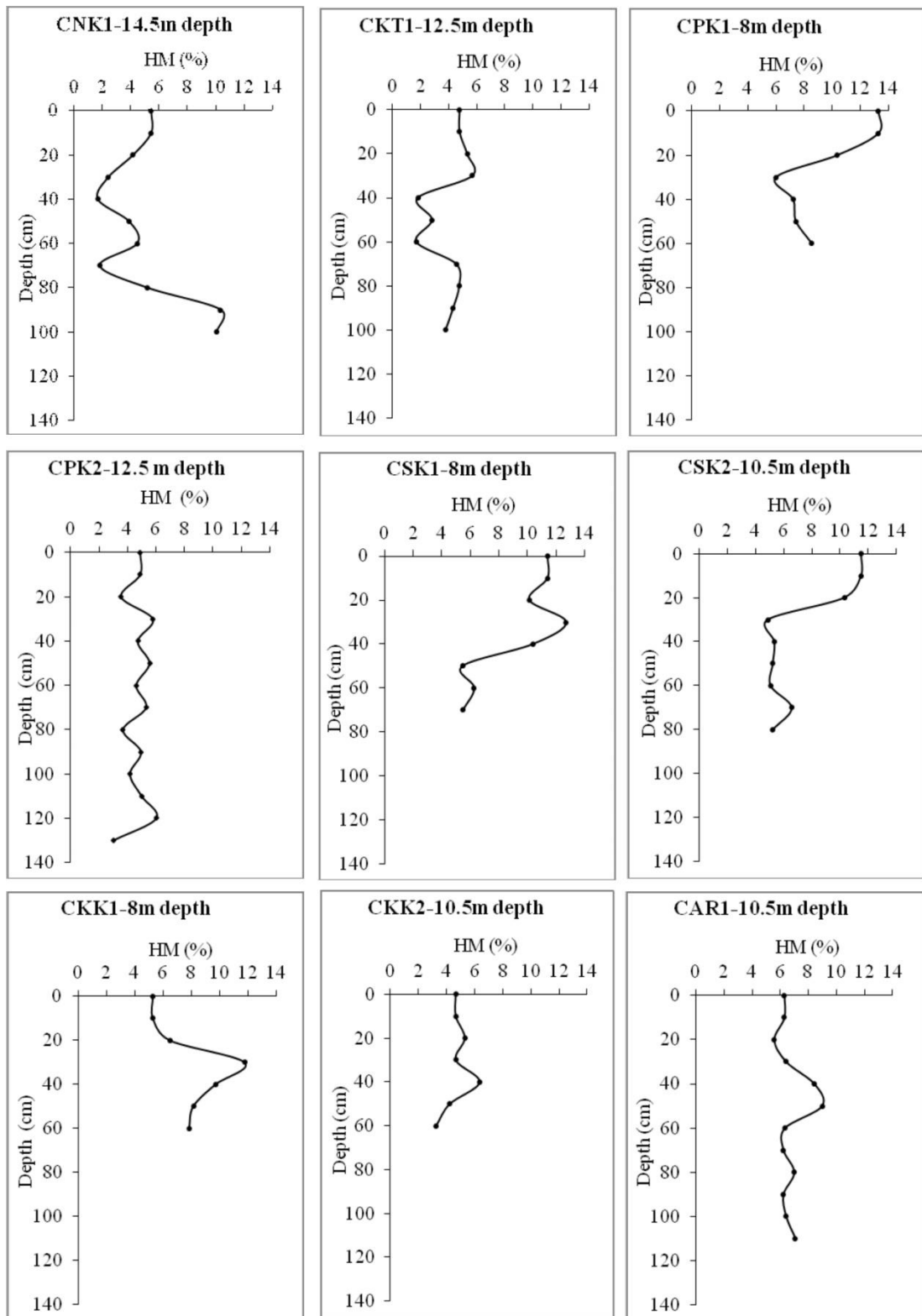


Fig. 5.9 Down-core variation in heavy mineral content at different stations of Neendakara-Arattupuzha coast

With regard to HM concentration in the innershelf, the total percentage in the shelf sediments varied between 3 and 30 % with an average value of 17 % in 1987 in the

Chavara coast (Prakash et al., 1991). GSI (1997) has reported the occurrence of HM in the offshore sediments off Chavara ranging from 5 to 32 % with an average value of 12 % which indicates that over a 10 year period the HM concentration has decreased. The HM content in the innershelf has decreased drastically after the 2004 tsunami with the average concentration decreasing to 2.3 % in 2005 (Narayanaswamy and Mallik, 2007). The average concentration in 2011, as seen in the present study, is around 8 % which indicates enrichment in the HM concentration in the innershelf of this coast during 2005-2011. But when we consider the overall scenario in the past two and a half decades time, it can be seen that the average HM concentration in the surficial sediments of innershelf of the Chavara coast has reduced from 17 % in 1987 to 8 % in 2011 (Table 5.11).

In the Arattupuzha sector (north of Kayamkulam inlet), the scenario is slightly different. The heavy mineral concentration in this sector was more or less comparable with the southern sector in 1987 (Table 5.11). The impact of tsunami on the heavy mineral concentration was severe in this sector too though not to the extent as observed in the south, with an average HM concentration of 6 %. In 2011 the concentration is relatively high with an average value of 10 % off Arattupuzha which indicates that the concentration has improved considerably in this sector also after the 2004 tsunami. However the overall reduction when compared to the 1987 values is very significant in this sector too.

Table 5.11 Long-term variation in average heavy mineral concentration in the surficial sediment samples of the innershelf

Year	Concentration (%)	
	Chavara	Arattupuzha
1987 ¹	17	17
1997 ²	12	-
2005 ³	2	6
2011 ⁴	8	10

¹Praksah et al., 1991; ²GSI, 1997; ³Narayanaswamy and Mallik, 2007; ⁴Present study

5.7.2 Sub-surface distribution

The data available from GSI (1997) who have estimated the sediment thickness and sub-surface variation of HM content by collection of core through vibro-coring have been used for a comparative study here. The thickness of sediment column for which the HM concentration is estimated by them in the innershelf is about 1, 2 and 3 m respectively off Neendakara - Kovilthottam light house (Sector I), Vellanathuruthu (Sector II) and Cheriazhikkal (Sector III). The average concentration of HM in the sediment columns of the three sectors mentioned above is reported as 10 % (0-1 m slice of the sea bed in Sector I), 8 % (0-2 m from the seabed in Sector II) and 6 % (0-3 m from the seabed in Sector III). A gradual decrease in the HM concentration with depth is also reported in all the three sectors.

In order to make comparison with the past data, the present data for Chavara coast discussed in the earlier section is grouped sector-wise and the average concentration in the 0-0.5 m and 0-1 m column has been worked out. The results are presented in Tables 5.12 & 5.13. The average HM concentration in the 0-0.5 m column of the sea bed in the Neendakara-Kovilthottam sector is 3.8 %. Along the Vellanathuruthu-Panikkarkadavu sector of the seabed the HM concentration is 6.9 % whereas in the Cheriazhikkal sector it is 8.7 %. The average heavy mineral concentrations in the 0-1 m column of the sea bed is 4.5 % in the Neendakara-Kovilthottam, and 4.7 % in the Vellanathuruthu-Panikkarkadavu sector (Table 5.13). No estimates could be made for the Cheriazhikkal sector since the core lengths are less than 1 m there. The heavy mineral data reported by GSI (1997) is exactly comparable for the Sector I since the thickness of sediment column is same. From the comparison (Table 5.14) it can be inferred that the average concentration of HM for the top 1 m slice of sea bed for the Neendakara-Kovilthottam sector has been reduced by 50 %. As regards Sector II, the data presented by GSI pertain to 0-2 m column and hence the data may not be exactly comparable with the present one. Keeping this limitation in mind it can be seen that in the Vellanathuruthu-Panikkarkadavu sector, the reduction is as much as 42 %.

From the comparison of the sub-surface variation of HM of the different sectors along the coast (Table 5.14) it can be inferred that the concentration of HM has been reduced by nearly half for the Neendakara-Panikkarkadavu sector (Sectors I and II referred above).

Table 5.12 Total average heavy mineral concentrations of 0-0.5 m column of seabed for different sectors along the Chavara coast

Sector	Location of sediment core	Down core depth (m)	Total HM concentration (%)	Total average HM % for the sector
Neendakara-Kovilthotam (Sector-I)	CNK1/1-CNK1/5	0-0.5	3.52	3.8
	CKT1/1-CKT1/5	0-0.5	4.08	
Vellanathuruthu (Sector-II)	CPK1/1-CPK1/5	0-0.5	8.87	6.89
	CPK2/1-CPK2/5	0-0.5	4.91	
Cheriazhikal (Sector-III)	CSK1/1-CSK1/5	0-0.5	10.03	8.74
	CSK2/1-CSK2/5	0-0.5	7.45	

Table 5.13 Total heavy mineral concentration of 0-1.0 m column of seabed for different sectors along the Chavara coast

Sector	Location of sediment core	Down-core depth (m)	Total HM concentration (%)	Total average HM % for the sector
Neendakara – Kovilthottam (Sector-I)	NK1/1 - NK1/10	0-1.0	4.94	4.5
	CKT1/1 - CKT1/10	0-1.0	3.95	
Vellanathuruthu (Sector-II)	CPK2/1 - CPK2/10	0-1.0	4.73	4.73

Table 5.14 Long-term variation in down-core average heavy mineral concentration in the innershelf at different sectors of the Chavara coast

Year	Sector	Average HM Concentration (%)
1997 (GSI 1997)	Sector I (0 - 1 m)	10
	Sector II (0 - 2 m)	8
	Sector III (0 - 3 m)	6
2011 (Present study)	Sector I (0 - 1 m)	4.5
	Sector II (0 - 1 m)	4.7
	Sector III (0 - 1 m)	-

Sector - I: Neendakara - Kovilthottam
Sector - II: Vellanathuruthu
Sector - III: Cheriazhikkal

5.8 Discussion

The results of the study shows that there was no appreciable change in the HM concentration in the beaches of the Chavara coast during 1981 – 2000 while there is depletion in concentration thereafter. In contrast, the concentration in the Arattupuzha sector has increased considerably. As regards the innershelf of Chavara coast, there is a reduction in the HM concentration from 12 % in 1987 to 8 % in 2011 with the concentration as low as 2 % in 2005 immediately after the tsunami. In the Arattupuzha sector, the concentrations were comparable with the Chavara sector in 1987 and the reduction over the 1987- 2011 period is only 2 %. The sub-surface concentrations show decrease of as much as 50 % during the period 1997-2011 along the Chavara innershelf. It will be interesting to look at the probable driving mechanisms for the long-term changes observed.

During the nearly two and a half decade period (1997-2011) under analysis in this study the coastal areas of this region had witnessed three extraneous factors viz. excessive mining by IREL and KMML, construction of two breakwaters at Kayamkulam inlet and the onslaught of the 2004 Tsunami in addition to the routine hydrodynamic forcing along this coast.

IREL and KMML are extracting considerable quantity of beach sand along the different sectors of the Chavara coast. According to Kurian et al. (2012) the quantum of extraction by IREL and KMML has almost doubled during the 2001-2010 decade over the previous decade. The material extracted is the material that is replenished from the offshore and this material is lost to the system for ever due to the extraction. The enrichment of HM seen in the beach sediment (Kurian et al., 2001) is due to the various sorting processes at work when the hydrodynamic forces act on the innershelf sediments (Komar, 1989). Thus the extraction of huge quantities of beach sediments reduces the level of sea bed and the quantum of sediment available for reworking by the hydrodynamic processes. Extraction of sand even at the present level can be expected to reduce the HM concentration in the coming years. It is pertinent to mention here that due to damming and excessive mining of river sand, there is no more input of sediment by the rivers to this coastal environment as it used to be a few decades back (Black and Baba, 2001).

Till 2000, the sector of the coast north of Neendakara was an open system. In an open system, sediments move uninterrupted in the alongshore/cross-shore direction both in the surf zone and in the innershelf. With the construction of two breakwaters jetting out into the sea upto a depth of around 7 m at the Kayamkulam inlet, the coast is no more an open one. Rather, the Neendakara-Kayamkulam sector of the coast became compartmentalized. In other words, it became a “sediment sub-cell”. The ‘*step-ladder*’ transport (Black et al., 2008) is nearly confined to this cell and the alongshore movement of sediment both in the surf zone and part of innershelf gets blocked by the breakwaters. Consequently, the breakwaters have modified the shoreline morphology within the study area with accretion immediately south of the breakwater and erosion in the sector immediately north of it in accordance with the predominant northerly transport (Fig. 5.10). Erosion of the barrier beach in the sector north of the inlet, where the sea walls have completely collapsed due to retreat of shoreline, leads to enrichment of heavies as documented by Komar (1989), Kurian et al. (2001) and Gujar et al. (2011). This explains the reason for the increase of HM concentration from as low as 15 % in 1981 to values as high as 80 % in the beach sediments of Arattupuzha sector. HM enrichment due to barrier beach erosion along the Chavara coast (Neendakara – Kayamkulam sector) is limited since most part of this coast is protected by seawall. Enrichment due to erosion is possible only at a few locations where gaps exist in the sea wall or the seawall is non-functional due to its collapse.

The 2004 Tsunami had a devastating effect on the coastal geomorphologic setting along this region and a huge deposit of heavy minerals with thickness of as much as 1 m was seen in the beach and hinterland areas of this coast (Narayana et al., 2005, 2007; Prakash et al., 2005; Kurian et al., 2006a). Komar (1989) while discussing the different sorting processes leading to beach placer formation underlines the phenomenon of transport sorting which can selectively transport the denser heavy minerals onshore due to long period waves. The observations of Kurian et al. (2006a), Prakash et al. (2007) and Narayana et al. (2005, 2007) conclusively prove this phenomenon. It is already established that paleo-beaches with high concentration of heavies exist in the offshore of this coast at depths of the order of 50 m (GSI, 1997). Tsunami being very long period waves with period of the order of 15 minutes is capable of inducing sediment motion even in the deep sea. Thus the source of the

huge quantum of heavy minerals transported onshore by the tsunami must have been from the whole shelf including the paleo-beaches.



Fig. 5.10 Satellite imagery (Source: Google image) and snapshots showing erosion immediately north of Kayamkulam breakwater and accretion towards south of the breakwater

Another important aspect regarding spatial variation in the innershelf sediment distribution needs to be noted here. Off the Chavara coast, the sediment column is resting directly on the hard lateritic bed which is not the case towards the Kayamkulam-Arattupuzha sector (GSI, 1994, 1997). The unconsolidated sediment column on a hard bed is easily susceptible to transport due to hydrodynamic forcing, particularly by very long period waves like the tsunami. The loss of huge quantum of HM might have brought down the average HM concentration in the innershelf surficial sediments to a meager 2 % off Chavara and 6 % off Arattupuzha coast. This lower surficial concentration in the innershelf during the post-tsunami scenario must have certainly contributed to the lower concentrations in the beaches during the subsequent period. Though the concentration of heavies has been restored to an average value of 8 % off Chavara and 10 % off Arattupuzha by 2011 by the sorting processes at work (Komar, 1989), the heavy mineral resources lost from the system are lost forever.

5.9 Summary

A study of the sedimentology and mineralogy of the beach and innershelf sediments of the Chavara coast which is well known for the rich beach placer deposits has been undertaken to understand the present status of HM distribution in the beach and innershelf sediments, to delineate the long-term trend in the HM distribution and to understand the mechanisms that drive these changes. The study confirms the depletion in the heavy mineral concentration in the beaches of the Chavara coast and drastic reduction in the heavy mineral concentration both in the surface as well as sub-surface sediments of the innershelf. The study establishes the contrasting pattern in the long-term changes in the HM concentration of the Chavara coast when compared to the sector north of it. While there is depletion in the HM concentration in the beaches of the Chavara coast after 2000, the Arattupuzha sector in the north shows an increasing trend during the study period due to erosion of the barrier beach. The surficial sediments of innershelf of both the sectors records reduction in the HM concentration, but the change is relatively less in the Arattupuzha sector. The 2004 tsunami brought down the HM concentration to as low as 2 % in the Chavara innershelf, but the impact was again relatively less in the Arattupuzha innershelf. The observed long-term changes are attributed to the excessive mining by the PSUs, the construction of two breakwaters at Kayamkulam inlet and the onslaught of the 2004 Tsunami. The extraction of huge quantities of beach sediments much beyond the sustainable limits reduces the level of sea bed and the quantum of sediment available in the innershelf for reworking by the hydrodynamic processes. With the construction of two breakwaters at Kayamkulam inlet the Neendakara-Kayamkulam sector of the coast has become compartmentalized due to which the inputs of sediments from the adjoining coastal sectors are curtailed. The 2004 Tsunami had a devastating effect on this coast and the innershelf was deprived of a huge quantum of HM by the selective onshore transport of HM by the tsunami. It is quite possible that the Chavara coast may cease to be a commercially viable beach extraction site in a few decades if the sand extraction is continued at the present level. The beaches in the Arattupuzha sector in the north may continue to record high concentrations of HM due to the erosion of the barrier beach rich in HM content.

CHAPTER 6

BEACH-INNERSHELF MORPHOLOGICAL CHANGES

6.1 Introduction

The beaches of the Chavara coast are undergoing drastic morphological changes as brought out by the recent studies (Rajith et al., 2008; Kurian et al., 2002). Since the beach and the innershelf are interlinked any morphological change in the beach will have its impact on the innershelf too. The morphology of the beach-innershelf system is decided by the sediment transport processes, which in turn is driven by various hydrodynamic processes and human-induced activities on the beach and the innershelf. Seasonal erosion of the beach is normally accompanied by accretion of sediments in the nearshore in the form of longshore bars and subsequent rebuilding of beach by erosion of these bars during the fair weather beach rebuilding process. Thus, while the seasonal erosion/accretion processes of the beach and the innershelf are complementary, the long-term erosion/accretion need not be so. In all likelihood, a sediment deficient eroding beach is accompanied by an eroding innershelf too and vice versa. While the short-term beach erosion/accretion of the Chavara coast has been studied by a couple of authors in the past (Kurian et al., 2001; Rajith et al., 2008; Sheela Nair et al., 2011, 2013), studies on long term changes, especially those linking the morphological changes of the beach and innershelf of the Chavara coast are lacking. This Chapter encompasses results of the study carried out focusing on the short- and long-term morphological changes of the beach and innershelf of the Chavara coast with the primary objective of identification of the causative factors responsible for the drastic morphological changes.

6.2 Short-Term Beach Morphological Changes

6.2.1 Short-term changes derived from beach profiles

Being a monsoon dominated coast, the observed short-term changes in beach morphology can be attributed to the major driving forces induced by the southwest monsoon (Black et al., 2008). The short-term beach profile changes for the three coastal stations NK-1, NK-5 and NK-6 are studied by analysing the monthly measured beach profiles for the period 2010 - 2015 which are presented in Figs. 6.1, 6.2 & 6.3. Though beach profiles were measured at a few other stations like NK-7 and

NK-8 in the south (see Fig. 3.14), they were not analysed since the data were incomplete due to lack of beaches at these locations. Fig. 6.4 shows the monthly volume changes at the three stations which are computed from the profiles. The computed cumulative beach volume changes are presented in Fig. 6.5.

6.2.1.1 Station NK-1

At station NK-1 (Figs. 6.1, 6.4a & 6.5), erosion is observed from June with the onset of the monsoon. The accretion phase starts from October 2010 and the beach volume goes upto $160 \text{ m}^3/\text{m}$ during May 2011. The beach volumes for the eight month period June 2011 to January 2012 are not presented as the monthly beach profile data are not available. From February to April 2012, the computed cumulative beach volume indicates a more or less stable state. The erosion phase starts from May 2012 and extends upto September 2012. This is followed by accretion in October 2012 and this continues till February 2013 with a high cumulative volume of $192 \text{ m}^3/\text{m}$. Again in 2013, a similar trend is observed with the erosion phase starting from March and continuing upto September. The beach building process starts from November and this is evident from the gradual increase in cumulative volume. The accreting process prevails till April 2014 by which time it attains a peak value of $135 \text{ m}^3/\text{m}$. Subsequently the erosional phase begins by May and this lasts till August 2014. From September till November even though accreting tendency is seen, the build-up is rather slow. In December the beach shows erosion and the eroding phase continues till January 2015, followed by accretion which extends upto March 2015. The period April to September 2015 is again notable for erosion followed by accretion towards the end of the year.

The seasonal erosion/accretion trend with erosion during the monsoon months and accretion during the fair weather period is quite evident from the beach profile and beach volume change data. The five year cumulative beach volume change data indicates a declining trend in the cumulative annual volume which was at its peak in February 2013 with a value of $192 \text{ m}^3/\text{m}$. This station being located very close to the southern arm of the Kayamkulam breakwater the seasonal erosion/accretion pattern differs from that of an open beach. The beach instead of acquiring the equilibrium profile continues to accrete under the influence of northerly longshore current which dominates throughout the fair season.

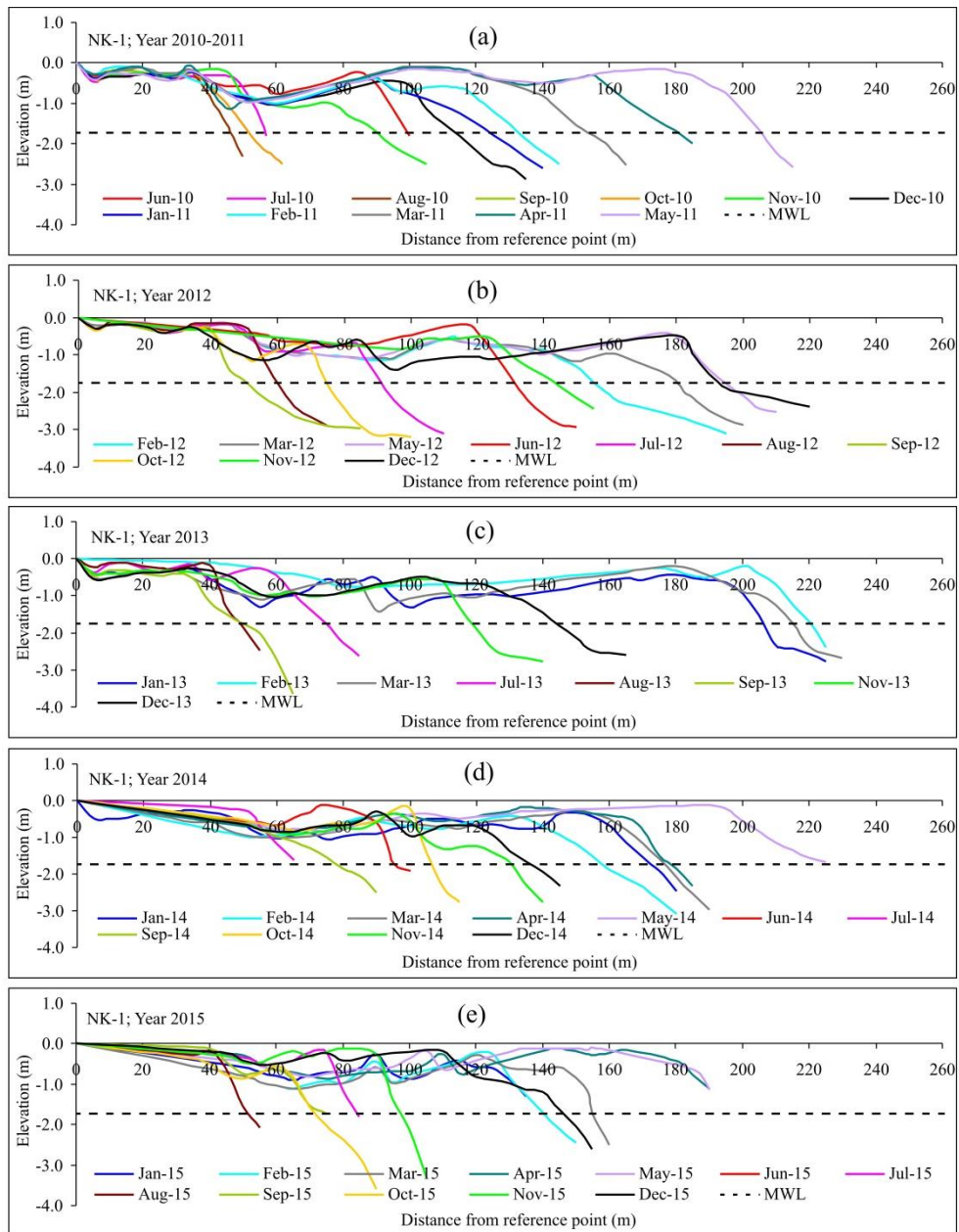


Fig. 6.1 Monthly beach profiles during (a) 2010-2011, (b) 2012, (c) 2013, (d) 2014 and (e) 2015 at Station NK-1

6.2.1.2 Station NK-5

The station NK-5 is at approximately 2 km to the south of the southern arm of the Kayamkulam breakwater. At this station erosion is observed during the initial peak monsoon period of 2010 followed by accretion during the latter part of monsoon which continues during the fair weather period till February 2011 with a maximum cumulative volume of $64 \text{ m}^3/\text{m}$ (Fig. 6.5). In 2011 the erosion phase commences from March and extends upto May. The profile data is not available during the period of June 2011 to January 2012. Unlike in 2011, the beach recovery in 2012 starts from February and lasts till March with a maximum cumulative volume of $70 \text{ m}^3/\text{m}$. The

erosion period is from May to September and the beach building is initiated by October with a maximum value of $60 \text{ m}^3/\text{m}$ observed in December 2012. The pattern is again different in 2013 with eroding trend starting from January itself. By the peak monsoon period of July-August, the beach disappears. From October onwards the beach building starts and reaches the peak value by January 2014. As observed in 2013, the eroding trend starts during the fair weather period itself and the beach is completely eroded by the monsoon time. From July onwards even though the beach building starts the peak value attained is only $37 \text{ m}^3/\text{m}$. The eroding phase starts much earlier compared to the previous year and the beach is completely eroded by February 2015 which is considered to be a typical beach building period. There is no beach at this station for the following 7 months. Though beach building commences in September, it is eroded completely by October.

The seasonal variation in beach profile and erosion/accretion pattern is quite evident in this station also. However, the overall trend shows a sharp decrease in the annual volume change towards the end of the five year period. The fact that the beach building which should have taken place during the fair weather period did not happen for the whole of 2015 is a serious issue. It indicates the emergence of a situation where the beach is totally starved of sediment.

6.2.1.3 Station NK-6

The Station NK-6, being proximate to the Vellanathuruthu mining site, is likely to show the influence of mining operation which involves the removal of sand from the foreshore followed by heaping and subsequent storing at the backshore. As there is hardly any beach during the period from June to October 2010 the profile data for this station is available only from November 2010. Beach building is observed from November and this continues till February 2011 by which time erosion commences. In 2012, erosion is observed from May and by the peak monsoon period there is hardly any beach and this situation continues till October. The build-up of the beach starts from November, attaining a maximum cumulative volume of $106 \text{ m}^3/\text{m}$ in February 2013. Erosion takes place subsequently and by June the beach is absent. From October onwards beach build-up starts with intermittent erosion and the cumulative volume reaches a maximum value of $88 \text{ m}^3/\text{m}$ in May 2014. During the monsoon months of June to September 2014 erosion is prevalent and the beach is completely eroded. Though the beach recovery takes place from September 2014 it

does not peak due to intermittent erosion. Hence the highest volume during the fair weather period of 2015 is only 18 m³/m. There is no beach during the monsoon months of July - September 2015 and the beach build-up starts from October.

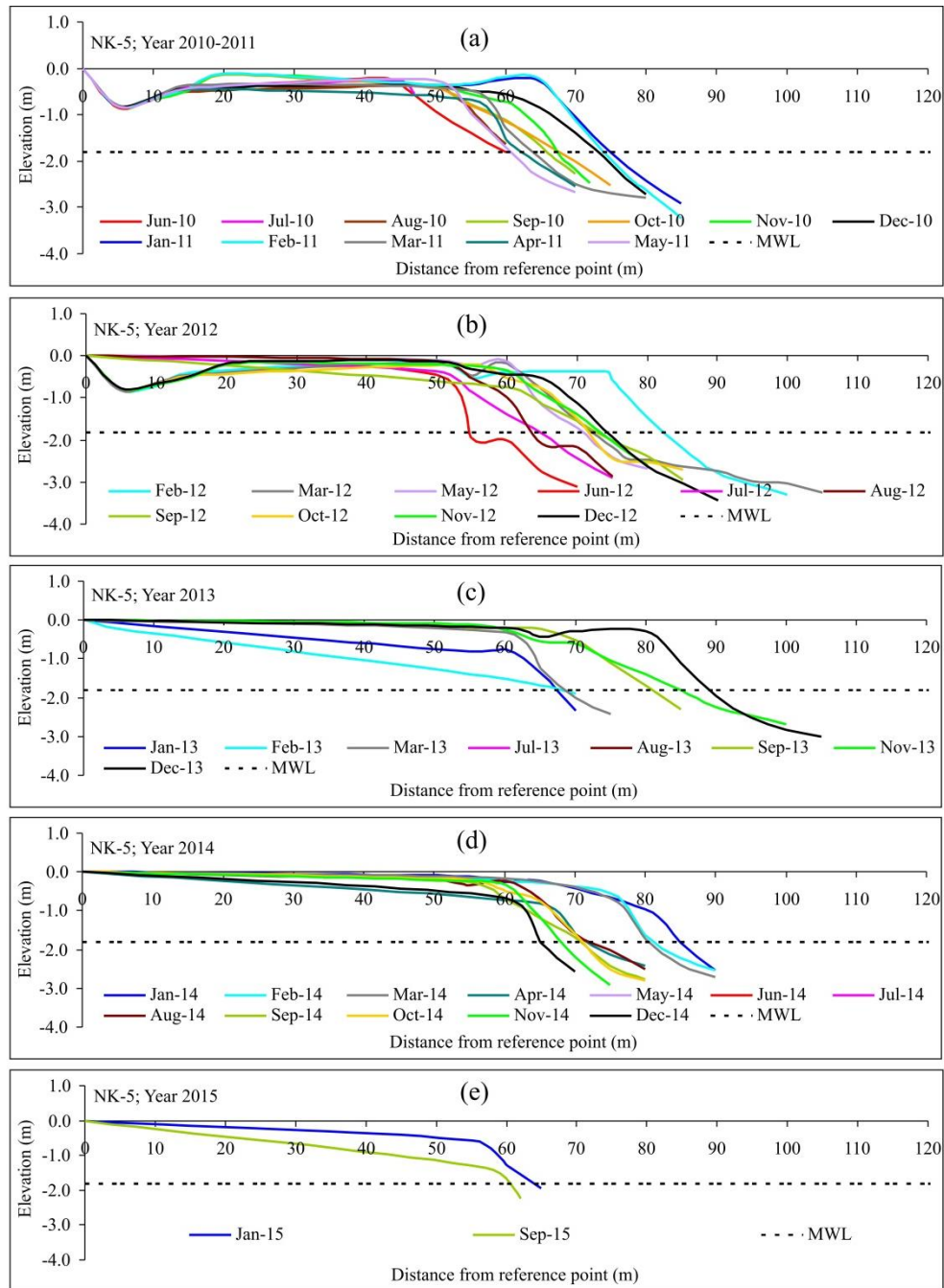


Fig. 6.2 Monthly beach profiles during (a) 2010-2011, (b) 2012, (c) 2013, (d) 2014 and (e) 2015 at Station NK-5

As in the case of other stations, the seasonal variation in beach profile and erosion/accretion pattern is evident in this station also. The cumulative volume which shows a high value of 88 m³/m in the pre-monsoon season of 2014 has not risen to that level subsequently. In the fair weather period of 2015, the highest value seen is

only 21 m³/m. As in the case of NK-5, and unlike NK-1, the extent of seasonal oscillation in the sediment volume is considerably reduced by 2015 which indicates short supply of sediment at this station.

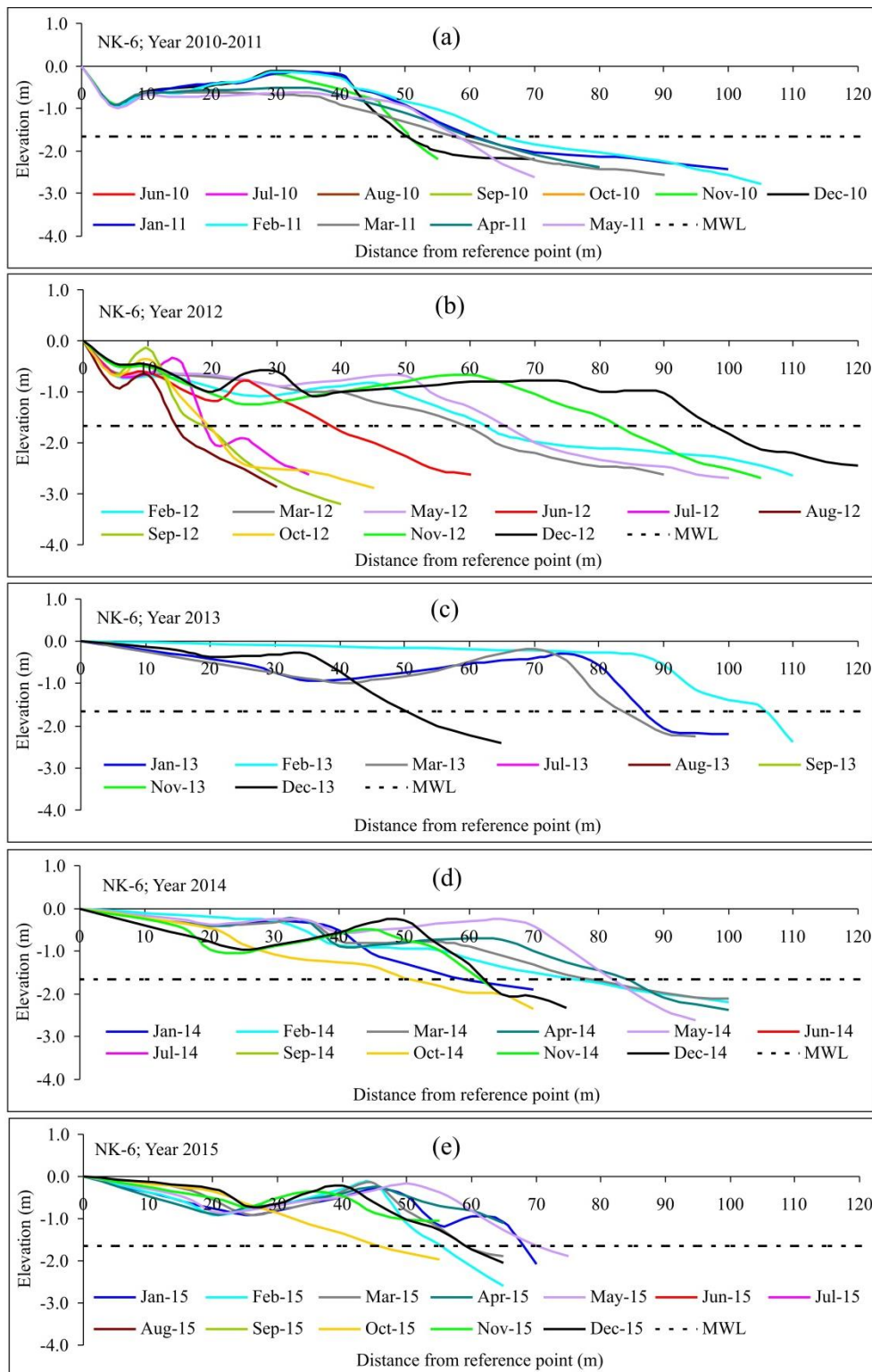


Fig. 6.3 Monthly beach profiles during (a) 2010-2011, (b) 2012, (c) 2013, (d) 2014 and (e) 2015 at Station NK-6

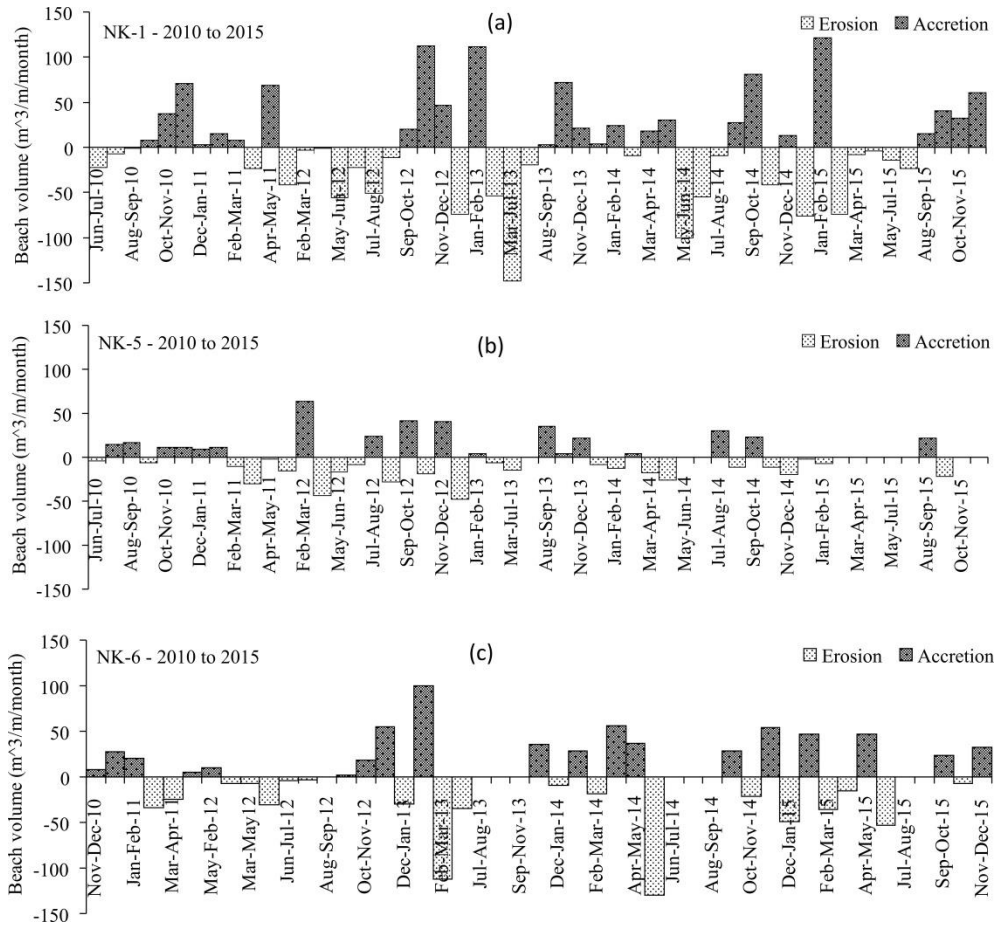


Fig. 6.4 (a-c) Beach volume change from June 2010 to December 2015: (a) NK-1, (b) NK-5 and (c) NK-6

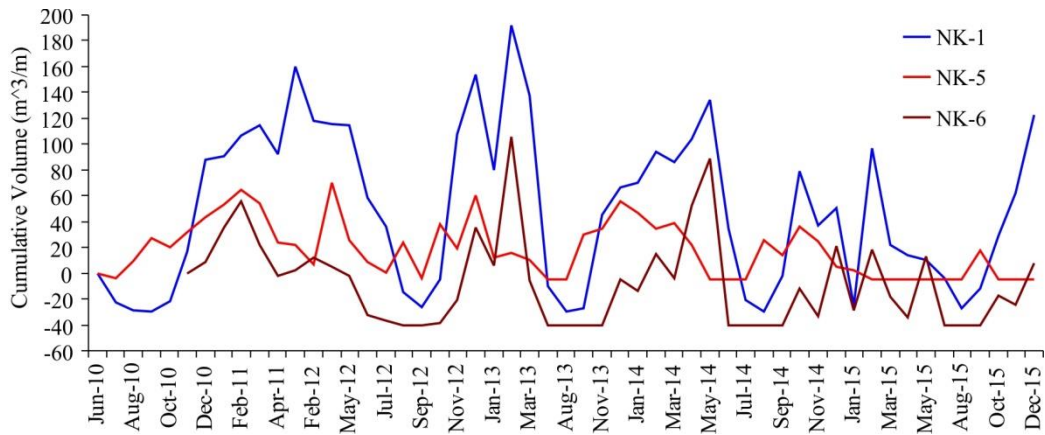


Fig. 6.5 Cumulative beach volume change (m^3/m) during the period of July 2010 to December 2015 for stations NK-1, NK-5 and NK-6 along the Neendakara-Kayamkulam coastal sector

6.2.1.4 Correlation between beach volume and beach width

The beach volume and beach width are calculated from the monthly beach profiles for the three stations viz. NK-1, NK-5 and NK-6 along the Neendakara-Kayamkulam

coastal sector. The scatter plot of beach volume and beach width for the above three stations are shown in Fig. 6.6. The analysis between beach volume and beach width shows a positive correlation for all the three stations. A strong correlation exists between beach volume and width for the station NK-5, with an R^2 value of 0.86. Moderate correlation is obtained for the station NK-1 and NK-6, with R^2 values of 0.73 and 0.72 respectively. This moderate correlation at station NK-1 may be due to the influence of Kayamkulam breakwater, and the station NK-6 is under the influence of strong mining activity. Both of these factors induce non-uniform changes in the beach profiles. A strong correlation is observed when there is a uniform change in the beach profiles.

6.2.2 Short-term shoreline changes

In this section the short-term shoreline changes during the period 2014 - 2015 are delineated from the monthly shoreline maps prepared based on GPS survey (see section 3.3.5 for methodology) and are presented in Figs. 6.7 & 6.8 and Tables 6.1 & 6.2. As this method has limitation with regard to spatial resolution of the mapping, only the northernmost sector of about 2 km length where there is considerable seasonal oscillation of the shoreline is considered for the study. Stations NK-1, NK-3 and NK-5 are located within this sector.

The shoreline variations during 2014 at the Azhikkal Station (NK-1, adjacent to the Kayamkulam south breakwater) show a retreat of the shoreline (erosion) during the months of May - July. The maximum variation (compared to the previous month) of 39 m is observed during May - June followed by June - July with a retreat of 37 m. During the remaining months, advancement of shoreline (accretion) is observed with maximum accretion during October - November (22 m) followed by March - April (14 m). Shoreline change is almost zero during November - December. The shoreline variation during 2015 again indicates beach build-up during January - May with the highest width observed in May. Subsequently erosion is observed from June - September with the highest erosion during May - July (66 m). Beach building occurs during the post-monsoon period, from September to December. Detailed analyses of the observed short-term shoreline changes at NK-1 points out that the period from October to April can be considered as the beach building or recovery phase subsequent to the retreat of the shoreline during June - September which represents

the typical monsoon season. The oscillatory trend of the shoreline is the highest at this station due to the ‘groin effect’ of the breakwater.

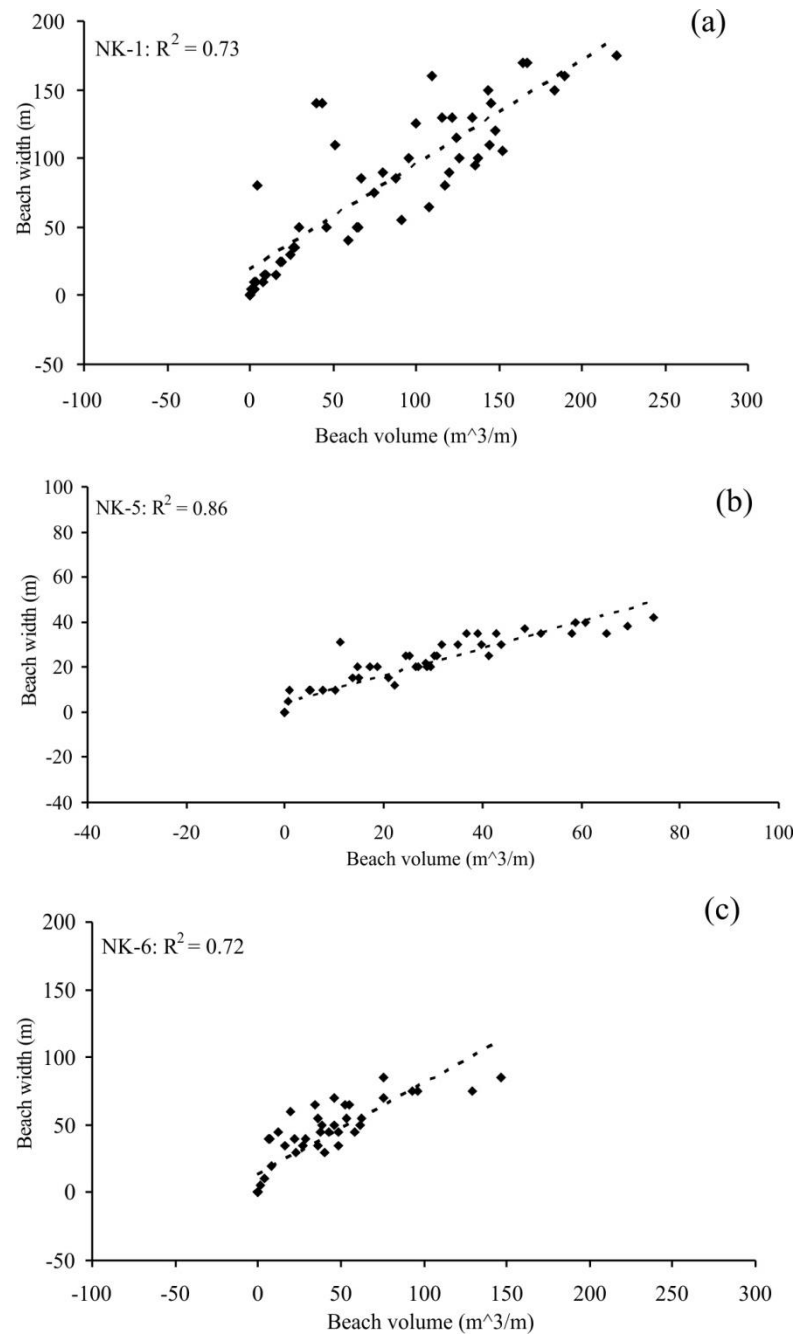


Fig. 6.6 Scatter plot of beach volume v/s beach width calculated from beach profiles for the stations (a) NK-1, (b) NK-5 and (c) NK-6

The station towards the south of Azhikkal i.e. NK-3 indicates relatively low oscillation when compared to NK-1. No significant change is seen during January to March 2014. Maximum seaward advancement of shoreline is observed during March to April (10 m). Eroding tendency of the beach starts from the pre-monsoon month of April itself and the retreat of the shoreline is as much as 29 m during April-May

followed by about 10 m during May-June. Since the beach was completely eroded by July, measurements could not be taken in July and August. From September onwards accreting tendency is observed and the shoreline advancement is as much as 26 m during September-November. However, retreat of the shoreline starts in December itself and the beach disappears by June in 2015. After a nominal recovery during July-August the retreat of the shoreline occurs again during August-September. However, significant build-up of the beach happens during the subsequent months with the shoreline advancing as much as 24 m during September-November.

Station NK-5 which is about 2 km south of the Kayamkulam breakwater exhibits the least oscillation of the shoreline when compared to NK-1 and NK-3. Though accretive tendency is observed during January-February 2014, retreat of the shoreline starts from February and by May the beach almost disappears. Hence no shoreline mapping was made for the period of May-July. Build-up of the beach and advancement of shoreline by about 5 m happens by November, but the retreat of the shoreline starts from December onwards and no beach build-up is seen during the pre-monsoon period when the conditions are normally favorable for beach building. No measurements are available for the February-June period when the beach is totally eroded. Even though the beach builds up during the latter part of monsoon period as indicated by some nominal deposition, it is totally nullified by the retreat of the shoreline during the October-December period.

Table 6.1 Monthly shoreline change (m) along the northern sector of Chavara coast estimated from shorelines mapped using GPS during the year 2014

Location	Shore term shoreline change (m) during the year 2014										
	Jan-Feb	Feb-Mar	Mar-Apr	Apr-May	May-Jun	Jun-Jul	Jul-Aug	Aug-Sep	Sep-Oct	Oct-Nov	Nov-Dec
Azhikkal (NK-1)	+12	+7	+14	+8	-39	-37	0	+9	+8	+22	+2
Azhikkal South (NK-3)	+1	+2	+10	-29	-10	#	#	+4	+16	+10	-4
Srayikkadu (NK-5)	+9	-8	+2	#	#	#	#	0	+3	+2	-7
# No beach; + ^{ve} Accretion; - ^{ve} Erosion											

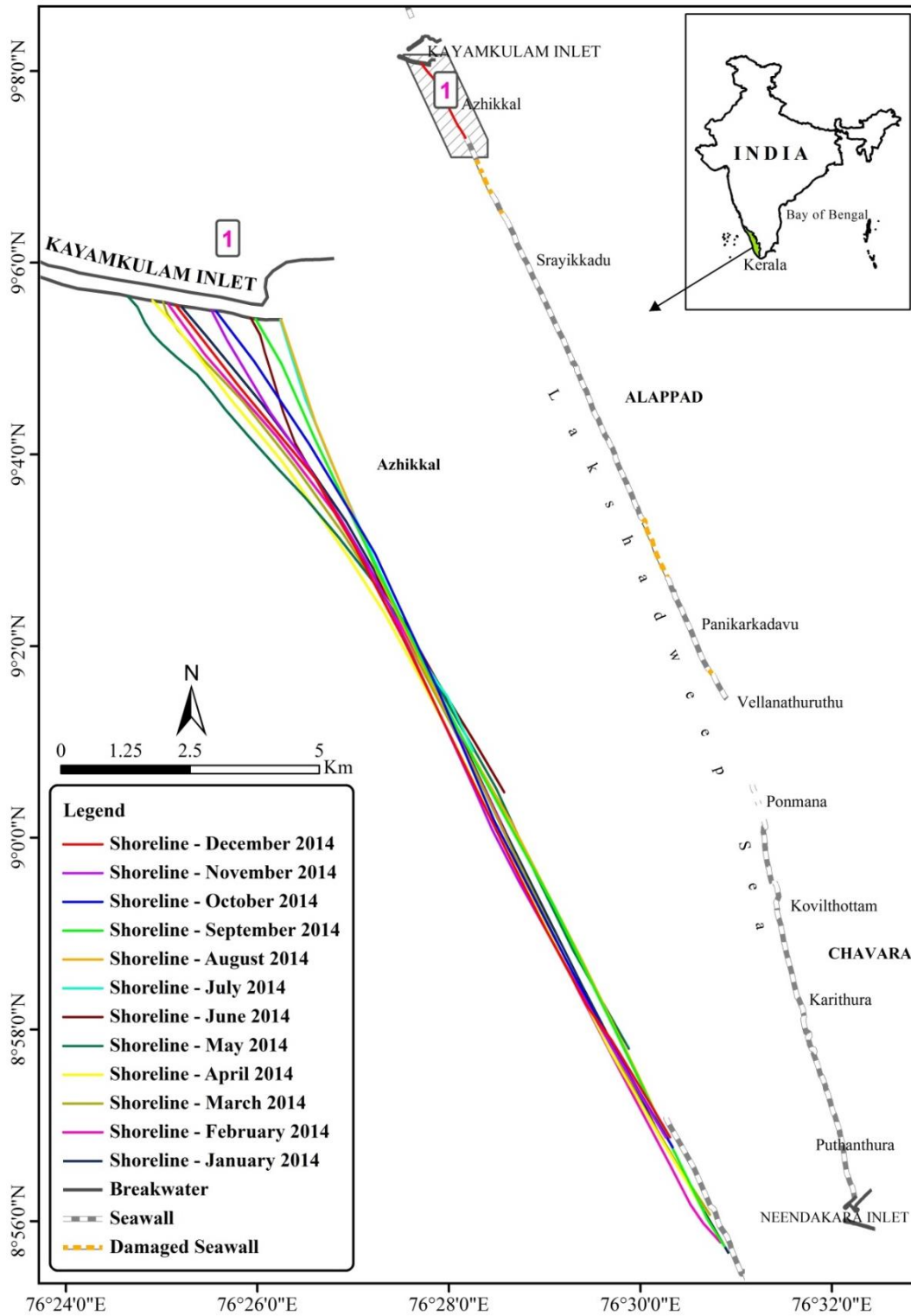


Fig. 6.7 Short-term shoreline change along the northern sector of the Chavara coast during 2014

6.3 Long-Term Shoreline Changes

The long-term shoreline changes are estimated using multi-dated toposheets of the Survey of India and satellite imageries taking numerous precautions to minimise

errors. The available toposheets are those of 1967-68 in 1:50000 and 1988-89 in 1:25000 scales. Toposheets of 1:25000 scale for the Ponmana to Neendakara sector (about 9 km long in the south) was not available and hence the comparisons with 1:25000 are limited to the available sector (Ponmana to Kayamkulam).

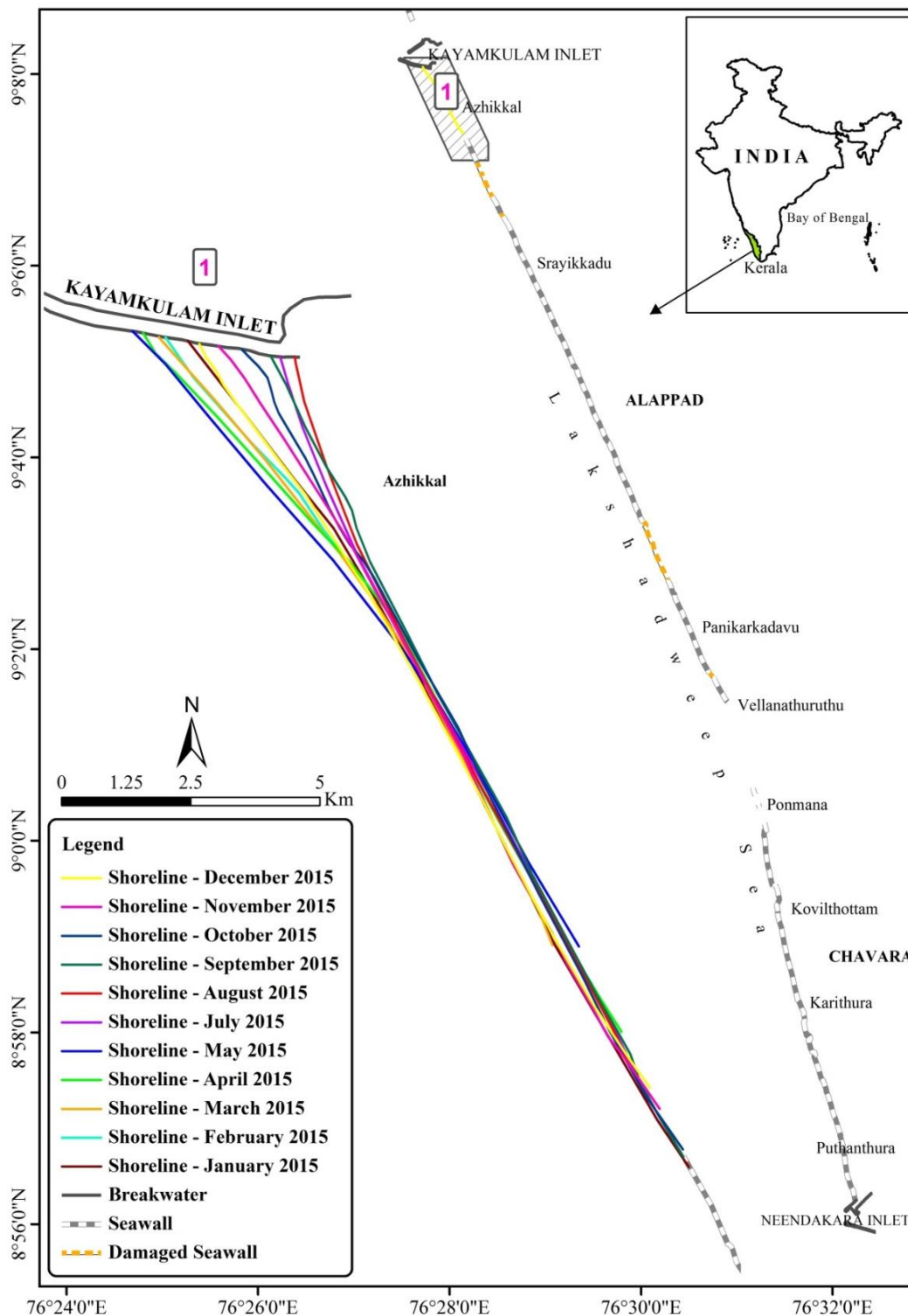


Fig. 6.8 Short-term shoreline change along the northern sector of the Chavara coast during 2015

Table 6.2 Monthly shoreline change (m) along the northern sector of Chavara coast estimated from shorelines mapped using GPS during the year 2015

Location	Short-term shoreline change (m) during the year 2015									
	Jan-Feb	Feb-Mar	Mar-Apr	Apr-May	May-Jul	Jul-Aug	Aug-Sep	Sep-Oct	Oct-Nov	Nov-Dec
Azhikkal (NK-1)	+14	+7	+4	+17	-66	-11	-12	+33	+2	+20
Azhikkal South (NK-3)	0	#	-10	-11	+5	+4	-11	+9	+15	0
Srayikkadu (NK-5)	#	#	#	#	-8	+4	-6	+5	-4	-5

No beach; +^{ve} Accretion; -^{ve} Erosion

The satellite images used are the IRS P6 LISS IV of 2007 and the Google imageries of 2003 - 2007. Shoreline mapping was carried out to delineate the shoreline position during the fair season of 2010 and 2015 (see section 3.5 for the methodology followed). The mapped/delineated shorelines for the different years are presented in Fig. 6.9. Shoreline changes in linear distance for a few representative locations along the coast are calculated after overlaying in ArcGIS and the results are presented in Table 6.3.

It can be seen from Fig. 6.9 and Table 6.3 that shoreline retreat is observed throughout the coast during the period of 1968-1989 along the Neendakara-Kayamkulam sector. Retreat of shoreline to the extent of 132 m and 118 m are observed at the stations NK-3 and NK-5 respectively located to the south of the Kayamkulam breakwater. Erosion is comparatively less during this period at the mining sites of Vellanathuruthu (NK-6), Ponmana north and Ponmana south with landward shifts of 52 m, 25 m, 26 m respectively. Comparison of the shoreline maps of 1968 and 2006 reveals that further south of the mining sites, the rate of erosion decreases as indicated by the shoreline retreat values of 19 m, 13 m and 10 m at Karithura (NK-8), Puthanthura and Neendakara locations respectively.

During the period of 1989-2006, the stations adjacent to the Kayamkulam breakwater show advancement of the shoreline with a maximum value of 152 m at NK-1 close to the breakwater, 63 m at NK-3 about 1 km south of the breakwater and 32 m at NK-5 further south. Obviously this accretion in contrast to the other stations is due to the 'groin effect' of the breakwater which was built during 2000-2005. Shoreline retreat of the order of 79 m is noticed at the mining locations of Vellanathuruthu (NK-6), and

still higher rate at the Ponmana mining location (175 m and 185 m at Ponmana north and Ponmana south respectively).

The shoreline change values for the period 1968-2006 presents a cumulative picture for the whole period. At NK-1, the shoreline is still in an advanced position when compared to 1968 due to the effect of the breakwater. The shoreline changes further south at NK-3 and NK-5, even though not considerable, indicate a net retreat and this can be attributed to the deposition subsequent to the breakwater construction at Kayamkulam. At the mining sites the retreat of the shoreline is considerably higher, reaching a maximum of 211 m at Ponmana south. The shoreline retreat at locations further south of the mining sites is insignificant with values around 10 - 20 m.

The comparison of shorelines during the period of 1968-2015 indicates higher retreat of the shoreline at the mining sites of Vellanathuruthu, Ponmana North and Ponmana South with values of 260 m, 388 m and 367 m respectively. The Kovilthottam mining site where the mining volumes are relatively low records a moderate retreat of only 100 m. Further south (eg. Karithura, Puthanthura, Neendakara), the shoreline retreat is much lesser with values in the range of 10 - 35 m during this period.

The shoreline change during 2006-2015 enables a closer look at the trend in shoreline change during the past one decade. The retreat of the shoreline continues unabated throughout, with the highest values at the mining sites. The mining sectors of Vellanathuruthu (NK-6), Ponmana North and Ponmana South show retreat of the order of 130, 187 and 155 m respectively during the past decade. At the three stations NK-1, NK-3 and NK-5 in the northern sector, the shoreline retreat shows values of 122 m, 133 m and 110 m respectively. The Kovilthottam mining site (NK-7) has less erosion compared to the other mining locations, with a shoreline retreat of only 22 m. The locations towards the south of the mining area exhibit marginal retreat of the order of 10 m.

In a nutshell, it is seen that the entire coast barring the northernmost sector is under erosion during all the four periods, viz. 1968-89, 1968-2006, 1968-2015 and 2006-2015 considered for the study. But the retreat of the shoreline is quite high in the mining sites of Vellanathuruthu, Ponmana North and Ponmana South with values in the range of 250 - 400 m during 1968-2015. The retreat is moderate in the northern sector due to the groin effect of the Kayamkulam breakwater. The northern most

stations which was showing some net accretionary trend during 1989-2006 has started showing significant shoreline retreat during the past one decade (2006-2015). Shoreline erosion, even though present, is not critical at the locations south of the mining site as they are protected by well-maintained seawalls.

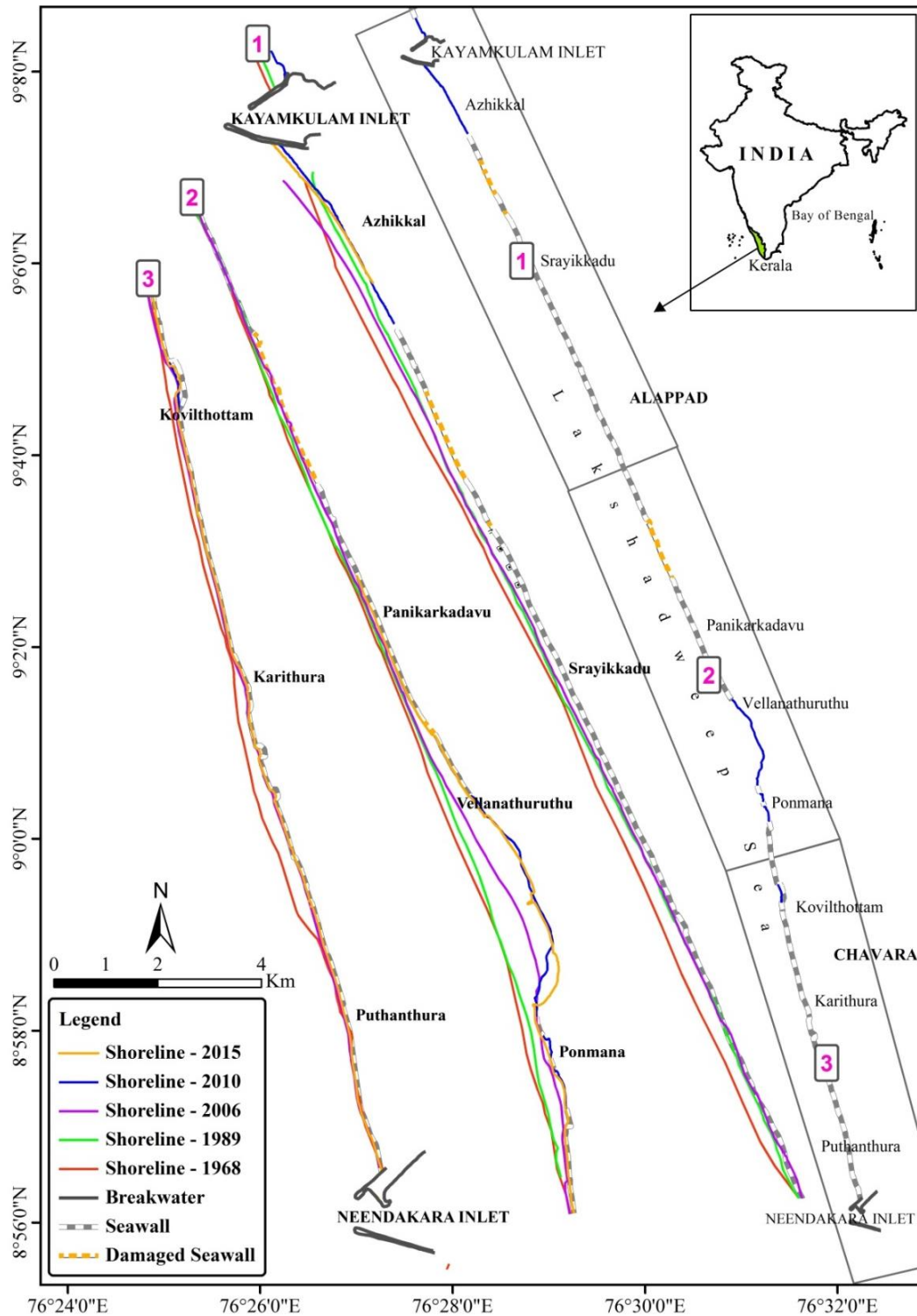


Fig. 6.9 Long-term shoreline change along the Chavara coast during different time periods starting from 1968

Table 6.3 Long-term shoreline change (m) along the Chavara coast during different periods

Location	Shoreline change (m)				
	1968-1989	1989-2006	1968-2006	1968-2015	2006-2015
Azhikkal (NK-1)	-57	+152	+95	-30	-122
Azhikkal South (NK-3)	-132	+63	-69	-178	-113
Srayikkadu (NK-5)	-118	+32	-86	-195	-110
*Vellanathuruthu (NK-6)	-52	-79	-131	-260	-130
*Ponmana (North)	-25	-175	-200	-388	-187
*Ponmana (South)	-26	-185	-211	-367	-155
*Kovilthottam (NK-7)	#	#	#	-100	-22
Karithura (NK-8)	#	#	-19	-34	-12
Puthanthura	#	#	-13	-22	-12
Neendakara	#	#	-10	-10	+2

* Mining sites; # No beach; +^{ve} Accretion; -^{ve} Erosion

6.4 Empirical Orthogonal Function Analyses of Beach Profiles

The Empirical Orthogonal Function (EOF) analysis is a statistical tool which can also be used to analyse the beach profile data. It can separate out the dominant modes of changes in the beach topographical data and is used to investigate the patterns in the beach variations and other coastal features. The monthly beach profiles over the period of December 2010 to December 2014 at station NK-5 located approximately 2 km south of the Kayamkulam breakwater is used for the EOF analysis. The dominant modes of the beach changes are obtained from the first three eigen functions (Aubrey, 1979). Eigen function does not consider a single point in the beach for the analysis, instead it decomposes the entire beach into spatial and temporal modes. The spatial mode is represented by first three eigen functions U1, U2 and U3 and the temporal mode by V1, V2 and V3. Using the first three eigen functions, the seasonal erosional / accretional behaviour of the beach is well established. Table 6.4 presents the percentage of variance contained by each eigen function from the EOF analysis. It can be seen that the first three eigen functions account for 97.9 % of the total variability in the beach profile data. The first eigen function comprehends the greatest portion of the mean square value (91.3 %). The 2nd and 3rd eigen functions comprises of the residual part having the variance of 5.1 and 1.5 % respectively. The remaining eigen functions have very little information to communicate.

Table 6.4 Results of EOF analysis showing the percentage of variance contained by each eigen function

Sl. No.	Eigen functions	Percentage of variance
1	1 st Eigen function (U1, V1)	91.3
2	2 nd Eigen function (U2, V2)	5.1
3	3 rd Eigen function (U3, V3)	1.5
Total		97.9

The first three eigen functions at station NK-5 representing spatial configuration and temporal dependence is shown in Fig. 6.10a-b. The 1st spatial eigen function (U1) represents the mean beach profile having moderately sloping foreshore. The corresponding component in the temporal mode (V1) shows an overall eroding tendency during the end of the fourth year i.e. December 2014. This is in line with the observation from the beach volume changes, where the rate of erosion is higher during the end of the year 2014. The 2nd spatial eigen function (U2) shows a broad maximum at 60 - 70 m from the bench mark. This clearly indicates the location where the beach profile experiences maximum variation. The erosion is initiated from approximately 70 m, whereas very less variability upto 50 m from the bench mark. The distribution of the corresponding temporal function (V2) shows the cyclic nature of the erosion/accretion. Here the beach is subjected to rapid erosion during April-May (2011), May-June (2012), February (2013), December (2013), April (2014) and December (2014). The cyclic erosion/accretion during the south-west monsoon is established from the 2nd eigen function. The 3rd spatial eigen function (U3) shows a maximum variability at 5 m at the backshore and about 60 - 80 m on the foreshore. The corresponding temporal function (V3) has no periodicity or seasonality and this shows the irregular changes of the beach due to severe erosion. The effect of south west monsoon on the beach is reflected in the eigen functions. Hence it can be concluded that the erosional tendency is more pronounced during the year 2014 which is in par with the results of beach volume computations also.

6.5 Numerical Simulation of Shoreline Evolution

Shoreline evolution along the Chavara coast has been modeled by using the LITLINE module of LITPACK modelling suite. The LITLINE calculates the shoreline evolution by solving a continuity equation for the sediment in the littoral zone. The influence of structures, sources (beach nourishment) and sinks (mining) is also included. The coastline position is calculated by LITLINE based on the time series

wave climate as input to the model. The shoreline change calculation is based on the 1-line theory (Hanson and Kraus, 2011) in which the cross-shore profile is assumed to remain unchanged during erosion/accretion. The coastal morphology is described by the shoreline position (in the cross-shore direction) and the coastal profile at a given longshore position.

The theoretical background, input data, calibration and validation along with the numerical simulations of the model are presented in the following sections.

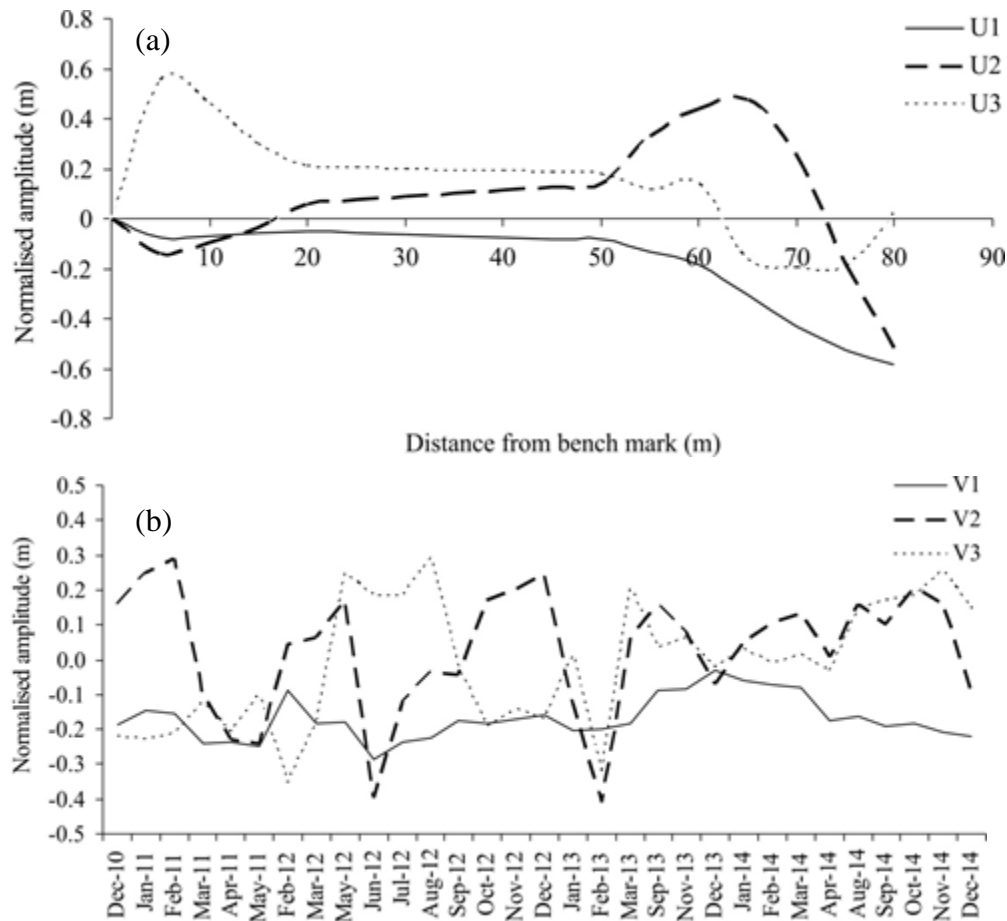


Fig. 6.10 First three eigen functions for the beach profiles at station NK-5: (a) spatial and (b) temporal dependence

6.5.1 Theoretical background

The basic assumption in the LITLINE model is that the longshore sand transport occurs uniformly over the beach profile from the berm height D_B down to the depth of closure D_c . The definition sketch for shoreline change calculation according to 1-line theory is shown in Fig. 6.11 and the baseline orientation used in LITLINE is shown in Fig. 6.12. The parameters are specified based on a coordinate system in which x-axis is the baseline quasi-parallel to the initial coastline, and y is perpendicular to the x

axis. By considering a control volume of sand balanced during an infinitesimal interval of time and neglecting the cross-shore transport, the following differential equation is obtained,

$$\frac{\partial y(x)}{\partial t} = - \frac{1}{h_{act}(x)} \frac{\partial Q_l(x)}{\partial x} \dots\dots\dots(6.1)$$

where $y(x)$ is the coastline position, t is the time, $h_{act}(x) = (D_B + D_C)$ is the height of the active cross-shore profile or total height of the control volume (where D_B is the berm height and D_C is the depth of closure), $Q_l(x)$ is the longshore sediment transport expressed in volume, and x is the longshore position or space coordinate along the axis parallel to the trend of the shoreline.

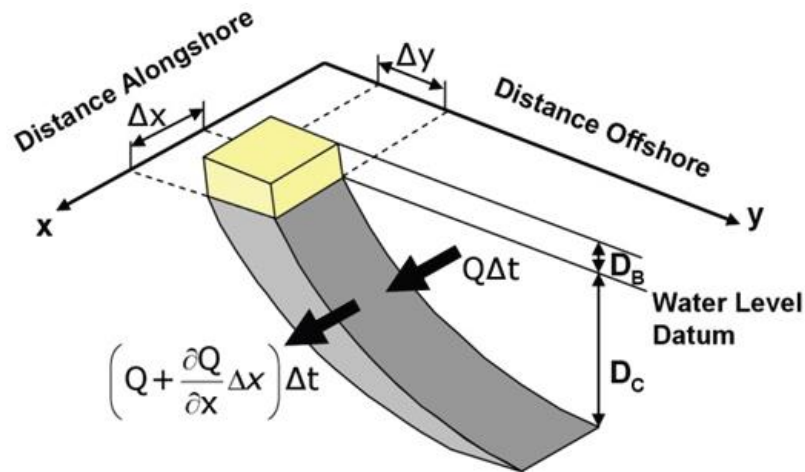


Fig. 6.11 Definition sketch for shoreline change calculation according to 1-line theory (Source: Hanson and Kraus, 2011)

The Eqn. (6.1) was extended to include the line discharges of sediment representing a source or sink of sand on the shoreline following the work of Kraus and Harikai (1983) and is given by

$$\frac{\partial y(x)}{\partial t} = - \frac{1}{h_{act}(x)} \frac{\partial Q_l(x)}{\partial x} + \frac{Q_{sou}(x)}{h_{act}(x) \Delta x} \dots\dots\dots(6.2)$$

where $Q_{sou}(x)$ is the source / sink term expressed in volume and is derived from the table of sediment transport rate in the surf zone, Δx is the alongshore discretization step. The alongshore discretization used in the LITLINE is shown in Fig. 6.13. From an initial coastline position $y_{intl}(x)$, the evolution in time is determined by solving the above equation. The continuity equation for sediment volumes is solved by using implicit Crank-Nicholson scheme which gives the development of the coastline position in time.

The continuity equation can be written as

$$a_i y_{i-1,t+1} + b_i y_{i,t+1} + c_i y_{i+1,t+1} = d_i \dots\dots\dots(6.3)$$

where

$$a_i = (1 - \alpha_{CN})dQ_{i-1} \dots\dots\dots(6.4)$$

$$b_i = \frac{\Delta x^2 h}{\Delta t} - a_i - c_i \dots\dots\dots(6.5)$$

$$c_i = (1 - \alpha_{CN})dQ_i \dots\dots\dots(6.6)$$

$$d_i = a_i y_{i-1,t} + b_i y_{i,t} + c_i y_{i+1,t} - \Delta x(Q_{i,t} - Q_{i-1,t} - QS_i) \dots\dots\dots(6.7)$$

where α_{CN} is the Crank-Nicholson factor which determine the implicit or explicit solution scheme ($\alpha_{CN} = 0$ gives fully implicit solution, $\alpha_{CN} = 1$ gives fully explicit solution). The system of equation for all longshore position can be solved by Gauss elimination and a_i , b_i , c_i and d_i can be found from the present time step.

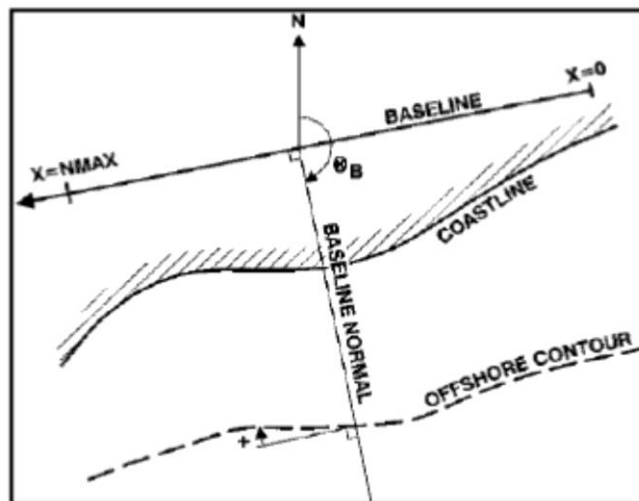


Fig. 6.12 Baseline orientation used in the LITLINE module of LITPACK

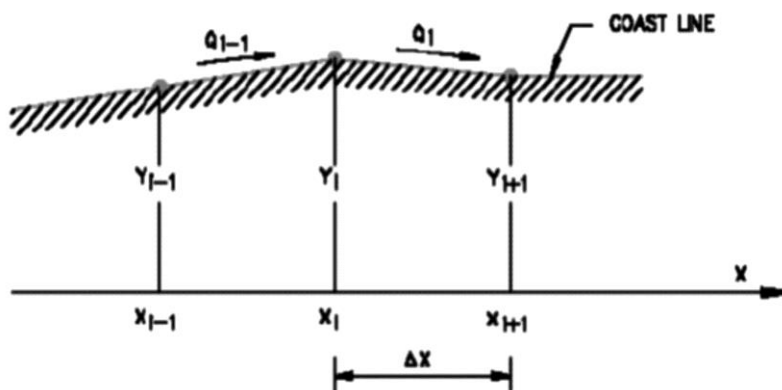


Fig. 6.13 Alongshore discretization used in the LITLINE module of LITPACK

6.5.2 Input data

The basic input data for the LITLINE model are the alongshore relative coastline alignment along with profile description, active depth of transport and depth contour angles at each grid point, cross-shore profile bathymetries, wave properties (wave height, period and angle), water levels, wind, position and size of structures and position and magnitudes of sources/sinks. The coastline position was given for the 24 km coastal stretch extending from Neendakara inlet in the south to the Kayamkulam inlet in the north at 10 m grid spacing for an accurate representation of the shoreline. The initial coastline is given as a distance from baseline and for the preparation of this coastline position, the shoreline for the year 2000 was used as the baseline data. The baseline is drawn at a shore parallel angle of 154° N which is close to the general shoreline orientation along the coast. The wave and cross-shore profile including the sediment characteristics are the additional inputs to the LITLINE module which are similar to that of LITDRIFT, and the same climatic conditions are used for the simulation of coastline evolution (see Tables 4.2 & 4.3). The cross-shore bathymetric profile extracted from the measured bathymetry was given as the basic input for the model. Four numbers of cross-shore profiles extending to a depth of 10 m is used as the input for simulating the actual field conditions. The cross-shore interval is about 1 m for these cross-shore profiles.

Sediment characteristics such as grain size were estimated from the collected sediment samples from the beach and innershelf from which the bed roughness and fall velocity were estimated. The LITLINE sediment transport table generation program, LINTABL is used for the computation of longshore sediment transport and LINTABL serves as another input for the coastline evolution model, which is a substitute for the LITDRIFT in the LITLINE module. The LINTABL calculates and tabulates sediment transport rates by the method of interpolation in the tables as functions of the water level, the surface slope due to regional currents, wave period, height and direction with respect to the shoreline normal. The same transport table can be applied along the whole coast if the coastline is straight and uniform.

Since this coastal sector is subjected to rampant beach sand mining, appropriate value of the mining quantity which acts as sink was given as one of the major input for the model. Mining volumes of 67,000 m³/year for the period 2000 - 2010 (Kurian et al., 2002) and 134,000 m³/year for the period 2011 - 2022 (Kurian et al., 2012) are

converted and given as sink input (negative value for the sink) for a 2 km mining stretch and 10 m grid spacing along the selected mining locations of Kovilthottam, Ponmana and Vellanathuruthu. The sink values are distributed over the three mining sites at 6.4 - 6.8 km, 8.8 - 9.6 km and 9.8 - 10.6 km towards north from the northern arm of the Neendakara breakwater.

Coastal protection structures such as breakwaters, groins and seawall constructed along the coastal sector of Neendakara-Kayamkulam are given as input using the appropriate grid no. starting from northern arm of the Neendakara breakwater. It is not possible to include all the 26 groins available along this coastal sector, since the model can accommodate only 20 groins as input. Thus only 20 major groins were given as input to the model.

6.5.3 Calibration and validation of the model

The model outputs were calibrated and validated using satellite imageries and the measured shorelines. The baseline shoreline was the surveyed shoreline of the year 2000. The surveyed shorelines for different years viz. 2006, 2010 and 2015 were used for the calibration and validation of the model. Thus the trend in the shoreline orientation for both the short and long time span i.e. 2000-2006, 2000-2010 and 2000-2015 was examined and was compared with the Google imageries for the same period. Several statistical parameters can be used to assess the quality of the performance of the numerical models. Among this, Relative Mean Absolute Error (RMAE) is used to evaluate the accuracy and performance of the LITLINE model (van Rijn et al., 2003; Pender and Karunarathna, 2013) and is given by

$$RMAE = \frac{\langle |Y-X| \rangle}{\langle |X| \rangle} \dots\dots\dots(6.8)$$

where Y is the simulated value (shoreline change), X is the measured value and <.> denotes the averaging procedure.

For the modeling of shoreline evolution, a baseline is fixed and the distance from the coastline to the baseline is set as the initial coastline. The initial coastline is divided into grid spacings of 10 m for the 24 km coastal stretch, starting from the extreme south of Neendakara breakwater and extending upto the Kayamkulam breakwater. The model run has been performed for the period 2000-2015, by accommodating the coastal protection structures constructed during different years. Appropriate sink input

is provided to the model at the mining sites of Kovilthottam, Ponmana and Vellanathuruthu so that the effect of beach sand mining is also incorporated. The observed shoreline of 2006, 2010 and 2015 show good corroboration with the simulated one as can be seen in Fig. 6.14a, b & c. The simulation result during the year of 2015 is superimposed with the Google image for the same period (Fig. 6.15a & b). The statistical error estimates for the simulated and measured shoreline along the Chavara coast for the years 2006, 2010 and 2015 is shown in Table 6.5. The Relative Mean Absolute Error (RMAE) is about 0.04 (4 %) during 2000-2006 shoreline simulation. But RMAE is about 0.05 (5 %) during the simulation period of 2000-2010 and 2000-2015. Thus the model is calibrated for both short- and long-term scenarios.

Table 6.5 Statistical error estimates for the simulated and measured shoreline along the Chavara coast for the years 2006, 2010 and 2015

Year	*RMAE
2000-2006	0.04
2000-2010	0.05
2000-2015	0.05
*RMAE - Relative Mean Absolute Error	

For validation of the model, the simulation was performed for each period by introducing the coastal structures relevant for the period. No mining was considered in the model at the mining sites (i.e. sink input is given as zero) and omitted the breakwater at the Kayamkulam inlet. It can be seen from the Fig. 6.16a that the dent in the mining site is completely filled due to the advancement of shoreline by the year of December 2006. The erosion/recession of the shoreline is observed at the northern end of the Kayamkulam inlet (Fig. 6.16b). This observation corroborates well with the results from the long-term shoreline change during 1968-1989 (Table 6.3), where the erosion is predominant at the northern end of the coastal stretch. But after the construction of Kayamkulam breakwater at the northern end during the period of 2000-2007, the accretion is dominant.

6.5.4 Shoreline evolution along the Chavara coast

The calibrated and validated model has been used for further simulation. The simulation was performed for the period of 2000 - 2022 by inserting groins in tally with the field scenarios of different years. The simulated shorelines for 2006, 2010,

2015, 2018 and 2022 are presented in Figs. 6.17 & 6.18. For better presumption, the shoreline evolution is superimposed on the recent satellite image (Google image) for the year of 2016 and is shown in Fig. 6.19a & b for both the northern sector near to Kayamkulam breakwater and mining sites.

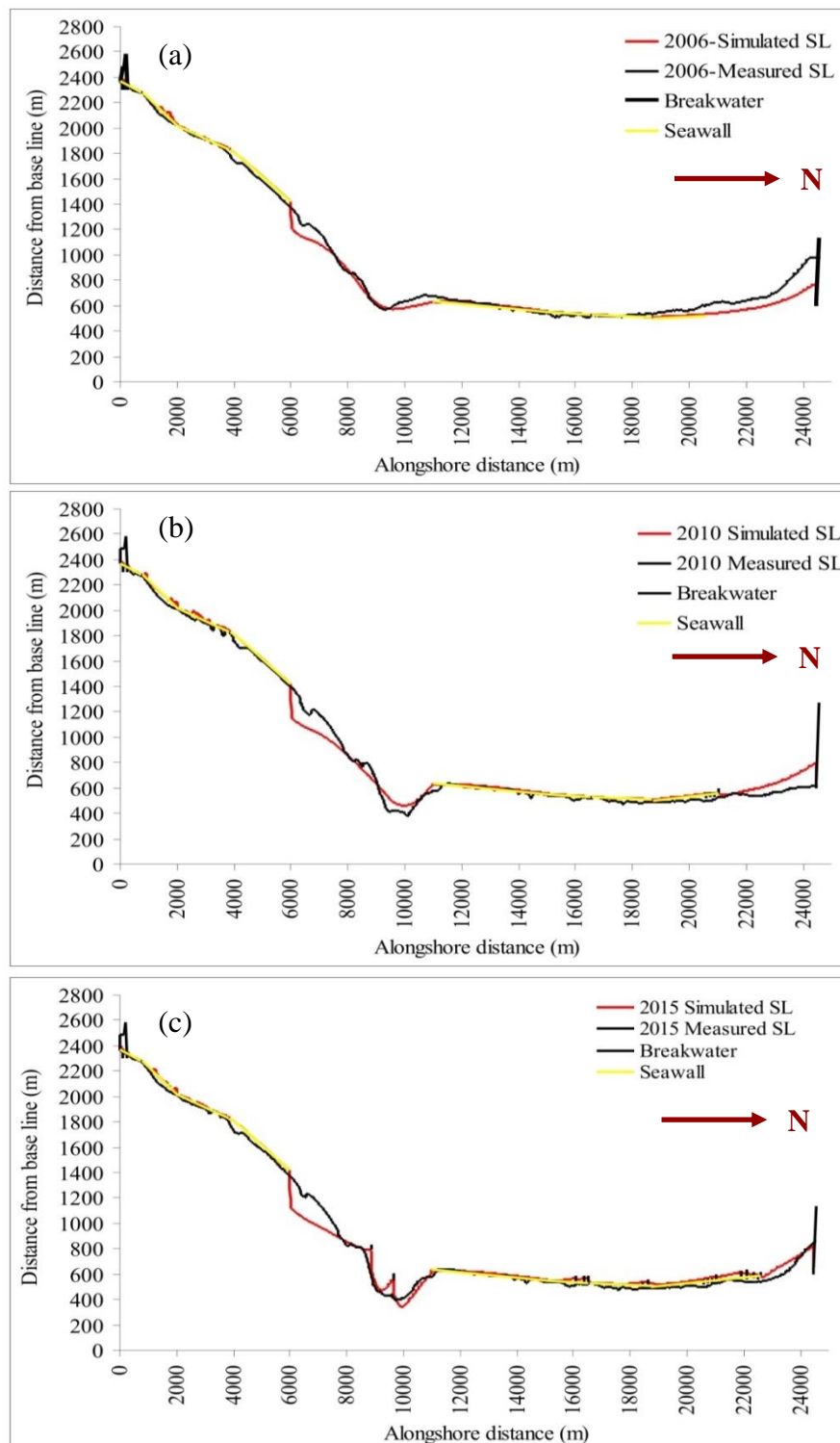


Fig. 6.14 Simulated and measured shoreline along the Neendakara-Kayamkulam coastal sector for the years (a) 2006, (b) 2010 and (c) 2015

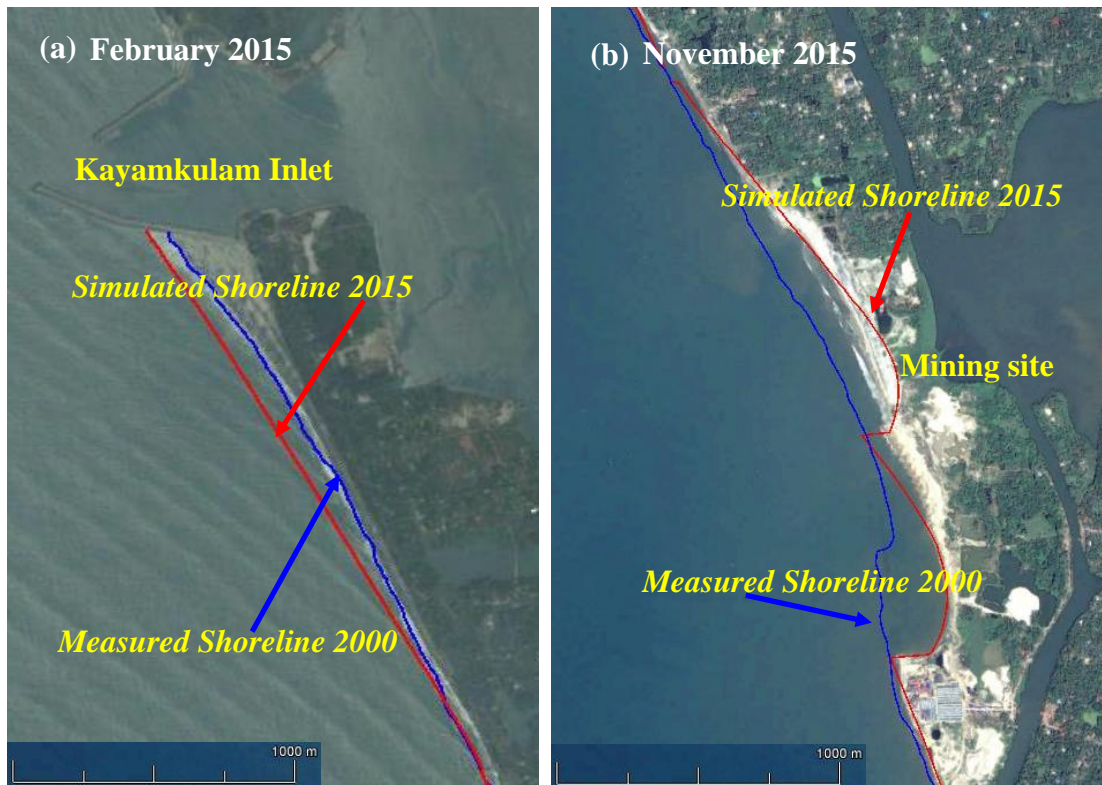


Fig. 6.15 Simulated shoreline along the Neendakara-Kayamkulam coastal sector for the year 2015 superimposed on satellite image (Google image) for the (a) northern sector near to Kayamkulam inlet and (b) Ponmana mining site

The simulated shorelines of 2006 and 2010 at the mining site (Fig. 6.17a) are not under the influence of the groins and hence a realignment of the shoreline with overall retreat is observed in 2006 and 2010. However the scenario changed after 2013, when two more groins were constructed at the Ponmana mining site. Due to the impact of intense mining, the recession in the shoreline will be even upto 300 m from the initial shoreline by the end of December 2022 (Fig. 6.17a). The influence of the short and long groins is predominant at the northern end, near to the Kayamkulam breakwater. If the present scenario persists, the accumulation at the northern arm of the breakwater will be stabilized by the year of 2022. Advancement in the shoreline is noticed in between the groin field, due to the predominant northerly transport along the coastal stretch. End point erosion is observed at the end of the groin field which is about 2 km south of Kayamkulam breakwater (Fig. 6.17b). The extent of erosion is upto the seawall (assuming that the sea wall will be well maintained) since all the other locations except the mining sites and 2 km south of Kayamkulam breakwater are protected by seawall.

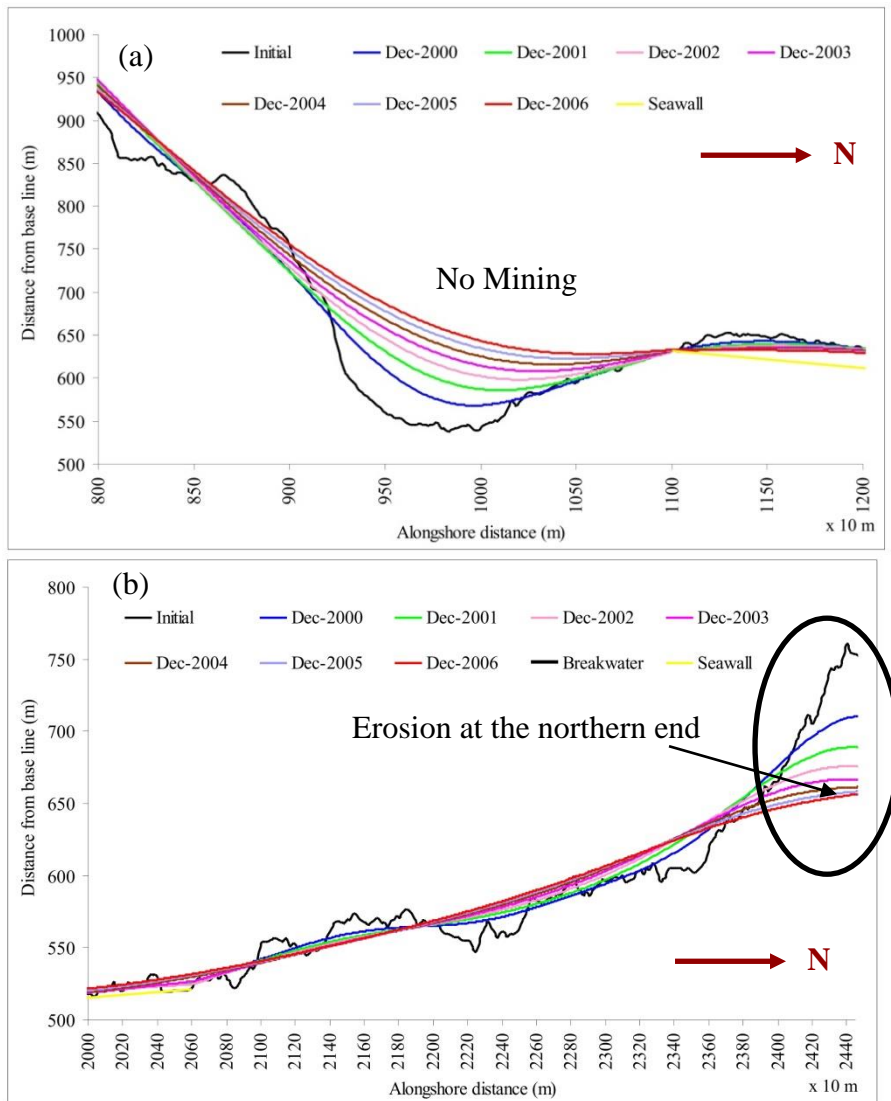


Fig. 6.16 Simulated shoreline for the years 2001-2006 (a) at mining site and (b) south of Kayamkulam inlet. The simulation was performed (i) without incorporating breakwaters and groins and (ii) by providing zero sink i.e. no mining

6.6 Innershelf Morphological Changes

The morphological changes in the innershelf are estimated from the bathymetry collected and collated for different years, viz. 2000, 2005 and 2010 (Fig. 6.20). In order to quantify the shift in isobaths over the ten year period, the bathymetry data for the three years were overlaid on an ArcGIS platform. Shore normal transects of one kilometre width each were drawn from nearshore to offshore off seven locations identified for computation of the isobath shift. The isobaths of 10 m, 14 m and 20 m were chosen for the computation of the shift and the area enclosed by the shift of the above isobaths over the periods 2000-2005, 2005-2010 and 2000-2010 were estimated. The shift of each isobath over different time periods per unit width is

presented in Fig. 6.21. The area calculated from bathymetric contours per unit width over different time periods for 10 m, 14 m and 20 m depth is shown in Table 6.6.

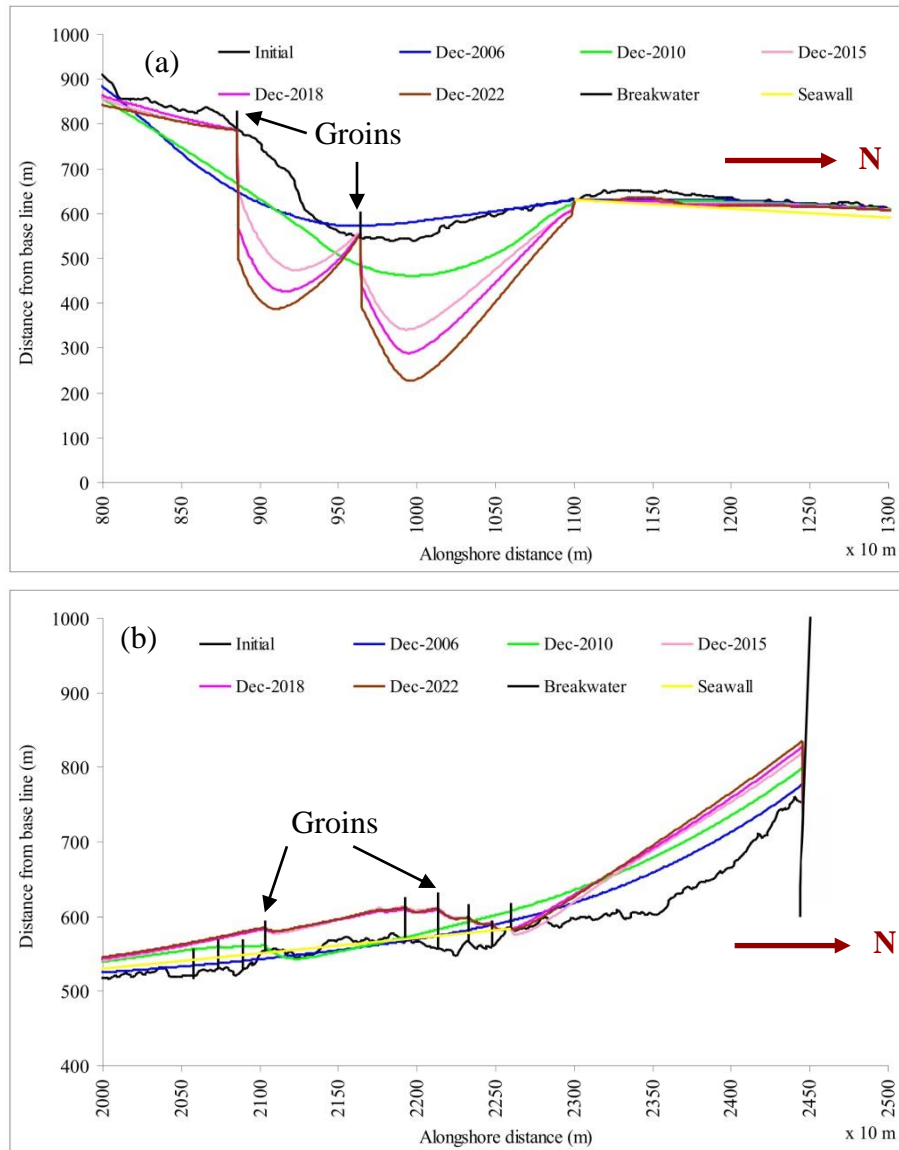


Fig. 6.17 Simulated shoreline for the years 2006, 2010, 2015, 2018 and 2022 (a) at the mining site and (b) south of Kayamkulam inlet. The simulation was performed with the influence of breakwaters, groins and seawall

It can be seen that the 10 m isobath (Fig. 6.21a) has shifted onshore at almost all the locations during the different time periods indicating that there is a deepening of the nearshore areas. The deepening is more pronounced at the mining locations of Ponmana and Vellanathuruthu. It can also be seen that the deepening is accelerated during the 2005-2010 period.

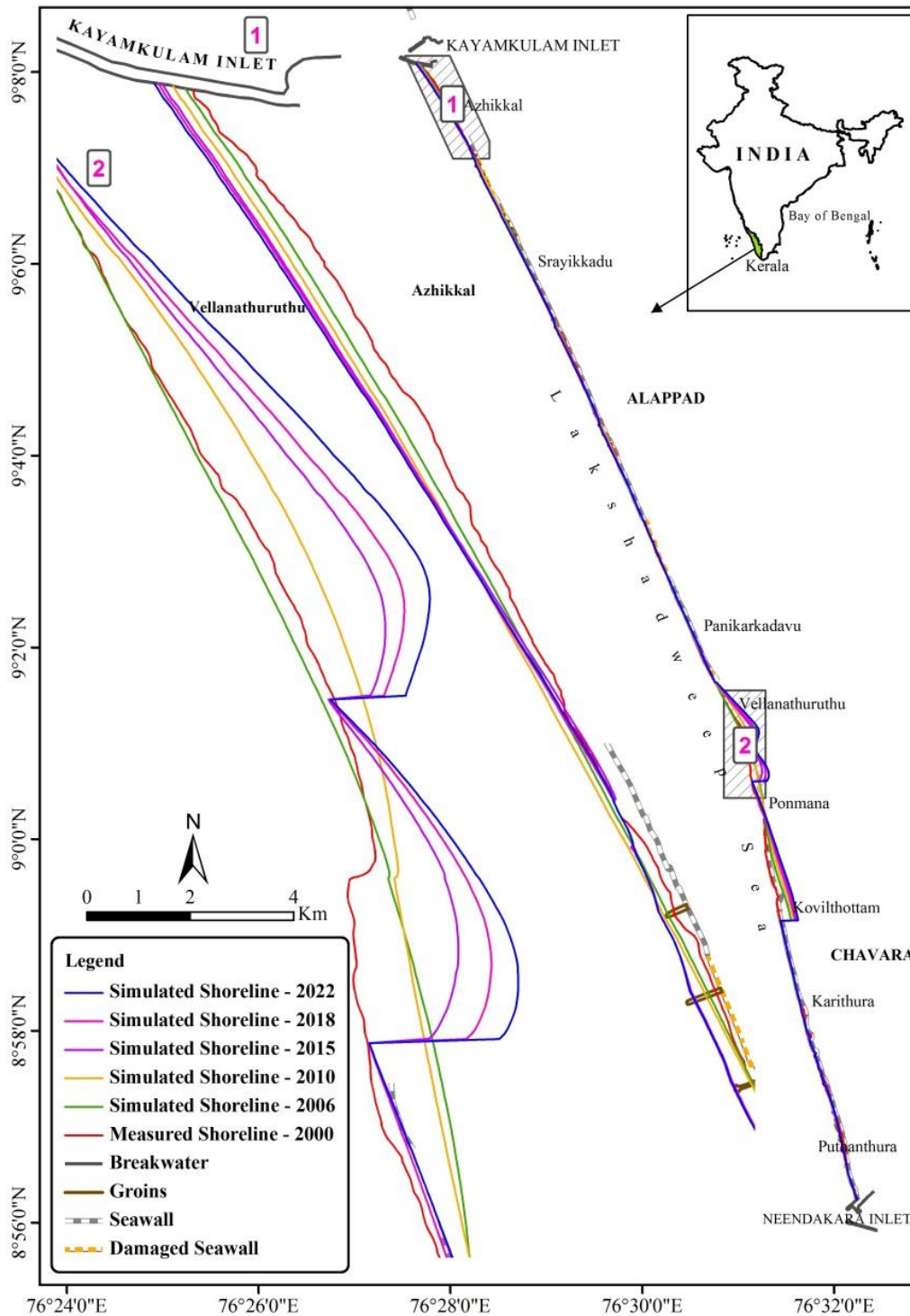


Fig. 6.18 The simulated shoreline for the selected sectors of the Chavara coast for the years 2006, 2010, 2015, 2018 and 2022. The measured shoreline for the year 2000 which is the baseline for the simulation is also shown in the figure

The 14 m isobath (Fig. 6.21b) shows a slightly different trend. During the period of 2000-2005 the isobaths at all the locations have shifted onshore. However, during the subsequent five year period of 2005-2010 the shift is reversed in the southern and northern sectors with a shallowing of this zone. Even at the central sectors

encompassing the mining zones, the shifts of the isobaths are either reversed or are of minimal values. If we take the overall trend during the 2000-2010 period, it can be seen that the 14 m isobath zone has migrated onshore at almost all the locations.

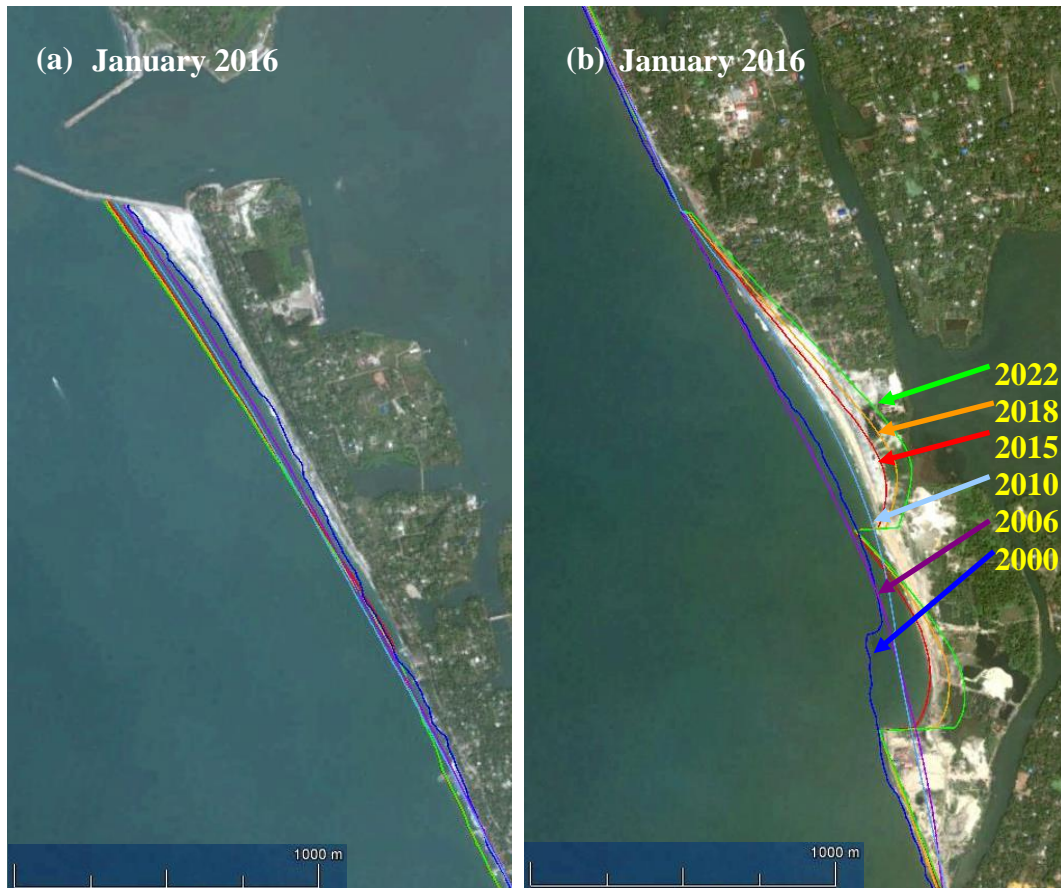


Fig. 6.19 Shoreline evolution simulated for the Chavara coast for different years (2000, 2006, 2010, 2015, 2018 and 2022): (a) south of Kayamkulam inlet and (b) Vellanathuruthu - Ponmana mining site. The simulated shorelines are superimposed on the Google image for January 2016

Further offshore, at 20 m depth (Fig. 6.21c), the overall deepening is observed at all locations during the 2000-2005 period barring Neendakara. In contrast, during the 2005-2010 period, deposition occurs at a majority of the offshore locations barring those off the mining sites of Ponmana and Vellanathuruthu. Even off these mining locations, the scale of deepening is minimal. Overall, during the 2000-2010 period, the innershelf of the 20 m depth zone deepens at most of the locations.

In general, the long-term trend indicates deepening of the nearshore zones of the whole coast during the 2000-2010 period. Further offshore at 14 m and 20 m depth zones, though overall deepening is seen, the post-tsunami period (2005-2010) shows pronounced deposition in the southern and northern sectors barring the mining sites.

Frihy et al. (1990) compared bathymetric maps of 1919/22 and 1986 for the continental shelf of northern Nile delta and found shifting of bottom contours due to accreted sands coming from eroded promontory tips as well as from offshore sources. In the present case the source for the pronounced deposition during the post-tsunami period could be the submerged palaeo-beaches offshore (Prakash, 2000; Hegde et al., 2006).

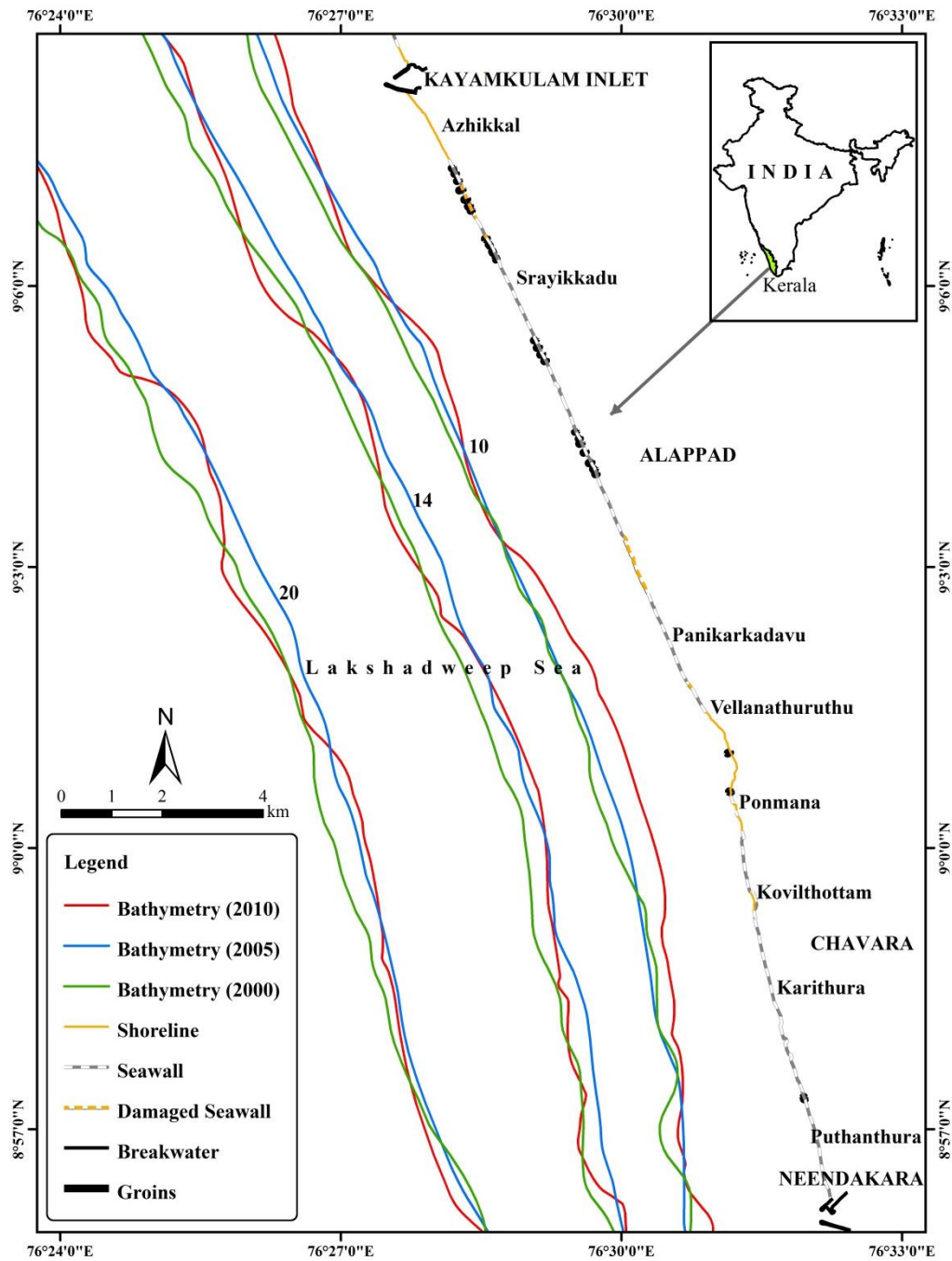


Fig. 6.20 Comparison of bathymetry of the innershelf of the Chavara coast during the years 2000, 2005 and 2010

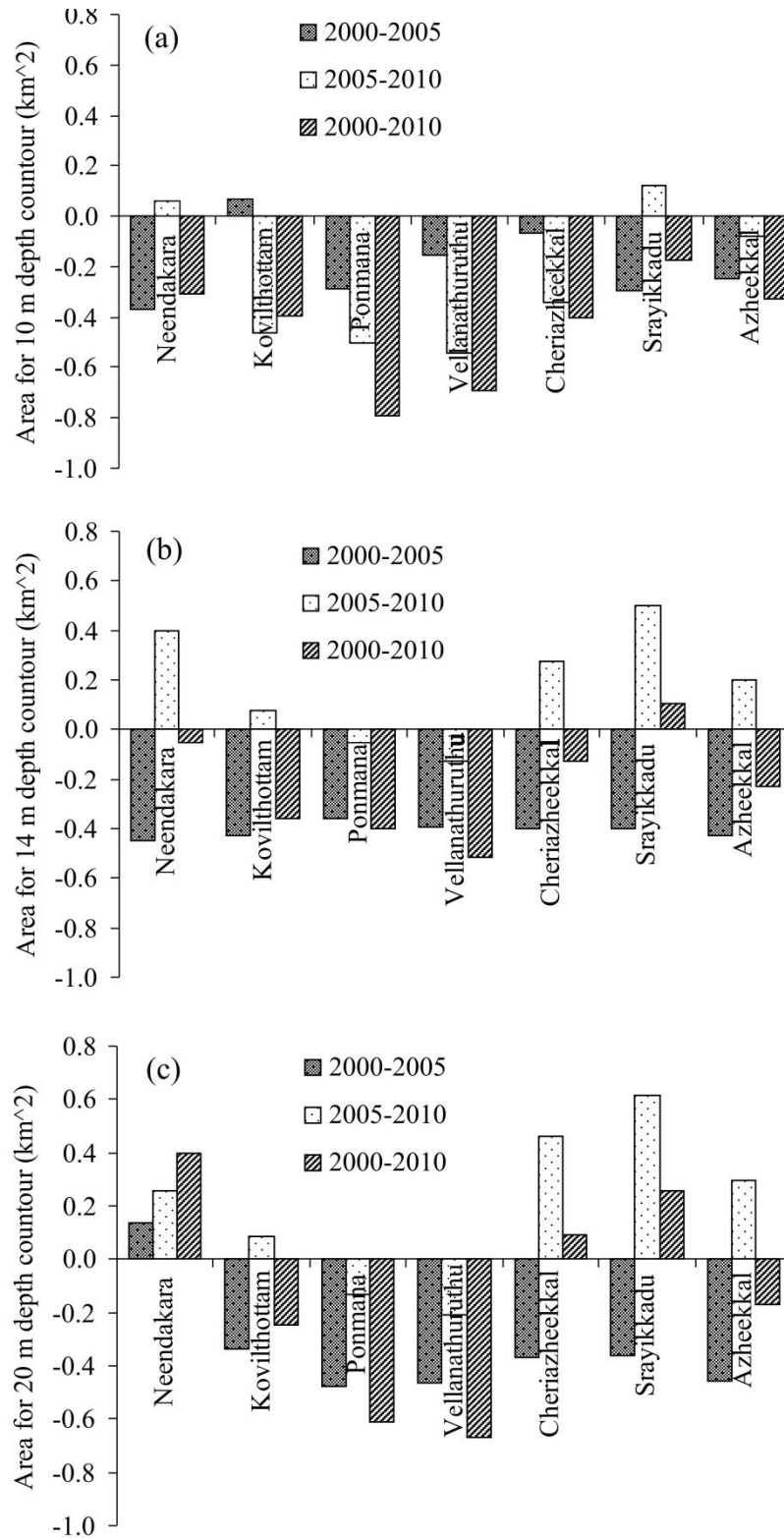


Fig. 6.21 Shift in isobaths at different locations of the Chavara coast as observed in the isobaths of (a) 10 m, (b) 14 m and (c) 20 m

6.7 Discussion

The study using shoreline change mapping and numerical modelling has brought out unequivocally the morphological changes that the whole Chavara coast has undergone

during the past four and a half decades. That the beaches of this coast are eroding since a long time is evident from the earlier studies (Prakash and Verghese, 1987; Sreekala et al., 1998), though no such studies are available for the innershelf. Construction of seawalls along this coast started in 1957-58 which is also an indication of the erosive nature of this coast since then.

Table 6.6 Shift in isobaths at different locations of the Chavara coast: area calculated from bathymetric contours per unit width over different time periods for 10 m, 14 m and 20 m depth

Location	Area calculated from shift in isobaths per unit width (km ²)								
	10 m contour			14 m contour			20 m contour		
	2000	2005	2000	2000	2005	2000	2000	2005	2000
	-	-	-	-	-	-	-	-	-
	2005	2010	2010	2005	2010	2010	2005	2010	2010
Neendakara	-0.37	0.06	-0.31	-0.45	0.40	-0.05	0.13	0.26	0.39
Kovilthottam	0.07	-0.46	-0.39	-0.43	0.07	-0.36	-0.34	0.09	-0.25
Ponmana	-0.29	-0.50	-0.79	-0.36	-0.05	-0.40	-0.48	-0.13	-0.61
Vellanathuruthu	-0.15	-0.54	-0.69	-0.39	-0.13	-0.52	-0.46	-0.21	-0.67
Cheriazheekkal	-0.06	-0.34	-0.40	-0.40	0.27	-0.13	-0.37	0.46	0.09
Srayikkadu	-0.30	0.12	-0.17	-0.40	0.50	0.10	-0.36	0.62	0.26
Azheekkal	-0.25	-0.08	-0.33	-0.43	0.20	-0.23	-0.45	0.29	-0.17

The spatial variation of the extent of shoreline change (intensity of erosion) and results of numerical modelling studies provide ample evidence of the driving force behind the observed changes. As seen already, the retreat of the shoreline is highest at the mining sites of Vellanathuruthu, Ponmana North and Ponmana South with values in the range of 250-400 m. This shows that the beach sand extraction by the two public sector companies is the main driver of the observed morphological changes. Beach sand extraction by IREL, KMML and its predecessor companies has been continuing on this coast since 1930. According to Kurian et al. (2002), 0.14 million tonnes of beach sand (which is roughly 67,000 m³ when converted to volume using the porosity factor worked out by them for the beach sand of this coast) is the yearly average extraction of IREL during the period 1990-2001. The intake by KMML was minimal till 2001, but increased manifold subsequently and in the decade 2001-2010, the average intake by both the firms together was almost double that of the previous decade. The volume of extraction prior to the 1990s is not available, but even assuming that these were smaller figures, the total volumes that have been mined so far for nearly one century could be a huge quantity. The sand extracted from the coast

is not returned to the system, or in other words is lost forever. When sand is extracted from the beach, the volumes available to be returned to the innershelf during the erosive phase are reduced and the ultimate impact of mining is to deplete the innershelf sand resource and lower the overall level of the shelf. The impact could be all the more serious considering the fact that there has been a drastic increase in the quantity of beach sand mining over the years. This unprecedented increase in mining volume is no match for offshore replenishment and thus leads to the caving-in of the beaches at the respective mining sites and adjoining areas (Fig. 6.22). The total length of the three mining sites put together is around 1.7 km. At the rate of onshore transport computed under the present study which is $77 \text{ m}^3/\text{m}/\text{year}$, the annual replenishment is around $131,000 \text{ m}^3$. This shows that the volume of sediment mined is much higher than the offshore replenishment. Thus the impact of mining is twofold. Firstly it will cause the beach to cave in at the mining sites since the material over and above the offshore replenishment is taken only from the beach (Kurian et al., 2002). Fig. 6.22 presents the sequence of morphological changes at the mining sites starting from 2003 through Google images. The remnants of the sea wall which was at the shore in 2003 is seen offshore due to the retreat of the shoreline; the beach has also caved in at this point by about 200 m during the 12 year period. This supports the long-term shoreline change values estimated under the present study which estimates recession of the shoreline by about 260 m at Vellanathuruthu, 388 m at Ponmana North, 367 m at Ponmana South and 100 m at Kovilthottam during the past four and a half decades.

The shoreline evolution modelling conducted for the Chavara coast shows that the mining at the present rate may have a devastating effect on the mining sites, particularly at Ponmana, where the shoreline retreats upto 250 m by 2022, from the shoreline of 2006. The recession in the shoreline during the period of 1968-2006 is about 200 m (Table 6.3). So by integrating both the results of observation and shoreline evolution modelling during the period of 1968 – 2022, about 450 m of the shoreline recession will take place at the mining site during these five and a half decades.

The second impact of mining is the lowering of the sea bed which is already seen to be occurring in the innershelf of the study area. As already stated, the material mined is the material that is replenished from offshore and is lost from the system. The

material that is mined during the 1990-2015 period itself is around 2,680,000 m³. No statistics is available for the period prior to that. Even assuming a very nominal mining volume equal to the above quantity during the 60 year period (1930-1990), the total mining volume till 2015 is about 5,360,000 m³. Assuming that the volume of material that is mined comes from a 15 km stretch of the innershelf of this coast, and assuming that the source of this sand is a width of 7 km of the innershelf limited to the 20 m isobath, this intake could cause a deepening of the shelf by about 5.1 cm during the period 1930-2015. In fact the loss to the system may be much higher since illegal mining by unauthorised individuals/agencies (Times of India, 2013) is not accounted for in the mining data. Hence the deepening of the shelf as observed is well explained.

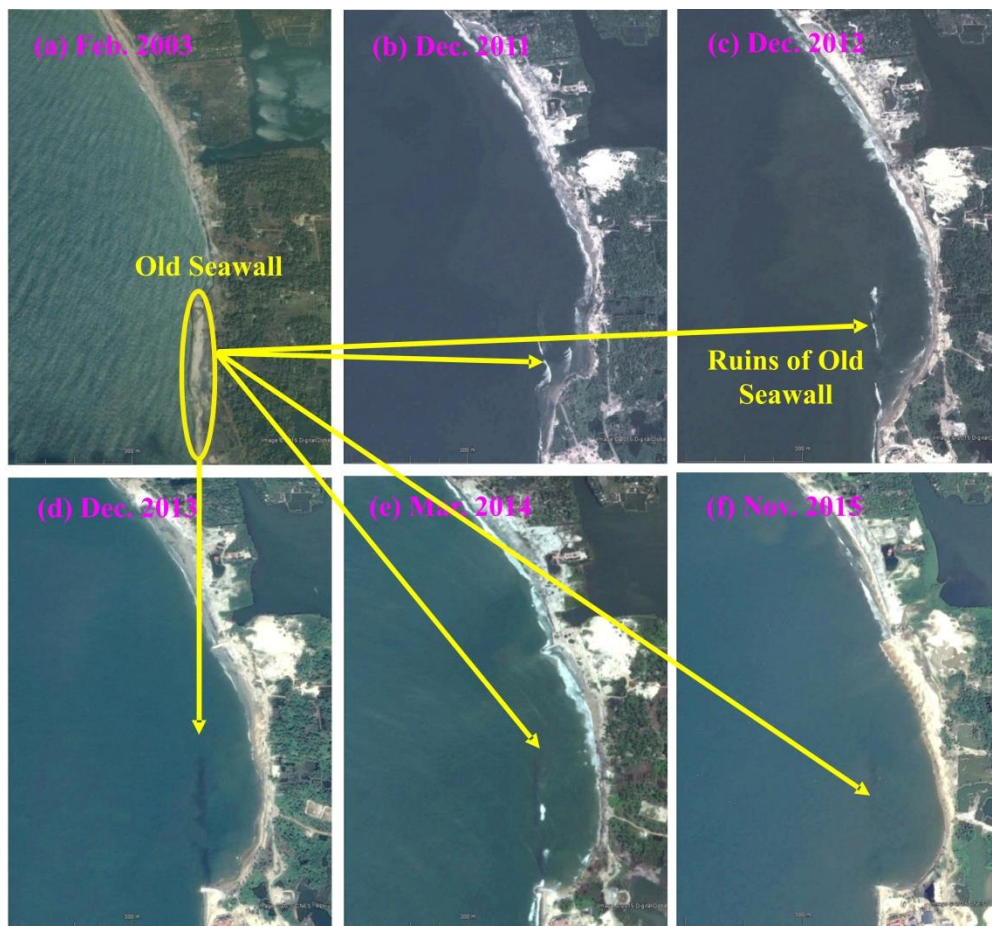


Fig. 6.22 Satellite images (Google images) of the Ponmana-Vellanathuruthu mining site during 2003 - 2015 showing the ruins of the old seawall at the mining site and two newly constructed groins during 2013

Another important forcing factor which has contributed to the morphological changes is the 2004 Tsunami which had a devastating effect on this coast with a run-up level as high as 5 m in the northern sector (Kurian et al., 2006a). The tsunami brought in huge deposits of heavy minerals from offshore which got deposited in the beach and

hinterland areas of this coast with a thickness of as much as 1 m at a few locations (Narayana et al., 2005; Kurian et al., 2006a, b). The tsunami waves being long period waves have immense potential for churning the bottom sediments and selectively transporting the heavy sands by the phenomenon of transport sorting (Komar, 1989). Hence the source of the backshore and hinterland deposits is the offshore causing a deepening of the innershelf. This has been confirmed by Kurian et al. (2006a) based on bathymetric data for 2000 and 2005 which are used as baseline data in the present studies too. The important role played by the tsunami in effecting innershelf morphological changes is evident from the results of the present study which shows a pronounced deepening of the innershelf during the 2000-2005 period after which it has reduced. This reduction can be attributed to the onshore transport of sediments from further offshore and longshore transport from the adjoining shelf.

The coast under study extending from Thangassery in the south was a more or less straight open coast till the 1950s as the sediments could move uninterrupted in the alongshore as well as cross-shore directions both in the surf zone and in the innershelf. In an open system, even if there is an intake of sediment at one location, the stability of the coast will not be affected as long as the intake is within the sustainable limit. However, the coastal engineering interventions along this coast, starting with construction of breakwaters (training walls) for the Neendakara harbour during 1982-88 and the Kayamkulam harbor during 2001-05, have compartmentalized this coast and made it a sediment sub-cell (van Rijn, 1997a). The long breakwaters jutting out into the offshore have restricted the surf zone longshore sediment transport within this cell and modified the shoreline morphology with accretion immediately south of the breakwater and erosion north of it. Similar observations have been made by Vaselali and Azarmsa (2009) for Pozm Bay coast, Iran and Noujas et al. (2014) southern Kerala coast, India. The southern Neendakara - Kovilthottam sector became starved of sediments and to stabilize this coast seawalls were constructed and are well maintained. The severe erosion in the northern sector in the 1980s and 1990s (see Table 6.3) has been defused to some extent by the accretion due to the breakwater at the Kayamkulam inlet. The construction of 26 groins during the period 2009-15 to protect individual stretches of the coast also had its impact on the morphology as observed by some researchers (Guimaraes et al., 2016; Mohanty et al., 2012). The satellite images (Google image) of the old and newly constructed groins near to

Kayamkulam inlet and further south of the inlet are shown in Figs. 6.23 & 6.24 respectively. The short-term erosion/accretion scenario presented in Figs. 6.4 & 6.5 for the station NK-5 is a classic example of the impacts of such ill-conceived shore protection measures.

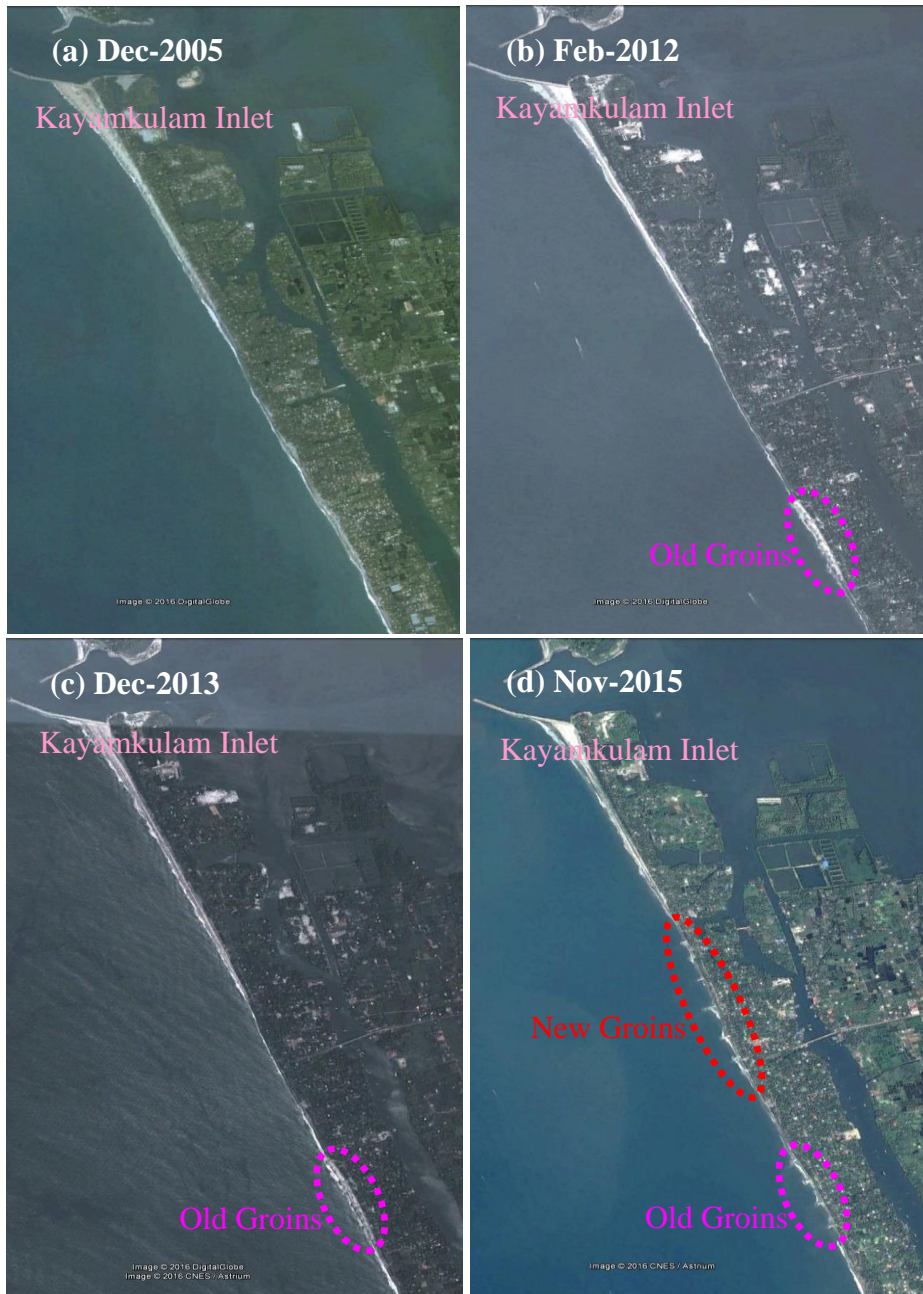


Fig. 6.23 Google images of the coastal sector immediately south of Kayamkulam inlet: (a) 2005, (b) 2012, (c) 2013 and (d) 2015. The old and new groins constructed along the coastal stretch is marked in the figure

For the years 2011, 2012, 2013 and 2014 the onshore transport is quite sizable and comparable with a cumulative value in the range of 60 - 65 m³/m. However after the

monsoon of 2014, the beach build-up during the post-monsoon period is reduced. In the fair weather period of 2015 the situation has become all the more precarious with absolutely no build-up. From a look at the physiographic set up it can be seen that a groin was built about 100 m south of this location after 2013. Starvation of this beach of sediments could be due to this groin which has obstructed the northerly longshore transport. The construction of such shore protection measures without due impact assessment will lead to creation of critically eroding zones in an already sediment starved beach environment.



Fig. 6.24 Google images of the north central sector of Chavara coast: (a) 2005, no groins are available; (b) 2012, no groins are available; (c) 2013, a groin field of 4 nos. is seen and (d) 2015, another groin field consisting of 7groins is added

6.8 Summary

A study of the short- and long-term morphological changes of the beach-innershelf system of the Chavara coast using multi-dated maps/images/data for the period of 1968-2015 indicates an overall retreat of the shoreline and relative deepening of the innershelf. During the period of 1968-2015, the shoreline retreat has been quite alarming at the mining sites with a staggering figure of nearly 400 m at the Ponmana mining site. While the build-up of the beach due to the effect of breakwater at the Kayamkulam inlet has neutralized to some extent the high erosion in the northernmost sector, the shoreline south of the mining site has not undergone significant changes due to the presence of well-maintained seawalls. Study of the beach profile data using the EOF analysis and volume change computations for the period 2010-2014 for the northern sector of the coast where beaches are present indicates the increasing erosive tendency of the beach towards the latter period. The deepening of the innershelf is more pronounced in the shallower portions upto a depth of 10 m. The observed changes in the beach-innershelf morphology can be mainly attributed to the intensified mining of the beach by the two public sector companies. The December 2004 Tsunami onslaught which resulted in the transport of a sizable quantity heavy mineral-rich innershelf sediments to the hinterland areas has also contributed to the deepening of the shelf. The construction of structures like breakwaters, groins and seawalls is another contributing factor to the morphological changes. The LITLINE model which was calibrated and validated for the coast using the shoreline data for different years has been used to simulate the shoreline changes till 2022. The simulations show that the caving in at the mining sites will aggravate further in the coming years. The intake of beach sediments by the two public sector firms has to be regulated to sustainable levels in order to minimize the negative impacts of sand mining. Introduction of any hard structure on this coast should be based on comprehensive scientific studies and impact analysis followed by systematic post-construction monitoring.

CHAPTER 7

SUMMARY, CONCLUSIONS AND RECOMMENDATIONS

7.1 Summary

The Chavara coast of 22 km length located along the southwest coast of India, extending from the Neendakara inlet in the south to the Kayamkulam inlet in the north, is well known for its rich Heavy Mineral (HM) deposits, also called as black sand deposits. Since 1930, the Indian Rare Earths Ltd. (IREL) and its predecessor companies have been engaged in beach sand mining along the Chavara coast for the extraction of heavy minerals. In 2000, the Kerala Minerals and Metals Ltd. (KMML), another Public Sector Undertaking situated at Chavara which was also engaged in beach sand extraction, entered the scene with large-scale mining of beach sand. As per the available data, the mining of beach sand by both these firms together is much beyond the annual replenishment by the hydrodynamic forces. Replenishment of these resources by the hydrodynamic processes is essential for maintaining the stability of the coast as well as for sustenance of mining. Depletion of heavy minerals in the beach sediments has been reported by the industries in the recent years. In addition, severe erosion and caving in of the beach at the mining sites have also been reported. The reported depletion of HM content in the beach sediments and the drastic beach morphological changes offered an interesting and important topic which has remarkable societal implications for this research under the Ph.D. programme.

The investigation carried out during 2010-2016 has been taken up with the following aim and objectives:

- Study the sediment dynamics and beach processes of the Neendakara-Kayamkulam coast through field observations and numerical modelling techniques
- Estimate the short- and long-term morphological changes in the beach and innershelf using multi-date data
- Estimate the short- and long-term changes in the heavy mineral content of the beach and innershelf sediments

- Decipher the beach-innershelf morphological changes and heavy mineral depletion with reference to the hydrodynamics and other forcing factors

As part of the investigation, an extensive review of literature that was intended to give the status of research in the topic of research was carried out. The literature study was confined to 4 themes encompassing the topic of research viz. coastal hydrodynamics, nearshore sediment transport, beach placers and beach-innershelf morphological changes. In addition to getting to know the emerging trend in research, both in the global as well as national scenario, the review has helped in fine tuning the methodology adopted for the work. The status of our knowledge on the topic of research and the lacuna relevant for the SW coast of India was summarized based on the literature review. It is found from the review that there are several studies on estimation of Longshore Sediment Transport (LST) for the surf zone of different coastal locations of the country using bulk formulas, but estimates using processes based numerical models are lacking. Computation of cross-shore sediment transport is rather scanty for the Indian coastline. Numerical modelling is emerging as an important tool in the country for analyzing and studying sediment dynamics in the coastal zone. The local wind data are not being incorporated in the models which is crucial while doing the numerical modelling of nearshore processes. Fine grid bathymetry also is critical in getting the desired accuracy in simulations using numerical models. Studies on erosion/accretion scenario of different locations of the coastline are several, but integration of the results of such studies with the sediment transport regime through numerical modelling is scarce. The studies point to the occurrence of erosion at many coastal locations which hitherto were stable and the role of anthropogenic factors as causative factors in such cases is quite evident.

A comprehensive field measurement and data collation programme taking care of the requirements of the study including numerical modelling was meticulously planned and implemented during the period 2010-2015. Beach profiling, bathymetric survey and sedimentological investigations which are essential to confirm the reported beach morphological changes and depletion in HM concentration were initiated in 2010 itself. Monthly beach profiles at selected stations and GPS based shoreline survey were conducted during the period 2010-2015 to study the beach morphological changes. Seasonal surficial sediment sampling from the beach and nearshore, suspended sediment sampling from two stations in the nearshore and one-time sub-

surface core sampling from selected stations in the innershelf were systematically carried out during 2010-2011. Bathymetric survey was carried out in the month of April 2010 in the innershelf of Chavara coast along transects at 1 km interval and extending up to 20 m depth. The bathymetric chart prepared out of this survey was used in conjunction with bathymetric data collected by the Centre for Earth Science Studies (CESS) for the years 2000 and 2005 to understand the innershelf morphological changes over the 10 year period. Year round wave data for 2014, which is the most important one as far as the sediment transport computations and numerical modelling studies are concerned, were acquired through a wave rider buoy deployed at 22 m water depth off Ponmana, located in the central Chavara coast. Synchronous with the wave data, wind was also measured by using an automatic weather station installed at the beach. Monthly littoral environmental observations which include the measurement of longshore current, breaker wave and beach characteristics were also carried out at selected coastal locations during 2014. Further, hydrodynamic data analysis, analysis of the sediment samples, empirical orthogonal function analysis for the beach profiles, geo-spatial analysis for the beach-innershelf morphological changes and numerical modelling studies were carried out in the laboratory.

A study of the nearshore sediment transport regime of the Chavara coast has been carried out combining field measurements with computations using different mathematical formulations. The LST in the surf zone was computed by using both bulk formulae (CERC and Kamphuis) and process-based numerical model (LITDRIFT). The longshore (3-10 m depth excluding surf zone) and cross-shore sediment fluxes in the innershelf were estimated using the validated LITDRIFT and LITPROF modules of LITPACK modelling system respectively. The model results indicate dominance of annual onshore transport over offshore transport. The longshore transport in the surf zone is northerly while it is consistently southerly in the innershelf. The two counter-directional pathways are linked through the cross-shore transport. The domination of the computed onshore flux is actually not reflected in the observed beach volume change, probably due to the influence of excessive sand mining by the industries. The actual quantity of sand available for onshore transport could be reduced due to the mining. This reduction in the replenishment of sand from

offshore will affect the stability of the coast with a net offshore transport instead of a net onshore transport computed by the model.

A study of the sedimentology and mineralogy of the beach and innershelf sediments of the Chavara coast and the Arattupuzha sector north of it has been undertaken to understand the present status of HM distribution in the beach and innershelf sediments, to delineate the long-term trend in the HM distribution and to understand the mechanisms that drive these changes. The study establishes the contrasting pattern spatially in the long-term changes in the HM concentration. While there is depletion in the HM concentration in the beaches of the Chavara coast after 2000, the Arattupuzha sector north of Chavara coast shows an increasing trend during the study period. The innershelf records reduction in the HM concentration in both the sectors, but the change is relatively less in the Arattupuzha sector. The 2004 Tsunami brought down the HM concentration to as low as 2 % in the Chavara innershelf, but the impact was relatively less in the Arattupuzha innershelf. The observed long-term changes are attributed mainly to the unsustainable mining by the Public Sector Undertakings (PSUs). The construction of two breakwaters at Kayamkulam inlet and the onslaught of the 2004 Tsunami are the other two contributing factors. The extraction of huge quantities of beach sediments much beyond the sustainable limits reduces the level of sea bed and the quantum of sediment available in the innershelf for reworking by the hydrodynamic processes. With the construction of two breakwaters at Kayamkulam inlet, the Neendakara-Kayamkulam sector of the coast has become compartmentalized, thereby curtailing the sediment input from the adjoining coastal sectors. The 2004 Tsunami also had a devastating effect on this coast and the innershelf was deprived of a huge quantum of HM by the selective onshore transport of HM by the tsunami. It is quite possible that the Chavara coast may cease to be a commercially viable beach extraction site in a few decades if the sand extraction is continued at the present level. The beaches in the Arattupuzha sector in the north may continue to record high concentrations of HM due to the erosion of the barrier beach rich in HM content.

A study of the short- and long-term morphological changes of the beach-innershelf system of the Chavara coast using multi-dated maps/images/data for the period of 1968-2015 indicates an overall retreat of the shoreline and relative deepening of the innershelf. Simulation of the shoreline evolution using the LITLINE module of

LITPACK corroborates the observed retreat of the shoreline. The shoreline retreat has been quite alarming in the mining sites with a staggering figure of nearly 400 m at the Ponmana mining site during the period of 1968-2015. While the build-up of the beach due to the effect of breakwater at the Kayamkulam inlet has neutralized to some extent the high erosion in the northernmost sector, the shoreline south of the mining site has not undergone significant changes due to the presence of well-maintained seawalls. Study of the beach profile data using the Empirical Orthogonal Function (EOF) analysis and volume change computations for the period 2010-2014 for the northern sector of the coast where beaches are present indicates the increasing erosive tendency of the beach towards the end of the period. The deepening of the innershelf is noticed in general, and is more pronounced in the shallower portions up to a depth of 10 m. The observed changes in the beach-innershelf morphology can be mainly attributed to the intensified mining of the beach by the two public sector companies. The December 2004 Tsunami onslaught which resulted in the transport of a sizable quantity of innershelf sediments to the hinterland areas also has played some role. The construction of structures like breakwaters, groins and seawalls is another contributing factor to the morphological changes. Simulations using the LITLINE model show that the caving in at the mining sites will aggravate further in the coming years.

7.2 Conclusions and Recommendations

The major conclusions and recommendations that emanate from the present investigation are:

- The nearshore sediment transport regime of a representative location of the Chavara coast comprises of:
 - Net northerly longshore sediment transport of 79,000 m³/year in the surf zone
 - Southerly longshore transport of 43,000 m³/year in the innershelf limited to 10 m depth; the direction is consistently southerly
 - Onshore transport of 77 m³/m/year
 - Offshore transport of 47 m³/m/year

- Domination of onshore flux as seen in the computations is not reflected in the yearly beach volume change, probably due to excessive sand mining
- Shoreline has retreated by as much as 260 m at Vellanathuruthu and nearly 400 m at Ponmana mining sites during the past 4 ½ decades
- An overall deepening of the innershelf is observed. The deepening is more pronounced off the mining sites where the 10 m isobath has advanced towards shore by 790 m and 690 m, and 20 m isobath by 610 m and 670 m off Ponmana and Vellanathuruthu respectively
- Depletion in the heavy mineral concentration in the beaches of the Chavara coast started after 2000
- The innershelf also shows considerable reduction in the heavy mineral concentration both in the surface as well as sub-surface sediments. Though the 2004 Tsunami brought down the surficial heavy mineral concentration to as low as 2 %, sorting processes during the subsequent period have raised the average innershelf concentration to 8 % in 2011
- Shoreline evolution model outputs show that the erosive tendency of the beach in general and the caving in at the mining sites will intensify in the coming years
- The main forcing factor for the beach-innershelf morphological changes and heavy mineral depletion is the mining by IREL and KMML. The 2004 Tsunami onslaught and construction of coastal structures are the other important contributing factors
- There is an urgent need to reduce the intake of sediments by the IREL and KMML to the sustainable mining volumes
- If the sand extraction is not limited to the sustainable mining limit, the Chavara coast may cease to be a commercially viable black sand extraction site in a few decades
- Introduction of hard structures without proper impact analysis has to be strictly curtailed

Coastal erosion is a serious problem faced by the coastal community. The Government is incurring huge expenditure towards coastal protection measures. Many

of the coastal protection and other coastal engineering projects like harbor development are being implemented without proper understanding of the coastal processes. Study of sediment dynamics, estimation of sediment budget and identification of the driving forces as done in the present study should be made mandatory for taking up coastal protection or other coastal engineering projects.

7.3 Recommendations for Future Research

Due to the increasing anthropogenic activities arising out of population pressure, resources exploitation and demand for infrastructural projects, the stability of the coastal zone in general is under threat. In order to solve coastal engineering problems, R & D efforts in the field of sediment dynamics modelling and sediment budgeting have to be further vigorously taken up, and the methodology fine-tuned using updated monitoring and numerical modelling techniques. The following up-gradations as regards observational and numerical modelling techniques are proposed for future studies.

- Measurement of nearshore wave characteristics: Measurement of wave characteristics at the breaker line will fetch reliable results for sediment transport computations
- Measurement of nearshore profiles: The fine tuning of the morphological model can be achieved by utilising measured monthly cross-shore profiles up to a depth of 15 m
- Deployment of Streamer traps for LST measurement: The usage of sediment traps such as Streamer traps that can be exclusively used in the surf zone for measurement of LST facilitates the calibration/validation of computed LST
- Installation of shore based video imaging system: Video cameras can be installed on the beach for round the clock imaging of the beach-nearshore system. Using appropriate software, the littoral environmental parameters like breaker wave height and angle, beach nearshore morphological changes, etc. can be derived
- Incorporation of wind in the cross-shore transport model: Wind influences cross-shore transport significantly. Wind has to be incorporated in the cross-shore transport model

- Utilization of processes based morphological models: Processes based morphological models such as CROSMOR, SBEACH, XBeach etc. can be utilised for simulating the cross-shore profiles

The incorporation of the above suggestions in the future research will greatly improve the accuracy of the computations / model outputs and thereby enhance the capability of the numerical models to resolve the issues faced by the coast.

REFERENCES

- Aagaard, T., 2014. Sediment supply to beaches: Cross-shore sand transport on the lower shoreface. *Journal of Geophysical Research: Earth Surface* 119, 913–926, doi: 10.1002/2013JF003041.
- Aagaard, T. and Greenwood, B., 1995. Longshore and cross-shore suspended sediment transport at far infragravity frequencies in a barred environment. *Continental Shelf Research* 15(10), 1235–1249.
- Aagaard, T., Black, K.P. and Greenwood, B., 2002. Cross-shore suspended sediment transport in the surf zone: a field-based parameterization. *Marine Geology* 185, 283–302.
- Aboobacker, V.M., Vethamony, P., Sudheesh, K. and Rupali, S.P., 2009. Spectral characteristics of the nearshore waves off Paradip, India during monsoon and extreme events. *Natural Hazards* 49(2), 311–323.
- Aboobacker, V.M., Rashmi, R., Vethamony, P. and Menon, H.B., 2011. On the dominance of pre-existing swells over wind seas along the west coast of India. *Continental Shelf Research* 31, 1701–1712.
- Ackers, P. and White, W.R., 1973. Sediment transport: new approach and analysis. *Journals of Hydraulics Division* 99(1), 2041–2060.
- Adegoke, J.O., Fageja, M., James, G., Agbaje, G. and Ologunorisa, T.E., 2010. An assessment of recent changes in the Niger Delta coastline using satellite imagery. *Journal of Sustainable Development* 3(4), 277–296, ISSN 1913-9063.
- Anctil, F. and Ouellet, Y., 1990. Preliminary evaluation of impacts of sand extraction near Iles-de-la-Madeleine Archipelago, Quhbec, Canada. *Journal of Coastal Research* 6(1), 37–51, ISSN 0749-0208.
- Angusamy, N., Loveson, V.J. and Rajamanickam, G.V. 2004. Zircon and ilmenite from the beach placers of southern coast of Tamil Nadu, east coast of India. *Indian Journal of Marine Sciences* 33(2), 138–149.
- Anooja, S., Padmalal, D., Maya, K., Vishnu Mohan, S. and Baburaj, B., 2013. Heavy mineral contents and provenance of late Quaternary sediments of southern Kerala, Southwest India. *Indian Journal of Geo-Marine Sciences* 42(6), 749–757.
- Anoop, T.R., Sanil Kumar, V. and Glejin, J., 2014. A study on reflection pattern of swells from the shoreline of peninsular India. *Natural Hazards* doi: 10.1007/s11069-014-1282-5.
- Anoop, T.R., Sanil Kumar, V., Shanas, P.R., Glejin, J. and Amrutha, M.M., 2016. Indian Ocean Dipole modulated wave climate of eastern Arabian Sea. *Ocean Science* 12, 1–10, doi: 10.5194/os-12-1-2016.
- Appendini, C.M., Salles, P., Mendoza, E.T., Lopez, J. and Torres-Freyermuth, A., 2012. Longshore sediment transport on the northern coast of the Yucatan Peninsula. *Journal of Coastal Research* 28(6), 1404–1417, ISSN 0749-0208.
- Aubrey, D.G., 1979. Seasonal patterns of onshore / offshore sediment movement. *Journal of Geophysical Research* 84, C10, 6347–6354.

- Baba, M., 1986. Computation of wave transmission over a shore protecting submerged breakwater. *Ocean Engineering* 13(3), 227–237.
- Baba, M., 1987. Wave power potential off the south-west Indian coast. *Energy* 12(6), 501–507.
- Baba, M. and Kurian N.P., 1988. Ocean waves and beach processes of southwest coast of India and their prediction. Centre for Earth Science Studies, Thiruvananthapuram, India, pp. 249.
- Baba, M., Harish, C.M. and Kurian, N.P., 1986. Influence of record length and sampling interval on ocean wave spectral estimates. *Mahasagar, Bulletin of National Institute of Oceanography* 19(2), pp. 79–85.
- Babu, K.S., Dwarakish, G.S. and Jayakumar, S., 2003. Modeling of sediment transport along Mangalore coast using Mike 21. *Proceedings of the International Conference on Coastal and Ocean Technology, December 10-12, 2003*, pp. 301–312.
- Bailard, J.A., 1981. An energetics total load sediment transport model for a plane sloping beach. *Journal of Geophysical Research* 86, 10938–10954.
- Bailard, J.A. and Inman, D.L., 1981. An energetics bedload model for plane sloping beach: local transport. *Journal of Geophysical Research* 86(C3), 2035–2043.
- Baptista, P., Cunha, T., Bernardes, C., Gama, C., Ferreira, O. and Dias, A., 2011. A precise and efficient methodology to analyse the shoreline displacement rate. *Journal of Coastal Research* 27(2), 223–232, ISSN 0749-0208.
- Baptista, P., Coelho, C., Pereira, C., Bernardes, C. and Veloso-Gomes F., 2014. Beach morphology and shoreline evolution: Monitoring and modelling medium-term responses (Portuguese NW coast study site). *Coastal Engineering* 84, 23–37.
- Baquerizo, A., Losada, M.A. and Losada, I.J., 2002. Edge wave scattering by a coastal structure. *Fluid Dynamics Research* 31, 275–287.
- Barbaro, G., Foti, G., Sicilia, L. and Malara, G., 2014. A formula for the calculation of the longshore sediment transport including spectral effects. *Journal of Coastal Research* 30(5), 961–966, ISSN 0749-0208.
- Barrie, J.V., 1980. Hydrodynamic factors controlling the distribution of heavy minerals (Bristol Channel). *Estuarine, Coastal and Shelf Science* 12, 609–619.
- Battjes, J.A., 1974. Surf similarity. *Coastal Engineering* 466–480, doi: 10.1061/9780872621138.029.
- Battjes, J.A. and Janssen, J.P.F.M., 1978. Energy loss and set-up due to breaking of random waves. *Coastal Engineering* 569–587, doi: 10.1061/9780872621909.034.
- Bayram, A., Larson, M., Miller, H.C. and Kraus, N.C., 2001. Cross-shore distribution of longshore sediment transport: comparison between predictive formulas and field measurements. *Coastal Engineering* 44, 79–99.
- Bayram, A., Larson, M. and Hanson, H., 2007. A new formula for the total longshore sediment transport rate. *Coastal Engineering* 54, 700–710.
- Benedet, L., Finkl, C.W., Campbell, T. and Kleing, A., 2004. Predicting the effect of beach nourishment and cross-shore sediment variation on beach morphodynamic assessment. *Coastal Engineering* 51, 839–861.

- Best, J.L. and Brayshaw, A.C., 1985. Flow separation-a physical process for the concentration of heavy minerals within alluvial channels. *Journal of Geological Society of London* 142, 747–755.
- Bijker, E.W., 1967. Some considerations about scales for coastal models with movable bed. Delft Hydraulics Laboratory, Publication 50, Delft, The Netherlands, pp. 142.
- Birben, A.R., Ozolcer, I.H., Karasu, S. and Komurcu, M.I., 2007. Investigation of the effects of offshore breakwater parameters on sediment accumulation. *Ocean Engineering* 34, 284–302.
- Biria, H.A., Neshaei, M.A.L., Ghabraei, A. and Mehrdad, M.A., 2014. Investigation of sediment transport pattern and beach morphology in the vicinity of submerged groin (case study: Dahane Sar Sefidrood). *Frontiers of Structural and Civil Engineering*, doi: 10.1007/s11709-014-0275-5.
- Black, K.P., 2001. Artificial surfing reefs for erosion control and amenity: Theory and application. *Journal of Coastal Research Special Issue* 34, 1–14, ISSN 0749-0208.
- Black, K.P. and Baba, M., 2001. Developing management plan for Ashtamudi estuary, Kollam, India. ASR Limited, Marine and Freshwater Consultant, Hamilton, New Zealand, pp. 546.
- Black, K.P., Kurian, N.P., Mathew, J. and Baba, M., 2008. Open coast monsoonal beach dynamics. *Journal of Coastal Research* 24(1), 1–12, doi: 10.2112/04-0289.
- Bruce, J.G., Johnson, D.R. and Kindle, J.C., 1998. Evidence of eddy formation in the eastern Arabian Sea during the northeast monsoon. *Journal of Geophysical Research* 99, 7651–7664.
- Bruun, P., 1954. Coast erosion and the development of beach profiles. Beach Erosion Board Technical Memorandum, 44, U.S. Army Engineer Waterways Experiment Station, Coastal Engineering Research Centre, Vicksburg, MS.
- Callaghan, D.P., Nielsen, P., Short, A. and Ranasinghe, R., 2008. Statistical simulation of wave climate and extreme beach erosion. *Coastal Engineering* 55, 375–390.
- Cartier, A. and Hequette, A., 2011. Variation in longshore sediment transport under low to moderate conditions on barred macrotidal beaches. *Journal of Coastal Research Special Issue* 64, 45–49, ISSN 0749-0208.
- Carver, R.E., 1971. Procedures in sedimentary petrology. Wiley-Interscience, New York, pp. 653.
- Cavaleri, L. and Rizzoli, P.M., 1981. Wind wave prediction in shallow water: Theory and Applications. *Journal of Geophysical Research* 86(C11), 10961–10973.
- Caviglia, F.J., 1994. Computation of longshore currents and sediment transport. *Computers and Geosciences* 20(6), 905–917.
- CEM, 2002. Coastal Engineering Manual. U.S. Army Corps of Engineers, Engineer Manual 1110-2-1100. Washington D.C.
- Chandramohan, P. and Rao, R.P., 1986. Mathematical prediction of long term shoreline changes at Visakhapatnam. *The Institution of Engineers (India)* 66 (Part CI 3&4), pp. 121–128.

- Chandramohan, P. and Nayak, B.U., 1991. Longshore sediment transport along the Indian coast. *Indian Journal of Marine Sciences* 20, 110–114.
- Chandramohan, P. and Nayak, B.U., 1992. Longshore sediment transport model for the Indian west coast. *Journal of Coastal Research* 8(4), 775–787.
- Chandramohan, P., Nayak, B. and Raju V.S., 1990. Longshore transport model for south Indian and Srilankan coasts. *Journal of Waterway, Port, Coastal and Ocean Engineering-ASCE* 116(4), 408–424, ISSN 0733-950X/90/0004-0408.
- Chandramohan, P., Sanil Kumar, V. and Nayak, B.U., 1991. Wave statistics around the Indian coast based on ship observed data. *Indian Journal of Marine Sciences* 20, 87–92.
- Chandramohan, P., Sanil Kumar, V., Nayak, B.U. and Pathak, K.C., 1993a. Variation of longshore current and sediment transport along the south Maharashtra coast, West coast of India. *Indian Journal of Marine Sciences* 22, 115–118.
- Chandramohan, P., Sanil Kumar, V. and Nayak, B.U. 1993b. Coastal processes along the shorefront of Chilka lake, east coast of India. *Indian Journal of Marine Sciences* 22, 268–272.
- Chandramohan, P., Nayak, B.U. and Sanil Kumar, V., 1994. Numerical modelling of nearshore wave transformation. *Ocean Technology: Perspectives*, pp. 389–399.
- Chandramohan, P., Jena, B.K. and Sanil Kumar, V., 2001. Littoral drift sources and sinks along the Indian coast. *Current Science* 81, 292–297.
- Chandrasekar, N., Saravanan, S., Cherian, A., Loveson, J.I., Rajamanickam, M. and Rajamanickam, G.V., 2010. Features sustaining the formation of beach placers along the southern east coast of India. *Marine Georesources and Geotechnology* 28, 240–249, doi: 10.1080/1064119X.2010.483782.
- Chandrasekar, N., Joevieviek, V. and Saravanan, S., 2013. Coastal vulnerability and shoreline changes for southern tip of India - remote sensing and GIS approach. *Journal of Earth Science and Climate Change* 4(144), doi: 10.4172/2157-7617.1000144.
- Chaudry, M.A., Memon, M.Q. and Danish, M., 2002. Heavy minerals concentration along the Baluchistan Coast, Pakistan from Gadani to Phornala. *Marine Georesources and Geotechnology* 20, 73–83.
- Chen, Q., Kirby, J.T., Dalrymple, R.A., Shi, F. and Thornton, E.B., 2003. Boussinesq modeling of longshore currents. *Journal of Geophysical Research* 108(C11), 3362, doi: 10.1029/2002JC001308.
- Cuadrado, D.G., Gomez, E.A. and Ginsberg, S.S., 2005. Tidal and longshore sediment transport associated to a coastal structure. *Estuarine, Coastal and Shelf Science* 62, 291–300.
- Darsan, J. and Alexis, C., 2014. The impact of makeshift sandbag groins on coastal geomorphology: A case study at Columbus Bay, Trinidad. *Environment and Natural Resources Research* 4(1), 94–116, ISSN 1927-0488.
- Datawell, 2009. Wave rider reference manual, DWR-MkIII. Datawell BV Oceanographic Instruments, The Netherlands.

- Dattatri, J., Raman, H. and Jothi Sankilr, N., 1979. Height and period distribution for waves off Mangalore harbour-west coast. *Journal of Geophysical Research* 84, 3767–3772.
- Davidson, M.A., Lewis, R.P. and Turner, I.L., 2010. Forecasting seasonal to multi-year shoreline change. *Coastal Engineering* 57, 620–629.
- Dean, R.G., 1973. Heuristic models of sand transport in the surf zone. *Proceedings Conference in the Engineering Dynamics in the Surf Zone*. Institution of Engineers, Sydney, Australia, pp. 208–214.
- Dean, R.G., 1977. Equilibrium beach profiles: U.S. Atlantic and Gulf Coasts. Department of Civil Engineering, Ocean Engineering Report No. 12, University of Delaware.
- Dean and Dalrymple, 2001. *Coastal processes with engineering applications*. Cambridge University Press, Cambridge, pp. 43, ISBN 0-511-03791-0.
- Deigaard, R., Fredsoe, J. and Hedegaard, I.B., 1986. Mathematical model for littoral drift. *Journal of Waterway, Port, Coastal and Ocean Engineering* 112(3), 351–369, ISSN 0733-950X/86/0003-0351.
- Delft Hydraulics, 1993. Yearly averaged sediment transport along the Dutch shore: Upgrading of UNIBEST-TC. Report H2129.
- DHI, 2004. Danish Hydraulic Institute. User manual and reference guide for MIKE21 and LITPACK modules. Danish Hydraulic Institute, Horsholm, Denmark.
- DHI, 2007. Danish Hydraulic Institute. MIKE C-MAP. User guide for the extraction of world wide bathymetry data and tidal information. Danish Hydraulic Institute, Horsholm, Denmark.
- DHI, 2008. Danish Hydraulic Institute. LITPROF User Guide. Danish Hydraulic Institute, Horsholm, Denmark.
- Dinesh Kumar, P.K., Manimurali R., Babu, M.T., Sudheesh, K., Vethamony, P. and Naveen Kumar, K.R., 2014. What drives nearshore sediment transport controls on the depletion of beach placers at Manavalakurichi, Southwest Coast of India? *Physical Geography* 35(5), 411–428.
- Diwan, S.G., Suryavaunshi, A.K. and Nayak, B.U., 1985. NIO's experience in Datawell wave rider buoys. *Proceedings of 1st National Conference on Dock and Harbour Engineering, Bombay*, 2, pp. E143–156.
- Eckart, C., 1952. The propagation of gravity waves from deep to shallow water. *National Bureau of Standards Circular* 521, Washington D.C., pp. 165–173.
- Elfrink, B. and Baldock, T., 2002. Hydrodynamics and sediment transport in the swash zone: A review and perspectives. *Coastal Engineering* 45, 149–167.
- Elmoustapha, A.O., Levoy, F., Monfort, O. and Koutitonsky, V.G., 2007. A numerical forecast of shoreline evolution after harbour construction in Nouakchott, Mauritania. *Journal of Coastal Research* 23(6), 1409–1417, ISSN 0749-0208.
- Elsayed, M.A.K. and Mahmoud, S.M., 2007. Groins system for shoreline stabilization on the east side of the Rosetta promontory, Nile Delta coast. *Journal of Coastal Research* 23(2), 380–387, ISSN 0749-0208.

- Elsayed, M.A.K., Younan, N.A., Fanos, A.M. and Baghdady, K.H., 2005. Accretion and erosion patterns along Rosetta Promontory, Nile Delta coast. *Journal of Coastal Research* 21(3), 412–420, ISSN 0749-0208.
- Engelund, F. and Hansen, E., 1967. A monograph on sediment transport in alluvial streams. Teknisk Forlag, Copenhagen, Denmark, pp. 63.
- Esteves, L.S., Williams, J.J., Lisniowski, M.A., 2009. Measuring and modelling longshore sediment transport. *Estuarine, Coastal and Shelf Science* 83, 47–59. doi: 10.1016/j.ecss.2009.03.020.
- Farris, A.S. and List, J.H., 2007. Shoreline change as a proxy for sub-aerial beach volume change. *Journal of Coastal Research* 23(3), 740–748, ISSN 0749-0208.
- Folk, R.L., 1980. Petrology of sedimentary rocks. Austin, Texas, U.S.A. Hemphill Publishing Co., 2nd Edition, pp. 184.
- Folk, R.L. and Ward, W.C., 1957. Brazos river bar: A study in the significance of grain size parameters. *Journal of Sedimentary Petrology* 27, 3–26.
- Fredsoe, J., 1984. The turbulent boundary layer in combined wave-current motion. *Journal of Hydraulic Engineering-ASCE* 110(HY8), 1103–1120.
- Fredsoe, J., Andersen, O.H. and Silberg, S., 1985. Distribution of suspended sediment in large waves. *Journal of Waterway, Port, Coastal and Ocean Engineering* 111(6), 1041–1059, ISSN 0733-950X/85/0006-1041.
- Frihy, O.E., 1988. Nile delta shoreline changes: Aerial photographic study of a 28-year period. *Journal of Coastal Research* 4(4), 597–606, ISSN 0749-0208.
- Frihy, O.E. and Komar, P.D., 1993. Long-term shoreline changes and the concentration of heavy minerals in beach sands of the Nile Delta, Egypt. *Marine Geology* 115, 253–261.
- Frihy, O.E., Nasr, S.M., Ahmed, M.H. and Raey, M., 1990. Temporal shoreline and bottom changes of the inner continental shelf off the Nile Delta, Egypt. *Journal of Coastal Research* 7(2), 465–475, ISSN 0749-0208.
- Frihy, O.E., Lotfy, M.F. and Komar, P.D., 1995. Spatial variations in heavy minerals and patterns of sediment sorting along the Nile Delta. *Egypt Sedimentary Geology* 97, 33–41.
- Galvin, C.J. Jr., 1963. Longshore currents on a laboratory beach. Ph.D. Thesis, Massachusetts Institute of Technology at Cambridge, Massachusetts.
- Galvin, C.J. Jr., 1968. Breaker type classification on three laboratory beaches. *Journal of Geophysical Research* 73, 3651–3659.
- Galvin, C.J. Jr., 1987. The continuity equation for longshore current velocity with breaker angle adjusted for wave-current interactions. *Coastal Engineering* 11, 115–129.
- Glejin, J., Sanil Kumar, V., Balakrishnan Nair, T.M. and Singh, J., 2013a. Influence of winds on temporally varying short and long period gravity waves in the near shore regions of the eastern Arabian Sea. *Ocean Science* 9, 1–11, doi: 10.5194/os-9-1-2013.

- Glejin, J., Sanil Kumar, V., Balakrishnan Nair, T.M., Singh, J. and Mehra, P., 2013b. Observational evidence of summer shamal swells along the west coast of India. *Journal of Atmospheric and Ocean Technology* 30, 379–388.
- Goda, Y., 1970. Numerical experiments on wave statistics with spectral simulation. Report of Research Institute of Port and Harbour, Japan, 9, pp. 3–57.
- Goda, Y., 1991. Longshore current generation by directional random waves in a planar beach. Proceedings of XXIXth IAHR Congress, Madrid, Spain, pp. B223–B230.
- Gowthaman, R., Sanil Kumar, V., Dwarakish, G.S., Shanas, P.R., Jena, B.K. and Jai Singh, 2015. Nearshore waves and longshore sediment transport along Rameshwaram Island off the east coast of India. *International Journal of Naval Architecture and Ocean Engineering* 7, 939–950, ISSN 2092-6782.
- Grace, R.A., 1976. Near bottom water motion under ocean waves. Proceedings of the 15th Coastal Engineering Conference, Honolulu, Hawaii, pp. 2371–2386.
- GSI, 1994. Geological Survey of India, Marine Wing. Report on detailed exploration for heavy mineral placer deposit off Chavara, Kerala (Southern Block). pp. 2–94.
- GSI, 1997. Geological Survey of India. Marine Wing. Report on detailed exploration for heavy mineral placer deposit off Chavara, Kerala (Northern Block). pp. 2–40.
- Guimaraes, A., Lima, M., Coelho, C., Silva, R. and Veloso-Gomes, F., 2016. Groin impacts on updrift morphology: Physical and numerical study. *Coastal Engineering* 109, 63–75.
- Gujar, A.R., Ambre, N.V., Mislankar, P.G. and Iyer, S.D., 2010. Ilmenite, magnetite and chromite beach placers from south Maharashtra, central west coast of India. *Resource Geology* 60(1), 71–86, doi: 10.1111/j.1751-3928.2010.00115.x.
- Gujar, A.R., Ganesan, P., Iyer, S.D., Gaonkar, S.S., Ambre, N.V., Loveson, V.J. and Mislankar, P.G., 2011. Influence of morphodynamic variability over seasonal beach sediments and its probable effect on coastal development. *Ocean and Coastal Management* 54, 514–523, doi:10.1016/j.ocecoaman.2011.03.007.
- Guza, R.T. and Thornton, E.B., 1985. Observations of surf beat. *Journal of Geophysical Research* 90, 3161–3172.
- Hallermeier, R.J., 1981. A profile zonation for seasonal sand beaches from wave climate. *Coastal Engineering* 4, 253–277.
- Hameed, T.S.S., 1988. Wave climatology and littoral processes at Alleppey. In: Baba, M. and Kurian, N.P. (Eds.), *Ocean waves and beach processes of south-west coast of India and their prediction*. Centre for Earth Science Studies, Thiruvananthapuram, India, December 1988, pp. 67–90.
- Hameed, T.S.S., 1989. Spectral and statistical characteristics of shoaling waves off Alleppey west coast of India. Ph.D. Thesis, Cochin University of Science and Technology, Cochin, Kerala, India, pp. 209.
- Hameed, T.S.S., Unpublished. FORTRAN programme for the computation of beach volume from the beach profiles. Centre for Earth Science Studies, Thiruvananthapuram, India.
- Hameed, T.S.S., Baba, M. and Thomas, K.V., 1986. Computation of longshore currents. *Indian Journal of Marine Sciences* 15, 92–95.

- Hameed, T.S.S., Kurian, N.P., Thomas, K.V., Rajith, K. and Prakash, T.N., 2007. Wave and current regime off the southwest coast of India. *Journal of Coastal Research* 23(5), 1167–1174.
- Hanamgond, P.T. and Chavadi, V.C., 1993. Sediment movement on Aligadde Beach, Uttara Kannada District, west coast of India. *Journal of Coastal Research* 9(3), 847–861, ISSN 0749-0208.
- Hanamgond, P.T. and Mitra, D., 2007. Dynamics of the Karwar coast, India, with special reference to study of tectonics and coastal evolution using remote sensing data. *Journal of Coastal Research Special Issue* 50, 842–847, ISSN 0749.0208.
- Hanson, H. and Kraus, N.C., 1991. Numerical simulation of shoreline change at Lorain, Ohio. *Journal of Waterway Port Coastal and Ocean Engineering* 117, 1–18.
- Hanson, H. and Kraus, N.C., 2011. Long-term evolution of a long-term evolution model. *Journal of Coastal Research, Special Issue* 59, 118–129, doi: 10.2112/SI59-012.1, ISSN 0749-0208.
- Hanson, H., Larson, M. and Kraus, N.C., 2010. Calculation of beach change under interacting cross-shore and longshore processes. *Coastal Engineering* 57, 610–619.
- Harish, C.M., 1988. Waves and related nearshore processes in a complex bay at Tellicherry. In: Baba, M. and Kurian, N.P. (Eds.), *Ocean waves and beach processes of south-west coast of India and their prediction*. Centre for Earth Science Studies, Thiruvananthapuram, India, December 1988, pp. 111–127.
- Hasselmann, K., 1974. On the spectral dissipation of ocean waves due to white capping. *Boundary-Layer Meteorology* 6, 107–127.
- Hegde, V.S., Shalini, G. and Kanchanagouri, D.G., 2006. Provenance of heavy minerals with special reference to ilmenite of the Honnavar beach, central west coast of India. *Current Science* 91(5), 644–648.
- Hegde, V.S., Shalini, G., Nayak, S.R., Rajawat, A.S., Suryanarayana, A., Jaykumar, S., Koti, B.K. and Girish, G.K., 2009. Low-scale foreshore morphodynamic processes in the vicinity of a tropical estuary at Honnavar, central west coast of India. *Journal of Coastal Research* 25(2), 305–314, ISSN 0749-0208.
- Hema Malini, B. and Rao, N.K., 2004. Coastal erosion and habitat loss along the Godavari delta front – a fallout of dam construction (?) *Current Science* 87(9), 1232–1236.
- Hilton, M.S. and Hesp, P., 1996. Determining the limits of beach-nearshore sand systems and the impact of offshore coastal sand mining. *Journal of Coastal Research* 12(2), 496–519, ISSN 0749-0208.
- Holthuijsen, L.H., 2007. *Waves in oceanic and coastal waters*. Cambridge University Press, New York, U.S.A. pp. 387, ISBN 13 978-0-511-27021-5.
- Horikawa, K., 1988. *Nearshore dynamics and coastal processes: Theory, measurement, and predictive models*. University of Tokyo Press, Tokyo. pp. 522, ISBN 0-86008-418-3.

- Hume, T.M., Bell, R.G., Black, K.P., Healy, T.R. and Nichol, S.L., 1999. Mangawhai-Pakiri sand study. Final Report. Sand movement and storage and nearshore sand extraction in the Mangawhai-Pakiri embayment. NIWA Client Report ARC 60201/10 prepared for the Working Party, Mangawhai-Pakiri Sand Study, ARC Environment, Auckland Regional Council, New Zealand.
- Huntley, D.A. and Hanes, D.M., 1987. Direct measurement of suspended sediment transport. *Proceedings Coastal Sediment '87*, New Orleans, pp. 723–737.
- Hwang, P.A., Ocampo-Torres, F.J. and Garcia-Nava, H., 2012. Wind sea and swell separation of 1D wave spectrum by a spectrum integration method. *Journal of Atmospheric and Oceanic Technology* 29, 116–128, doi: 10.1175/JTECH-D-11-00075.1.
- Ingram, R.L., 1971. Sieve analysis. In: Carver, R.E. (Ed.), *Procedures in sedimentary petrology*. Wiley Interscience, New York, pp. 49–68.
- IREL, 2010. Primary data provided by Indian Rare Earths Limited (IREL), Chavara. Kerala, India.
- Isla, F.I., 1991. Spatial and temporal distribution of beach heavy minerals: Mar Chiquita, Argentina. *Ocean and Shoreline Management* 16, 161–173.
- Jackson, N.L., 1999. Evaluation of criteria for predicting erosion and accretion on an estuarine sand beach, Delaware Bay, New Jersey. *Estuaries* 22(2A), 215–223.
- Jayakumar, S., Naik, K.A., Ramanamurthy, M.V., Ilangovan, D., Gowthaman, R. and Jena, B.K., 2008. Post-tsunami changes in the littoral environment along the southeast coast of India. *Journal of Environmental Management* 89, 35–44, doi:10.1016/j.jenvman.2007.01.050.
- Jayappa, K.S., 1996. Longshore sediment transport along the Mangalore coast, west coast of India. *Indian Journal of Marine Sciences* 25, 157–159.
- Jena, B.K. and Chandramohan, P. 1997. Sediment transport near the peninsular tip of India. *Proceedings of 2nd Indian National Conference on Harbour and Ocean Engineering (INCHOE-97)*, Thiruvananthapuram, India, pp. 1054–1060.
- Jeyar, M., Chaabelasri, E. and Salhi, N., 2015. Effect of coastal waves on hydrodynamics in one-inlet coastal Nador Lagoon, Morocco. *Modelling and Simulation in Engineering*, Hindawi Publishing Corporation, Article ID: 156967, 1–8, <http://dx.doi.org/10.1155/2015/156967>.
- Jignesh, K., Sarkar, A. and Raj Kumar, 2005. Determination of ocean wave period from altimeter data using wave-age concept. *Marine Geodesy* 28, 71–79, doi: 10.1080/01490410590884575.
- Johnson, H.K. and Kofoed-Hansen, H., 2000. Influence of bottom friction on sea surface roughness and its impact on shallow water wind wave modeling. *Journal of Physical Oceanography* 30, 1743–1756.
- Jose, F., 2000. Coastal hydrodynamics and sediment transport along SW coast of India with special reference to heavy sand. Unpublished Ph.D. Thesis. Cochin University of Science and Technology, pp. 207.

- Jose, F., Kurian, N.P. and Prakash, T.N., 1997. Longshore sediment transport along the southwest coast of India. Proceedings of 2nd Indian National Conference on Harbour and Ocean Engineering (INCHOE-97), Thiruvananthapuram, India, pp. 1047–1053.
- Jun Tang, Yong-Ming Shen and Lei Cui, 2008. Modeling nearshore currents induced by irregular breaking wave. *Journal of Coastal Research Special Issue* 52, 245–252, ISSN 0749-0208.
- Kaliraj, S., Chandrasekar, N. and Magesh, N.S., 2013. Evaluation of coastal erosion and accretion processes along the southwest coast of Kanyakumari, Tamil Nadu using geospatial techniques. *Arabian Journal of Geosciences* 8(1), doi: 10.1007/s12517-013-1216-7.
- Kamphuis, J.W., 1991. Alongshore sediment transport rate. *Journal of Waterway, Port, Coastal and Ocean Engineering-ASCE* 117, 624–640.
- Kamphuis, J.W., 2002. Alongshore transport of sand. Proceedings of the 28th International Conference on Coastal Engineering, American Society of Civil Engineers, Cardiff, Wales, pp. 2478–2490.
- Kamphuis, J.W., Davies M.H., Nairn, R.B. and Sayao, O.J., 1986. Calculation of littoral sand transport rate. *Coastal Engineering* 10, 1–21.
- Karambas, T.V., 2006. Prediction of sediment transport in the swash zone by using a nonlinear wave model. *Continental Shelf Research* 26(5), 599–609.
- Kelley, S.W., Ramsey, J.S. and Byrnes, M.R., 2004. Evaluating shoreline response to offshore sand mining for beach nourishment. *Journal of Coastal Research* 20(1), 89–100, ISSN 0749-0208.
- Kim, C.S. and Lim, H., 2009. Sediment dispersal and deposition due to sand mining in the coastal waters of Korea. *Continental Shelf Research* 29, 194–204.
- Kirby, J.T. and Dalrymple, R.A., 1994. Combined refraction/Diffraction Model, REF/DIF 1. Version 2.5. Documentation and User's Manual. Center for Applied Coastal Research, Department of Civil Engineering, University of Delaware, Newark 19716.
- Kobayashi, N. and Lawrence, A.R., 2004. Cross-shore sediment transport under breaking solitary waves. *Journal of Geophysical Research* 109, 1–13, C03047, doi: 10.1029/2003JC002084.
- Kokpinar, M.A., Darama, Y. and Guler, I., 2007. Physical and numerical modeling of shoreline evaluation of the Kizilirmak river mouth, Turkey. *Journal of Coastal Research* 23(2), 445–456, ISSN 0749-0208.
- Komen, G.J., Hasselmann, S. and Hasselmann, K., 1984. On the existence of a fully developed wind-sea spectrum. *Journal of Physical Oceanography* 14, 1271–1285.
- Komen, G.J., Cavaleri, L., Donelan, M., Hasselmann, K., Hasselmann, S. and Janssen, P.A.E.M., 1994. Dynamics and modelling of ocean waves. Cambridge University Press, pp. 532.
- Komar, P.D., 1976. Beach processes and sedimentation. Prentice Hall Inc., Englewood Cliffs, New Jersey, pp. 429.
- Komar, P.D., 1989. Physical processes of waves and currents and the formation of marine placers. *CRC Critical Reviews in Aquatic Sciences* 1(3), 393–423.

- Komar, P.D. and Inman, D.L., 1970. Longshore sand transport on beaches. *Journal of Geophysical Research* 75(30), 5914–5927.
- Komar, P.D. and Wang, C., 1984. Processes of selective grain transport and the formation of placers on beaches. *Journal of Geology* 92, 637–655.
- Koomans, R.L. and de Meijer, R.J., 2004. Density gradation in cross-shore sediment transport. *Coastal Engineering* 51, 1105–1115.
- Kraus, N.C. and Harikai, S., 1983. Numerical model of the shoreline change at Oarai Beach. *Coastal Engineering* 7(1), 1–28.
- Kroon, A., Larson, M., Moller, I., Yokoki, H., Rozynski, G., Cox, J. and Larroude, P., 2008. Statistical analysis of coastal morphological data sets over seasonal to decadal time scales. *Coastal Engineering* 55, 581–600.
- Kunte, P.D. and Wagle, B.G., 2000. Littoral transport studies along west coast of India - A review. *Indian Journal of Marine Sciences* 30, 57–64.
- Kurian, N.P., 1987. Wave height and spectral transformation in the shallow waters of Kerala coast and their prediction. Ph.D. Thesis, Cochin University of Science and Technology, Cochin, Kerala, India, pp. 150.
- Kurian, N.P., 1988. Waves and littoral processes at Calicut. In: Baba, M. and Kurian, N.P. (Eds.), *Ocean waves and beach processes of south-west coast of India and their prediction*. Centre for Earth Science Studies, Thiruvananthapuram, India, December 1988, pp. 91–110.
- Kurian, N.P., 1989. Shallow water wave transformation. In: Baba M. and Hameed, T.S.S. (Eds.), *Ocean wave studies and applications*, Centre for Earth Science Studies, Thiruvananthapuram, India, pp. 15–32.
- Kurian, N.P. and Baba, M., 1987. Wave attenuation due to bottom friction across the southwest Indian continental shelf. *Journal of Coastal Research* 3, 485–490.
- Kurian, N.P., Baba, M. and Hameed, T.S.S., 1985. Prediction of nearshore wave heights using a refraction programme. *Coastal Engineering* 9, 347–356.
- Kurian, N.P., Prakash, T.N., Jose, F. and Black, K.P., 2001. Hydrodynamic processes and heavy mineral deposits of the southwest coast, India. *Journal of Coastal Research Special Issue* 34, 154–163, ISSN 0749-0208.
- Kurian, N.P., Prakash, T.N., Thomas, K.V., Hameed, T.S.S., Chattopadhyay, S., Baba, M., Black, K.P. and Mathew, J., 2002. Heavy mineral budgeting and management at Chavara. Final report submitted to Indian Rare Earths Ltd. by Centre for Earth Science Studies, Thiruvananthapuram, India, Vol. 1 and 2, pp. 513.
- Kurian, N.P., Baba, M., Hameed, T.S.S., Thomas, K.V. and Harish, C.M., 2004. Hydrodynamics of the coastal waters of SW coast of India. *Earth System Science and Natural Resources Management Centre for Earth Science Studies Silver Jubilee Compendium*, pp. 181–199.
- Kurian, N.P., Rajith, K., Hameed, T.S.S. and Thomas, K.V., 2005. Currents in the innershelf off Chavara, south-west coast of India. *National Workshop on Oceanographic Features of the Indian Coastal Waters*, 6-7 October 2005, pp. 67–71.

- Kurian, N.P., Pillai, A.P., Rajith, K., Muralikrishnan, B.T. and Kalairasan, P., 2006a. Inundation characteristics and geomorphological impacts of December 2004 tsunami on Kerala coast. *Current Science* 90, 240–249.
- Kurian, N.P., Prakash, T.N., Baba, M. and Nirupama, N., 2006b. Observations of tsunami impact on the coast of Kerala, India. *Marine Geodesy* 29, 135–145, doi: 10.1080/01490410600748301.
- Kurian, N.P., Thomas, K.V., Hameed, T.S.S., Ramachandran, K.K., Sheela Nair, L., Subramanian, B.R., Ramana Murthy, M.V., Bhat, M., Rajan, E., Pillai, A.P., Kalaiarasan, P., Rajith, K., Murali Krishnan B.T., Indulekha K.P., Sreejith, C., Anil T., Asha V. and Shamji, V.R., 2007. Shoreline Management Plan for Munambam–Kayamkulam sector, south-west coast of India. Final Project Report Submitted to ICMAM Project Directorate, Ministry of Earth Sciences by Centre for Earth Science Studies, Thiruvananthapuram, pp. 188.
- Kurian, N.P., Rajith, K., Hameed, T.S.S., Sheela Nair, L., Ramana Murthy, M.V., Arjun, S. and Shamji, V.R., 2009. Wind waves and sediment transport regime off the south-central Kerala coast, India. *Natural Hazards* 49, 325–345, doi: 10.1007/s11069-008-9318-3.
- Kurian, N.P., Hameed, T.S.S., Prakash, T.N., Sheela Nair, L., Thomas, K.V., Reji S., Raju, D., Ajitkumar, M., Prasad, R., Sandeep, K.K. and Linikrishna, K.L., 2012. Study on depletion of heavy mineral content in the beach washings of IREL, Chavara. Final report submitted to Indian Rare Earths Ltd. by Centre for Earth Science Studies, Thiruvananthapuram, India, pp. 290.
- Kuriyama, Y. and Sakamoto, H., 2014. Cross-shore distribution of long-term average longshore sediment transport rate on a sandy beach exposed to waves with various directionalities. *Coastal Engineering* 86, 27–35.
- Larson, M. and Kraus, N.C., 1989. SBEACH: Numerical model for simulating storm-induced beach change. Report 1: Empirical foundation and model development. Technical Report No. CERC-89-9. Vicksburg, Mississippi: U.S. Army Engineer Waterways Experiment Station, U.S. Army Corps of Engineers.
- Larson, M. and Kraus, N.C., 1995. Prediction of cross-shore sediment transport at different spatial and temporal scales. *Marine Geology* 126, 111–127.
- Larson, M., Kraus, N.C. and Wise, R.A., 1999a. Equilibrium beach profiles under breaking and non-breaking waves. *Coastal Engineering* 36, 59–85.
- Larson, M., Hanson, H., Kraus, N.C. and Newe, J., 1999b. Short- and long-term responses of beach fills determined by EOF analysis. *Journal of Waterway, Port, Coastal, and Ocean Engineering* 125, 285–293.
- Lee, K.K., 1975. Longshore currents and sediment transport in west shore of Lake Michigan. *Water Resources Research* 11(6), 1029–1032.
- Li, M.Z. and Komar, P.D., 1992. Selective entrainment and transport of mixed size and density sands: flume experiments simulating the formation of black-sand placers. *Journal of Sedimentary Petrology* 62(4), 584–590.
- Liu, K.W., 1999. Nature and distribution of heavy minerals in the Natal Group, South Africa. Geological Society, London, Special Publications 163, 311–325, doi: 10.1144/GSL.SP.1999.163.01.24.

- Longuet-Higgins, M.S., 1970. Longshore currents generated by obliquely incident sea waves, 1 and 2. *Journal of Geophysical Research* 75(33), 6778–6801.
- Longuet-Higgins, M.S., 1975. On the joint distribution of the periods and amplitudes of sea waves. *Journal of Geophysical Research* 80(18), 2688–2693.
- Longuet-Higgins, M.S. and Stewart, R.W., 1964. Radiation stresses in water waves; a physical discussion, with applications. *Deep-Sea Research* 2, 529–562.
- Lopez-Ruiz, A., Ortega-Sanchez, M., Baquerizo, A. and Losada, M.A., 2012. Short and medium-term evolution of shoreline undulations on curvilinear coasts. *Geomorphology* 159-160, 189–200.
- Luepke, G. and Clifton, H.E., 1983. Heavy mineral distribution in modern and ancient bay deposits, Willapa Bay, Washington, U.S.A. *Sediment Geology* 35, 233–247.
- Mahalder, B. and Navera, U.K., 2010. Cross-shore sediment transport due to wave: a laboratory study. *Proceedings of MARTEC 2010, The International Conference on Marine Technology*, 11-12 December 2010, BUET, Dhaka, Bangladesh, pp. 341–346.
- Makota, V., Sallema, R. and Mahika, C., 2004. Monitoring shoreline change using remote sensing and GIS: A case study of Kunduchi area, Tanzania. *Western Indian Ocean Journal of Marine Science* 3(1), 1–10.
- Mallik, T.K., Samsuddin, M., Prakash, T.N., Vasudevan, V. and Terry Machado., 1987. Beach erosion and accretion-An example from Kerala, southwest coast of India. *Environmental Geology and Water Sciences* 10(2), 105–110.
- Manimurali, M., Shrivastava, D. and Vethamony, P., 2009. Monitoring shoreline environment of Paradip, east coast of India using remote sensing. *Current Science* 97(1), 79–83.
- Masria, A., Abdelaziz, K., Negm, A., 2015. Testing a combination of hard and soft measures to enhance the stability of Rosetta outlet. *Journal of Oceanography and Marine Research* 4, 138, doi: 10.4172/jomr.1000138.
- Masselink, G. and Hughes, M., 1998. Field investigation of sediment transport in the swash zone. *Continental Shelf Research* 18, 1179–1199.
- Masselink, G., Evans, T.D., Hughes, M.G. and Russell, P., 2005. Suspended sediment transport in the swash zone of a dissipative beach. *Marine Geology* 216, 169–189.
- Masselink G., Austin, M., Tinker, J., O'Hare, T. and Russell, P., 2008. Cross-shore sediment transport and morphological response on a macrotidal beach with intertidal bar morphology, Truc Vert, France. *Marine Geology* 251, 141–155, doi:10.1016/j.margeo.2008.01.010.
- McCall, R.T., Masselink, G., Poate, T.G., Roelvink, J.A. and Almeida, L.P., 2015. Modelling the morphodynamics of gravel beaches during storms with XBeach-G. *Coastal Engineering* 103, 52–66.
- McDougal, W.G. and Hudspeth, R.T., 1989. Longshore current and sediment transport on composite beach profiles. *Coastal Engineering* 12, 315–338.

- Mei, C.C. and Liu, P.L.F., 1977. Effects of topography on the circulation in and near the surf zone - linear theory. *Estuarine and Coastal Marine Science* 5, 25–37.
- Meyer-Peter, E. and Mueller, R., 1948. Formulas for bed-load transport. 2nd International IAHR Congress, Stockholm, Sweden.
- Mil-Homens, J., Ranasinghe, R., van Thiel de Vries, J.S.M. and Stive, M.J.F., 2013. Re-evaluation and improvement of three commonly used bulk longshore sediment transport formulas. *Coastal Engineering* 75, 29–39.
- Miller, H.C., 1999. Field measurements of longshore sediment transport during storms. *Coastal Engineering* 36, 301–321.
- Miller, J.K. and Dean, R.G., 2004. A simple new shoreline change model. *Coastal Engineering* 51, 531–556.
- Mishra, P., Mohanty, P.K., Murty, A.S.N. and Sugimoto, T., 2001. Beach profile studies near an artificial open-coast port along south Orissa, East Coast of India. *Journal of Coastal Research Special Issue* 34, 164–171, ISSN 0749-0208.
- Moeini, M.H. and Shahidi, A.E., 2007. Application of two numerical models for wave hindcasting in Lake Erie. *Applied Ocean Research* 29, 137–145, doi:10.1016/j.apor.2007.10.001.
- Mohanty, P.K., Patra, S.K., Bramha, S., Seth, B., Pradhan, U., Behera, B., Mishra, P. and Panda, U.S., 2012. Impact of groins on beach morphology: a case study near Gopalpur Port, east coast of India. *Journal of Coastal Research* 28(1), 132–142, ISSN 0749-0208.
- Mohanty, P., Barik S.K., Kar, P.K., Behera, B. and Mishra, P., 2015. Impacts of Ports on shoreline change along Odisha coast. 8th International Conference on Asian and Pacific coast (APAC 2015), *Procedia Engineering* 116, pp. 647–654.
- Moore, B.D., 1982. Beach profile evolution in response to changes in water level and wave height. MCE Thesis, Department of Civil Engineering, University of Delaware, pp. 164.
- Morton, A.C. and Smale, D., 1990. The effects of transport and weathering on heavy minerals from the Cascade river, New Zealand. *Sedimentary Geology* 68, 117–123.
- Morton, R.A., Leach, M.P., Paine, J.G. and Cardoza, M.A., 1993. Monitoring beach changes using GPS surveying techniques. *Journal of Coastal Research* 9(3), 702–720, ISSN 0749-0208.
- Morton, R.A., Miller, T. and Moore, L., 2005. Historical shoreline changes along the US Gulf of Mexico: A summary of recent shoreline comparisons and analyses. *Journal of Coastal Research* 21(4), 704–709, ISSN 0749-0208.
- Munk, W.H., 1949. The solitary wave theory and its applications to surf problems. *Annals of the New York Academy of Sciences* 51, 376–462.
- Muraleedharan, G., Mourani Sinha, Rao, A.D., Unnikrishnan Nair, N. and Kurup, P.G., 2009. Estimation of wave period statistics using numerical coastal wave model. *Natural Hazards* 49, 165–186, doi: 10.1007/s11069-008-9311.
- Murty, C.S. and Varadachari, V.V.R., 1980. Topographic changes of the beach Valiathura, Kerala. *Indian Journal of Marine Sciences* 9, 31–34.

- Murty, C.S. and Veerayya, M., 1985. Longshore currents and associated sediment transport in the nearshore areas of Kerala and Goa, west coast of India. *Mahasagar, Bulletin of the National Institute of Oceanography* 18 (20), pp. 163–177.
- Murty, C.S., Sastry, J.S. and Varadachari, V.V.R., 1979. Shoreline deformations in relation to shore protection structures along Kerala coast. *Indian Journal of Marine Sciences* 9, 77–81.
- Mwakumanya, M.A. and Bdo, O., 2007. Beach morphological dynamics: A case study of Nyali and Bamburi beaches in Mombasa, Kenya. *Journal of Coastal Research* 23(2), 374–379, ISSN 0749-0208.
- Nair, A.G., Suresh Babu, D.S., Damodaran, K.T., Shankar, R. and Prabhu, C.N., 2009. Weathering of ilmenite from Chavara deposit and its comparison with Manavalakurichi placer ilmenite, southwestern India. *Journal of Asian Earth Sciences* 34, 115–122.
- Narayana, A.C., Tatavarti, R. and Shaktwipi, M., 2005. Tsunami of 26 December 2004: Observations on Kerala coast. *Journal of Geological Society of India* 65, 239–246.
- Narayana, A.C., Tatavarti, R., Shinu, N. and Subeer, A., 2007. Tsunami of December 26, 2004 on the southwest coast of India: Post-tsunami geomorphic and sediment characteristics. *Marine Geology* 242, 155–168.
- Narayananaswamy, N. and Mallik, T.K., 2007. Heavy mineral studies of the innershelf area off Chavara, Kerala - A preliminary note. In: Loveson, V.J., Sen, P.K. and Sinha, A., (Eds.), *Exploration, Exploitation, Enrichment and Environment of Coastal Placer Minerals (PLACER-2007)*, Macmillan Advanced Research Series, pp. 91–97.
- Nascimento, do.L. and Lavenere-Wanderely, A.A., 2006. Effect of shore protection structures (Groins) on Sao Miguel Beach, Ilheus, Bahia, Brazil. *Journal of Coastal Research Special Issue* 39, 858–862, ISSN 0749-0208.
- Nayak, B.U. and Chandramohan, P., 1992. A longshore sediment transport estimation for the Indian coast. *Proceedings in 1st Convention, ISPO, 1990*, pp. 111–116.
- Noujas, V., Thomas, K.V., Sheela Nair, L., Hameed, T.S.S., Badarees K.O. and Ajeesh, N.R., 2014. Management of shoreline morphological changes consequent to breakwater construction. *Indian Journal of Geo-Marine Sciences* 43(1), 54–61.
- Ozolcer, I.H. and Komurcu, M.I., 2007. Effects of straight groin parameters on amount of accretion. *Indian Journal of Marine Sciences* 36(3), 173–182.
- Payo, A., Baquerizo, A. and Losada, M., 2008. Uncertainty assessment: Application to the shoreline. *Journal of Hydraulic Research* 46, 96–104, doi: 10.1080/00221686.2008.9521944.
- Pender, D. and Karunarathna, H., 2013. A statistical process based approach for modelling beach profile variability. *Coastal Engineering* 81, 19–29.
- Peterson, C.D., Komar, P.D. and Scheidegger, K.F., 1986. Distribution, geometry, and origin of heavy mineral placer deposits on Oregon beaches. *Journal of Sedimentary Petrology* 56(1), 67–77.

- Pham Thanh Nam, Larsson, M., Hanson, H. and Le, X.H., 2009. A numerical model of nearshore waves, currents, and sediment transport. *Coastal Engineering* 56, 1084–1096.
- Pierson, W.J. Jr. and Moskowitz, L., 1964. A proposed spectral form for fully developed wind seas based on the similarity theory of S.A. Kitaigorodskii. *Journal of Geophysical Research* 69, 5181–5190.
- Plomaritis T.A. and Collins, M.B., 2013. Hydrodynamic and sediment dynamic modifications of tidal flow in the near-field area of offshore breakwaters. *Ocean Dynamics* 63, 225–241, doi: 10.1007/s10236-013-0592-6.
- Portilla, J., Ocampo-Torres, F.J. and Monbaliu, J., 2009. Spectral partitioning and identification of wind sea and swell. *American Meteorological Society* 26, 107–122, doi: 10.1175/2008JTECHO609.1.
- Prakash, T.N., 2000. Sediment distribution and placer mineral enrichment in the innershelf of Quilon, SW coast of India. *Indian Journal of Marine Sciences* 29, 120–127.
- Prakash, T.N. and Verghese, A.P., 1987. Seasonal beach changes along Quilon district coast, Kerala. *Journal of the Geological Society of India* 29, 390–398.
- Prakash, T.N. and Prithvi Raj, M., 1988. A study of seasonal longshore transport direction through grain-size trends: An example from the Quilon coast, Kerala, India. *Ocean and Shoreline Management, Elsevier Applied Science, England* 11, 195–209.
- Prakash, T.N., Raju, G.K. and Prithvi Raj, M., 1991. Radioelement distribution in river, beach and offshore areas and their significance to Chavara placer deposit, southern Kerala coast of India. *Geo-Marine Letters* 11, 32–38.
- Prakash, T.N., Kurian, N.P., Rajith, K., Pillai, A.P., Murali Krishnan, B.T., Kalaiarasan, P. and Varghese, T.I., 2005. December 2004 Tsunami: Some results of field surveys along the Kerala coast. *Workshop on Tsunami Effects and Mitigation Measures, IIT Madras, Chennai*, pp. 307–320.
- Prakash, T.N., Black, K.P., Mathew, J., Kurian, N.P., Thomas, K.V., Hameed, T.S.S., Vinod, M.V. and Rajith, K., 2007. Nearshore and beach sedimentary dynamics in a placer dominated coast, southwest India. *Journal of Coastal Research* 23(6), 1391–1398.
- Prasad, K.V.S.R., Arun Kumar, S.V.V., Ch. Venkata Ramu and Patnaik, K.V.K.R.K., 2010. Wave refraction and energy patterns in the vicinity of Gangavaram, east coast of India. *Indian Journal of Geo-Marine Sciences* 39(4), 509–515.
- Prasada Rao, C.V.K., Hareesh Kumar, P.V. and Mohan Kumar, N., 1996. Pre-monsoon current structure in the shelf water off Cochin. *Proceedings of 2nd Workshop on Scientific Results, FORV Sagar Sampada*, pp. 19–24.
- Prasannakumar, S., 1985. Studies on sediment transport in the surf zone along certain beaches of Kerala. Unpublished Ph.D. Thesis, Cochin University of Science and Technology, pp. 110.
- Prasannakumar, S., Shenoi, S.S.C. and Kurup, P.G., 1983. Littoral drift along shoreline between Munambam and Andhakaranazhi, Kerala coast. *Indian Journal of Marine Sciences* 12, 209–212.

- Prasanna Kumar, S., Vethamony, P. and Murty, C.S., 1990. Wave-induced nearshore flow patterns in the vicinity of Cochin harbour, India. *Ocean and Shoreline Management* 13, 111–125, 0951-8312/90.
- Praveen, K.K., 2006. Shoreline changes and land use land cover of Kollam coast. Dissertation, Mangalore University, Mangalore, India.
- Pritchard, D. and Hogg, A.J., 2003. Cross-shore sediment transport and the equilibrium morphology of mudflats under tidal currents. *Journal of Geophysical Research* 108(C10), 3313, doi: 10.1029/2002JC001570.
- Prithvi Raj, M. and Prakash, T.N., 1988. Sediment distribution and transport studies of the inner shelf zone off the central coast of Kerala, India. *Journal of Coastal Research* 5(2), 271–280, ISSN 0749-0208.
- Pujos, M., Bouysse, P. and Pons, J.C., 1990. Sources and distribution of heavy minerals in Late Quaternary sediments of the French Guiana continental shelf. *Continental Shelf Research* 10(1), 59–79.
- Quick, M.C., 1991. Onshore-offshore sediment transport on beaches. *Coastal Engineering* 15, 313–332.
- Quick, M.C. and Ametepe, J., 1991. Relationship between longshore and cross-shore transport. *Proceedings of Coastal Sediments '91*, Seattle, Washington, June 25–27, 1991, Vol. 1, pp. 184–196.
- Rajawat, A.S., Chauhan, H.B., Ratheesh, R., Rode, S., Bhanderi, R.J., Mahapatra, M., Mohit, K., Yadav, R., Abraham, S.P., Singh, S.S., Keshri, K.N. and Ajai, 2015. Assessment of coastal erosion along the Indian coast on 1:25,000 scale using satellite data of 1989–1991 and 2004–2006 time frames. *Current Science* 109(2), 347–353.
- Rajith, K., 2006. Sediment budgeting studies for the Kollam coast. Ph.D. Thesis, Cochin University of Science and Technology, Cochin, Kerala, India, pp. 212.
- Rajith, K., Kurian, N.P., Thomas, K.V., Prakash, T.N. and Hameed, T.S.S., 2008. Erosion and accretion of a placer mining beach of SW Indian coast. *Marine Geodesy* 31, 128–142.
- Rao, C.B., 1957. Beach erosion and concentration of heavy mineral sands. *Journal of Sedimentary Petrology* 27(2), 143–147.
- Rao, N.C., Anu Radha, B., Reddy, K.S.N., Dhanamjayarao, E.N. and Dayal, A.M., 2012. Heavy mineral distribution studies in different microenvironments of Bhimunipatnam coast, Andhra Pradesh, India. *International Journal of Scientific and Research Publications* 2(5), 1–10, ISSN 2250-3153.
- Rashmi, R., Aboobacker, V.M., Vethamony, P. and John, M.P., 2013. Co-existence of wind seas and swells along the west coast of India during non-monsoon season. *Ocean Science* 9, 281–292, doi: 10.5194/os-9-281-2013.
- Reddy, M.P.M., 1979. A systematic study of wave conditions and sediment transport near Mormugao harbour. Supplement to *Mahasagar*, National Institute of Oceanography, Goa, India, 3(1), pp. 1–18.

- Reddy, K.S.N., Varma, D.D., Rao, E.N.D., Veerananarayana, B. and Prasad, T.L., 2012. Distribution of heavy minerals in Nizampatnam-Lankavanidibba coastal sands, Andhra Pradesh, east coast of India. *Journal Geological Society of India* 79, 411–418.
- Requejo, S., Medina, R. and González, M., 2008. Development of a medium–long term beach evolution model. *Coastal Engineering* 1–15, doi: 10.1016/j.coastaleng.2008.04.005.
- Revichandran, C., Pylee, A., Josanto, V. and Sankaranarayanan, V. N., 1993. Suspended sediment transport and shoaling in the Munambam fishery harbour, Kerala. *Proceedings of the 5th Kerala Science Congress, January 1993*, pp. 499–501.
- Roelvink, J.A. and Stive, M.J.F., 1989. Bar-generating cross-shore flow mechanisms on a beach. *Journal of Geophysical Research* 94, 4785–4800.
- Rogers, A.L. and Ravens, T.M., 2008. Measurement of longshore sediment transport rates in the surf zone on Galveston Island, Texas. *Journal of Coastal Research* 24(2B), 62–73, ISSN 0749-0208.
- Rosati, J.D., 2005. Concepts in sediment budgets. *Journal of Coastal Research* 21(2), 307–322.
- Roy, P.S., 1999. Heavy mineral beach placers in southeastern Australia: Their nature and genesis. *Economic Geology* 94, 567–558.
- Roy Chowdhury, B. and Sen, T., 2013. Coastal erosion and its impact on Sagar Island, (S) 24 Parganas. *W.B. International Journal of Science and Research* 4(3), 2319–7064, ISSN 2319-7064.
- Sahu, H.K., Hariharan, V. and Katti, R.J., 1991. Seasonal fluctuation in the coastal currents off Mangalore. *Environment and Ecology* 9, 521–525.
- Sajeev, R., Sankaranarayanan, V.N., Chandramohan, P. and Namboodiripad, K.S.N., 1996. Seasonal changes of the sediment distribution and stability along the beaches of Kerala, southwest coast of India. *Indian Journal of Marine Sciences* 25, 216–220.
- Sajeev, R., Chandramohan, P. and Sanil Kumar, V., 1997a. Wave refraction and prediction of breaker parameters along the Kerala coast, India. *Indian Journal of Marine Sciences* 26, 128–134.
- Sajeev, R., Chandramohan, P., Josanto, V. and Sankaranarayanan, V. N., 1997b. Studies on sediment transport along Kerala coast, southwest coast of India. *Indian Journal of Marine Sciences* 26, 11–15.
- Sajiv Philip, C., Sanil Kumar, V., Glejin J., Udhaba Dora, G. and Vinayaraj, P., 2012. Interannual and seasonal variations in nearshore wave characteristics off Honnavar, west coast of India. *Current Science* 103(3), 286–292.
- Sajiv Philip, C., Sanil Kumar, V., Udhaba Dora, G. and Glejin, J., 2014. Nearshore waves, longshore currents and sediment transport along micro-tidal beaches, central west coast of India. *International Journal of Sediment Research* 29(3), 402–413.

- Samiksha, S.V., Vinodkumar, K., and Vethamony, P., 2014. Impact of shamal winds and swells on the coastal currents along the west coast of India. *Indian Journal of Marine Sciences* 43(7), 1236–1240.
- Samsuddin, M. and Suchindan, G.K., 1987. Beach erosion and accretion in relation to seasonal longshore current variation in the northern Kerala coast, India. *Journal of Coastal Research* 3(1), 55–62, ISSN 0749-0208.
- Samsuddin, M., Ramachandran, K.K. and Suchindan, G.K., 1991. Sediment characteristics, processes and stability of the beaches in the northern Kerala coast, India. *Journal of Geological Society of India* 38, 82–95.
- Sanil Kumar, V. and Anand, N.M., 2004. Variations in wave direction estimated using first and second order Fourier coefficients. *Ocean Engineering* 31, 2105–2119.
- Sanil Kumar, V. and Ashok Kumar, K., 2008. Spectral characteristics of high shallow water waves. *Ocean Engineering* 35, 900–911.
- Sanil Kumar, V., Sarma, K.D.K.M., Joseph, M.X. and Viswambaram, N.K., 1989. Variability in current and thermohaline structure off Visakhapatnam during late June, 1986. *Indian Journal of Marine Sciences* 18, 232–237.
- Sanil Kumar, V., Chandramohan, P., Kumar, K.A., Gowthaman, R. and Pednekar, P., 2000. Longshore currents and sediment transport along Kannirajapuram coast, Tamil Nadu, India. *Journal of Coastal Research* 16, 247–254.
- Sanil Kumar, V., Ashok Kumar, K. and Raju, N.S.N., 2001. Nearshore processes along Tikkavanipalem beach, Visakhapatnam, India. *Journal of Coastal Research* 17, 271–279.
- Sanil Kumar, V., Anand, N.M. and Gowthaman, R., 2002. Variations in nearshore processes along Nagapattinam coast, India. *Current Science* 82, 1381–1389.
- Sanil Kumar, V., Anand, N.M., Chandramohan, P. and Naik, G.N., 2003. Longshore sediment transport rate - measurement and estimation, central west coast of India. *Coastal Engineering* 48, 95–109.
- Sanil Kumar, V., Pathak, K.C., Pednekar, P., Raju, N.S.N. and Gowthaman, R., 2006. Coastal processes along the Indian coastline. *Current Science* 91, 530–536.
- Sanil Kumar, V., Ashok Kumar, K., Pednekar, P. and Gowthaman, R., 2007. Sea and swell along west coast of India: A study based on measured data. 4th Indian National Conference on Harbour and Ocean Engineering, 12 to 14 December 2007 at NITK, Surathkal, pp. 736–745.
- Sanil Kumar, V., Sajiv Philip, C. and Balakrishnan Nair, T.M., 2010. Waves in shallow water off west coast of India during the onset of summer monsoon. *Annales Geophysicae* 28, 817–824.
- Sanil Kumar, V., Jai Singh, Pednekar, P. and Gowthaman, R., 2011. Waves in the nearshore waters of northern Arabian Sea during the summer monsoon. *Ocean Engineering* 38(2-3), 382–388.
- Sanil Kumar, V., Glejin, J., Udhaba Dora, G., Sajiv Philip, C., Singh, J. and Pednekar, P., 2012. Variations in nearshore waves along Karnataka, west coast of India. *Journal of Earth System Science* 121(2), 393–403.

- Saravanan, S., Chandrasekar, N. and Jeevivek, V., 2013. Temporal and spatial variation in the sediment volume along the beaches between Ovari and Kanyakumari (SE India). *International Journal of Sediment Research* 28, 384–395.
- Sarma, M.S.S. and Rao, L.V.G., 1986. Currents and temperature structure off Godavari (east coast of India) during September, 1980. *Indian Journal of Marine Sciences* 15, 88–91.
- Sarma, K.G.S. and Reddy B.S.R., 1988. Longshore sediment transport near Visakhapatnam Port, India. *Ocean and Shoreline Management* 11, 113–127.
- Schneider, C., 1981. The littoral environment observations (LEO) data collection program. Coastal Engineering Technical Aid 81-5, Coastal Engineering Research Center, U.S. Army Engineers Waterways Experiment Station, Vicksburg, Mississippi.
- Shah Alam Khan, M., 2003. Cross-shore net sediment transport change to equilibrium: A wave tank study. *Journal of Civil Engineering, The Institutions of Engineers, Bangladesh*, CE31(1), pp. 1–8.
- Shamji, V.R., Hameed, T.S.S., Kurian, N.P. and Thomas, K.V., 2010. Application of numerical modelling for morphological changes in a high energy beach during the south-west monsoon. *Current Science* 98(5), 691–695.
- Shanas, P.R. and Sanil Kumar, V., 2014. Coastal processes and longshore sediment transport along Kundapura coast, central west coast of India. *Geomorphology* 214, 436–451.
- Shankar, D. and Shetye, S.R., 1997. On the dynamics of the Lakshadweep high and low in the southeastern Arabian Sea. *Journal of Geophysical Research* 102, 12551–12562.
- Shankar, D., Vinayachandran, P.N. and Unnikrishnan, A.S., 2002. The monsoon currents in the north Indian Ocean. *Progress in Oceanography* 52, 63–120.
- Shankar, R., Thompson, R. and Prakash, T.N., 1996. Estimation of heavy and opaque mineral contents of beach and offshore placers using rock magnetic techniques. *Geo-Marine Letters* 16, 313–318.
- Sheela Nair, L., Sundar, V. and Kurian, N.P., 2011. Numerical model studies on the effect of breakwaters on coastal processes - A case study along a stretch of the Kerala coast, India. *International Journal of Ocean and Climate Systems* 2(4), 291–302, doi: <http://dx.doi.org/10.1260/1759-3131.2.4.291>.
- Sheela Nair, L., Sundar, V. and Kurian, N.P., 2013. Shore protection for a placer deposit rich beach of the southwest coast of India. *International Journal of Ocean Climate Systems* 4(1), 41–62.
- Sheela Nair, L., Sundar, V., Kurian, N.P., 2015. Longshore sediment transport along the coast of Kerala in southwest India. *Procedia Engineering* 116, 40–46, doi: 10.1016/j.proeng.2015.08.262.
- Shemdin, O.H., Hsiao, H., Carlson, H.E., Hasselmann, K. and Schulze, K., 1980. Mechanisms of wave transformation in finite-depth water. *Journal of Geophysical Research* 85(C9), 5012–5018.

- Shenoi, S.S.C. and Prasannakumar, S., 1982. Littoral processes along shoreline from Andhakaranazhi to Azhikode along Kerala coast. *Indian Journal of Marine Sciences* 11, 201–207.
- Shenoi, S.S.C. and Antony, M.K., 1991. Current measurements over western continental shelf of India. *Continental Shelf Research* 11, 81–93.
- Shenoi, S.S.C., Murty, C.S. and Veerayya, M., 1987. Monsoon-induced seasonal variability of sheltered versus exposed beaches along the west coast of India. *Marine Geology* 76, 117–130.
- Shepard, F.P., 1954. Nomenclature based on sand-silt-clay ratios. *Journal of Sedimentary Petrology* 24 (3), 151–158.
- Shepard, F.P., Emery, K.O. and La Fond, E.C., 1941. Rip currents: a process of geological importance. *Journal of Geology* 49, 337–369.
- Shetye, S.R., 1998. West India coastal current and Lakshadweep high/low. *Sadhana* 23, pp. 637–651.
- Shetye, S.R., Gouveia, A.D., Shenoi, S.S.C., Sundar, D., Michael, G.S., Almeida, A.M. and Santanam, K. 1990. Hydrography and circulation off the west coast of India during the southwest monsoon 1987. *Journal of Marine Research* 48, 359–378.
- Short, A.D., 1999. Beach hazards and safety. In: Short, A.D. (Ed.), *Handbook of beach and shoreface morphodynamics*. John Wiley and Sons, Chichester, pp. 293–304.
- Short, A.D., 2006. Australian beach systems - nature and distribution. *Journal of Coastal Research* 22(1), 11–27, ISSN 0749-0208.
- Siddiquie, H.N. and Mallik, T.K., 1972. Trend-surface analysis of distribution of some heavy minerals in shelf sediments off Mangalore, India. *Mathematical Geology* 4(4), 277–290.
- Simon, B., 2007. Grain size distribution and statistic package for the analysis of unconsolidated sediments by sieving or laser granulometer. *Gradistat programme, Version 4.0*.
- Singh, A.K., Deo, M.C. and Sanil Kumar, V., 2008. Prediction of littoral drift with artificial neural networks. *Hydrology and Earth System Sciences* 12, 267–275.
- Slingerland, R. and Smith, N.D., 1986. Occurrence and formation of water-laid placers. *Annual Review of Earth and Planetary Sciences* 14, 113–147.
- Smith, E.R., Bruce, A.E. and Wang, P., 2004. Dependence of total longshore sediments transport rates on incident wave parameters and breaker type. ERDC/CHL CHETN-IV-62, U.S. Army Engineer Research and Development Center, Vicksburg, USA.
- Smith, E.R., Wang, P., Ebersole, B.A. and Zhang, J., 2009. Dependence of total longshore sediment transport rates on incident wave parameters and breaker type. *Journal of Coastal Research* 25(3), 675–683, ISSN 0749-0208.
- Smith, S.E. and Abdel-Kader, A., 1988. Coastal erosion along the Egyptian delta. *Journal of Coastal Research* 4(2), 245–255, ISSN 0749-0208.

- Sorensen, R.M., 2006. Basic coastal engineering. 3rd Edition, Springer, U.S.A., pp. 324, ISBN 0-387-23332-6.
- Splinter, K.D. and Slinn, D.N., 2003. Three-dimensional modeling of alongshore current dynamics. Canadian Coastal Conference 2003, pp. 1–14.
- SPM, 1984. Shore Protection Manual. U.S. Army Corps of Engineers, Vol. 1 and 2, Coastal Engineering Research Centre, Waterways Experiment Station, Vicksburg, Mississippi.
- Sreeja, S., 2005. Geoinformatics for cataloguing of shoreline stability. Dissertation, College of Engineering and Centre for Earth Science Studies, Thiruvananthapuram, India.
- Sreekala, S.P., Baba, M. and Muralikrishna, M., 1998. Shoreline changes of Kerala coast using IRS data and aerial photographs. Indian Journal of Marine Science 27(1), 144–148.
- Srinivas, K. and Dinesh Kumar, P.K., 2002. Tidal and non-tidal sea level variations at two adjacent ports on the southwest coast of India. Indian Journal of Marine Sciences 31(4), 271–282.
- Srivastava, A.K., Ingle, P.S. and Khare, N., 2010. Textural characteristics, distribution pattern and provenance of heavy minerals in glacial sediments of Schirmacher Oasis, east Antarctica. Journal of the Geological Society of India 75, 393–402.
- Stramma, L., Fischer, J. and Schott, F., 1996. The flow field off southwest India at 8°N during the southwest monsoon of August 1993. Journal of Marine Research 54, 55–72.
- Suresh, P.K. Sundar, V. and Selvaraj, A., 2011. Numerical modelling and measurement of sediment transport and beach profile changes along southwest coast of India. Journal of Coastal Research 27(1), 26–34, ISSN 0749-0208.
- Suresh, R.R.V., Annapurnaiah, K., Reddy, K.G., Lakshmi, T.N. and Balakrishnan Nair, T.M., 2010. Wind sea and swell characteristics off east coast of India during southwest monsoon. International Journal of Oceans and Oceanography 4(1), 35–44, ISSN 0973-2667.
- Sutherland, J., Peet, A.H., Soulsby, R.L., 2004. Evaluating the performance of morphological models. Coastal Engineering 51, 917–939, doi:10.1016/j.coastaleng.2004.07.015.
- Swift, D.J.P., Dili, C.E. and McHone, J., 1971. Hydraulic fractionation of heavy mineral suites on an unconsolidated retreating coast. Journal of Sedimentary Petrology 41 (3), 683–690.
- Tai-Wen Hsu, John, R.C.H., Wen-Kai Weng, Swun-Kwang Wang and Shan-Hwei Ou, 2006. Wave setup and setdown generated by obliquely incident waves. Coastal Engineering 53, 865–877.
- Thomas, K.V., 1988. Waves and nearshore processes in relation to beach development at Valiyathura. In: Baba, M. and Kurian, N.P. (Eds.), Ocean waves and beach processes of south-west coast of India and their prediction. Centre for Earth Science Studies, Thiruvananthapuram, India, December 1988, pp. 47–66.

- Thomas, K.V., Kurian, N.P., Sundar, V., Sannasiraj, S.A., Badarees, K.O., Saritha, V.K., Abhilash, S., Sarath, L.G. and Srikanth, K., 2010. Morphological changes due to coastal structures along the southwest coast of India. Proceedings of the Joint Indo-Brazil Workshop on Coastal Processes Modelling Relevant to Understand the Causes of Shoreline Changes, ICMAM, Chennai, India, March 23-25, pp. 125–133.
- Thornton, E.B. and Krapohl, R.F., 1974. Water particle velocities measured under ocean waves. *Journal of Geophysical Research* 79, 847–852.
- Thornton, E.B., Sallenger, A., Sesto, J.C., Egley, L., McGee, T. and Parsons, R., 2006. Sand mining impacts on long-term dune erosion in southern Monterey Bay. *Marine Geology* 229, 45–58.
- Times of India, 2013. Lack of proper mining policy hits industry. Times of India, Kochi, India, Date: November 22, 2013.
- Trujillo, A.P. and Thurman, H.V., 2010. *Essentials of Oceanography*. 10th Edition, Prentice Hall, pp. 551, ISBN 032166812X.
- Tsujimoto, G., Kakinoki, T., Hamaura, Y., Shigematsu, T. and Uno, K., 2007. A study on sediment transport inside and outside a permeable submerged breakwater with the Macroscopic turbulence model. *Journal of Coastal Research Special Issue* 50, 206–210, ISSN 0749.0208.
- Turker, U. and Kabdas, M.S., 2006. The effects of sediment characteristics and wave height on shape-parameter for representing equilibrium beach profiles. *Ocean Engineering Technical Note* 33, pp. 281–291, doi: 10.1016/j.oceaneng.2004.12.016.
- Turker, U. and Kabdas, M.S., 2007. Verification of sediment transport rate parameter on cross-shore sediment transport analysis. *Ocean Engineering* 34, 1096–1103.
- Udhaba Dora, G., Sanil Kumar, V., Glejin, J., Sajiv Philip, C. and Vinayaraj, P., 2012. Short-term observation of beach dynamics using cross-shore profiles and foreshore sediment. *Ocean and Coastal Management* 67, 101–112.
- Udhaba Dora, G., Sanil Kumar, V., Vinayaraj, P., Sajiv Philip, C. and Glejin, J., 2014a. Quantitative estimation of sediment erosion and accretion processes in a micro-tidal coast. *International Journal of Sediment Research* 29(2), 218–231.
- Udhaba Dora, G., Sanil Kumar, V., Sajiv Philip, C. and Glejin, J., 2014b. Observation on foreshore morphodynamics of microtidal sandy beaches. *Current Science* 107(8), 1324–1330.
- van der Wegen, M., Jaffe, B.E. and Roelvink, J.A., 2011. Process-based morphodynamic hindcast of decadal deposition patterns in San Pablo Bay, California. *Journal of Geophysical Research* 116(F02008), 1856–1887, doi: 10.1029/2009JF001614.
- van Lancker, V., Lanckneus, J., Hearn, S., Hoekstra, P., Levoy, F., Miles, J., Moerkerke, G., Monfort, O. and Whitehouse, R., 2004. Coastal and nearshore morphology, bedforms and sediment transport pathways at Teignmouth (UK). *Continental Shelf Research* 24, 1171–1202.
- van Rijn, L.C., 1997a. Sediment transport and budget of the central coastal zone of Holland. *Coastal Engineering* 32, 61–90.

- van Rijn, L.C., 1997b. Cross-shore modelling of graded sediments. Report H Z2181, Delft Hydraulics, The Netherlands.
- van Rijn, L.C., 1998. The effect of sediment composition on cross-shore bed profiles. ICCE, Copenhagen, Denmark.
- van Rijn, L.C., 2011. Coastal erosion and control. *Ocean and Coastal Management* 54, 867–887, doi:10.1016/j.ocecoaman.2011.05.004.
- van Rijn, L.C., 2012. Principles of sediment transport in rivers, estuaries and coastal seas. Aqua Publications, Amsterdam, The Netherlands, pp. 386.
- van Rijn, L.C., 2014. A simple general expression for longshore transport of sand, gravel and shingle. *Coastal Engineering* 90, 23–39.
- van Rijn, L.C. and Wijnberg, K.M., 1996. One-dimensional modelling of individual waves and wave-induced longshore currents in the surf zone. *Coastal Engineering* 28, 121–145.
- van Rijn, L.C., Walstra, D.J.R., Grasmeijer, B., Sutherland, J., Pan, S. and Sierra, J.P., 2003. The predictability of cross-shore bed evolution of sandy beaches at the time scale of storms and seasons using process-based profile models. *Coastal Engineering* 47, 295–327.
- Varma, U.P., Rama Raju, V.S., Abraham P. and Narayanaswamy, G., 1981. Sediment budget of a portion of Trivandrum beach (Kerala). *Mahasagar - Bulletin of National Institute of Oceanography* 14(1), pp. 17–21.
- Vaselali A. and Azarmsa S.A., 2009. Analysis of breakwater construction effects on sedimentation pattern. *Journal of Applied Sciences* 9(19), 3522–3530.
- Vethamony, P. and Sastry, J.S., 1985. On the characteristics of multi-peaked spectra of ocean waves. *Journal of the Institution of Engineers (India)* 66(Part CI 3&4), 129–132.
- Vethamony, P., Sudheesh, K., Rupali, S.P., Babu, M.T., Jayakumar, S., Saran, A.K., Basu, S.K., Kumar, R. and Sarkar, A., 2006. Wave modelling for the north Indian ocean using MSMR analysed winds. *International Journal of Remote Sensing* 27(18), 3767–3780.
- Vinayaraj, P., Glejin, J., Udhaba Dora, G., Sajiv Philip, C., Sanil Kumar, V., and Gowthaman, R., 2011. Quantitative estimation of coastal changes along selected locations of Karnataka, India: A GIS and remote sensing approach. *International Journal of Geosciences* 2, 385–393, doi: 10.4236/ijg.2011.24041.
- Wagle, B.G., Gujar, A.R. and Mislankar, P.G., 1989. Impact of coastal features on beach placers - a case study using remote sensing. *Proceedings of 21st Offshore Technology Conference, Houston, Texas*, pp. 229–233.
- Walton T.L. Jr. and Dean, R.G., 2010. Longshore sediment transport via littoral drift rose. *Ocean Engineering* 37, 228–235.
- Wang, P. and Kraus, N.C., 1999. Longshore sediment transport rate measured by short-term impoundment. *Journal Waterway Port Coastal and Ocean Engineering* 125, 118–126.
- Wang, P., Kraus, N.C. and Davis, R.A. Jr., 1998. Total longshore sediment transport rate in the surf zone: Field measurements and empirical predictions. *Journal of Coastal Research* 14(1), 269–282, ISSN 0749-0208.

- Wang, P., Ebersole, B.A. and Smith, E.R., 2002a. Longshore sand transport – Initial results from large scale sediment transport facility. ERDC/CHL CHETNII-46, U.S. Army Engineer Research and Development Center, Vicksburg, Mississippi, <http://chl.erd.c.usace.army.m>.
- Wang, P., Ebersole, B.A., Smith, E.R. and Johnson, B.D., 2002b. Temporal and spatial variations of surf zone currents and suspended sediment concentration. *Coastal Engineering* 46, 175–211.
- Wang, P., Beck, T.M., and Robberts, T.M., 2011. Modeling regional-scale sediment transport and medium-term morphology change at a dual-inlet system examined with the Coastal Modeling System (CMS): A case study at Johns Pass and Blind Pass, West-Central Florida. In: Roberts, T.M., Rosati, J.D. and Wang, P. (Eds.), *Proceedings, Symposium to Honor Dr. Nicholas C. Kraus, Journal of Coastal Research Special Issue 59*, pp. 49–60, ISSN 0749-0208.
- Winant, C.D., Inman, D.L. and Nordstrom, C.E., 1975. Description of seasonal beach changes using empirical eigen functions. *Journal of Geophysical Research* 80, 15, 1979–1986.
- WMO, 1998. World Meteorological Organization. Guide to wave analysis and forecasting. Secretariat of the World Meteorological Organization, Geneva, Switzerland, WMO-No. 702, 2nd Edition, pp. 159, ISBN 92-63-12702-6.
- Wright, L.D., Boon, J.D., Kim, S.C. and List, J.H., 1991. Modes of cross-shore sediment transport on the shoreface of the Middle Atlantic Bight. *Marine Geology* 96, 19–51.
- Yalcin, M.G., 2009. Heavy mineral distribution as related to environmental conditions for modern beach sediments from the Susanoglu (Atakent, Mersin, Turkey). *Environmental Geology* 58, 119–129, doi: 10.1007/s00254-008-1499-2.
- Yalin, M.S., 1977. *Mechanics of sediment transport*. Pergamon, Oxford, 1st Edition, pp. 290.
- Yang, W.H., 1993. Breaking wave spectrum and set-down set-up in shallow water. *Journal of Marine Science and Technology* 1(1), 73–79.
- Yang, Z., Wang, T., Cline, D. and Williams, B., 2014. Hydrodynamic modeling analysis to support nearshore restoration projects in a changing climate. *Journal of Marine Science and Engineering* 2, 18–32, doi: 10.3390/jmse2010018.

Appendix

**Cover and First Page of
Publications from the Thesis**

Erosion and heavy mineral depletion of a placer mining beach along the south-west coast of India: Part I— Nearshore sediment transport regime

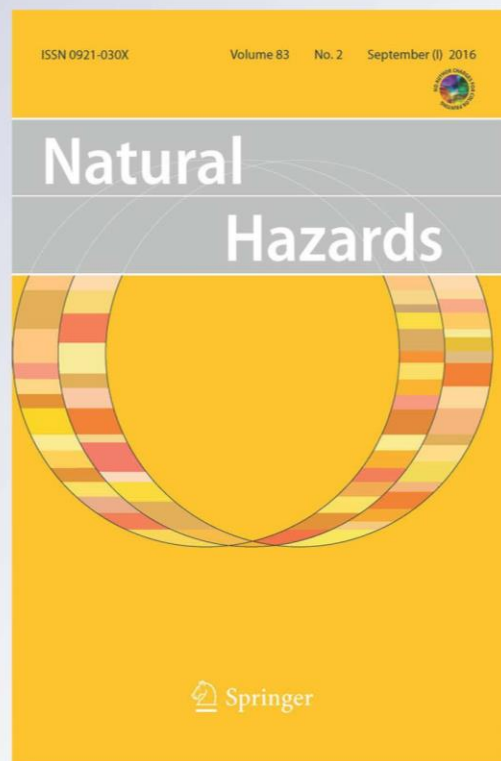
R. Prasad, L. Sheela Nair, N. P. Kurian & T. N. Prakash

Natural Hazards

Journal of the International Society
for the Prevention and Mitigation of
Natural Hazards

ISSN 0921-030X
Volume 83
Number 2

Nat Hazards (2016) 83:769-796
DOI 10.1007/s11069-016-2368-z



 Springer



Erosion and heavy mineral depletion of a placer mining beach along the south-west coast of India: Part I—Nearshore sediment transport regime

R. Prasad¹ · L. Sheela Nair¹ · N. P. Kurian¹ · T. N. Prakash¹

Received: 13 February 2016 / Accepted: 18 May 2016 / Published online: 27 May 2016
© Springer Science+Business Media Dordrecht 2016

Abstract The Chavara coast of southwest India is well known for its rich beach placer deposits which are being commercially exploited by the industries. Replenishment of these resources, which consist of heavy minerals of varying densities, by the hydrodynamic processes is essential for maintaining the stability of the coast as well as sustenance of mining. Rich concentrations of heavy minerals were reported consistently in the beach sediments of this coast in the past, but a systematic reduction in the concentration of the heavies has been reported during the past one-and-a-half decades. This paper, the first in a series of three, emanates from a programme of study launched to understand the mechanisms that manifest the reported changes in the morphology and mineralogy along this coast. In this study the longshore and cross-shore sediment transport rates along this coast have been estimated adopting numerical model studies. The validated LITDRIFT and LITPROF modules of the LITPACK modelling system have been used for computing the longshore and cross-shore sediment fluxes in the surf zone and innershelf region. The net annual longshore sediment transport is northerly in the surf zone where as it is southerly in the innershelf. Detailed analysis of the computed results shows domination of onshore transport over offshore transport. The beach volume change estimated from the measured beach profile on the other hand shows a reduction in the annual replenishment. The domination of the onshore flux as seen in the computations is actually not reflected in the field observations, and this can be attributed to the influence of excessive sand mining by the industries.

Keywords Innershelf · Nearshore · Numerical modelling · Sediment transport · Surf zone

✉ L. Sheela Nair
sheela.nair@nic.in;
<http://www.ncess.gov.in>

¹ Coastal Processes Group, National Centre for Earth Science Studies (NCESS), Akkulam, Thiruvananthapuram, Kerala 695 011, India

Erosion and heavy mineral depletion of a placer mining beach along the south-west coast of India: Part II—Sedimentological and mineralogical changes

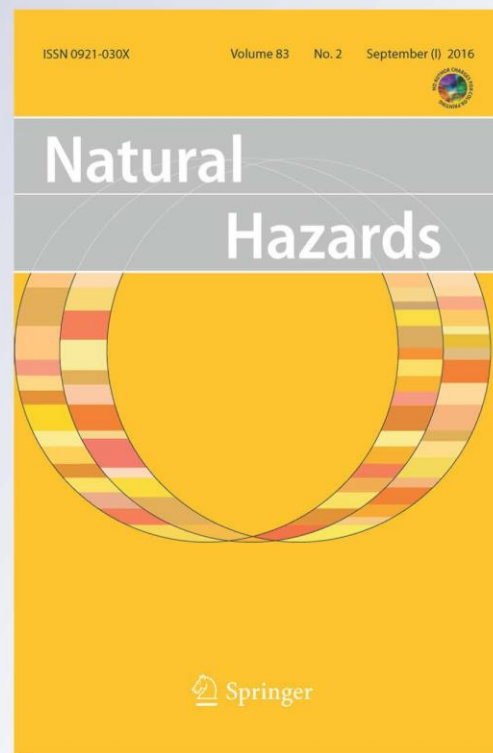
**T. N. Prakash, Tiju I. Varghese,
R. Prasad, L. Sheela Nair & N. P. Kurian**

Natural Hazards

Journal of the International Society
for the Prevention and Mitigation of
Natural Hazards

ISSN 0921-030X
Volume 83
Number 2

Nat Hazards (2016) 83:797-822
DOI 10.1007/s11069-016-2350-9



 Springer



Erosion and heavy mineral depletion of a placer mining beach along the south-west coast of India: Part II—Sedimentological and mineralogical changes

T. N. Prakash¹ · Tiju I. Varghese¹ · R. Prasad¹ ·
L. Sheela Nair¹ · N. P. Kurian¹

Received: 13 February 2016 / Accepted: 3 May 2016 / Published online: 13 May 2016
© Springer Science+Business Media Dordrecht 2016

Abstract Mining of beach placers or heavy minerals (HM) has been going on along the Neendakara–Kayamkulam coastal sector of the SW India for the past several decades by two public sector undertakings. Rich concentrations of HM were reported consistently in the beach sediments of this coast in the past, but a systematic reduction in the concentration of the heavies has been reported during the past one and a half decades. This paper emanates from a programme of study launched to understand the mechanisms that manifest the reported changes in the morphology and mineralogy along this coast. A detailed study of the sedimentology and mineralogy of the beach and innershelf has been carried out based on surficial sediment sampling from the beach and innershelf and core sampling from the innershelf. The study confirmed the depletion in the HM concentration in the beaches of the Chavara coast after 2000. One of the factors that led to the depletion in HM concentration along this coast was the 2004 tsunami which brought down the concentration to as low as 2 % in the innershelf. In addition to the tsunami, the other factors responsible for the observed depletion of beach placers along the coast are excessive beach sand mining and construction of coastal structures.

Keywords Beach · Erosion · Heavy mineral depletion · Innershelf · Sedimentology

1 Introduction

Rich concentration of heavy minerals, known as ‘Chavara placer deposit’, occurs along the Neendakara–Kayamkulam coastal sector of SW India. Commonly occurring minerals in the deposits are ilmenite, leucoxene, rutile, sillimanite, garnet, zircon, monazite that have a

✉ L. Sheela Nair
sheela.nair@nic.in

¹ Coastal Processes Group, National Centre for Earth Science Studies (NCESS), Akkulam, Thiruvananthapuram 695 011, Kerala, India

Erosion and heavy mineral depletion of a placer mining beach along the south-west coast of India: part III—short- and long-term morphological changes

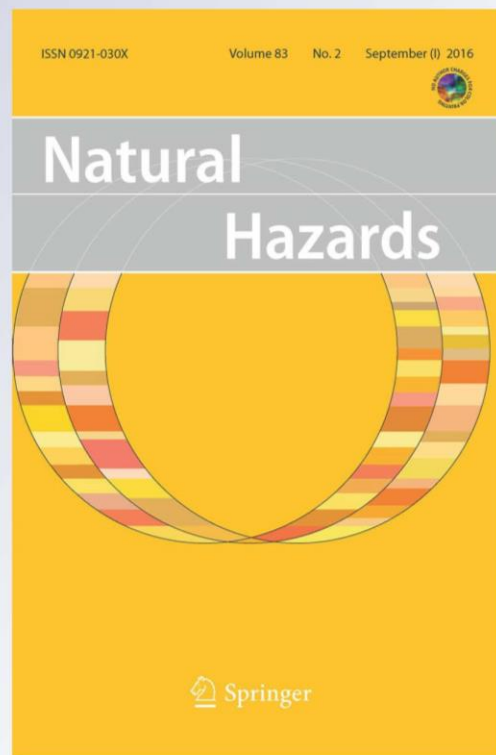
**R. Prasad, L. Sheela Nair, N. P. Kurian,
T. N. Prakash & Tiju I. Varghese**

Natural Hazards

Journal of the International Society
for the Prevention and Mitigation of
Natural Hazards

ISSN 0921-030X
Volume 83
Number 2

Nat Hazards (2016) 83:823-847
DOI 10.1007/s11069-016-2346-5



 Springer



Erosion and heavy mineral depletion of a placer mining beach along the south-west coast of India: part III—short- and long-term morphological changes

R. Prasad¹ · L. Sheela Nair¹ · N. P. Kurian¹ · T. N. Prakash¹ · Tiju I. Varghese¹

Received: 13 February 2016 / Accepted: 27 April 2016 / Published online: 11 May 2016
© Springer Science+Business Media Dordrecht 2016

Abstract The Chavara coast of south-west India is well known for its rich beach placer deposits which are being commercially mined by two public sector firms. The erosion of the beach and innershelf and the depletion of heavy mineral content of this coast have attracted a lot of attention of late, and an investigation of the mechanisms that drive these changes was taken up recently. The results of the investigation are presented in three parts. This paper, which is the last in the series, presents a study of the morphological changes of the beach and innershelf and integrates the results from the other two papers with an analysis of multi-dated shoreline and bathymetry data. The analysis of the multi-dated data showed an overall retreat of the shoreline and a relative deepening of the innershelf. The shoreline retreat has been quite alarming at the mining sites with one of the mining sites showing a retreat of nearly 400 m. The sediment deposition adjacent to the breakwater (built during 2000–2007) at the northern inlet has defused to some extent the high erosion observed earlier in the northernmost sector, and the presence of well-maintained seawalls has nearly maintained the shoreline south of the mining site. The erosion of the beach is accompanied by a deepening of the innershelf which is more pronounced in the shallower portions up to 10 m depth. The observed changes in the beach–innershelf morphology are analysed with respect to the nearshore sediment transport regime and heavy mineral distribution of the coast. It is observed that the combined intake of sediments by the two firms during the past one and a half decade is much above the sustainable mining level. Another contributing factor is the 2004 tsunami which drained off a sizable quantity of innershelf sediments rich in heavy minerals to the hinterland regions. The breakwaters at the two inlets bordering this coast have virtually compartmentalized this coast from the rest of the south-west coast making it a sediment sub-cell. In addition, the breakwaters act as groins

✉ L. Sheela Nair
sheela.lnair@nic.in;
<http://www.ncess.gov.in>

¹ Coastal Processes Group, National Centre for Earth Science Studies (NCESS), Akkulam, Thiruvananthapuram, Kerala 695 011, India